

## Deodorization of polluted air streams

**Author:**

Hardwick, Bruce Alfred

**Publication Date:**

1972

**DOI:**

<https://doi.org/10.26190/unsworks/13989>

**License:**

<https://creativecommons.org/licenses/by-nc-nd/3.0/au/>

Link to license to see what you are allowed to do with this resource.

Downloaded from <http://hdl.handle.net/1959.4/69322> in <https://unsworks.unsw.edu.au> on 2024-04-20

The University of New South Wales  
School of Chemical Engineering

DEODORIZATION OF POLLUTED AIR STREAMS  
WITH PARTICULAR REFERENCE TO THE  
REMOVAL OF TRACES OF HYDROGEN SULPHIDE  
AND ETHYL MERCAPTAN USING AQUEOUS  
SYSTEMS CONTAINING MANGANESE COMPOUNDS

A Thesis submitted for the degree of  
DOCTOR OF PHILOSOPHY  
by  
Bruce Alfred Hardwick  
December, 1972

Candidate's Certificate

The work described in this thesis was carried out by the candidate in the School of Chemical Engineering of the University of New South Wales and has not been submitted to any other University or Institution for a higher degree.

.....

B.A. Hardwick

## ACKNOWLEDGEMENTS

Sincere thanks are due to the staff of the School of Chemical Engineering for their help and encouragement, and in particular to Professor R.T. Fowler for his assistance in this study.

Sincere thanks are also due to Mr. D.K.B. Thistlethwayte whose encouragement and assistance was particularly appreciated, and whose comments and suggestions has improved this work far beyond that which would have been possible otherwise.

Acknowledgement is also made to the Department of Education and Science of the Commonwealth of Australia who provided financial assistance.



### ABSTRACT

The absorption of hydrogen sulphide and ethyl mercaptan from polluted air streams by alkaline buffered solutions of potassium permanganate has been examined in a simple gas bubbler. The same gas/liquid system has also been used, in conjunction with a series of three short wetted wall columns, to study the case of mass transfer from a gas in laminar flow.

For analysis of the low concentrations of hydrogen sulphide and ethyl mercaptan involved, an analytical method based on the two fluorescent reagents fluorescein mercuric acetate and tetra-acetoxymercurifluorescein, has been developed. Extensive tests have shown that the accuracy and reproducibility of the calibration data, and the method in general, is excellent.

The results of the bubbler tests demonstrate the ability of the permanganate test solution to continue to absorb the gaseous sulphide from the polluted air stream well beyond the point at which all permanganate ion has been reduced. Examination of the precipitate formed in such solutions using X-ray diffraction techniques and the appropriate oxidation potential diagrams has indicated a probable reaction path which emphasises the powerful catalytic properties of the precipitated manganese species in the presence of air.

The mass transfer measurements obtained using the short wetted wall columns and laminar flow conditions are in good agreement with the Graetz equation for parabolic flow.

## SUMMARY

The recent awakening of interest in environmental protection, and the subsequent governmental action, has stimulated a demand for more efficient methods of pollution control. The elimination of odorous substances from gaseous discharges, an important aspect of air pollution control, has benefited little from this interest, relying mainly on methods of deodorization developed some time ago. However, a particularly promising technique, and one which has only recently been suggested as a means of general odour control, is that involving absorption in alkaline buffered solutions of potassium permanganate.

Assessment of the effectiveness of an odour abatement technique is complicated by the lack of a universally acceptable method of odour measurement. Where the odorous substance is a pure chemical, the concentration level in relation to the odour threshold is usually sufficient to define the efficiency of the technique. In this work, where hydrogen sulphide and ethyl mercaptan were chosen as representative of the odour problem, chemical analyses were used. An attempt to correlate the analytical result with the appropriate A.S.T.M. odour level measurement was unsuccessful.

To perform the analysis a new analytical method was

developed. The method depended on the rapid absorption of the sulphide pollutant in an alkaline solution of one of two fluorometric reagents, fluorescein mercuric acetate or tetra-acetoxymercurifluorescein. The reading obtained on measurement of the solution fluorescence was then related directly to the concentration of pollutant in the reagent solution by previously determined calibration curves. Examination of the reliability of the calibration data showed that consistently reproducible curves could be obtained when both the crystalline reagent and the reagent solution were stored under carefully controlled conditions.

An overall check on the method, using air streams containing known concentrations of the pollutant, showed that there were no differences between the observed and known values at the 95% level of significance.

The behaviour of alkaline buffered permanganate solution during the deodorization of air streams containing low concentrations of the sulphidic contaminant was examined using a simple absorber comprising a 500 ml Drechsel bottle. Generation of the gas stream was achieved by steady injection of a pure sample of the material under test into a carbon dioxide free air stream.

Overall the results confirmed those reported in the

literature. However, it was also found that in this particular case, where the sulphidic contaminant was contained in a reactive carrier, air, the precipitate remaining after all permanganate ion had been reduced was an efficient catalyst capable of continuing the oxidation.

Examination of this precipitate after a reaction period well in excess of that necessary to remove all permanganate ion, using X-ray diffraction methods in conjunction with the appropriate theoretical oxidation potential diagrams, revealed a probable reaction path. The key to this path is the oxide  $\text{Mn}_3\text{O}_4$ , trimanganese tetroxide, which is capable of reacting with the sulphide to form manganese sulphide,  $\text{MnS}$ , a relatively unstable compound easily oxidised by the oxygen in the air.

The gas/liquid system described above has also been used, in conjunction with short wetted wall columns of three different lengths to examine the case of mass transfer from an air stream in laminar flow. This form of transfer is of little practical interest, but of great theoretical and experimental interest, since it can be easily analysed from first principles to yield a solution which most investigators have found difficult to verify experimentally. By critical analysis it was possible to determine the sources of error in most of these investigations, and to eliminate them from this

investigation by careful design of the experimental apparatus and procedures.

In this manner good agreement was obtained between the results and the Graetz equation for a parabolic velocity distribution. Generally the agreement was better for the case of hydrogen sulphide absorption than that of ethyl mercaptan absorption

As a final check on the reliability of the experimental apparatus, the wetted wall columns were used to determine physical absorption coefficients for the system involving the desorption of carbon dioxide from water.

The results showed good agreement with those reported in the literature, yielding the equation,

$$K_L \sqrt{\frac{L}{D_L}} = 7.41 \left( \frac{T}{\sqrt{\epsilon}} \right)^{0.33}$$

with a correlation coefficient of 0.8 and a standard deviation on a log-log scale of 0.037.

## Table of Contents.

Acknowledgements	ii
Abstract	iii
Summary	v
Table of Contents	ix
Nomenclature	xx

## Chapter 1.

### Odours and Deodorization with Special Reference to Hydrogen Sulphide and Ethyl Mercaptan.

1.1	Introduction	2
1.1.1	Odours and Odour Theories	2
1.1.2	The Odour Problem	4
1.2	Methods of Deodorization	5
1.2.1	General Methods of Deodorization	5
1.2.2	Specific Methods of Deodorization	6
1.3	Assessment of the Odour Abatement Method	7
1.3.1	Odour Evaluation	7
1.3.2	Odour Thresholds and the Minimum Identifiable Odour	9
1.3.3	Methods of Measuring the Odour Level	11
1.3.4	The Odour Panel	11
1.3.5	Odorometers and Odour Measurement Techniques	12

1.4	Hydrogen Sulphide and Ethyl Mercaptan and Their Odours	13
1.4.1	Occurrence	13
1.4.2	Environmental Dangers	14
1.4.3	Odour Threshold and Minimum Identifiable Odour Values for Hydrogen Sulphide and Ethyl Mercaptan	16

## Chapter 2.

### Development of a Fluorometric Method for the Determination of Hydrogen Sulphide and Ethyl Mercaptan in Air.

2.1	Review of Available Methods for the Measurement of Low Concentrations of Hydrogen Sulphide in Air	22
2.1.1	Test Requirements	24
2.2	Method Selected for Trial	24
2.2.1	Reagents	25
2.2.2	Sample Stream Gas Absorber	25
2.2.3	Fluorescence Measurement	25
2.3	Details of the Analytical Procedure for H <sub>2</sub> S Concentration Measurement	27
2.3.1	Preparation and Storage of Reagent Solutions	27
2.3.2	Calibration of the Reagent Solution	27
2.3.3	Preparation and Standardisation of Solutions	28



2.3.4	Determination of the H <sub>2</sub> S Equivalent of the Stock Sulphide Solutions	29
2.3.5	Preparation of Calibration Curves for the Fluorescent Reagent	30
2.3.6	The Test Procedure for the Measurement of H <sub>2</sub> S in Air	30
2.4	A Check on the Stability of the Crystalline Reagent and the Reagent Solution.	33
2.4.1	Effect of Light on the Reagent Solution.	33
2.4.2	Resistance of the Reagent Solution to Degradation with Age	34
2.4.3	Resistance of the Solution to Degradation by Air	42
2.4.4	The Reacted Solution Stability	42
2.4.5	The effect of temperature on the Stability of the Reagent Solution	42
2.4.6	Crystalline reagent Storage Conditions	43
2.4.7	Reproducibility of the Calibration Curves	44
2.5	An overall check on the Reliability of this method of H <sub>2</sub> S Measurement	44
2.5.1	Measurement of the H <sub>2</sub> S Purity	47
2.5.2	Experimental Apparatus	47
2.5.3	Experimental Method	49
2.5.4	Calculations	51

2.5.5	Results and Conclusions	52
2.6	Comparison of the Reagents FMA and TMF for H <sub>2</sub> S Measurement	52
2.7	Analysis of Low Concentrations of Ethyl Mercaptan in Air	53
2.7.1	Assessment of TMF and FMA as Reagents for C <sub>2</sub> H <sub>5</sub> SH Measurement	54
2.8	Detailed Analytical Procedure for C <sub>2</sub> H <sub>5</sub> SH Concentration Measurement using TMF Solutions	54
2.8.1	Examination of Suitable Solvents for the Calibrating Solution	55
2.8.2	Calibration of the Reagent Solution	55
2.8.3	Determination of the C <sub>2</sub> H <sub>5</sub> SH Content of the Stock Solution	56
2.8.4	Preparation of Calibration Curves	57
2.9	Stability of the Data	58
2.10	The Test Procedure for C <sub>2</sub> H <sub>5</sub> SH Analysis	60
2.11	An Overall Check on the Reliability of the Fluorometric Method of C <sub>2</sub> H <sub>5</sub> SH Measurement	61
2.11.1	Experimental Apparatus	61
2.11.2	Experimental Procedure	62
2.11.3	Calculations	62
2.11.4	Results and Conclusions Regarding the Reliability of the Method	64
2.12	Discussion of Results and Conclusions	65

Chapter 3.  
The Use of Potassium Permanganate  
and Associated Compounds  
for Deodorization.

3.1	Introduction	68
3.1.1	Optimum Solution pH	70
3.1.2	Experimental Program	71
3.2	Experimental Apparatus	71
3.2.1	The Air Scrubbing Train	72
3.2.2	The Hydrogen Sulphide Injection System, Reaction Vessel and Ancillary Equipment	74
3.2.3	The Ethyl Mercaptan Injection System	80
3.2.4	pH Measurement	82
3.3	Chemicals	82
3.3.1	Hydrogen Sulphide Storage System	83
3.4	Experimental Procedures	85
3.4.1	Adjustment of the Internal Gas Pressures	85
3.4.2	The Test Solution	85
3.4.3	Procedure During Gas Bubbling Runs	86
3.4.4	Normal Runs	86
3.4.5	Extended Runs	88
3.4.6	Measurement of the Gas Stream Pollutant Concentration	88
3.5	Odour Measurement	89

3.6	Calculations	90
3.7	Discussion of Results and Conclusions	90

#### Chapter 4.

##### The Reaction of Hydrogen Sulphide and Ethyl Mercaptan with Potassium Permanganate in the Presence of Air.

4.1	Introduction	99
4.2	The Reaction of $\text{H}_2\text{S}$ with $\text{KMnO}_4$	100
4.2.1	The Relevant Solid Phases of Manganese	100
4.2.2	Discussion	103
4.3	The Stability Field Diagram	103
4.3.1	The Reaction of $\text{H}_2\text{S}$ with Aqueous $\text{KMnO}_4$ in the Presence of Air	104
4.4	Examination of the Reaction Products from the $\text{H}_2\text{S}$ - $\text{KMnO}_4$ Reaction	109
4.4.1	Preparation and Examination of the Product	109
4.4.2	X-Ray Diffraction Evidence	110
4.4.3	The Probable Reaction Path	111
4.5	The Oxidation of Ethyl Mercaptan in Alkaline $\text{KMnO}_4$ Solution.	112
4.5.1	Examination of Reaction Products	112

#### Chapter 5.

##### Mass Transfer Measurements

5.1	Fundamentals of Gas Absorption	115
5.2	Mass and Heat Transfer to Fluids and Gases in Laminar Flow	118

5.2.1	Previous Experimental Results	121
5.3	The Wetted Wall Column as an Experimental Unit	125
5.3.1	The Short Wetted Wall Column	126
5.4	Film Flow	126
5.4.1	The Regimes of Film Flow	126
5.4.2	Analysis of Film Flow	127
5.4.3	Wave Inception and Suppression in the Laminar Film	129
5.4.4	A Critical Examination of Film Flow in the Short Wetted Wall Column	131
5.5	The Diffusion Coefficients	132
5.5.1	The Diffusivity of $H_2S$ in Air and $C_2H_5SH$ in Air	133
5.5.2	The Diffusivity of $CO_2$ in Water	133
5.6	Experimental Apparatus	133
5.6.1	Experimental Apparatus for the Examination of the Absorption of $H_2S$ and $C_2H_5SH$ into Alkaline Solutions	134
5.6.1.1	The Wetted Wall Column and Ancillary Equipment	137
5.6.1.2	Liquid Streams Around the Column	144
5.6.2	Experimental Apparatus for Examination of the Desorption of $CO_2$ from Water	146
5.7	The Desorption of $CO_2$ from Water	148
5.7.1	Theory	158
5.7.2	Experimental Procedure	149

5.7.3	Calculations and Results	151
5.7.4	Discussion of Results	152
5.8	Mass Transfer from a Gas in Laminar Flow	157
5.8.1	Experimental Apparatus	158
5.8.2	Experimental Procedure	158
5.8.3	Calculation of Results	161
5.8.4	Discussion of Results	161

## Chapter 6.

<u>Recommendations and Conclusions.</u>	167
---	-----

<u>Appendix A</u>	Experimental and Calculated Results for Chapter 2.	172
<u>Appendix B</u>	Experimental and Calculated Results for Chapter 3.	192
<u>Appendix C</u>	Experimental and Calculated Results for Chapter 4.	220
<u>Appendix D</u>	Experimental and Calculated Results for Chapter 5.	227
<u>Appendix E</u>	Sample Calculations	238
<u>Appendix F</u>	References	247
<u>Appendix G</u>	Published Papers	257

# LIST OF FIGURES

FIGURE 2.1	Sample Stream Absorption Vessel	26
FIGURE 2.2	Calibration Curves, 0.00025% FMA, Showing the Effect of Crystalline Reagent Storage Conditions	31
FIGURE 2.3	Calibration Curves, 0.00025% FMA Solution No. FMA 25/1	35
FIGURE 2.4	Calibration Curves, 0.00025% FMA Solution No. FMA 25/7	36
FIGURE 2.5	Calibration Curves, Reagent Test Solutions No. FMA 75/1 to FMA 75/3	37
FIGURE 2.6	Calibration Curves, 0.00075% FMA Solution, Showing Effect of Reagent Solution Age	38
FIGURE 2.7	Calibration Curves, 0.00075% FMA, Showing Curves Prepared 105 Days Apart	39
FIGURE 2.8	Calibration Curves, 0.012% TMF Reagent Test Solution No. TMF 120/1	40
FIGURE 2.9	Calibration Curves, 0.012% TMF Reagent Test Solutions No. TMF 120/2 and TMF 120/3	41
FIGURE 2.10	Calibration Curve, 0.012% TMF Reagent Test Solution No. TMF 120/4	45
FIGURE 2.11	Calibration Curves, 0.012% TMF Reagent Test Solution No. TMF 120/9	46
FIGURE 2.12	Apparatus for the Production and Measurement of Air Streams Containing Known Concentrations of H <sub>2</sub> S	48
FIGURE 2.13	Calibration Curve, 0.012% TMF, Ethyl Mercaptan Measurement	59
FIGURE 3.1	Air Scrubbing Train	73
FIGURE 3.2	Reaction Vessel and Ancillary Equipment	75
FIGURE 3.3	Hydrogen Sulphide Injection System	76
FIGURE 3.4	Details, Absorption-Reaction Vessel	79

FIGURE 3.5	Mercaptan Injection System	81
FIGURE 3.6	Hydrogen Sulphide Storage System	84
FIGURE 3.7	Variation of the Outlet Hydrogen Sulphide Concentration with Time (Run 3.19)	93
FIGURE 3.8	Ethyl Mercaptan Absorption, Runs No. 3.35 and 3.36	96
FIGURE 4.1	Stability Field Diagram for Manganese Species at 25°C	105
FIGURE 4.2	Stability Field Diagram for the System Shown in Figure 4.1 in the Presence of CO <sub>2</sub>	106
FIGURE 4.3	Stability Field Diagram for the System S-H <sub>2</sub> O	107
FIGURE 5.1	Theoretical Curves, Mass Transfer to Fluids and Gases in Streamline Flow	122
FIGURE 5.2	Flowsheet, Odour Injection and Measuring System	135
FIGURE 5.3	Photograph, Showing the Apparatus Used for Gas Absorption and Desorption Measurements	136
FIGURE 5.4	Flowsheet, Showing the Gas and Liquid Streams Around the Column	138
FIGURE 5.5	Photograph of the Tower Section	139
FIGURE 5.6	Details of Wetted Wall Column	142
FIGURE 5.7	Assembly, Wetted Wall Column	143
FIGURE 5.8	Gas and Liquid Streams - CO <sub>2</sub> Desorption Experiments	147
FIGURE 5.9	Experimental Results - Desorption of CO <sub>2</sub> from Water	153
FIGURE 5.10	Comparison of Experimental and Theoretical Data - Desorption of CO <sub>2</sub> from Water	154



FIGURE 5.11	Comparison of Experimental Results with Theory - Absorption of $C_2H_5SH$ from Air Streams in Laminar Flow	162
FIGURE 5.12	Comparison of Experimental Data with Theory - Absorption of $H_2S$ from Air Streams in Laminar Flow	163

NOMENCLATURE.

$A$	Interfacial area
$a$	Multiplier (see eq.5.25)
$a_{ox}$	Activity of products
$a_{red}$	Activity of reactants
$c$	Specific heat
$C_1, C_2$	Concentration of reactive component in inlet and outlet liquid streams
$C_a, C_{ai}$	Concentration of component A in the bulk liquid stream and at the interface respectively
$C_a^*$	Concentration of component A in the liquid phase in equilibrium with $P_a$
$D$	Diameter
$D_L, D_V$	Diffusion coefficients in the liquid and gas phases respectively
$E_h$	Oxidation potential
$E^0$	Reaction voltage
$f$	Faraday constant
$\Delta F^0$	Standard free energy change
$g$	Acceleration due to gravity
GMV	Volume registered by gas meter
$K$	Equilibrium constant
$k_G, k_L$	Gas and liquid phase mass transfer coefficients
$K_G, K_L$	Overall gas and liquid phase mass transfer coefficients
$L$	Column length

$m$	Defined by equation 5.16
$n$	Number of electrons involved
$N_A$	Transfer rate
$P$	Total internal pressure
$P_A$	Vapour pressure of $C_2H_5SH$
$P_{a1}, P_{a2}$	Partial pressure of component A in the inlet and outlet streams respectively
$P_a, P_{ai}$	Partial pressure of component A in the bulk gas stream and at the interface respectively
$P_a^*$	Partial pressure of component A in the gas phase in equilibrium with $C_a$
$Q$	Volumetric flowrate
$R$	Universal gas constant
$R$	Radius (eq. 5.25)
$R''$	Stoichiometric ratio
$r$	Radial distance
RPM	Gear train input shaft speed
$Re_i$	Critical film Reynolds Number
$Re'$	Film Reynolds Number
$Re$	Reynolds Number
$S$	Rate of surface renewal
$Sc$	Schmidt number
$S_d$	Standard deviation
STI, STO	Sample times, inlet and outlet streams respectively
$T$	Temperature

$t$	Time
$t'$	"t" statistic
$t_e$	Time of exposure
$T_m$	Time occupied by run
$T_W$	Wall Temperature
$T_1, T_2$	Temperature of inlet and outlet streams respectively
$T_r$	Time from start of run
$T_a$	Absolute temperature
$u$	Velocity
$v$	Film velocity
$\bar{v}$	Average film velocity
$V_s$	Syringe volume per unit length
$v_r, v_\theta, v_z$	Velocity components
$W$	Liquor flowrate
$W'$	Width of the two dimensional system
$W_{TI}, W_{TO}$	Weight of $H_2S$ or $C_2H_5SH$ in reagent solution
$x$	Distance from wall into the film
$X$	The reagent solution mercaptan (or $H_2S$ ) content
$x_F$	Thickness of the Whitman film
$Y$	Photofluorometer reading
$Y_a$	Mole fraction of $C_2H_5SH$
$z$	Rectangular co-ordinate
$n$	n th. root of a Bessel Function (see eq. 5.13)
$\Gamma$	Mass flowrate of liquid per unit perimeter

$\delta$	Film thickness
$\epsilon$	Defined by eq. 5.30
$u_y$	Mean value of Y
$\mu$	Viscosity
$\rho$	Density
$\theta$	Slope of two dimensional system
$\phi$	Defined by eq. 5.15

CHAPTER 1.

ODOURS AND DEODORIZATION

WITH SPECIAL REFERENCE

TO

HYDROGEN SULPHIDE AND ETHYL

MERCAPTAN.

## 1.1 Introduction.

Of recent years, public concern at the dangers associated with environmental pollution has manifested itself in an increase in the severity of the relevant legislation, often with limits being set on the allowable levels of pollutants discharged to the environment.

Odours are a form of environmental pollution which generally lead to bitter complaints from all within the vicinity of the discharge. Whilst odour is not the direct cause of organic disease, as was believed last century (19), some odorous gases are toxic. The dangers associated with indiscriminant discharge of gaseous waste products, particularly from industrial sources, have been amply demonstrated on a number of occasions, where suitable climatic conditions and heavy gaseous emissions have led to disasters in which numerous deaths have been recorded (18) (32).

### 1.1.1 Odours and Odour Theories

Many insects and fish rely on a highly specific and very sensitive olfactory mechanism to guide them in their search for food, a mate, a suitable ovipository site or to warn them of danger, (20) (21). Thus, for example, both the homing instinct and the alarm reaction evident in the migratory salmon have been shown to be a function of odour detection and recognition. As little as one part of 1-serine,  $C_3H_5O(OH)_2N$  in  $8 \times 10^{10}$  parts of water is sufficient to evoke the latter

phenomenon (18) (20).

The sense of smell in man is classified as a distance receptor (22) and is distinctive insofar as the perception of odours requires the incorporation of a particle of the external environment into the organism.

However, without a knowledge of the interpretative ability of the sensory receiving section of the brain of creatures using olfactory mechanisms, an odour can only be defined in terms of man's own perception. Thus an odour can be thought of as being the interpretation of a specialised stimulation occurring in some, or all, osmoceptor cells. Despite continuing intense research, no universally accepted theory describing odours and odour perception has been devised. This has handicapped researchers attempting to build instruments capable of direct odour measurement, and, although some success has been claimed (26), it is generally accepted (12)(25) that the replacement of the human observer as the means of odour evaluation is still far in the future.

MONCRIEFF (27) in 1951 listed 24 theories of odour. AMERINE et al (23) have indicated that the theories that have been proposed to date depend on such recognizable properties as adsorption on the olfactory membrane, molecular shape, cohesive energy density, surface tension and certain chemical properties. Some, they found, involved the concept of infra-red absorption whilst others were related to the molecular vibration, and the corresponding Raman Effect. Delocalised



II-electrons have also been proposed by SHAH et al (24) as being related to the odour characteristics of a molecule.

Two theories are of particular interest at present, the Amoore Stereochemical theory and Wright's Molecular Vibration theory. Both are under constant review. The former theory (28)(29) attempts to correlate the odour quality of a compound with the physical fit of its molecules into certain receptor sites at the olfactory nerve endings. WRIGHT (20) based his theory on the relationship between the low frequency vibrations of the molecule of a chemical compound and its odour.

#### 1.1.2 The Odour Problem

While odours may arise from both industrial and natural sources, by far the most widespread and difficult to control are those from the former. Where the emissions are malodorous, complaints from nearby residents generally force the development of odour abatement methods.

It is difficult to assign a greater share of odour problem responsibility to any one family of chemicals more than another. However, the sulphidic compounds, generally, are very representative of this overall problem. They are, mostly, extremely malodorous, and have some of the lowest reported odour thresholds. In addition their production, both naturally and industrially, is widespread and, usually, the odour nuisance thus produced is very difficult to eliminate.

## 1.2 Methods of Deodorization of Vapours and Gases.

There are literally scores of methods of deodorization. However, broadly, they may be divided into non-specific methods which remove a wide spectrum of odours, and specific methods which are geared to the nature of the odorous gas.

### 1.2.1 General Methods of Deodorization.

For general odour elimination there is perhaps no better method than that of high temperature oxidation (57). While this method is often used directly, the required oxidation temperature may be greatly reduced by the use of a suitable catalyst.

When the concentrations of the odorous constituents are low, and the gas flow rates relatively small, it is often possible to economically remove the odours by adsorption on activated carbon (61). This system involves low capital investment, and is capable of removing a wide range of contaminants (58)(60). Regeneration of the carbon may be achieved using steam or hot air, either directly, or in the presence of a catalyst (58). However, where the adsorbed contaminants are sulphidic, the regeneration is complicated by the sulphur which can form under certain conditions (73)(79) on the surface and within the pores of the carbon during the adsorption step.

For general deodorization there are many other processes available. Absorption by aqueous chlorine, a method commonly used for the control of general sewage odours, is one such technique (67). Bacteria have also been shown to

be efficient deodorizing agents (62)(63).

Two methods of deodorization which are of little industrial significance are those of "odour masking" and "odour neutralisation". The former method simply relies on the covering of an odour of a melodorous or offensive nature by another, more pleasant odour. The latter method depends on the cancellation of one odour by another. It is, in fact, a highly specific phenomenon, the efficiency being strongly dependent on the choice of the correct neutralising odour and odour concentration.

Potassium permanganate has also been shown to be an effective deodorising agent for a wide range of odours (see section

#### 1.2.2 Specific Methods of Deodorization.

Where the odorous constituents of the gas stream can be identified with certainty, it may be possible to use a specific method of removal. The methods of deodorization mentioned below are specific for  $H_2S$  and certain organic sulphur compounds.

The iron oxide process, a common method of gas stream purification in the gas industry, is one such method. In this process the sulphidic contaminant reacts with a bed of solid ferric oxide yielding a sulphide, the oxide being regenerated by contacting the sulphide with oxygen. Only the and forms of the oxide have been used with any degree of success (64).

Ferric oxide has also been used in the form of a hydrated suspension in an alkaline solution. This use of the oxide is well established in the gas industry, and forms the basis for the Ferrox, Manchester and Gluud purification processes.

There are a large number of chemical compounds which, in aqueous solution, will rapidly absorb  $H_2S$  and certain other sulphidic substances, yielding intermediate compounds which readily decompose in the presence of heat or oxygen to regenerate the reactive absorbent. Alkanolamine solutions, sodium and ammonium thioarsenate solutions and solutions of complex ferric compounds have all been successfully used in this field (66).

Solutions containing alkaline salts, organic oxidation catalysts such as hydroquinone, ammonia, ammonium salts (84), copper sulphate (82) and zinc salts (85) have also been used for  $H_2S$  removal from gaseous streams.

### 1.3 Assessment of the Odour Abatement Method.

The aim of the designer of odour abatement equipment is either to reduce the concentration of the odorous gas below the statutory or other prescribed level where such a level exists, or to produce an effluent gas which will not lead to complaints from nearby residents.

#### 1.3.1 Odour Evaluation.

When assessing odour abatement equipment, or an odour problem, a quantitative measure of the minimum stimulus required

to cause an odour sensation in the human subject is important. The concentration of odorous material in the atmosphere which can just be detected by the human olfactory system is known as the "odour threshold" (O.T.) concentration. When the odour level is such that the odorous material can just be identified, the concentration of material in the atmosphere has reached the "minimum identifiable odour" (M.I.O.) level. SULLIVAN et al (42) have also mentioned an "objectionability threshold" which they define as the minimum concentration of a particular substance which will elicit an unpleasant response from the subject. These thresholds may differ considerably. In fact, it is not unusual to have an O.T. and a M.I.O. concentration differing by a factor of a power of 10.

Once the concentration of odorous material has moved above these levels, a method of odour intensity measurement must be found. KATZ and TALBERT (43) have used the following scale:

0	no odour	3	easily noticeable
1	very faint	4	strong
2	faint	5	very strong

which is, in reality, an opinion scale.

Odour intensity may be expressed quantitatively relative to the odour threshold concentration by using the "odour unit" (44). The odour unit is defined as one cubic foot of air at the odour threshold.

### 1.3.2 Odour Thresholds and the Minimum Identifiable Odour.

There are a number of O.T. and M.I.O. values for single compounds, reported in the literature. Typical values are reported below in Tables 1.1 and 1.2.

Many of the values recorded before the advent of modern analytical tools, such as the gas chromatograph, must be viewed with some suspicion, since even small traces of certain impurities can alter the values considerably.

Reliable sources of O.T. and M.I.O. values must record the type of test instrument and method used, the composition, experience and other relevant details of the odour panels and the purity of the materials under test. The remarkable discrepancies to be found in the values reported in the literature cannot be completely attributed to differences in the olfactory properties of the testing personnel. A number of other reasons have been suggested;

- a) M.I.O. values reported as O.T. values or vice versa,
- b) the use of impure test chemicals and gases,
- c) incorrect re-reporting of previously determined values, and
- d) direct mathematical errors.

Throughout the literature there are numerous examples of each of these. SUMMER (18) for instance, has

reported the M.I.O. value for  $\text{H}_2\text{S}$  given by McCORD and WITHERIDGE (19) as a minimum stimulus (O.T.) value. Again, as indicated by JONES (46), the threshold values given in the International Critical Tables (47) were calculated using an incorrect conversion factor. Although the tables were published in 1926, it was not until 1953 that he drew attention to this error, which when corrected, altered threshold values by a factor of 100.

The Manufacturing Chemists' Association, disillusioned by the apparent lack of agreement in reported O.T. and M.I.O. values, has instigated an experimental determination of a comprehensive list of threshold data. LEONARDOS et al. (40) has listed M.I.O. values for 53 chemicals determined under this authorisation.

The degree of compounding of errors in the reported threshold values may be more easily observed by reference to the following example. The O.T. value for  $\text{H}_2\text{S}$  is given by SUMMER (18) as 0.0011 mg/l. These authors have, in turn, taken the value from DALLAVALLE and DUDLEY (48), who do not define the source of their data. However, they appear to have taken the number 2 intensity of KATZ and TALBERT (43). When we consider the fact that the latter experimenters used a crude  $\text{H}_2\text{S}$  for their determinations, together with the fact that there are, by definition, distinct differences between the No. 2 intensity of Katz and Talbert and the "just noticeable odour" of Dallavalle and Dudley, then the reliability of the value is even more doubtful.

### 1.3.3 Methods of Measuring the Odour Level.

Where the odour is due to a pure constituent for which an accurate odour threshold concentration value (or M.I.O. value,) is available, then chemical assessment of an odour level may be possible. Generally however, the odour is due to a combination of odorous gases and a quantitative measure of odour is required. With no reliable instrument available for such a measurement the procedure for measurement must necessarily depend on the notoriously variable human olfactory system. Values thus derived can vary considerably, not only due to observer differences, but also because of such factors as humidity variations, variation in the method of presentation of the test gas, and choice of olfactometer or test method. Individual differences between observers are also common.

### 1.3.4 The Odour Panel

For accurate odour evaluation a panel of observers is required. PRINCE and INCE (36) and WITTES and TURK (35) have suggested that the panel members be carefully selected and trained to improve their reliability. Observer panels have been developed for evaluation of odour levels using both the syringe dilution technique (37)(39), and the dynamic dilution technique (38)(40). The variability of threshold values determined by a panel has been analysed in detail (36) (38).

STERN (12) has suggested that the initial screening



of panel members be carried out on the basis of their eating habits, the "fussy" eater being the best choice. Final screening of panel members is carried out on the basis of their odour acuity. He considers that a three membered panel, chosen in this way, should suffice. MILLS et al (39) believe that odour panels should contain at least eight persons, while LEONARDOS et al (40) used a panel of four trained members in their odour threshold determinations for the Manufacturing Chemists' Association.

When evaluating the results obtained from an odour panel, one has to decide how many of the panel must elicit a consistently positive response before the odour concentration is accepted as the O.T., or M.I.O, whichever the case may be. STERN (12) prefers to use the concentration corresponding to a consistently positive answer from only one member of the panel, while LEONARDOS et al (40) use the concentration corresponding to consistently positive answers from all members of the panel. SULLIVAN et al (42) suggest that the concentration used should be that corresponding to a positive answer from 50% of the panel members.

#### 1.3.5 Odorometers and Odour Measurement Techniques.

For test purposes odours of known concentrations are generated by either a static or a dynamic method. The latter system is superior insofar as it is not subject to surface adsorption phenomena and is thus the method used by most investigators requiring O.T. or M.I.O. values for pure

compounds in air. Nevertheless certain static methods afford a simple and rapid means of measuring thresholds.

An odorometer constructed using the dynamic method for odorising air streams can be made to nearly approach actual conditions by a correctly designed presentation method. Thus those odorometers which directly inject the odour-air mixtures into the nostrils (50) are inferior in this respect, whilst those which bring the mixtures into contact with the whole head (49), or especially, the whole body (40) are superior.

The American Society for Testing and Materials (A.S.T.M.) has based its standard method for the measurement of odour in the atmosphere (44) on a static dilution system. The procedure requires that a sample of the atmosphere or gas under test be diluted with odour free air until a dilution is achieved in which the odour can be barely perceived by the human olfactory system. The evaluation of the odour is carried out by direct injection into the subjects' nostril while he is in odour free surroundings.

#### 1.4 Hydrogen Sulphide and Ethyl Mercaptan and Their Odours.

Both of these gases are widespread in industry, are relatively hard to remove from industrial effluent gas, and have objectionable odours and low odour threshold concentrations.

##### 1.4.1 Occurrence.

Both can occur through leakages from petroleum refineries, wood pulp treatment plants where the kraft process is used, and phosphoric and sulphuric acid manufacturing

plants (30). Hydrogen sulphide is also one of the constituents of the odorous gases evolved during the putrefaction of food processing wastes.

Both gases are also present in sewer atmospheres. In these circumstances  $H_2S$  is particularly annoying since it is both dangerous to workmen in the sewers, and is one of the main agents in sewer corrosion.

#### 1.4.2 Environmental Dangers.

##### Hydrogen Sulphide.

Hydrogen sulphide is an extremely toxic gas, 600 ppm proving fatal within 30 minutes (33). The malodorous nature of the gas may give ample warning of its presence, but olfactory adaption or fatigue (18)(23), wherein there is a loss of the olfactory faculty under continuous odour stimulation, can lead to a person unknowingly remaining within an area containing a toxic concentration.

In industrial surroundings even low concentrations of  $H_2S$  can have a detrimental effect on copper and silver electrical contacts (32), the resultant sulphide coating leading to an increase in contact resistance and fusing. LYNN and ELSEY (86) consider that  $H_2S$  is a controlling cause of poor electric motor commutation and brush life.

Most countries have standards which limit the allowable atmospheric concentration of toxic substances to which people may be exposed either continuously or intermittently. Broadly they can be divided into two classes,

"air quality standards" which are for continual exposure of all living and non-living things, and "threshold limit values" which are for 8 hour day, 5 days per week exposure of healthy adult workers.

For  $H_2S$  the air quality standard values vary between 0.005 ppm by volume in the U.S.S.R. with a 20 minute averaging time to 0.1 ppm in the Federal Republic of Germany with a 30 minute averaging time (30). The American Conference of Governmental Industrial Hygienists (34) gives the 1968 threshold limit value as 10 ppm by volume.

Ethyl Mercaptan.

Ethyl mercaptan is listed by SAX (41) as being a moderately dangerous irritant which should not be ingested or inhaled to excess. The A.C.G.I.H. (34) sets the ceiling threshold limit value at 10 ppm by volume.

This vapour is particularly dangerous when heated to decomposition or when brought into contact with acids or acid fumes, since, under these circumstances it can emit toxic fumes of oxides of sulphur.

#### 1.4.3 Odour Threshold and Minimum Identifiable Odour Values for Hydrogen Sulphide and Ethyl Mercaptan.

A number of OT and MIO values for the above compounds have been reported in the literature. These are summarised in Tables 1.1 and 1.2. However, these have not been determined under exactly similar conditions and are thus not strictly comparable, a fact which LAFFORT (55), who summarised and averaged some early values of a large number of odorous compounds, failed to comprehend. Since there is no standard accurate method for the measurement of these values it is purely a matter of personal preference. It would appear that the best method would combine a dynamic system with a presentation method involving either whole body or whole face immersion, and a trained odour panel. The MIO determinations of LEONARDOS et al (40) appear to follow this criteria.

TABLE 1.1  
Hydrogen Sulphide, Odour Threshold and  
Minimum Identifiable Odour Values From  
Various Literature Sources.

VALUE (ppm by vol).	TYPE	REFERENCES	ORIGINAL REF.	YEAR OF DETERMINATION	PURITY	METHOD
0.0047	MIO	(40)	(40)	1969	PREPARED FROM Na <sub>2</sub> S (PROBABLY 95%)	DYNAMIC: Whole body presentation; 100% acceptance by trained panel.
0.00047	MIO	(40)	(40)	1969	TAKEN FROM CYLINDER (PROBABLY 99.6%)	"
0.0045	MIO	(38)	(38)	1969	N.A. **	DYNAMIC: facial presentation, Mean value of un- trained panel.
0.007	OT	(51)	(51)	1966	"pure"	DYNAMIC: facial presentation; acceptance by 50% of panel; compari- son with pure air.

TABLE 1.1 (Cont).

RANGE 0.0086-0.022	OT	(52)	(52)	1962	N.A.	DYNAMIC; facial presentation; com- parison with pure air.
0.025	OT	(83)	(83)	1943	"	N.A.
0.13	OT	(56) (43)	(43)	1930	Crude	DYNAMIC:Head mask or hood presentation.
0.8	APPROX. MIO	(18) (19) (48)	<u>PROBABLY</u> * (43)	1930 *	Crude	"
BEST PROBABLE OT VALUE : 0.007 ppm						
BEST PROBABLE MIO VALUE : 0.0047 ppm						
(H <sub>2</sub> S Prepared from Na <sub>2</sub> S)						
BEST PROBABLE MIO VALUE : 0.00047 ppm						
(H <sub>2</sub> S from Cylinder)						

\* See Section 1.3.2

\*\* Not given.

TABLE 1.2  
Ethyl Mercaptan; Odour Threshold and Minimum  
Identifiable Odour Values From  
Various Literature Sources

VALUE (ppm by vol.)	TYPE	REFERENCES	ORIGINAL REF.	YEAR OF DETERMINATION	PURITY	METHOD
0.001	MIO	(40)	(40)	1969	N.A. **	DYNAMIC: Whole body presentation; 100% acceptance by trained panel.
0.004	MIO	(38)	(38)	1969	"	DYNAMIC: facial presentation; mean value of untrained panel.
0.002	OT	(83)	(83)	1943	"	N.A.
0.00026 0.00097 0.0030 (AV.0.0014)	OT	(43)	(43)	1930	"pure"	DYNAMIC: head mask or hood presentation.
0.075	APPROX. MIO	(19) (48)	(43) *	<u>PROBABLY</u> 1930 *	"pure"	"



TABLE 1.2 (Cont.)

18	OT	(53)	(53)	1919	N.A.	DYNAMIC: facial presentation.
0.000016	OT	(18) (27) (54)	(54)	1886	"	Static
BEST PROBABLE OT VALUE				:	0.001 ppm	
BEST PROBABLE MIO VALUE				:	0.001 ppm	

\* See Section 1.3.2

\*\* Not given.

CHAPTER 2.

DEVELOPMENT OF A FLUOROMETRIC METHOD FOR  
THE DETERMINATION OF HYDROGEN SULPHIDE AND  
ETHYL MERCAPTAN IN AIR.

## 2.1 Review of Available Methods for The Measurement of Low Concentrations of Hydrogen Sulphide in Air.

There are a number of accurate methods of analysis available which are capable of measuring very low concentrations of  $H_2S$  in air streams. JACOBS (1) and SMITH et al (3) have summarised and critically compared the more successful of these.

One of the most popular methods, which has been widely used for measuring  $H_2S$  concentrations in sewerage (8), gas (4) and air (1)(2), is the colorimetric "Methylene Blue" method. Generally, when using this process to determine the  $H_2S$  content of air streams, the sulphide is trapped in an alkaline suspension of cadmium hydroxide, although cadmium chloride, cadmium acetate and zinc compounds have all been used (1)(4). The colour which develops in this solution after addition of p-aminodimethylaniline, ferric ion and acid, is then measured after a standard time interval and compared with previously determined calibration curves.

Where the  $H_2S$  concentration is very low, the reagent exposure time could range up to about 30 minutes. While this, in itself, is a disadvantage, the formation of light-sensitive sulphide during the reaction (6) must <sup>also</sup> be considered. This latter phenomenon can cause up to a ten-fold variation in results, depending on whether or not the absorber is shielded from light.

There are a number of other analytical methods which are used for determining low concentrations of  $H_2S$  in air. In the Lead Acetate method, the gaseous sulphide is allowed to react with a lead acetate impregnated surface to produce a dark stain of  $PbS$  (8). Comparison of the density of this stain with a range of standard stains leads to a good estimate of the  $H_2S$  concentration. A similar method, which uses silver nitrate as the reagent, has also been described (3).

The gas chromatograph, a useful instrument for general gas analysis, is somewhat limited in the field of gaseous pollutant measurement. Even when suitable columns are employed (9)(10)(11), direct measurement of the relatively low concentrations of pollutants encountered in this field is difficult.

In the case of  $H_2S$ , probably the most accurate of these methods has been developed by WALTER and AMBERG (98), who used the gas chromatograph to measure  $H_2S$  concentrations as low as 0.1 ppm.

WRONSKI (13)(14) has described a titrimetric procedure for the determination of sulphides and mercaptans using a fluorescent indicator consisting of tetra-acetoxymercurofluorescein (TMF),  $C_{20}H_8O_5$  ( $HgOOC.CH_3$ )<sub>4</sub>, dissolved in 0.01N NaOH. The procedure is based on the ability of the sulphidic compound to reduce (quench) the fluorescence of the TMF solution. ANDREW and NICHOLS (17) have described an instrument

in which almost instantaneous measurement of  $\text{H}_2\text{S}$  concentrations as low as  $5 \times 10^4$  ppm by volume, is achieved by use of this principle.

Since the reagent, TMF was not available commercially; it was prepared in accordance with the method described by WHITE (15). A commercially available compound, fluorescein mercuric acetate (FMA),  $\text{C}_{20}\text{H}_{10}\text{O}_5 (\text{HgOOC}.\text{CH}_3)_2$ , has been used by KARUSH et al (16) as a very sensitive test reagent for disulphide groups in proteins and peptides. Although it was found that the FMA appeared to undergo slow degradation in  $\text{NaOH}$ , as indicated by a decline of fluorescence, (this being accelerated by exposure to daylight) a  $10^{-4}$  molar solution in  $0.01\text{N}$   $\text{NaOH}$ , stored in the dark, showed no detectable degradation after several weeks. The reagent solution also appeared to be fairly stable to elevated temperature.

#### 2.1.1 Test Requirements.

It was required that the method of analysis chosen for the measurement of  $\text{H}_2\text{S}$  and  $\text{C}_2\text{H}_5\text{SH}$  throughout this work should be,

- a) easy to apply, yet accurate;
- b) substantially unaffected by the presence of air in the gaseous mixtures under test; and
- c) suitable for measuring  $\text{H}_2\text{S}$  and  $\text{C}_2\text{H}_5\text{SH}$  concentration levels from about 0.05 to 200 ppm by volume, in relatively short time intervals.

#### 2.2 Method Selected for Trial.

From the foregoing it was concluded that while there were

a number of well tried analytical methods which could be adapted to suit these test requirements, it appeared that methods of analysis based on the fluorescent indicators, TMF and FMA could prove more suitable.

The following trials were thus initiated

#### 2.2.1 Reagents.

The reagent, fluorescein mercuric acetate,  $C_{20}H_{10}O_5 (HgOOC.CH_3)_2$ , (FMA), mol.wt. 849.6, was a crystalline powder product of the Sigma Chemical Co. of U.S.A.

The tetra-acetoxymercuri-fluorescein (TMF)  $C_{20}H_8O_5 (HgOOC.CH_3)_4$ , mol.wt. 1366.9, was prepared in accordance with the method of WHITE (15) and purified following the instructions of WRONSKI (14).

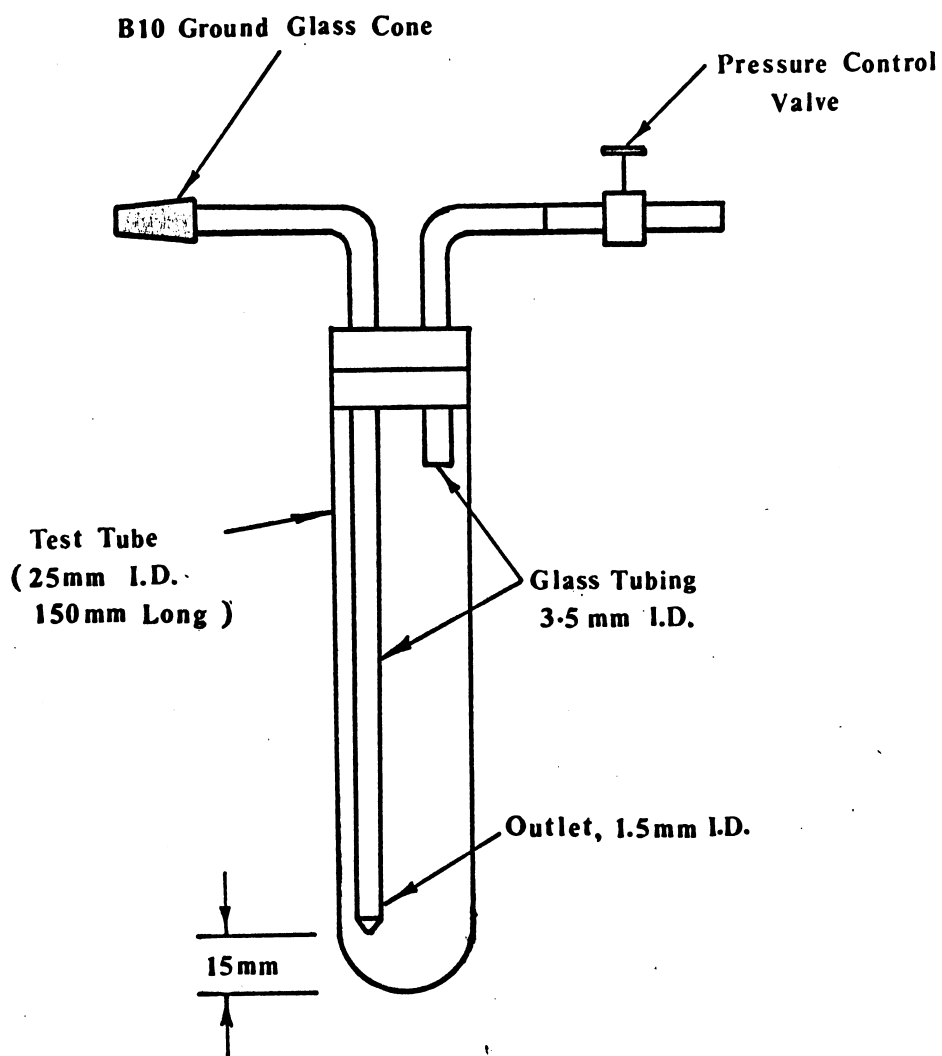
#### 2.2.2 Sample Stream Gas Absorber.

Absorption of the  $H_2S$  from the sample air stream by the fluorescent reagent solution was achieved using a simple absorber system based on a test tube of approximately 2.5 cm. I.D. This apparatus is shown in Figure 2.1.

When two such bubblers were used in series it was found that, for all sample stream flowrates used, up to the expected maximum of 1.5 litres/minute, even when the fluorescence of the reagent solution in the first tube had been substantially reduced, the photofluorometer reading for the second tube was not significantly different from the original reading.

#### 2.2.3 Fluorescence Measurement.

Measurement of solution fluorescence was made using

**FIGURE 2.1****SAMPLE STREAM ABSORPTION APPARATUS**

a model 12C electronic photofluorometer (Coleman Instruments Inc. U.S.A.) in conjunction with primary filter number 12-224 (Corning Glass No.5113) and secondary filter number 14-220 (Corning Glass No.2424). The transmission characteristics of these filters are listed in the "Handbook of Chemistry and Physics", 50th. edition, (96). Systematic tests on all the glass colour filters supplied with the instrument by the manufacturer, confirmed the superiority of the above filters for the fluorescence measurements involved in these experiments.

### 2.3 Details of the Analytical Procedure for H<sub>2</sub>S

#### Concentration Measurement.

##### 2.3.1 Preparation and Storage of Reagent Solutions.

Both the FMA and TMF reagent solutions were prepared by dissolving accurately weighed portions of the respective compound in aqueous 0.01N NaOH solutions. Complete solution of the reagent was assured by allowing a minimum of 24 hours between the time of preparation of the mixture and withdrawal of the first test portions.

Generally, the reagent solution was stored in the dark at room temperature. The solid crystalline reagents were stored over silica gel within a refrigerator at a temperature of about 7°C.

##### 2.3.2 Calibration of the Reagent Solution.

The stepwise procedure used for calibration of the reagent solution was as follows;



- (1) Prepare
  - (a) sodium sulphide ( $\text{Na}_2\text{S}$ ) solution
  - (b) 0.01N sodium thiosulphate ( $\text{Na}_2\text{S}_2\text{O}_3$ ) solution
  - (c) 0.01N iodine ( $\text{I}_2$ ) solution, and
  - (d) 0.01N potassium iodate ( $\text{KI}\text{O}_3$ ) solution.
- (2)
  - (a) Standardise the  $\text{Na}_2\text{S}_2\text{O}_3$  solution using the standard  $\text{KI}\text{O}_3$  solution.
  - (b) Standardise the  $\text{I}_2$  solution using the  $\text{Na}_2\text{S}_2\text{O}_3$  solution.
- (3)
  - (a) Determine the  $\text{H}_2\text{S}$  equivalent of the  $\text{Na}_2\text{S}$  solution (STOCK SOLUTION) using the standardised  $\text{Na}_2\text{S}_2\text{O}_3$  and  $\text{I}_2$  solutions.
- (4)
  - (a) Dilute the STOCK SOLUTION as required.
- (5)
  - (a) Prepare calibration curves for the fluorescent reagent solution as detailed below.

### 2.3.3 Preparation and Standardisation of Solutions.

The preparation and standardisation of the  $\text{Na}_2\text{S}_2\text{O}_3$  and  $\text{I}_2$  solutions, and the preparation of the standard  $\text{KI}\text{O}_3$  solutions, were carried out following the methods described by VOGEL (95).

The  $\text{Na}_2\text{S}$  stock solutions were prepared by dissolution of A.R. grade  $\text{Na}_2\text{S} \cdot 9\text{H}_2\text{O}$  crystals in  $\text{NaOH}$  solutions. The method, and the precautions necessary to prevent rapid decomposition of the inherently unstable sulphide, have been well documented (2)(3).

For some tests this solution was diluted further using freshly boiled and cooled distilled water containing about 5g. of A.R. grade NaOH per litre. The approximate  $H_2S$  equivalents of these solutions are shown below in Table 2.1.

TABLE 2.1

Approximate  $H_2S$  (equivalent) Content  
of the Sodium Sulphide  
Stock and Test Solutions.

Stock Solution	300	ug/ml. of solution		
Test Solution I	150	"	"	"
Test Solution II	15	"	"	"

2.3.4 Determination of the  $H_2S$  Equivalent of the Stock  
Sulphide Solutions.

To determine the  $H_2S$  equivalent of the sulphide solutions a method based on that described by TREADWELL and HALL (97) was used. About 7.5 ml of 0.5 N HCl plus 40 ml of 0.01N (standardised)  $I_2$  solution were diluted to 200 ml with distilled water, and 10 ml of the sodium sulphide solution slowly added with continuous mixing. The excess  $I_2$  was then titrated with the previously standardised 0.01N  $Na_2S_2O_3$  solution, using starch as the indicator

The  $H_2S$  equivalent of the stock solution was

given by the equation,

$$\mu\text{gH}_2\text{S equiv./ml.solution} = 1.704 \times 10^3 (40\text{Ni} - \text{Tna.Nna})$$

- - - - 2.1

where Tna = thiosulphate titration of the excess iodine  
and Ni,Nna= the normality of the iodine and thiosulphate  
solutions respectively.

### 2.3.5 Preparation of Calibration Curves for the Fluorescent Reagent.

A number of 25 ml. aliquots of the reagent solution under test were measured out and micro-pipetted quantities of the appropriate sodium sulphide solution added. Where the reagent solution strength was 0.00075% or under, enough distilled water was also added to make the total of the added fluid up to 0.50 ml. To control dilution errors in solutions of strength greater than 0.00075%, no more than 0.45 ml. of Na<sub>2</sub>S solution was added to any one aliquot.

The solutions were then shaken and allowed to stand for between 15 and 45 minutes in a dark place. At the end of this period the fluorescence was measured, and the photofluorometer reading plotted against the weight of H<sub>2</sub>S equivalent added.

Typical calibration curves are shown in Figure 2.2.

### 2.3.6 The Test Procedure for the Measurement of H<sub>2</sub>S in Air

For these experiments, only four different fluorescent solution concentrations were used, the solution chosen for a particular measurement depending on the expected H<sub>2</sub>S content of the air stream (see Table 2.2). The calibration curves for

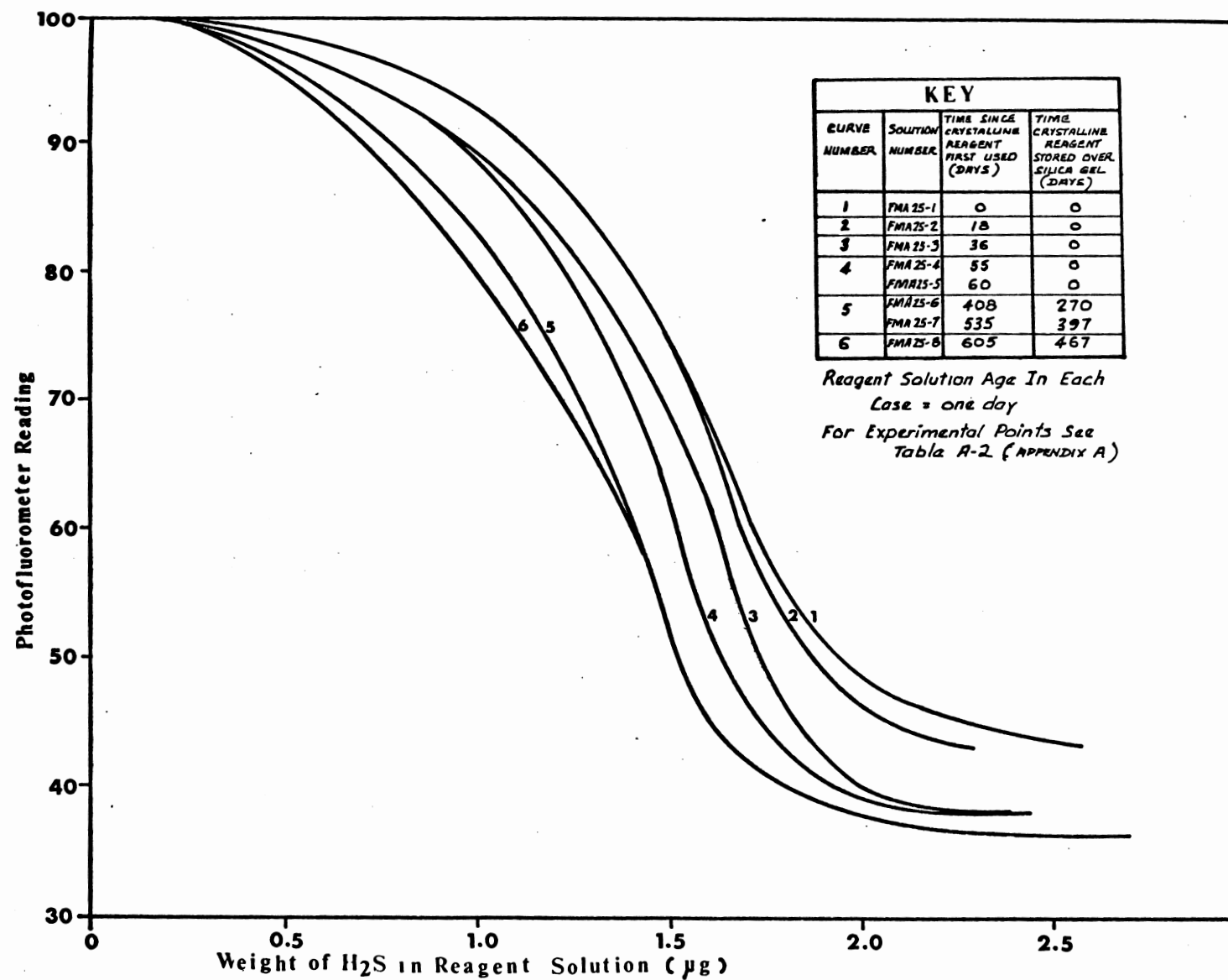


**FIGURE 2.2** CALIBRATION CURVES, 0.00025% FMA, SHOWING THE EFFECT OF CRYSTALLINE REAGENT STORAGE CONDITIONS

these solutions were prepared in the manner described above.

Taking care to expose the fluorescent solution to as little light as practicable, 25 ml. of the solution was pipetted into the absorber and the absorber connected to the apparatus sample offtake point. Where the fluorescent solution strength was 0.00075% or less, 0.50 mls. of distilled water were also added. An accurately measured quantity of the sulphide containing air was then passed through the solution, the absorber finally disconnected, and an appropriate portion of the solution transferred to the photofluorometer cuvette.

Between 15 and 45 minutes after this step the solution fluorescence was measured. Each recorded value was an average of at least three measurements.

From the value thus derived and the calibration curve for the particular fluorescent solution in use, the  $\text{H}_2\text{S}$  content of the air was determined.

TABLE 2.2  
The FMA and TMF Solution Concentrations  
and Their Useful Ranges for  
Hydrogen Sulphide Determination.

Solution Conc.	Ranges of Applicability ( $\mu\text{gH}_2\text{S}$ )	
	Precision $\pm 15\%$ or better	Precision $\pm 1\%$ or better
0.00025% FMA	0.4 - 1.7	1.0 - 1.7
0.00075% FMA	2.0 - 7.0	3.5 - 7.0
0.006% FMA	15 - 60	20.0 - 60.0
0.0120% TMF	7.5 - 70	20.0 - 70.0

## 2.4 A Check on the Stability of the Crystalline Reagent and the Reagent Solution.

In order to assess the stability of the reagent and the reagent solution under various conditions, a number of tests were carried out. These generally involved preparation of calibration curves, the results of which are tabulated in Appendix A.

### 2.4.1 Effect of Light on the Reagent Solution.

In order to quantitatively confirm initial experiments, which indicated that the fluorescent solution was light sensitive, a sample of the solution (No. FMA75/5) was exposed to normal laboratory bench top light while three control samples FMA75/4, FMA75/6 and FMA75/7 were stored in a cupboard. All solutions had been prepared 9 days prior to the commencement of this test.

From the experimental calibration data, which is shown in Table A3/2, Appendix A, it was apparent that exposure to light for a period of 7 days was sufficient to produce a small variation in photofluorometer readings. However, when this variation was examined statistically, by pairing the control sample and test sample data over the full range of the curve, and applying Students' t test, no variation was found at the 95% level of significance.

After 33 days exposure the three control samples still produced distinct calibration curves. However, the fluorescence of the test sample was found to have been destroyed

to such an extent that it was not measurable on the photo-fluorometer.

#### 2.4.2 Resistance of the Reagent Solution to Degradation With Age.

A number of tests were carried out to examine the resistance of the reagent solution to degradation on standing. Initial experiments had indicated that there was a gradual change in the calibration curve over extended storage intervals, even when the solution was stored in a dark place.

In these tests the reagent solutions were stored in a cupboard for periods of up to 51 days after preparation. At various intervals over this period samples were withdrawn and the calibration curves determined. The results are shown in Tables A2, A3 and A4, and;

- (a) Figures 2.3 and 2.4 for 0.00025% FMA solution,
- (b) Figure 2.6 for 0.00075% FMA solution, and
- (c) Figures 2.8 and 2.9 for 0.0120% TMF solution.

From these it is obvious that, under the storage conditions mentioned above, there is no significant change in the calibration data for at least the first 14 days after solution preparation.

However, when storage times exceeded 14-16 days the calibration curves were found to be significantly different from those determined above.

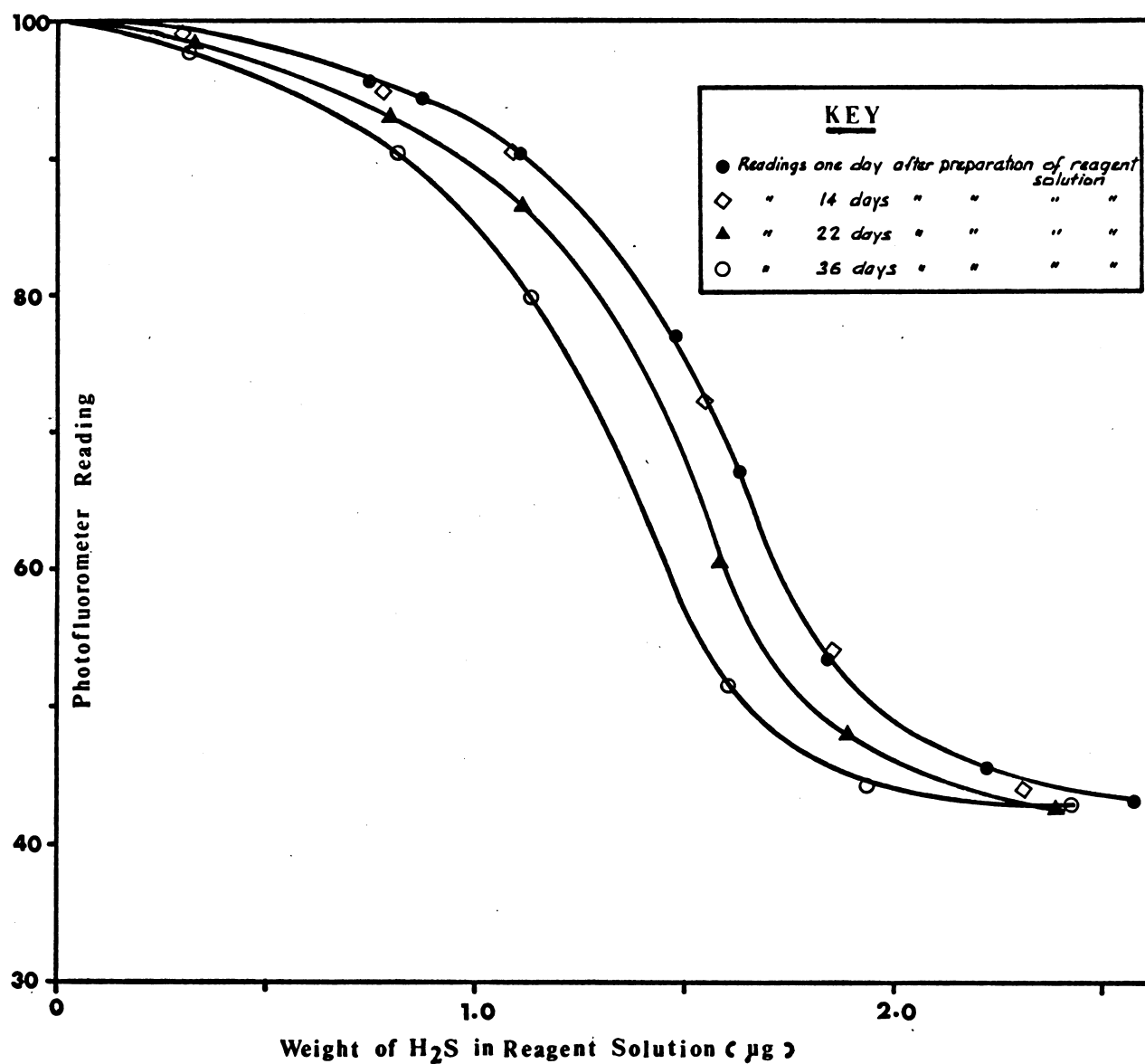


**FIGURE 2.3**  
**CALIBRATION CURVES, 0.00025% FMA SOLUTION N<sup>o</sup> FMA 25/1**  
**SHOWING EFFECT OF REAGENT SOLUTION AGE**



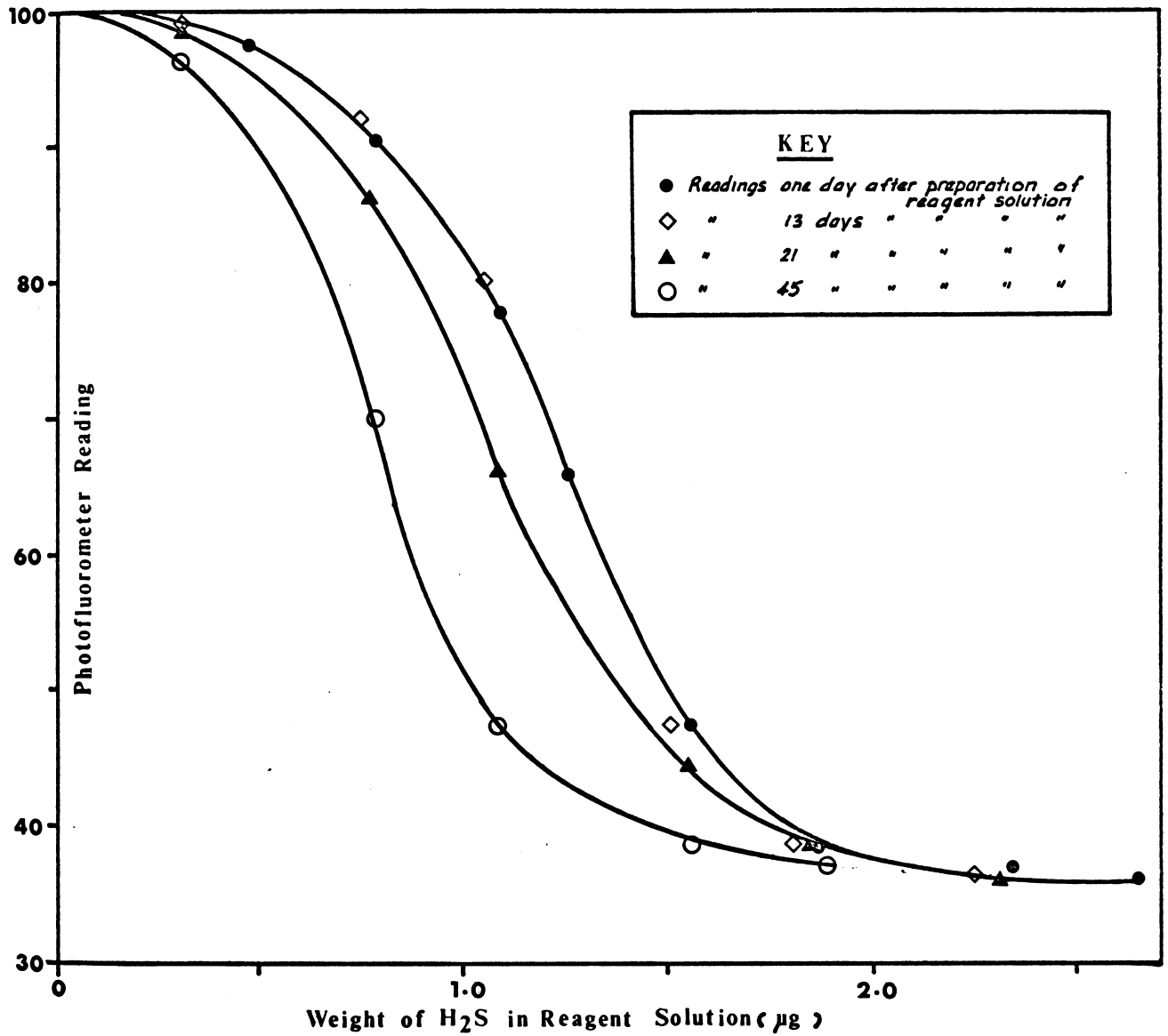


**FIGURE 2.4**

**CALIBRATION CURVES, 0.00025% FMA SOLUTION N<sup>o</sup> FMA 25/7  
SHOWING EFFECT OF REAGENT SOLUTION AGE**

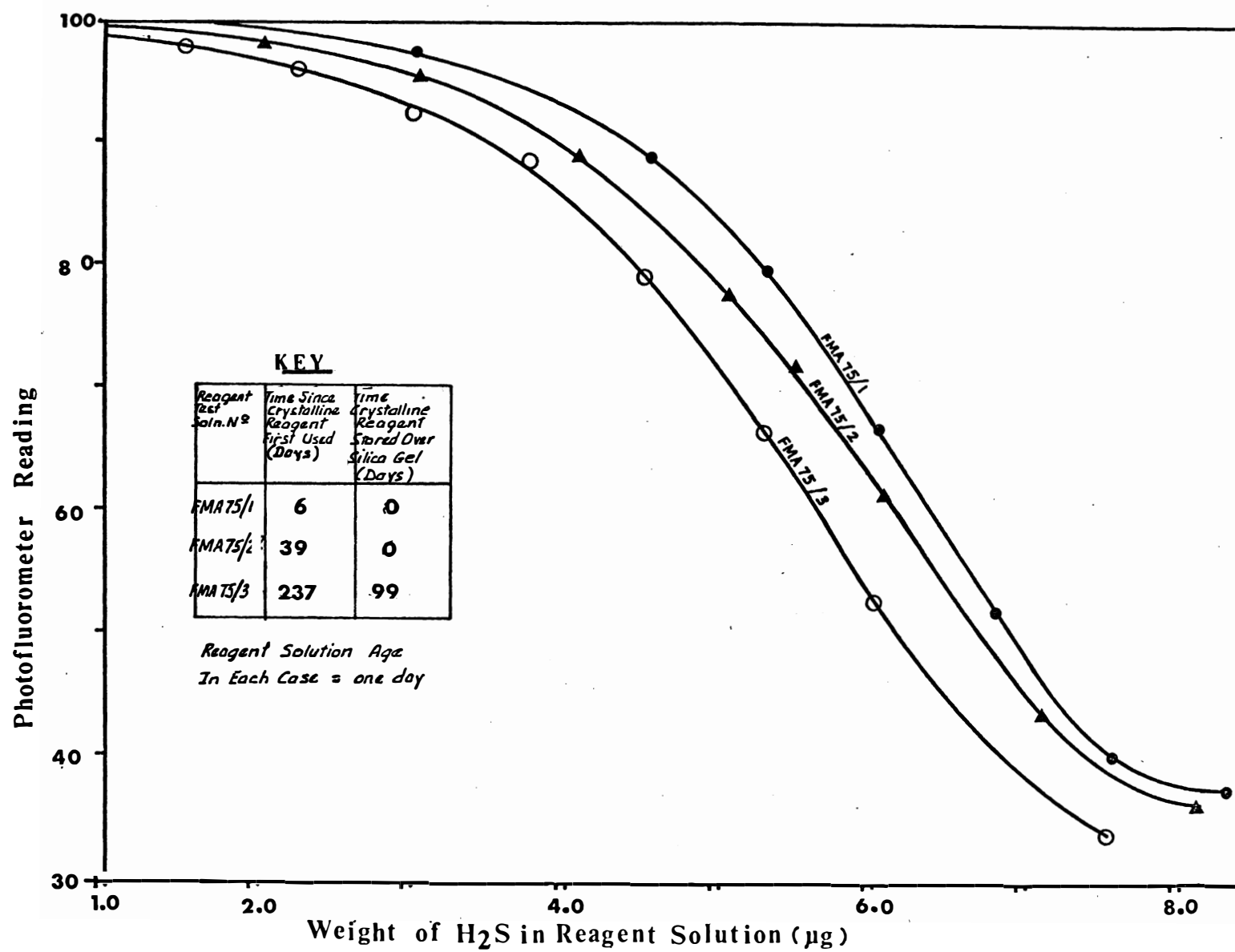
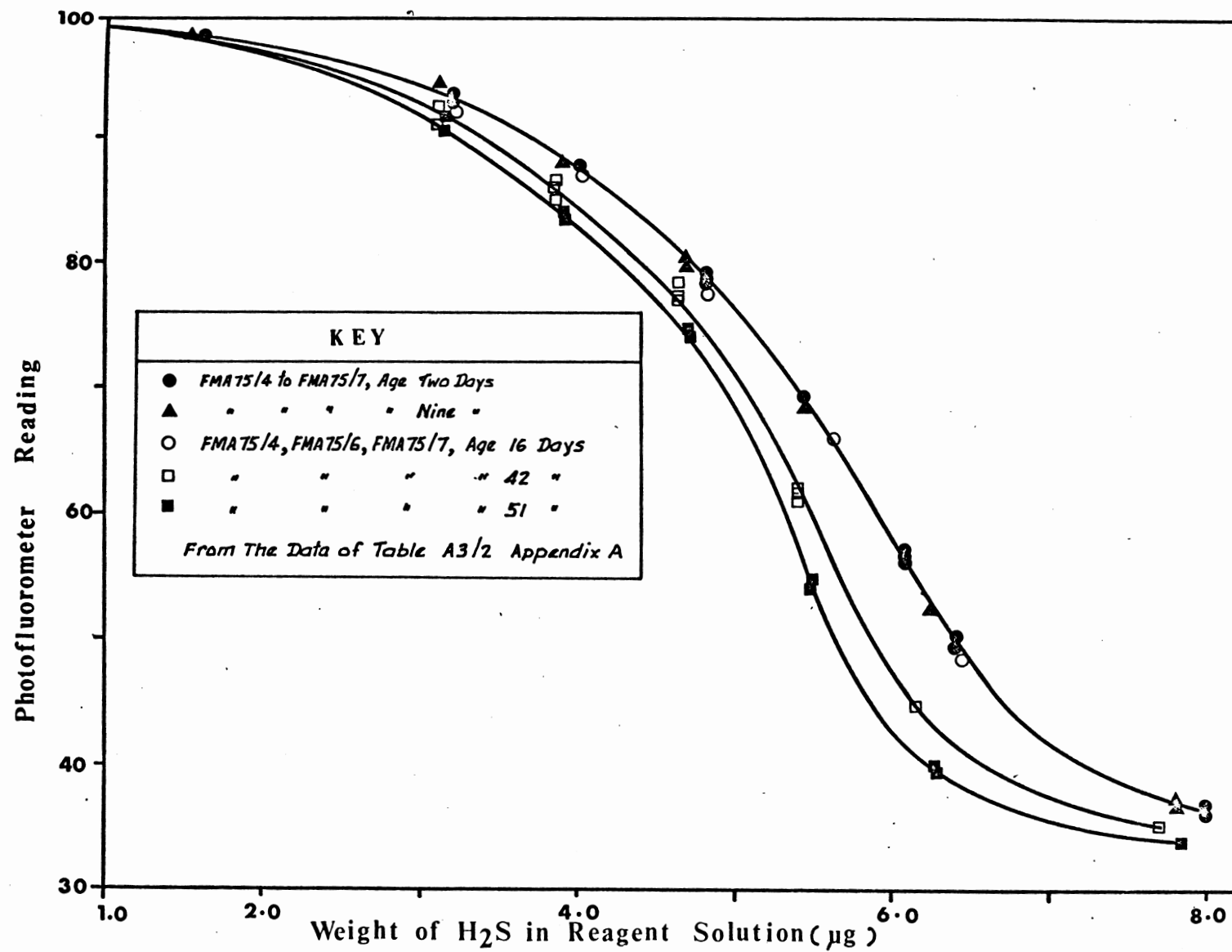
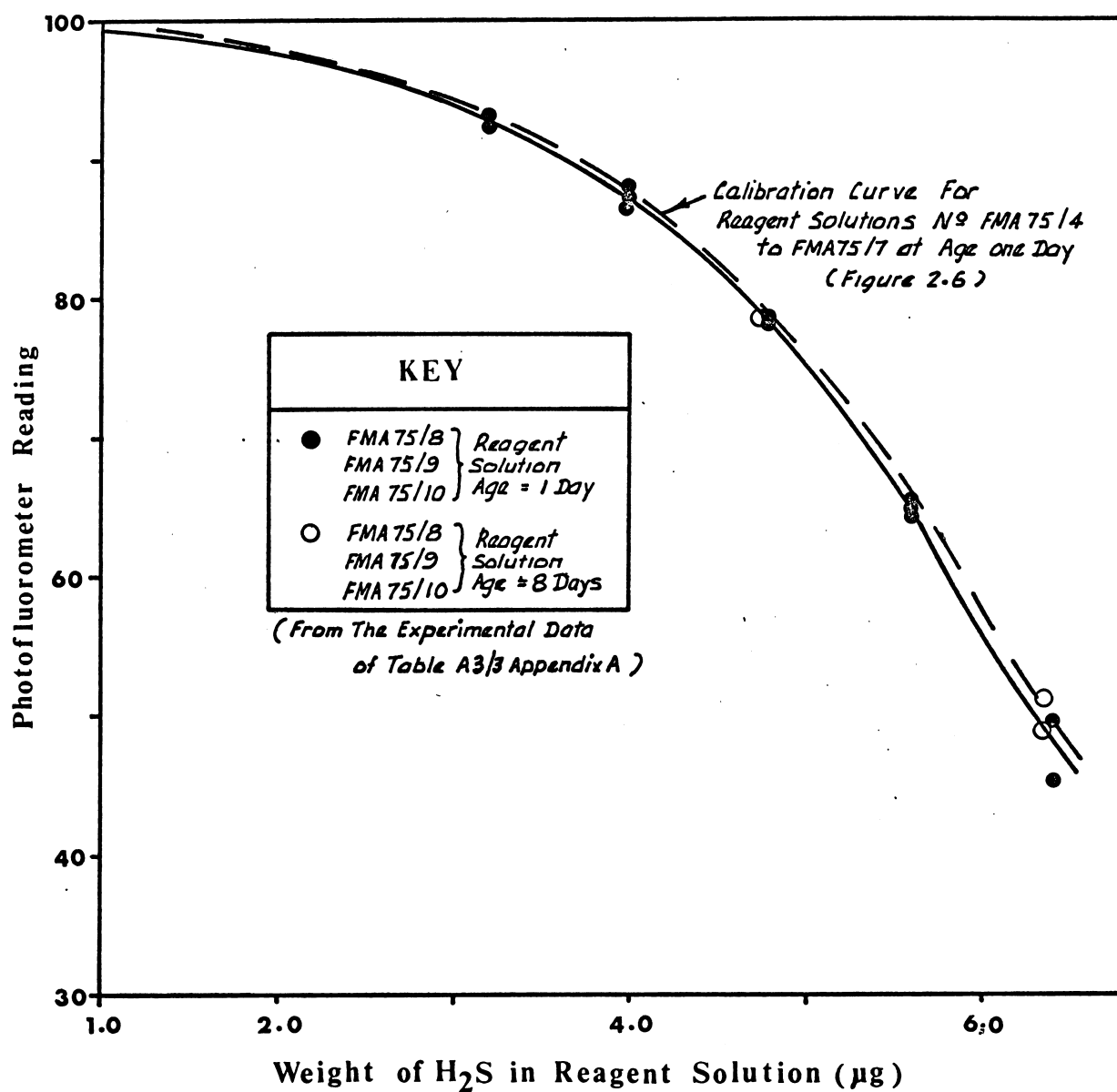


FIGURE 2.5 CALIBRATION CURVES, REAGENT TEST SOLUTIONS NO  
FMA75/1 to FMA75/3



**FIGURE 2.6 CALIBRATION CURVES, 0.00075% FMA SOLUTION, SHOWING EFFECT OF REAGENT SOLUTION AGE**



**FIGURE 2.7**

**CALIBRATION CURVES, 0.00075% FMA, SHOWING CURVES**  
**PREPARED 105 DAYS APART**

**(CRYSTALLINE REAGENT STORED OVER SILICA GEL)**

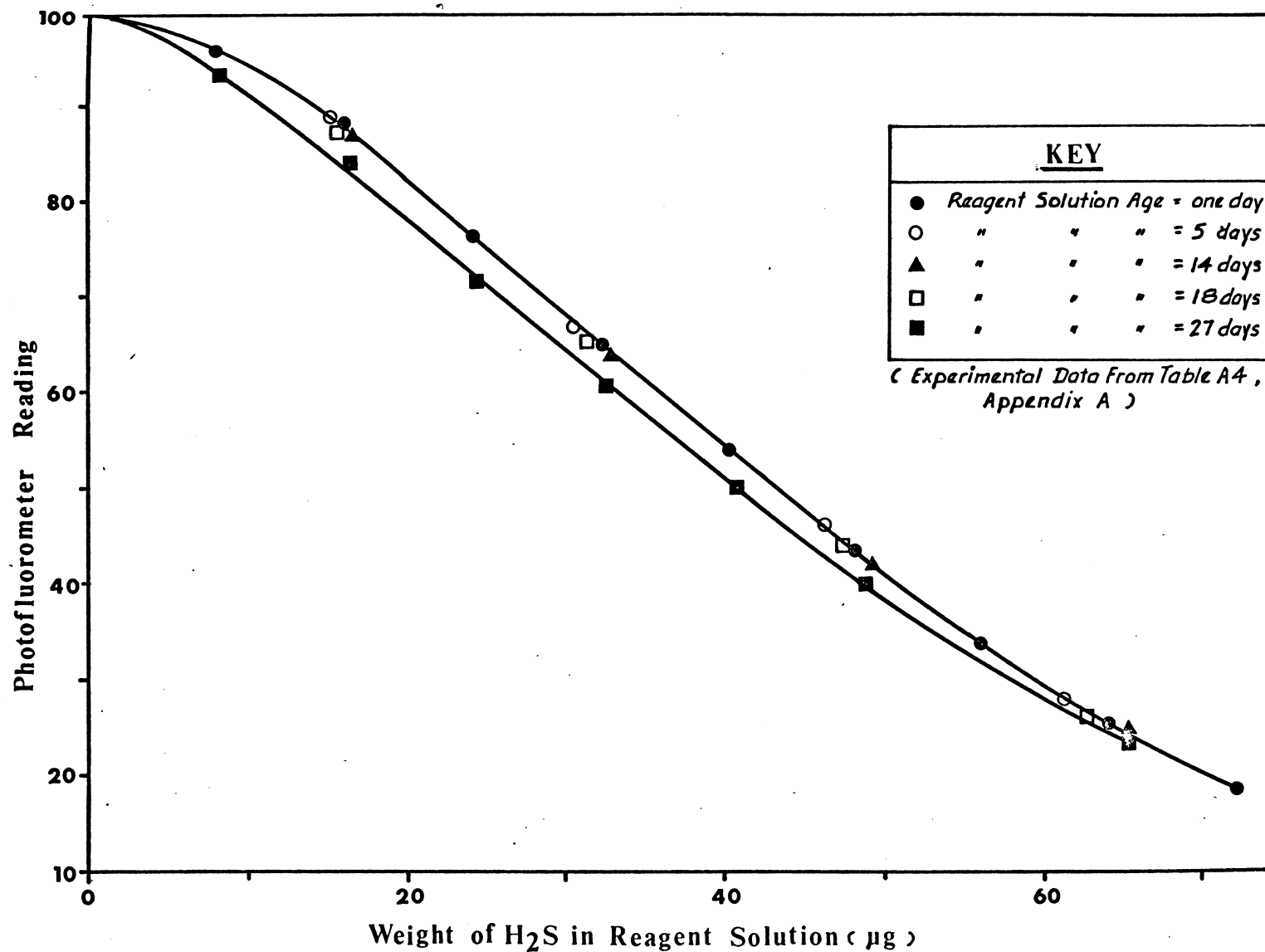


**FIGURE 2.8**    CALIBRATION CURVES, 0.012% TMF REAGENT TEST SOLUTION  
Nº TMF 120/1

SHOWING VARIATION WITH SOLUTION AGE

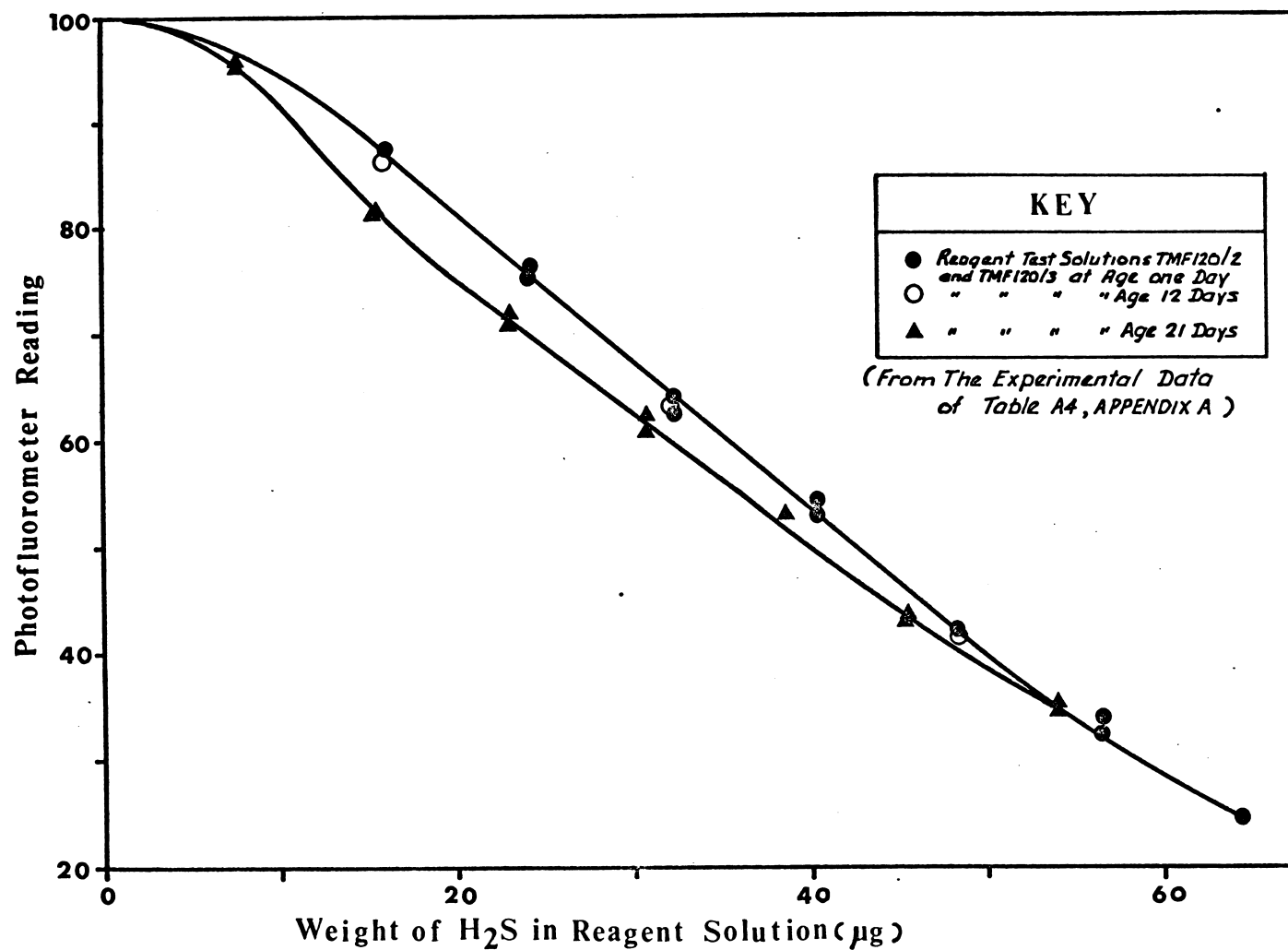


**FIGURE 2.9 CALIBRATION CURVES, 0.012% TMF REAGENT TEST SOLUTIONS  
NºTMF120/2 & TMF120/3**

SHOWING VARIATION WITH SOLUTION AGE

#### 2.4.3 Resistance of the Solution to Degradation By Air.

Nine litres of deodorised air were passed through sample portions of each of the solutions under test, at a rate of 1.5 l/min. In all cases there was no measurable change in solution fluorescence.

To verify the stability of the solutions in the presence of the acid gas,  $\text{CO}_2$ , 2ml. of  $\text{CO}_2$  were injected through a septum seal into a stoppered bottle containing 25 mls. of 0.00025% FMA in 0.01 NaOH solution. The solution was then vigorously shaken and the fluorescence determined using the photofluorometer. This was repeated using the 0.00075% FMA solution and the 0.0120% TMF solution. Again no measurable change in fluorescence occurred.

#### 2.4.4 The Reacted Solution Stability.

Table A1 sets out experimental data produced by measuring the fluorescence of the reagent solutions under test, at time intervals of 15 and 45 minutes after addition of the  $\text{Na}_2\text{S}$  calibrating solution.

When Students' t test was applied to the paired values in these photofluorometer readings, it was found that the differences, in all cases, were not significant at the 95% level. The results of this test are presented in Table A5.

#### 2.4.5 The Effect of Temperature on the Stability of the Reagent Solution.

In this test, reagent solution numbered FMA75/8

was stored at a temperature of about 11°C, while two control samples, FMA75/9 and FMA75/10 were stored at an average temperature of 19°C. As demonstrated by Figure 2.7 and Table A3/3, the calibration data at the end of eight days, for both the test and the control solutions, were almost exactly equivalent.

Small temperature variations would appear to have no effect on reagent solution stability.

#### 2.4.6 Crystalline Reagent Storage Conditions.

Initially the crystalline reagent was stored in a dark bottle in a cool place, as recommended by the Manufacturer. However, it was found that calibration curve stability was enhanced considerably if, in addition, the crystalline reagent was stored over silica gel. This is illustrated by Figures 2.2, 2.5 and 2.9 and Tables A2, A3 and A4.

In all cases, before the introduction of the silica gel system of storage, significant changes in calibration curve position occurred as the crystalline reagent aged. The movement was always in the one direction and suggested either an increasing crystalline material moisture content or a chemical breakdown of its structure.

However, after storage over silica gel was adopted, these calibration curve changes were arrested, and in some cases reversed. Eventually an equilibrium condition was attained within the crystalline reagent, such that the calibration curves became consistently reproducible.



#### 2.4.7 Reproducibility of the Calibration Curves.

The calibration data for reagent solutions of the same strength and age were examined for both short and long term reproducibility. The short term reproducibility provides a measure of the errors inherent in the calibration procedures, while the long term reproducibility provides a measure of the stability of the crystalline reagent.

The former is exemplified by Figure 2.6 for 0.00075% FMA, and Figure 2.10 for 0.0120% TMF. Here simultaneously prepared solutions FMA75/4 to FMA75/7 and TMF120/7 to TMF120/8 show only a random scatter of relatively small deviations from mean values.

Thus the short term reproducibility appears to be excellent.

The long term reproducibility is demonstrated by Figure 2.7 and Table A3 for samples of 0.00075% FMA prepared up to 105 days apart, and Figures 2.10 and 2.11 for solutions numbered TMF120/7 to TMF120/9 prepared up to 160 days apart. It is obvious that, when stored in the recommended manner, the crystalline reagents are stable, producing calibration curves which are reproducible over long periods.

#### 2.5 An Overall Check on the Reliability of This Method of H<sub>2</sub>S Measurement.

In this test H<sub>2</sub>S was injected at a known rate into a continuous, steady stream of air, and the H<sub>2</sub>S content of the

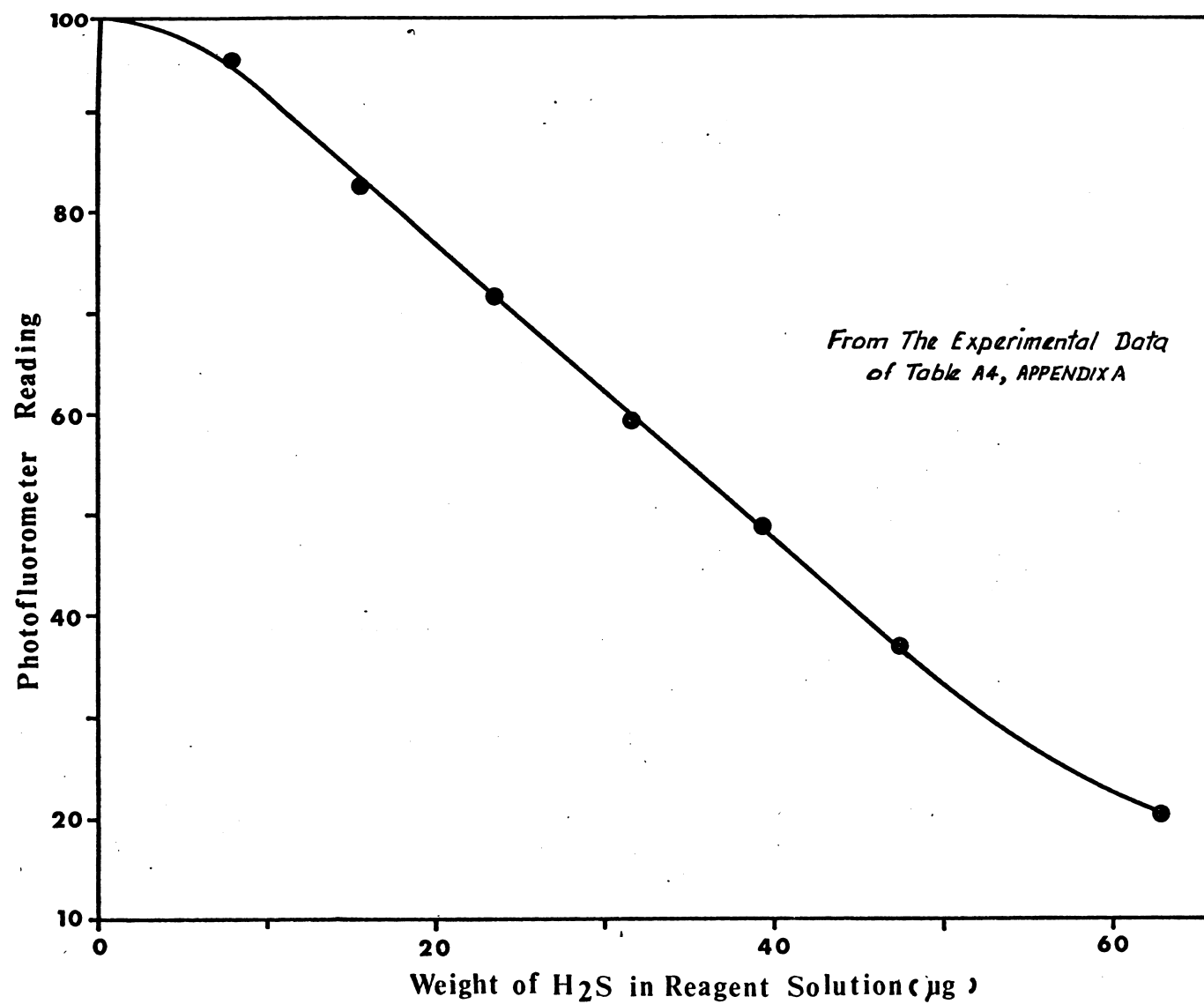


**FIGURE 2.10 CALIBRATION CURVE, 0.012% TMF REAGENT TEST SOLUTION N° TMF120/4**

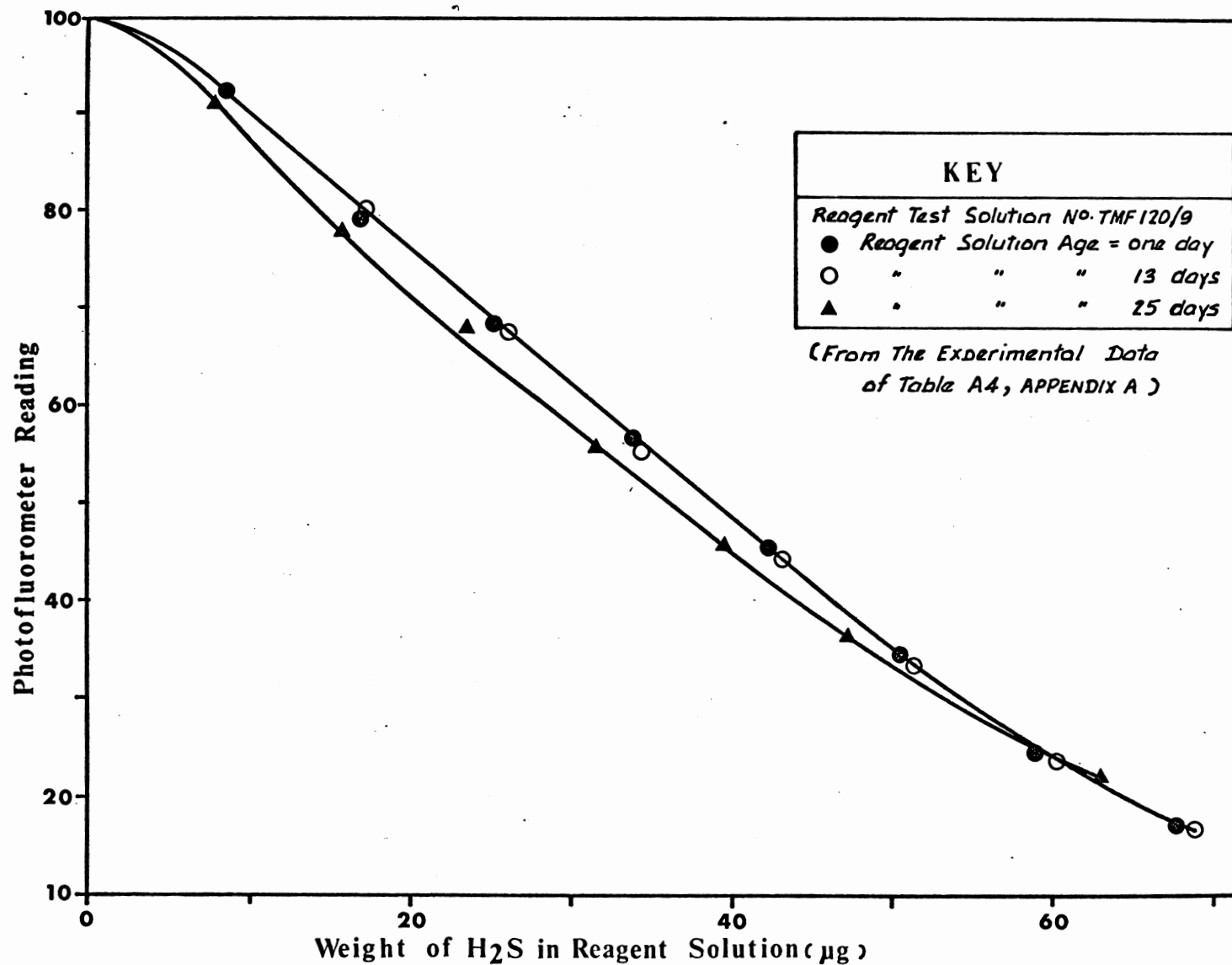


**FIGURE 2.11** CALIBRATION CURVES, 0.012% TMF REAGENT TEST SOLUTION NO. TMF120/9  
SHOWING VARIATION WITH SOLUTION AGE

dilute  $\text{H}_2\text{S}$ -air mixture determined experimentally using the fluorometric method described above.

#### 2.5.1 Measurement of the $\text{H}_2\text{S}$ Purity.

The  $\text{H}_2\text{S}$  for these tests was obtained from a cylinder supplied by the Mathieson Gas Co. Inc. of the U.S.A. Although the stated purity was 99.6% minimum, it was checked in the following manner.

Samples of the  $\text{H}_2\text{S}$  gas were taken in previously calibrated syringes and injected directly into 25 ml. volumes of standardised 0.01N iodine solution. The excess iodine was then titrated against standardised 0.01N  $\text{Na}_2\text{S}_2\text{O}_3$  solution using starch as the indicator.

To achieve the absorption and subsequent reaction without loss of  $\text{H}_2\text{S}$ , the iodine was contained in a 250 ml. bottle and the  $\text{H}_2\text{S}$  introduced through a self-sealing rubber stopper.

#### 2.5.2 Experimental Apparatus.

The apparatus for production of the air/ $\text{H}_2\text{S}$  mixture is illustrated in Figure 2.12. Briefly,  $\text{H}_2\text{S}$  of known purity was dosed into a continuous stream of purified air at a constant predetermined rate from a mechanically operated, all glass hypodermic syringe. The  $\text{H}_2\text{S}$  injection system is fully described in section 3.2.2.

The pressure within the apparatus was measured using a water-filled manometer calibrated to 0.1 cm  $\text{H}_2\text{O}$ . This pressure could be set to any reasonable level for any given

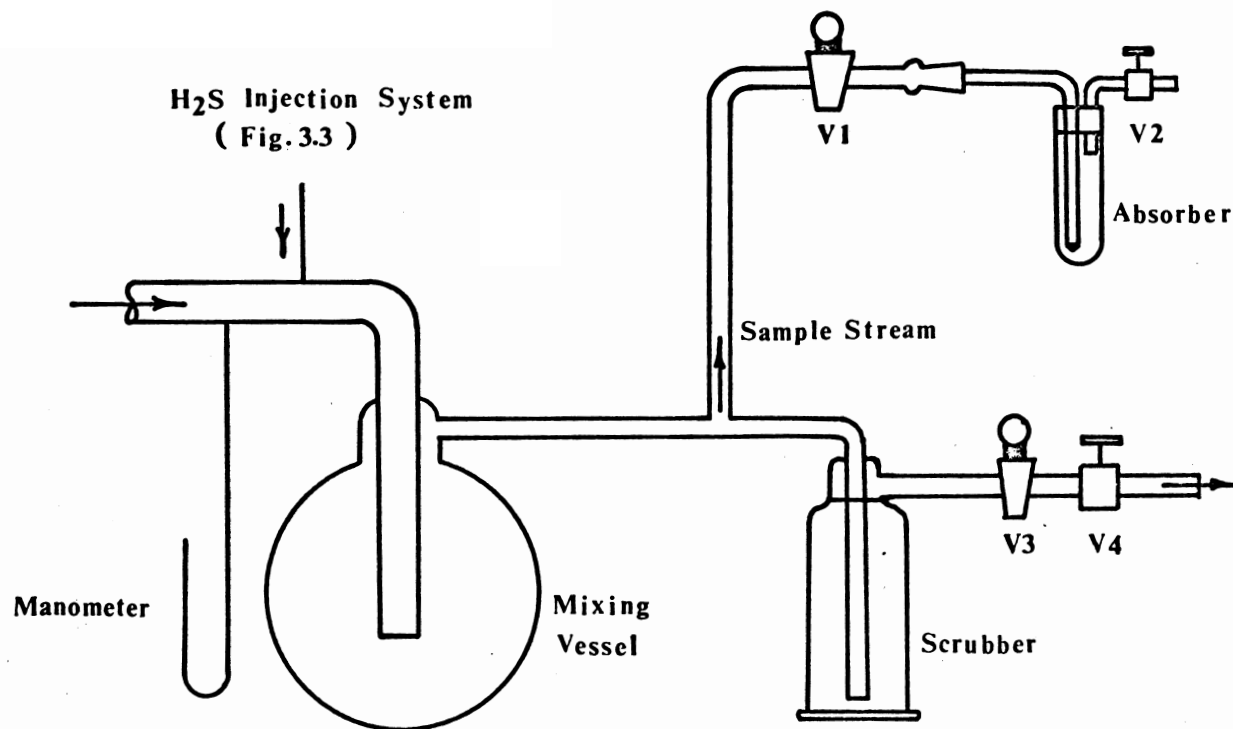


**FIGURE 2.12**

**APPARATUS FOR THE PRODUCTION AND MEASUREMENT OF AIR  
STREAMS CONTAINING KNOWN CONCENTRATIONS OF  $\text{H}_2\text{S}$**

flowrate merely by operation of valves V2 or V4.

The deodorised air was produced in the purification train described in section 3.2.1. All joints in the apparatus between the  $\text{H}_2\text{S}$  injection point and the sample absorber were of the ground glass socket and cone variety. The air/ $\text{H}_2\text{S}$  mixture leaving the main test apparatus was treated by passage through alkaline potassium permanganate solution before venting to the atmosphere.

A stopwatch, accurate to 0.1 second, was used to measure both the drive shaft speed, and the reagent solution reaction time. The ambient temperature was measured using a copper-constantan thermocouple coupled to a Cambridge portable potentiometer via an ice-water cold junction.

### 2.5.3 Experimental Method.

Before the commencement of the run the  $\text{H}_2\text{S}$  storage apparatus, described in section 3.3.1, was approximately three quarters filled with  $\text{H}_2\text{S}$  from the  $\text{H}_2\text{S}$  cylinder, and the remainder filled with deodorised air. After a storage period of a few hours the  $\text{H}_2\text{S}$  concentration of this mixture was determined using the method described above.

The air stream through the apparatus was then started and the flowrate set at a value of between 1.0 and 1.5 l/min. With valve V1 (Figure 2.12) closed and valve V3 fully open, the internal apparatus pressure was then set at some value between 5.0 and 16.5 cm water gauge by manipulation of valve V4.

The reagent absorption vessel, Figure 2.1, was then charged with a pipetted 25 ml. of water, and the vessel connected to the experimental apparatus. The air stream was then diverted through this vessel, by opening valve V1 and closing valve V3, and the apparatus internal pressure adjusted by operation of the absorber outlet valve V2, until the value recorded above had been attained. The vessel was then emptied, dried and recharged with a pipetted 25 ml. of the fluorescent reagent solution, 0.006% FMA in NaOH (0.01N aq.).

A syringe full of  $H_2S$  was then taken from the storage apparatus, the syringe connected into the experimental apparatus, and the gear train motor started.

After the syringe plunger movement had commenced, the main inlet valve into the air train, valve V1 (Figure 3.1) was gradually opened until full internal pressure had been achieved. The valve was then fully opened, control of the flowrate thus passing to the secondary control valve, valve V3, Figure 3.1, which had been previously set to achieve the air flowrate of between 1.0 and 1.5 l/min mentioned above. This operation was extended over several minutes thus minimising the possibility of air movement back into the syringe. The apparatus was allowed to come to equilibrium over about 10 minutes and an experimental determination of  $H_2S$  concentration achieved in the following manner. (refer to Figure 2.12).

By operating valves V3 and V1 simultaneously, the flow of air/ $H_2S$  mixture was diverted into the absorption vessel.

Since the outlet valve V2 on this vessel had been pre-set to maintain internal apparatus pressure at a constant level, variation in H<sub>2</sub>S injection rate due to pressure differences was avoided.

After a pre-determined accurately measured interval of time, valves V3 and V1 were again operated simultaneously, the gas again flowing via the scrubbing vessel to the atmosphere. The absorption vessel was then disconnected from the apparatus and the solution fluorescence determined. This process was then repeated using the 0.0120% TMF reagent solution.

The atmospheric pressure was determined using a Fortin barometer, the ambient temperature using a copper-constantan thermocouple, and the drive shaft speed by timing 50 to 100 revolutions directly.

#### 2.5.4 Calculations.

The weight of H<sub>2</sub>S introduced in a test of "t" minutes duration was calculated directly from the equation;

$$\begin{array}{l} \text{Wt. H}_2\text{S Passed} \\ \text{Into Solution} \\ (\mu\text{g}) \end{array} = \frac{Vs}{26} \times \frac{\text{RPM}}{50} \times C_H \times t \quad - - - - 2.2$$

where  $V_s$  = syringe volume per unit length (ml/inch)  
(Table 3.2)

RPM = gear train input shaft speed (RPM)

$C_H$  = H<sub>2</sub>S concentration ( $\mu\text{g/ml}$ ).

The constants used in this equation are defined in Table 3.2.



The values derived from this equation were then compared with the values determined from the reagent solution fluorescence measurements.

#### 2.5.5 Results and Conclusions.

The experimental and calculated results are shown in Tables A6 to A8, Appendix A. Tables A7 and A8 also give the results of a Student's "t" test which was applied to the paired calculated and observed values for  $H_2S$  concentration. The hypothesis that the observed and calculated values represented random deviations from the same populations was found to be valid at the 95% level of significance.

Individual differences between the paired readings are small, and in most cases less than 2% of the measured value. Since there are no significant trends in these differences, it was assumed that;

- (a) the method of generation of the air streams containing given  $H_2S$  concentrations is accurate enough for the purpose envisaged, and
- (b) the fluorometric method of  $H_2S$  concentration measurement is reliable and accurate.

#### 2.6 Comparison of the Reagents FMA and TMF for $H_2S$ Measurement.

In many respects FMA and TMF were found to act similarly when used as test reagents for  $H_2S$  measurement. However, FMA was found to have the disadvantage that complete fluorescence quenching did not occur under the experimental conditions

utilised herein. Nevertheless, the commercial availability of the crystalline FMA reagent, which obviates the necessity of a tedious preparation and purification step, was considered to be an advantage.

Accordingly, for the experimental work connected with odour removal, FMA reagent solutions were used for the determination of low concentrations of  $\text{H}_2\text{S}$ , and TMF solutions for the determination of relatively high concentrations.

## 2.7 Analysis of Low Concentrations of Ethyl Mercaptan in Air.

Generally, analytical procedures for the determination of low concentrations of ethyl mercaptan ( $\text{C}_2\text{H}_5\text{SH}$ ) in air have been given relatively little attention.

A method based on conversion of the thiol to  $\text{H}_2\text{S}$  with subsequent methylene blue analysis has been used by WILBY (38) with good results. The gas chromatograph has also long been used to separate and measure various sulphur containing gases, including thiols, from gas streams (10) and has, in fact, been used to measure certain gaseous thiols at concentration levels less than 1 ppm by volume .

However, the titrimetric fluorescent procedure for  $\text{H}_2\text{S}$  analysis described by WRONSKI (13)(14) and referred to in section 2.1 above, has also been used to analyse for thiols.

It was therefore considered likely that the TMF reagent, and possible also the FMA reagent, would prove satisfactory for accurate analysis of the  $\text{C}_2\text{H}_5\text{SH}$  content of polluted air streams, and that the methods developed above for  $\text{H}_2\text{S}$  measurement would apply.

### 2.7.1 Assessment of TMF and FMA as Reagents for $C_2H_5SH$ Measurement.

Reagent solutions containing 0.00075% FMA in NaOH (0.01N aq.) and 0.0014% TMF in NaOH (0.01N aq.) were prepared and calibrated using a calibrating solution containing about 90  $\mu g$  of  $C_2H_5SH$  per ml. Preparation and standardisation of this solution is described below in section 2.8.

These preliminary tests demonstrated that, whereas the TMF solution produced good calibration curves, the calibration curves for the 0.00075% FMA solution approached a minimum value at the photofluorometer reading = 76.0 line.

A more detailed examination of this latter phenomenon was then undertaken using calibrating solutions containing  $C_2H_5SH$  concentrations ranging between 33 and 350  $\mu g./ml$ .

Again the truncated and virtually useless calibration data thus obtained served to emphasise the uselessness of FMA as a reagent for  $C_2H_5SH$  determination.

## 2.8 Detailed Analytical Procedure for $C_2H_5SH$ . Concentration Measurement Using TMF Solutions.

The reagent solution used for measurement of the  $C_2H_5SH$  concentration of gas streams throughout these experiments contained 0.0120% TMF in NaOH (0.01Naq.). The method of preparation of this solution is described in section 2.3.1.

### 2.8.1 Examination of Suitable Solvents for the Calibrating Solution.

To calibrate the TMF solutions, small portions of a calibrating solution containing known quantities of  $C_2H_5SH$  dissolved in a suitable solvent were added to aliquots of the reagent solution and the photofluorometer readings taken.

During initial trials, it soon became apparent that calibration curves obtained using NaOH as the solvent for the  $C_2H_5SH$  were not reproducible. However, calibrating solutions made up using ethanol (constant boiling mixture) as the mercaptan solvent showed no such disadvantage, giving calibration curves which were reproducible over many months.

The failure of calibrating solutions prepared from NaOH to behave satisfactorily, may be explained by the observation that mercaptans are readily oxidised by air under alkaline conditions (92). In view of the excellent results obtained using ethanol as the solvent, the possible use of NaOH was not pursued further.

### 2.8.2 Calibration of the Reagent Solution.

Essentially the stepwise procedure used for calibration of the reagent solution followed that used during the calibration of the reagent solutions for  $H_2S$  analysis (section 2.3.2).

- (1) Prepare
  - (a) 0.01N  $\text{KI} \text{O}_3$  solution (95)
  - (b) 0.01N  $\text{Na}_2\text{S}_2\text{O}_3$  solution (95)
  - (c) 0.01N iodine solution (95)
  - (d) a solution of  $\text{C}_2\text{H}_5\text{SH}$  in ethanol as described below in section 2.8.3.
- (2) Standardise the  $\text{Na}_2\text{S}_2\text{O}_3$  and the  $\text{I}_2$  solutions in the manner described by VOGEL (95).
- (3) Determine the  $\text{C}_2\text{H}_5\text{SH}$  content of the calibrating solution (STOCK  $\text{C}_2\text{H}_5\text{SH}$  SOLUTION) using the titrimetric procedure described below in section 2.8.4.
- (4) Dilute the stock solution as described below to yield  $\text{C}_2\text{H}_5\text{SH}$  TEST SOLUTION I.
- (5) Thereafter as detailed below in section 2.8.5.

#### 2.8.3 Preparation of the Calibrating Solutions.

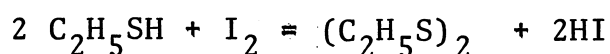
Two solutions were prepared for use in the calibration of the test method, a stock solution containing approximately 3500  $\mu\text{g.}$  of  $\text{C}_2\text{H}_5\text{SH}$  per ml, and a test solution containing approximately 350  $\mu\text{g.}$  of  $\text{C}_2\text{H}_5\text{SH}$  per ml. STOCK SOLUTION From 200 to 230 microlitres of liquid A.R. grade  $\text{C}_2\text{H}_5\text{SH}$  were transferred, using a micro-syringe, into a 50 ml. volumetric flask containing approximately 25 ml. of ethyl alcohol (constant boiling mixture), and the solution made up with more of the same solvent. The  $\text{C}_2\text{H}_5\text{SH}$  content of this solution was measured, using the method described below, immediately before use.

$\text{C}_2\text{H}_5\text{SH}$  TEST SOLUTION I. Immediately after the  $\text{C}_2\text{H}_5\text{SH}$  content

of the stock solution had been measured, five millilitres were pipetted into another 50 ml volumetric flask containing approximately 25 mls of ethyl alcohol, and the solution again made up to 50 ml using the same solvent. This solution was used for preparation of fluorescent solution calibration data immediately after its own preparation, and was discarded and made afresh if it was more than an hour old.

#### 2.8.4. Determination of The $C_2H_5SH$ Content of the Stock Solution.

This analysis is based on the reaction of a known volume of the mercaptan containing solution with a known volume of standardised iodine solution, and the titration of the excess iodine with standardised  $Na_2S_2O_3$  solution. The iodine oxidises the mercaptan smoothly and rapidly, according to the equation (102),



Method. A pipette was used to transfer 2.5 mls of the stock solution under test, to 25 mls of standardised 0.01N iodine solution in a flask. The flask was then stoppered and shaken, and the excess iodine titrated against standardised 0.01N  $Na_2S_2O_3$  solution.

A blank titration of the  $Na_2S_2O_3$  solution against 25 mls of iodine solution containing 2.5 mls of ethyl alcohol, showed that the alcohol had no effect on the results.

### 2.8.5 Preparation of Calibration Curves.

Calibration curves for the 0.0120% TMF were prepared in a manner similar to that described in section 2.3, using the  $C_2H_5SH$  Test Solution I mentioned above.

### 2.9 Stability of the Data.

Two sets of calibration data for 0.0120% TMF solution in 0.01 N NaOH are given in Table A9 and Figure 2.13. These sets of data were collected over a period of two months using crystalline reagent which had been stored over silica gel for a considerable period, and was thus free of any such changes as are referred to in section 2.4.6.

Figure 2.13 would appear to indicate that both sets of data could be assumed to be random samples from the same population. If the first and final points are ignored (i.e. points 0,100.0) and (254.9,28.0) the calibration data can be represented by a single straight line.

When this relationship was examined by a linear regression of Y on X, ignoring the two points mentioned above, the equation became;

$$X = 326.1 - 3.001Y \quad \dots \dots \dots 2.3$$

where X = The reagent solution mercaptan content ( $\mu g$ )  
and Y = The corresponding photofluorometer reading.

The standard error of the estimate was 1.15. The 95% confidence limits were also calculated, and representative values are listed in Table A10. As indicated in this table,

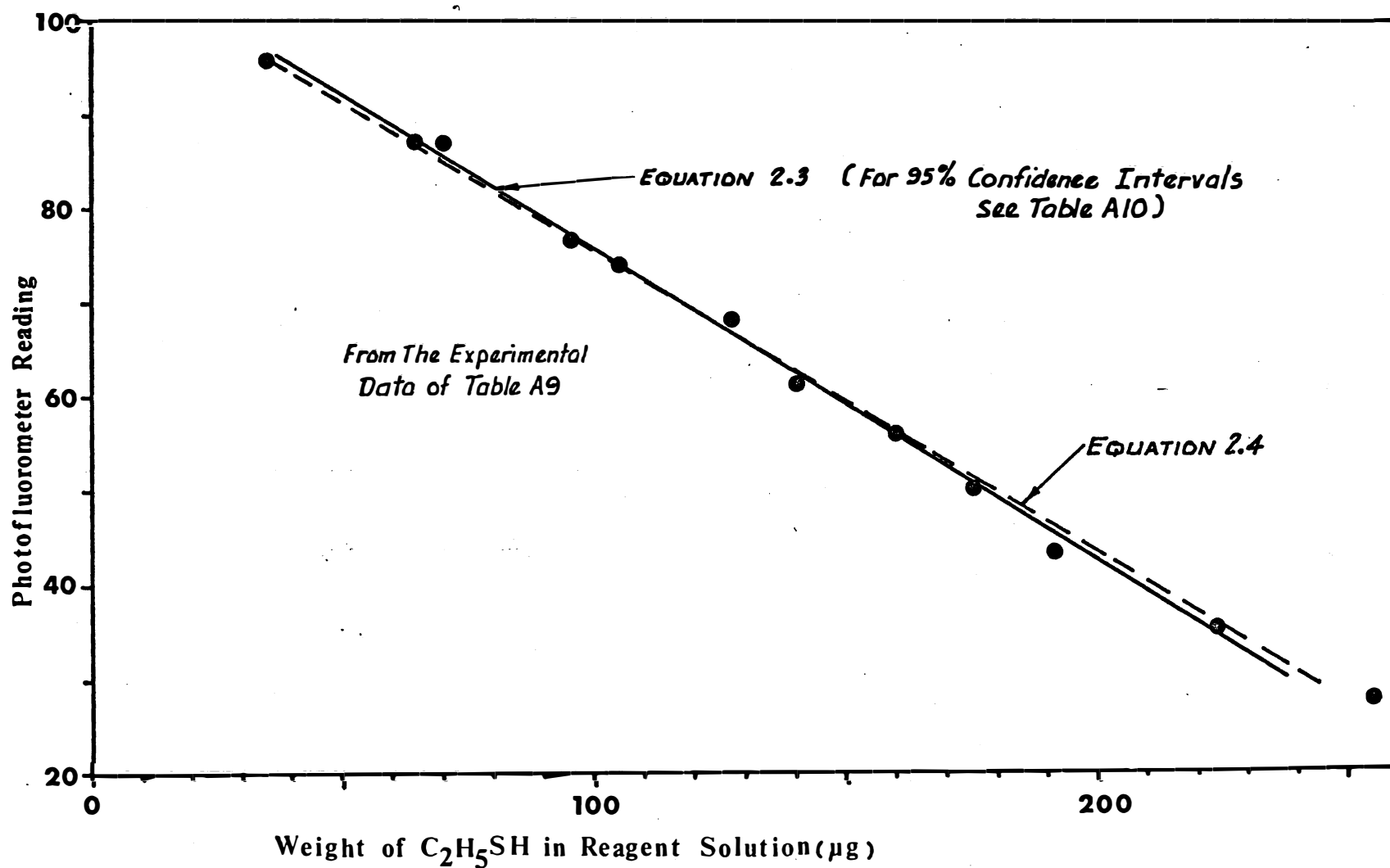


**FIGURE 2.13** CALIBRATION CURVE, 0.012% TMF, FOR ETHYL MERCAPTAN MEASUREMENT



the limits examined were;

- (a) The interval of estimation for the mean value ( $u_Y$ ) of a number of Y values for a particular value of X; with 95% confidence, and
- (b) the interval of estimation for a single Y value, corresponding to a single X value; with 95% confidence.

When the point (254.9,28.0) was included in the data, a linear regression of Y on X yielded the line,

$$X = 333.25 - 3.0966Y \quad - - - - 2.4$$

where X and Y are defined above. The standard error of the estimate was increased to 1.57.

Nevertheless, as indicated in Figure 2.13, there is little practical difference between the lines produced by equations 2.3 and 2.4.

#### 2.10 The Test Procedure for C<sub>2</sub>H<sub>5</sub>SH Analysis.

Only one reagent solution strength, that is, 0.0120% TMF in NaOH (0.01N aq.), was used throughout these experiments. This solution was prepared in accordance with the method set out above in section 2.8, and was stored in a dark place when not in use, and discarded and made afresh every 14 days.

Taking care to expose the fluorescent solution to as little light as possible, 25 ml. of the reagent solution were pipetted into the absorption vessel described in section 2.2.2, and one ml. of ethyl alcohol added. The absorber was then connected to the sample off-take point (see Figure 2.12), and

an accurately measured volume of the air-mercaptan mixture passed through the solution. The absorber was then disconnected, an appropriate portion of the solution transferred to a photofluorometer cuvette, and the fluorescence measured using the photofluorometer. This latter step was carried out between 15 and 45 minutes after the mercaptan containing air had ceased to contact the reagent solution.

#### 2.11 An Overall Check on the Reliability of the Fluorometric Method of $C_2H_5SH$ Measurement.

In this test an air stream containing a known concentration of  $C_2H_5SH$  was produced and the  $C_2H_5SH$  content determined experimentally using the fluorometric method described above.

Basically the test method was similar to that described in section 2.5.

##### 2.11.1 Experimental Apparatus.

The same basic apparatus as described in section 2.5.2 was used for this series of tests, but with additional provision for the vapourisation of the liquid  $C_2H_5SH$  at constant known rates. This provision is fully described in section 3.2.3 and illustrated in Figure 3.5. Briefly it consisted of a means whereby nitrogen, driven at a very slow but constant rate from a hypodermic syringe, was bubbled through a quantity of approximately 5 mls. of the mercaptan contained within a small glass vial, thus carrying thiol vapours through into the main air stream. The vial was totally immersed in a water bath of known temperature.

### 2.11.2 Experimental Procedure.

The vial in the  $C_2H_5SH$  vapourisation apparatus was disconnected from the apparatus and approximately 5 mls. of ethyl mercaptan added. While ever the apparatus was in constant use, this operation was repeated at intervals of 3 to 4 days, any remaining mercaptan at the end of this period being discarded due to the remote possibility (92) of contamination by oxidation products.

The procedure for operation of the apparatus and the taking of samples exactly followed that given in section 2.5, except that a reading of the water bath temperature was taken during each run.

### 2.11.3 Calculations.

From a knowledge of the rate at which the air was passing into the liquid mercaptan, the temperature at which the mercaptan was being held, and the vapour pressure-temperature relationship for the mercaptan, it was possible to estimate the mercaptan injection rate.

In this calculation a number of assumptions were made;

- (a) the air, and the ethyl mercaptan, were at the same temperature.
- (b) Raoult's law applied, and
- (c) the air became saturated with the mercaptan, at the temperature of the mercaptan, during the bubbling process.

Then,

$$W_{tm} = \frac{V_s}{26} \times \frac{RPM}{50} \times \frac{Y_a}{1-Y_a} \times \frac{62.13 \times 10^6}{V_{gm}} \times t \quad \text{--- 2.5}$$

where  $W_{tm}$  = the weight of  $C_2H_5SH$  introduced in a test of  $t$  minutes duration ( $\mu g$ )

$V_{gm}$  = the volume occupied by 1 g. mole at the total internal pressure of the apparatus and the temperature of the vapour (ml),

and  $Y_a$  = the mole fraction of  $C_2H_5SH$  in the air.

From Raoult's Law

$$Y_a = \left( \frac{P_A}{P} \right) \quad \text{--- 2.6}$$

where  $P_A$  = the vapour pressure of the  $C_2H_5SH$  at the temperature of the water bath

and  $P$  = the total internal pressure.

To apply this method, the vapour pressure of pure ethyl mercaptan at various temperatures was required. The data from WEAST (96) was plotted with co-ordinates  $\log$  (vapour pressure, mm.Hg.) versus  $\log$  (absolute temperature,  $^{\circ}K$ ). From this curve it was apparent that, for the range of vapour pressure values required for this experiment, the assumption of a linear relationship between the  $\log$  of the two variables was valid.

Thus an equation was derived for the vapour pressure,  $P_A$  (mm.Hg.), in terms of the absolute temperature,  $T_a$  ( $^{\circ}K$ ),

$$P_A = 400 \left( \frac{T_a}{290.86} \right)^{10.8} \quad \text{--- 2.7}$$

#### 2.11.4 Results and Conclusions Regarding the Reliability of the Method.

An IBM 1620 computer was used to compute the value of  $W_{tm}$  for the 16 sets of experimental data shown in Table A11. The results of these calculations are also shown in this Table, where they are compared with the values derived from the photofluorometer reading. The differences between pairs of data were also examined using Student's test, at the 95% level of significance. From this test, which is also shown in the above table, it was concluded that the hypothesis that the pairs of data were random samples from similar populations, should be accepted.

Nevertheless, the results are not as good as those for  $H_2S$ , presented above. The differences appear to have a preponderance of negative values, with some differences ranging up to  $6\frac{1}{2}\%$  of the measured value.

## 2.12 Discussion of Results and Conclusions.

The fluorescent compounds, TMF and FMA, were found to be excellent reagents for use in a simple, yet reliable method of analysis for the measurement of low concentrations of  $\text{H}_2\text{S}$  in air. The method was also found to be suitable for  $\text{C}_2\text{H}_5\text{SH}$  measurement, although, in this instance only the TMF reagent solution behaved satisfactorily.

The analytical technique required the preparation of calibration curves for each of the reagent solutions under test. For  $\text{C}_2\text{H}_5\text{SH}$  analysis, the resultant curves were found to be reasonably linear, allowing the derivation of a simple equation relating the two variables. No such linearity was found for the case of  $\text{H}_2\text{S}$  absorption, although a detailed examination of the calibration data for 0.00075% FMA in NaOH (0.01Naq), using an I.B.M. 1620 computer, revealed a good fit with the sixth order polynomial,

$$y = 99.904 + 13.270 x + 17.865 x^2 + 8.349 x^3 \\ - 1.848 x^4 + 0.182 x^5 - 0.00646 x^6 \quad \dots \dots \dots 2.8$$

with a standard error of the estimate of 0.66.

Here,  $x = \text{H}_2\text{S}$  content of the solution ( $\mu\text{g.}$ ) and  
 $y = \text{photofluorometer reading.}$

It was found that, for consistently reproducible calibration curves, it was necessary to store both the crystalline reagent and the reagent solution under carefully controlled conditions, and to discard reagent solutions which were more than 14 days old. Best results were obtained when the

crystalline reagents were stored over silica gel in a refrigerator at a temperature of about 7°C to 11°C, and the reagent solutions stored at room temperature in a dark place.

The fluorometric technique for the determination of low concentrations of H<sub>2</sub>S in air using FMA reagent solutions, has been used as the basis of a paper published by the author and co-workers in "Atmospheric Environment". A copy of this paper is included in Appendix G.

CHAPTER 3.

THE USE OF POTASSIUM PERMANGANATE

AND ASSOCIATED MANGANESE COMPOUNDS

FOR DEODORISATION.



### 3.1 Introduction.

The use of  $\text{KMnO}_4$  (potassium permanganate) in circumstances requiring a strong oxidant, has been restricted by its relatively high cost. Nevertheless it has been amply demonstrated that it is superior, both economically and otherwise, as a means of controlling taste and odour in water. In water treatment plants (68) (69) (70) it has been used to remove soluble iron and manganese compounds, and certain organic contaminants. Secondary benefits accrue because  $\text{KMnO}_4$  is a bactericide and algicide.

Buffered aqueous solutions of  $\text{KMnO}_4$  (and potassium and sodium dichromate) have been used to remove traces of  $\text{H}_2\text{S}$  from such industrial gases as carbon dioxide (66) (71). In this case, the solution used usually contains about 4%  $\text{KMnO}_4$  and 1% sodium carbonate, and is discarded after about 75% of the  $\text{KMnO}_4$  is converted to manganese dioxide, no attempt being made to utilise the oxidative power of the hydrated manganese dioxide itself.

KUEHNER (75) recognised the suitability of a dilute aqueous solution of  $\text{KMnO}_4$  as an agent for gaseous odour reduction. The process was apparently enhanced by the addition of lithium chloride to the solution (74). Perhaps greatest simplicity of application has been achieved by the use of filter beds of water absorbing substrates, such as hydrated alumina or silica gel, impregnated with  $\text{KMnO}_4$  (76) (77). Beds of this type have been used in air conditioner filters to remove odours of

all sorts.

EMANUEL (71) and POSSELT and REIDIES (72) have examined the deodorising properties of a 1% aqueous solution of  $\text{KMnO}_4$  in some detail, using a wide range of odorous substances, and a gas-liquid contact time of approximately one second. The comparative removal efficiency was determined by measuring the threshold odour number of an odour-air mixture, after contact with alkaline  $\text{KMnO}_4$  solution buffered to a pH of 8.5 in a gas-washing bottle fitted with a fritted disc diffuser, and comparing this value with the threshold odour number of a parallel odour-air stream after contact with water buffered to a pH of 8.5, under the same conditions. Threshold odour numbers were measured using the A.S.T.M. Method D1391-57 (44).

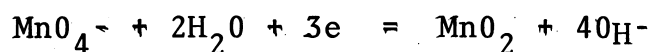
In most cases, even though the odorous materials under test included mercaptans, amines, phenols, and fat-rendering and asphalt plant off-gases, considerable, and in some cases complete odour reduction occurred. For example, they found that butanethiol contaminated air, which gave a threshold odour number of 200,000 at the buffered water exit, gave a value of 33 at the exit of the gas-washing bottle containing the  $\text{KMnO}_4$  solution.

Investigation of manganese compounds, other than  $\text{KMnO}_4$ , as deodorising agents has not been very intense. However, BAILEY and HUMPHREYS (73) have investigated the use of Manganese II, in the form of manganese chloride, as an agent for the oxidation of odorous sulphides from tannery wastes.

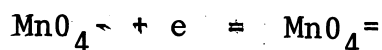
In this process, which they considered to be very effective, air is used as the oxidant and the MnII as a catalyst. The main product is the thiosulphate, although the more stable sulphate is also formed.

### 3.1.1 Optimum Solution pH.

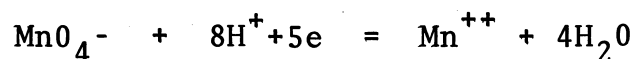
The optimum pH range for solutions of  $\text{KMnO}_4$  used for deodorisation is approximately 8-10 (72), although a pH as high as 11 may be used without significant loss of efficiency (71). In neutral or alkaline solution the generally accepted equation representing the reaction of  $\text{KMnO}_4$  with an oxidisable compound is (87),



Where the pH is high and the permanganate ion is in excess, the manganate ion is formed,



However in acid solution the oxidising power of the permanganate is much greater,



the manganous ion being formed.

Nevertheless, POSSELT and REIDIES (72) gave a number of definite reasons for the choice of the optimum pH range given above.

- i) in the strongly acid region,  $\text{KMnO}_4$  solution is extremely corrosive, necessitating the use of expensive materials for equipment construction,

- ii) a pH just below 7, in the barely acid region, generally halts most of the permanganate reaction,
- iii) hydroxyl ions catalyse the permanganate oxidation of organic compounds,
- iv) a pH in the alkaline region means that any malodorous lower fatty acids formed by the oxidation of the corresponding alcohols or aldehydes will be retained as odourless alkali metal salts in the scrubbing solution,
- v) a pH far beyond 10 may result in excessive consumption of  $\text{KMnO}_4$ , due to needless secondary oxidation of the primary oxidation products.

To maintain the solution alkalinity in the face of the possibly acidic nature of the polluted air stream, they suggested the use of suitable buffers, such as sodium bicarbonate, sodium carbonate or borax.

### 3.1.2 Experimental Program

The experiments described below were designed to examine the ability of aqueous buffered  $\text{KMnO}_4$  solution to destroy the odorous constituent of air streams containing low concentrations of either  $\text{H}_2\text{S}$  or  $\text{C}_2\text{H}_5\text{SH}$ .

### 3.2 Experimental Apparatus.

The apparatus was designed to produce a stream of air containing very small known concentrations of  $\text{H}_2\text{S}$  or  $\text{C}_2\text{H}_5\text{SH}$ , and to bring it into contact with the solution under test, usually alkaline  $\text{KMnO}_4$ , in a bubble type reaction vessel.

### 3.2.1 The Air Scrubbing Train.

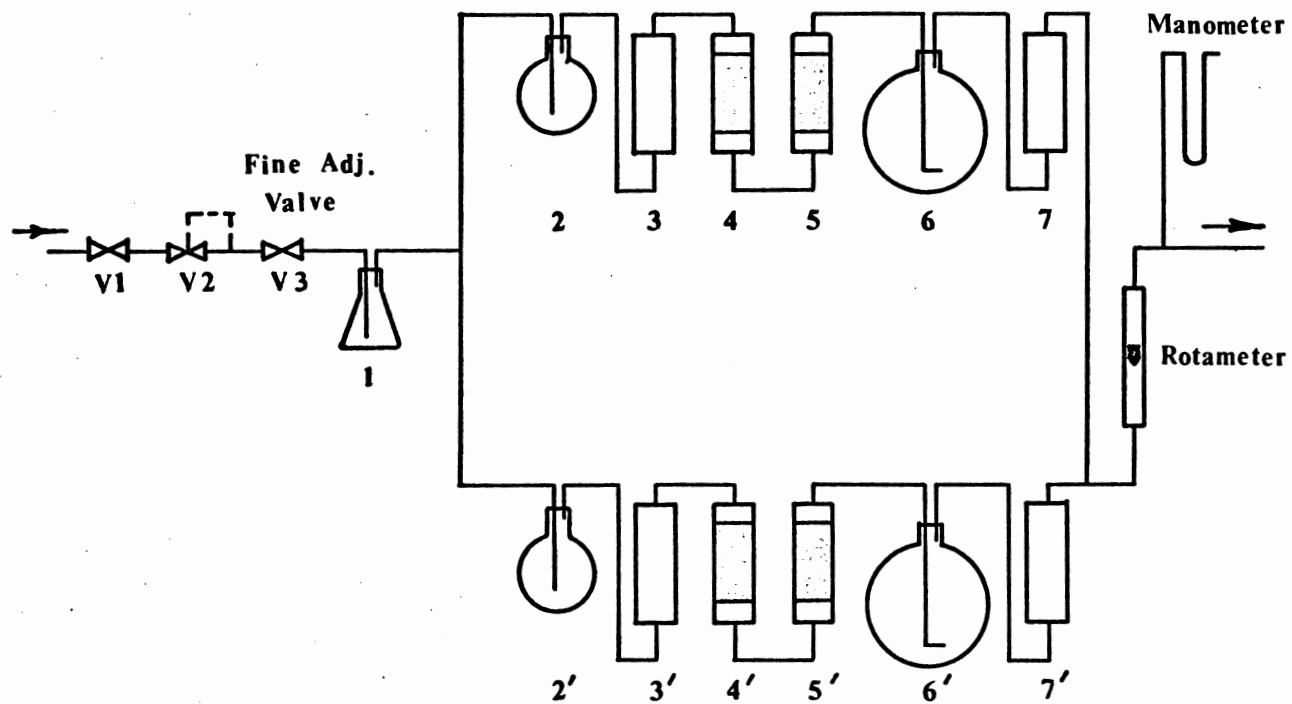
This section of the apparatus is shown in Figure 3.1. Air, from a compressor and pipeline system at a pressure of 120 psig, was fed into the apparatus via valve V1 and constant pressure regulator, V2. The regulator was set to give an outlet pressure of 5 psig.

TABLE 3.1.

#### Details of Air Purification System

(Refer to Figure 3.1).

VESSEL NO.	DESCRIPTION OF VESSEL AND CONTENTS	PRINCIPAL FUNCTION.
2,2'	2 litre conical flask, empty.	Removal of comparatively large particles.
2,2'	3 litre erlenmeyer flask containing 1.5 l. of 10% KOH solution; gas distribution through an 0.5 cm. I.D. tube.	CO <sub>2</sub> removal.
3,3'	6 cm. O.D. glass tube containing 750cc. of loosely packed glass wool.	Solid particles and droplet removal.
4,4'	6 cm. O.D. glass tube containing 330cc. of B.D.H. brand granular activated charcoal.	Vapour and odour removal.
5,5'	6 cm. O.D. glass tube containing 610 cc. of B.D.H. brand granular activated charcoal	Vapour and odour removal.
6,6'	3 litre erlenmeyer flask ("quickfit") containing 1.5 l. of distilled water; sintered glass (porosity No.1) gas distribution tube.	Humidification of the air stream.
7,7'	6 cm. O.D. glass tube containing 400 cc. of loosely packed glass wool.	Droplet removal.



**FIGURE 3.1**  
**AIR SCRUBBING TRAIN**

Because the air was supplied by an oil lubricated compressor, it was passed through an efficient purifying system prior to use. This system consisted of two parallel scrubbing trains, which taken together, provided the full airflow capacity required for the planned experiments. Details of the contents and purpose of each of the vessels in the trains are set out in Table 3.1.

### 3.2.2 H<sub>2</sub>S Injection System, Reaction Vessel and Ancillary Equipment. (Fig. 3.2)

This section of the apparatus was designed to continuously feed a small quantity of H<sub>2</sub>S gas at a controlled rate into the stream of purified air, and to achieve intimate contact between the pollutant rich air and the solution under test in a suitable reactor.

Both the wet and dry bulb temperatures of the incoming air stream were determined using copper-constantan thermocouples (T1 and T2) and an ice-water solution cold junction. The thermocouples were firstly calibrated against a thermometer accurate to 0.1°C. The cold junctions were contained in a vacuum insulated vessel. Leads from the junctions were connected via a multi-switch, to a Cambridge Portable Potentiometer calibrated to 0.01 mV.

The H<sub>2</sub>S was continuously fed into the purified air stream at a constant rate from a mechanically operated, all glass hypodermic syringe, as illustrated in Figure 3.3.

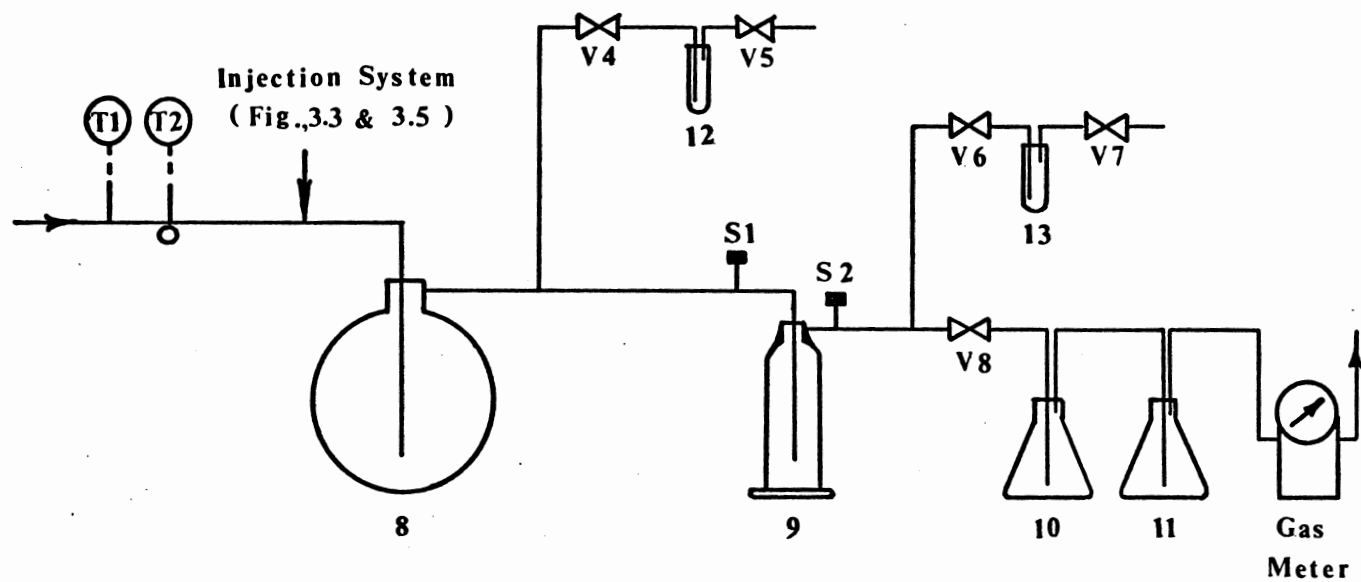


**FIGURE 3.2**

**REACTION VESSEL AND ANCILLARY EQUIPMENT**



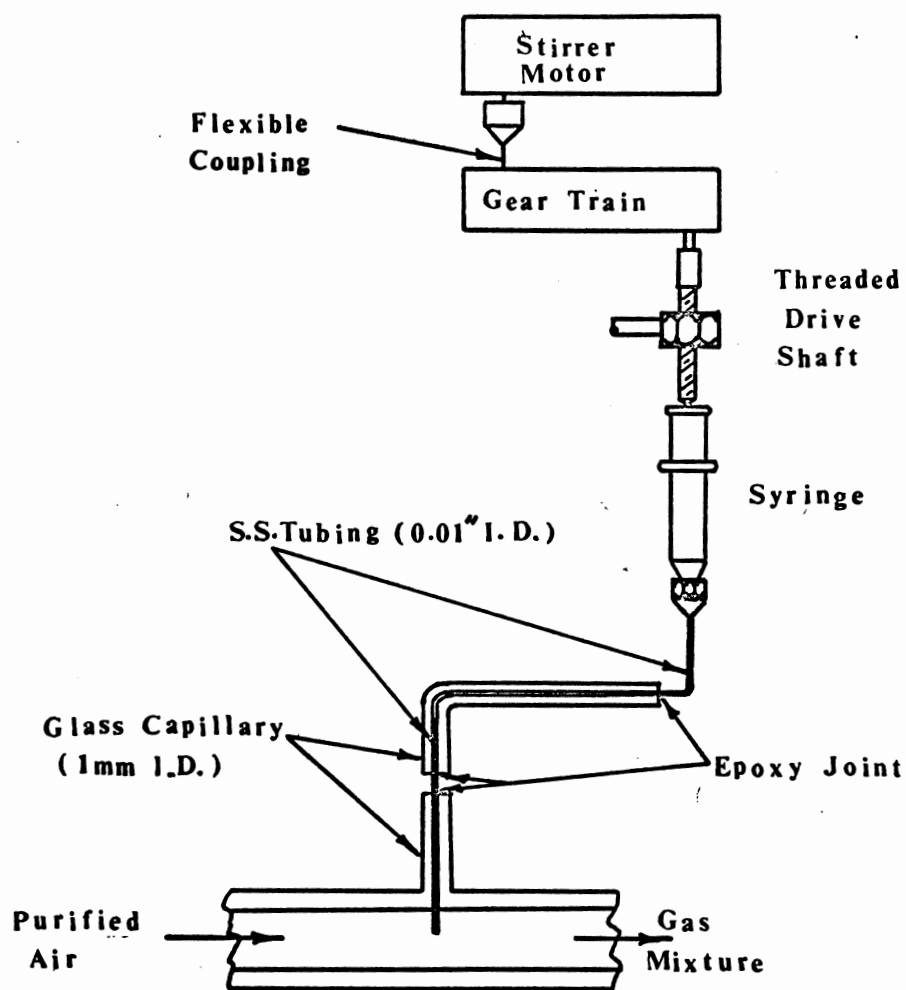


**FIGURE 3.3**

**HYDROGEN SULPHIDE INJECTION SYSTEM**

To assist in smooth, gas tight operation of the syringe, silicone grease was applied to both the barrel and the plunger.

The mechanical operating system consisted of a "Caframo" brand, variable speed laboratory stirrer, connected, via reduction gearing, to a threaded push-rod which drove the syringe plunger at rates between 1.54 and 0.04 inches/minute. Details of the gear train mechanical data and the syringe data are given in Table 3.2. Originally, the  $H_2S$  driven from the syringe was carried to the air stream through 9 inches of 0.01 inch I.D. stainless steel hypodermic syringe needle tubing. However, it was found that oxidation of the  $H_2S$  to sulphur within the tube lead to tube blockages after about 200 to 300 hours of operation. This difficulty was overcome by replacing part of the length of stainless steel tubing with glass capillary tubing, as detailed in Figure 3.3. An epoxy resin adhesive was used to join the stainless steel tubing and the glass capillary. As illustrated in the above figure, this joint was always made such that there were four or more centimetres between the adhesive and the air stream.

Particular attention was paid to the design of the joints in the air stream. Between the activated carbon-filled vessels in the air purifying train, (vessels 4, 5, 4', and 5') and the point of  $H_2S$  injection, all joints were made with polythene tubing. However, downstream of the  $H_2S$  injection point, were such plastic, or even rubber connections

might possibly have caused a significant change in the  $H_2S$  concentration, the joints were made with ground glass cones and sockets.

TABLE 3.2

Gear Train Mechanical Data and Syringe Data.

Gear train reduction ratio at main output shaft = 50:1

Number of output shaft turns per inch of travel

of plunger = 26 turns per inch.

Syringe Data.

Type - all glass hypodermic with stainless steel luer locking needle attachment.

Brand - "Superevaglass u-micromatic".

Volume expressed per inch of plunger movement.

10 ml syringe = 4.35 ml/inch.

5 " " = 2.73 "

2 " " = 1.70 "

The air/ $H_2S$  mixture leaving the injection point passed firstly to a 10 litre mixing vessel and then to the reaction system. The reactor was constructed from a 500 ml. Quickfit Drechsel bottle as shown in Figure 3.1.

Gas stream sample points for odour measurement, consisting of permanently fixed hypodermic syringe needles, were provided before and after this vessel. Samples for  $H_2S$  concentration measurement were taken via valves V4 and V6 (Figure 3.2) using the apparatus described in section 2.2.

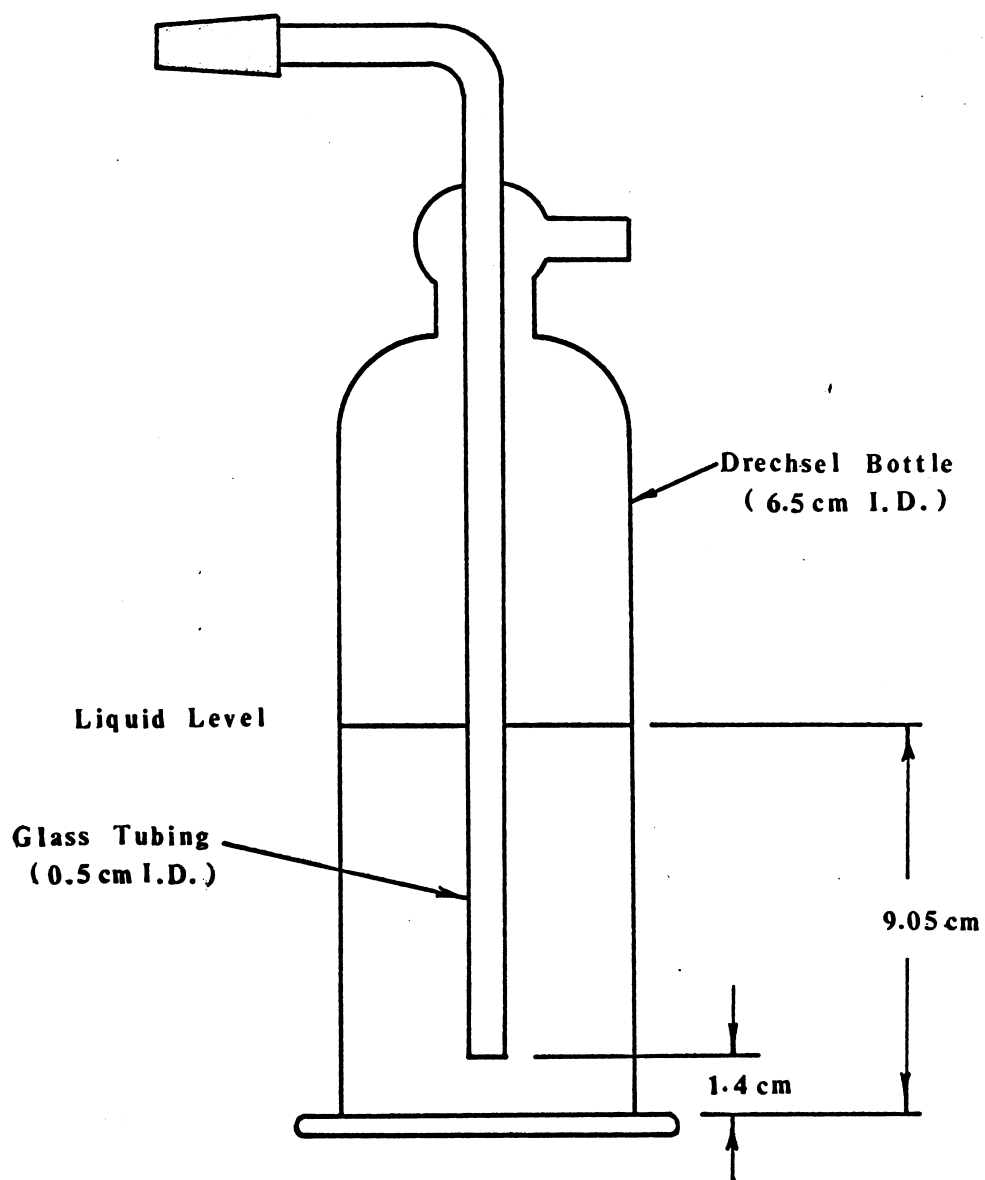


**FIGURE 3.4**

**DETAILS OF THE ABSORPTION-REACTION VESSEL**

Outlet valves (V5 and V7) were also provided on the sample absorbers so that the internal pressure of the apparatus could be regulated during sampling.

The gas leaving the reactor was then scrubbed of any remaining contaminants in a vessel containing a 5% alkaline solution of  $\text{KMnO}_4$ . From this it passed next through a glass tower loosely packed with glass wool, and finally through a "dry" gas meter (Smiths Meters Ltd., London) possessing a 6 inch dial and a minimum calibration of  $0.02\text{ft}^3$ .

### 3.2.3 Ethyl Mercaptan Injection System.

The dosing system for injecting gaseous ethane thiol (ethyl mercaptan) into the air stream is shown in Figure 3.5. In this system, the mechanical drive arrangement described above, in section 3.2.2., was used to force nitrogen (or air) from an all glass hypodermic syringe through about 9" of 0.01" I.D. stainless steel tubing into a glass vial of 10 ml. capacity containing about 5 ml. of the thiol. To maintain a steady, known rate of thiol vapourisation, the vial was contained within a water-bath whose temperature was measured using a mercury in glass thermometer capable of registering a minimum difference of  $0.1^\circ\text{C}$ .

The thiol enriched gas issuing from the vial then passed into the stream of deodorised and purified air leaving the air scrubbing train.

Although REID (92) has suggested that the oxidation of mercaptans by air, in the absence of a catalyst,

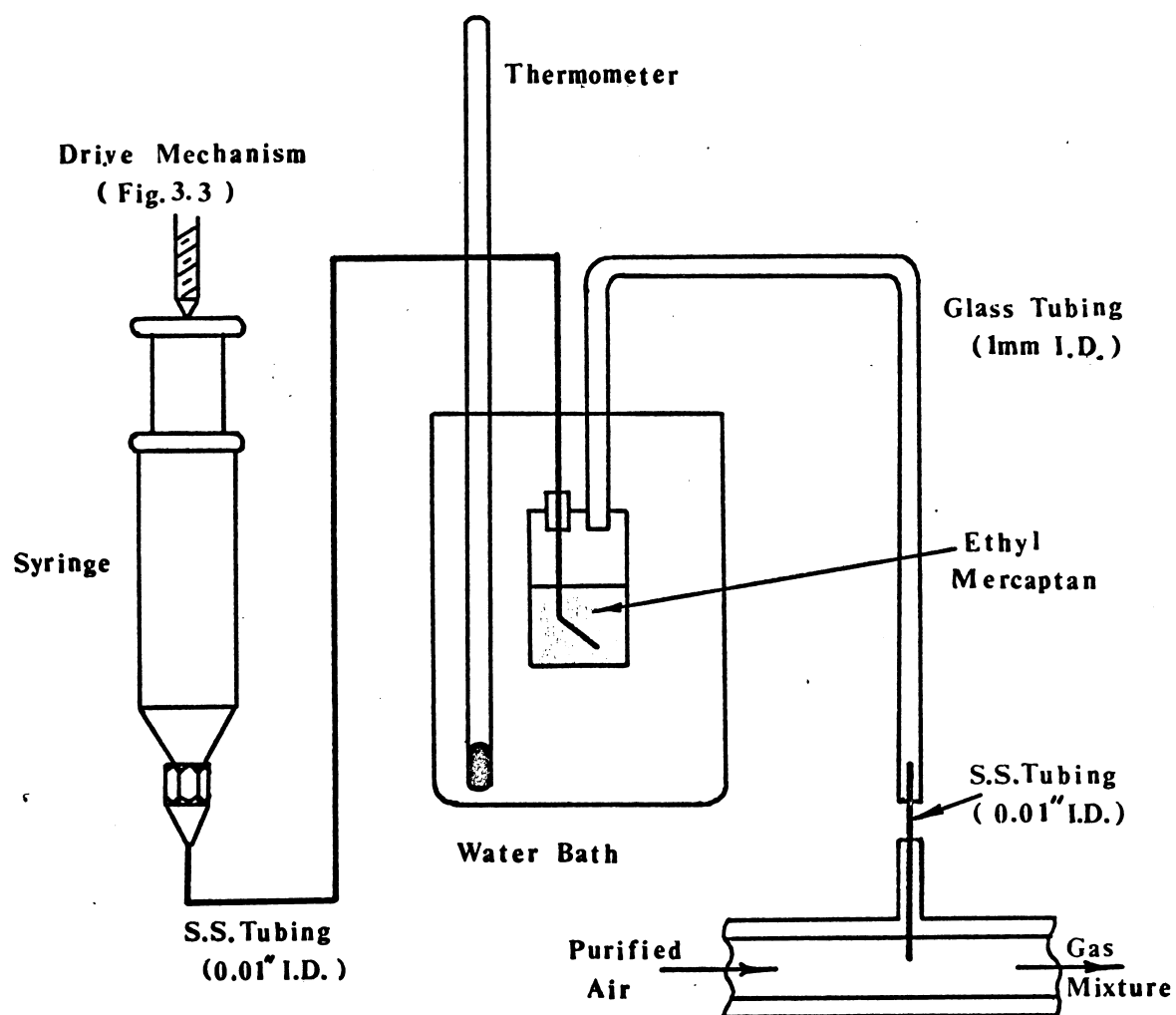


**FIGURE 3.5**  
**MERCAPTAN INJECTION SYSTEM**

is extremely slow, and may not even occur at all, precautions were taken against the possibility of oxidation of the thiol within the 10 ml. glass container. These comprised of,

- (a) the replacement of the air which was used as a carrier gas for the first few runs, by nitrogen, and
- (b) periodic replacement of the thiol.

#### 3.2.4 pH Measurement.

Measurement of pH was carried out using an EIL model 23A direct reading pH meter (Electronic Instruments Ltd., England) capable of reading down to 0.1 of a pH unit.

#### 3.3 Chemicals.

Two different sources of  $H_2S$  were employed during these experiments. The initial few experiments, Runs 3.1 to 3.6, were carried out using  $H_2S$  produced in a "quickfit" gas generating bottle by the gradual addition of deaerated 40%  $H_2SO_4$  solution to previously washed sodium sulphide crystals. The  $H_2S$  so evolved was passed through cold saturated barium hydroxide solution, yielding finally  $H_2S$  of about 95% purity. This method was based on the system described by MELVILLE and GOWENLOCK (103).

The remaining experiments were carried out by drawing C.P. grade  $H_2S$  direct from a cylinder supplied by the Mathieson Gas Co. Inc. of the U.S.A. This gas was of 99.6% purity, or better.

The ethane thiol was supplied by B.D.H. Ltd., with

a minimum purity of 99.5%.

All other chemicals used during these experiments were of A.R. grade.

### 3.3.1. Hydrogen Sulphide Storage System.

To facilitate the filling of the syringe for the  $\text{H}_2\text{S}$  injection system described above, a  $\text{H}_2\text{S}$  storage system was devised. In this system the  $\text{H}_2\text{S}$  was stored in a 250ml. gas storage bottle over water which had been previously acidified with  $\text{H}_2\text{SO}_4$  and saturated with  $\text{H}_2\text{S}$ . ( See Figure 3.6).

During storage and withdrawal of the gas, a positive pressure was maintained within the reservoir with the aid of the attached levelling bottle. So as to expose a minimum liquid surface area to the external air, the liquid within the levelling bottle was always maintained such that the surface fell within a narrow extension arm.

Withdrawal of gas from the reservoir required that the upper valve, V1 be turned on. The sample was then taken in a hypodermic syringe fitted with a 26 gauge stainless steel needle, by merely plunging the syringe needle through the septum seal and the valve orifice into the upper section of the gas storage vessel.

The septum seal was of the type used for gas chromatography, and was fixed in place with an epoxy resin adhesive.



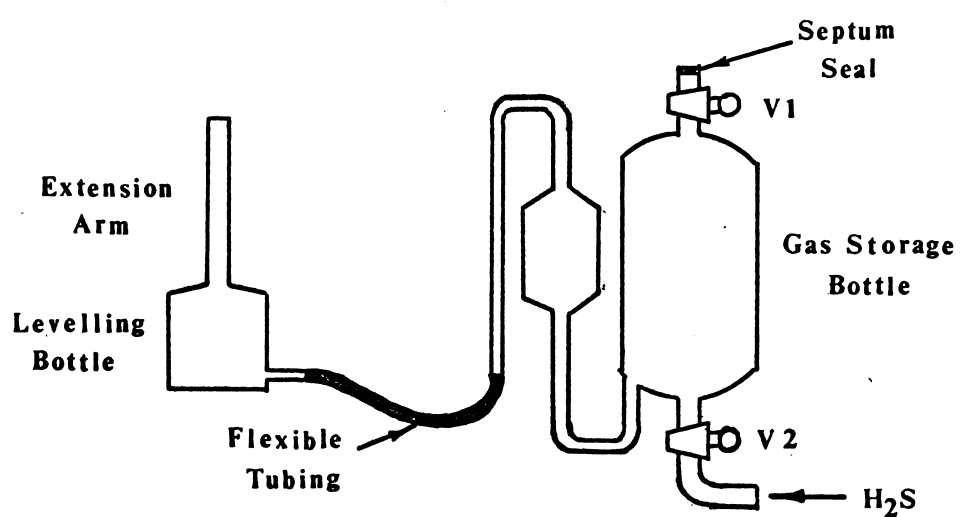


**FIGURE 3.6**  
**HYDROGEN SULPHIDE STORAGE SYSTEM**

### 3.4 Experimental Procedures.

Prior to the commencement of each run, the following items were examined and adjusted.

#### 3.4.1. Adjustment of the Internal Gas Pressure.

Maintenance of a continuous, steady  $\text{H}_2\text{S}$  or  $\text{C}_2\text{H}_5\text{SH}$  input rate demanded careful control of internal gas pressures. This was achieved by adjustment of valves V2, V3, V4 and V5 as detailed below.

Three hundred mls. of water were pipetted into the reactor, and 25mls. pipetted into each of the inlet and outlet sample bubblers (vessels 12 and 13, Figure 3.2). With the outlet pressure of the constant pressure regulator (V2, Figure 3.1) set to 5 p.s.i.g., the flowrate of the airstream was set to the required level using the fine adjustment valve V3. The internal pressure corresponding to this flowrate was then noted. The flow path was then altered to pass through the inlet sample bubbler (vessel 12, Figure 3.2) and the internal pressure set to the value noted above, by operation of outlet valve V5. This operation was repeated using the outlet sample bubbler (vessel 13) and outlet valve V7. The water was then removed, and the vessels dried.

#### 3.4.2 The Test Solution.

The test solution was prepared by dissolving the required amount of A.R. grade potassium permanganate in water, and adding a measured quantity of buffer reagent (eg.  $\text{K}_2\text{B}_4\text{O}_7 \cdot 5\text{H}_2\text{O}$ ). Just prior to the commencement of each run, the concentration

of  $\text{KMnO}_4$  in the solution was accurately determined by titration against 0.01 N.  $\text{As}_2\text{O}_3$  solution using the procedure described by VOGEL (95). The solution pH was also measured.

A fresh test solution was prepared daily.

#### 3.4.3 Procedure During Gas Bubbling Runs.

Three hundred mls. of test solution were pipetted into the reactor and 25 mls. of the fluorescent reagent, of the required strength, pipetted into each of the sample bubblers.

With fine adjustment valve V3 preset in the manner described above, it was necessary only to fully open the main valve V1, to automatically attain the desired gas flowrate.

#### 3.4.4 Normal Runs.

A hypodermic syringe of the desired volume filled with the appropriate gas ( $\text{H}_2\text{S}$  or nitrogen, depending on the absorption run in progress) was connected to the injection system. The variable speed stirrer motor was then started and adjusted to give the required gear train drive speed, and thus the required pollutant injection rate. The air flow was then brought to the desired level by opening valve V1, with valves V6 and V8 closed, and adjusting valve V4 to give an internal gas pressure equal to that noted above (section 3.4), vessel 12 being disconnected from the apparatus for this operation.

The gas issuing from valve V4 was allowed to impinge upon a filter paper saturated with lead acetate solution. Immediately the darkening of this paper had

indicated the presence of pollutant in the stream, V8 was opened and V4 closed, thus diverting the stream through the reactor. The internal gas pressure was again checked and re-adjusted if required.

The pollutant concentration and the odour intensity of the gas stream were then determined using the procedures described below. Measurements were taken on both inlet and outlet streams of the absorber reactor system. In some instances these were repeated several times at regular intervals throughout the run.

Generally, the syringe drive speed was such that the gas within the syringe was exhausted within 20 to 35 minutes. As soon as the plunger height indicated that this was the case, the run was stopped. To achieve this the air stream was first released to atmosphere by opening V4, the syringe drive motor stopped, and the air flow finally stopped by operation of V1.

At the end of the run, the time and the volume of gas registered by the gasmeter were recorded. The reactor was then disconnected from the apparatus and the  $\text{KMnO}_4$  solution pH and concentration measured. The latter was determined by titration against  $\text{As}_2\text{O}_3$ , again using the method described by VOGEL (95).

At the end of each run the wet and dry bulb gas temperatures were also recorded. During each run records were also made of the atmospheric pressure, atmospheric temperature,

the gas flowrate indicated by the rotameter and the syringe drive speed.

#### 3.4.5 Extended Runs.

It was required, in some cases, that the runs continue for 2-3 days, or more. This was achieved by stopping the run and refilling and replacing the syringe when required. The run was then re-started as detailed above.

One of the advantages of the syringe drive system was that on re-starting, it would return immediately and accurately to its preset speed. After the air flow had re-started, the stream was allowed to pass through valve V4 until the darkening of lead acetate soaked filter paper held at the outlet from this valve indicated the presence of pollutant. The stream was then diverted through the reactor and the run completed as described above.

#### 3.4.6 Measurement of the Gas Stream Pollutant Concentration.

The concentration of each of the two pollutants employed during these tests ( $\text{H}_2\text{S}$  and  $\text{C}_2\text{H}_5\text{SH}$ ) was measured using the fluorometric technique described in Chapter 2.

To apply this technique, the sample bubbler, shown in Figure 2.1, was filled with 25 mls. of the fluorescent reagent solution and connected to the main apparatus. As described in Section 3.4.1 above, the outlet valve on each bubbler (valves V5 and V7) had previously been set to maintain a constant internal gas pressure during all operations.

The inlet concentrations were measured by operating valves V4 and V8 such that the gas stream was diverted through the sample bubbler for the appropriate sampling period (measured by a stopwatch). These sampling periods were generally chosen on the basis of experience, to ensure that the solution fluorescence was measured within the "linear" portion of the calibration curve.

Outlet concentrations were determined in a similar manner by operation of valves V6 and V8. The differential weight of pollutant absorbed by the test solution was read directly from the appropriate calibration curve.

For conversion of this value to concentration units, the flowrate of gas through the fluorescent solution was taken equal to that which had been flowing through the main apparatus.

### 3.5 Odour Measurement.

Odour measurements were taken using the A.S.T.M. D1391-57 (44) procedure described above in section 1.3.5.

The samples for measurement were taken in 100 ml. all glass, luer locking hypodermic syringes, Caps for these syringes were constructed from shortened and sealed 26 gauge hypodermic syringe needles. A transfer needle was also constructed to the design recommended in the above A.S.T.M. procedure. For greater ease of operation the recommended "transfer" syringes of 2 ml. and 100 ml. capacity were supplemented by one of 10 ml. capacity. All of the 100 ml.

syringes were clearly marked to distinguish "sample", "dilution" and "transfer" syringes.

#### The Odour Panel.

The odour panel consisted of three members, each of whom was subjected to the restrictions stipulated in the above standard method. Maximum dilution was assumed to have been obtained when there was a consistently positive answer from at least two of these panel members.

#### 3.6 Calculations.

An I.B.M. 1620 computer was used to calculate the inlet and outlet  $\text{H}_2\text{S}$  and  $\text{C}_2\text{H}_5\text{SH}$  concentrations, the weights of the various reactants consumed in the reaction, the average air flowrate, and a number of cumulative values. The method is illustrated by a sample calculation given in Appendix E.

#### 3.7 Discussion of Results and Conclusions.

##### Hydrogen Sulphide Absorption.

The initial runs (3.1 to 3.11), the results of which are given in Tables B1 and B7, were designed to gather preliminary data for assessment purposes. In these runs the  $\text{KMnO}_4$  solution pH was varied between 6.8 and 9.3, the inlet gas  $\text{H}_2\text{S}$  concentration between 12.0 and 28.3 ppm (v/v), and the average gas flowrate between 1.8 and 3.1 l/min. In each case the molar ratio "R" of the  $\text{KMnO}_4$  reduced during the run to the  $\text{H}_2\text{S}$  absorbed by the solution, was calculated.

The results serve to emphasise the importance of buffering the pH to a suitable value during  $\text{H}_2\text{S}$  absorption.

Wherever the buffer was in excess of that required to maintain a high pH, the outlet  $\text{H}_2\text{S}$  concentration was low and relatively steady for long periods.

The results also emphasise the inconsistencies in the values of "R". These suggest the existence of complex side reactions considerably different from those postulated by the equations given in section 4.2

Runs numbered 3.12 and 3.13 were designed to examine the behaviour of the permanganate solution during extended absorption periods. The initial  $\text{KMnO}_4$  concentration was 0.01% by weight, in an aqueous solution buffered to pH 9.25 by 0.1% by weight potassium tetraborate ( $\text{K}_2\text{B}_4\text{O}_7 \cdot 5\text{H}_2\text{O}$ ).

The results are given in Tables B2, B3 and B8. The consistency of the readings for the outlet  $\text{H}_2\text{S}$  concentration can be taken as a measure, not only of the reliability of the analytical technique, but also of the stability of the  $\text{H}_2\text{S}$  injection system.

Run 3.13 also serves to demonstrate the ability of the reaction product within the liquor to continue the  $\text{H}_2\text{S}$  oxidation well beyond the point at which all permanganate ion disappears from solution. In this case, all evidence of the ion had disappeared before the fortieth operating minute had elapsed, that is, before approximately one quarter of the run had progressed.

This observation is also supported by the results of run 3.19, which are given in Tables B5 and B9. In this run an aqueous solution containing 0.02%  $\text{KMnO}_4$  by weight, buffered



to a pH of 9.25 by 0.4 g/l of potassium tetraborate, was used to absorb  $\text{H}_2\text{S}$  from an air stream containing an average of 47.4 ppm  $\text{H}_2\text{S}$  (v/v), until the concentration of  $\text{H}_2\text{S}$  in the outlet stream had risen to a value of about 30 ppm (v/v). The variation in the outlet  $\text{H}_2\text{S}$  concentration throughout this run is shown graphically in Figure 3.7.

In this case all evidence of the permanganate ion had disappeared before the end of run 3.19.2, that is, before  $8.5 \times 10^{-3}$  g. of  $\text{H}_2\text{S}$  had been absorbed by the solution. The total weight of  $\text{H}_2\text{S}$  absorbed during the run, computed from each individual gas stream  $\text{H}_2\text{S}$  measurement, was found to be 0.20g. This was in reasonable agreement with the value of 0.18g. determined by analysis of the final product.

As a qualitative measure of the importance of the reactive manganese species in this absorption process, runs 3.14 to 3.18, and run 3.26, were carried out in the absence of any such species, using only buffered and unbuffered water as the solvent. The absorption of  $\text{H}_2\text{S}$  in alkaline buffered water has been studied in detail by ASTARITA and GIOIA (165) (166), who showed that the chemical reaction occurring in the liquid phase could be considered instantaneous with respect to the diffusional processes.

As may be readily observed by reference to the results of these runs (Tables B4, B8, B6 and B10), saturation of the liquid phase was relatively rapid. The importance of the manganese species to the absorption process is obvious.

Av. Inlet  $\text{H}_2\text{S}$  Conc.  
= 47.4 ppm v/v

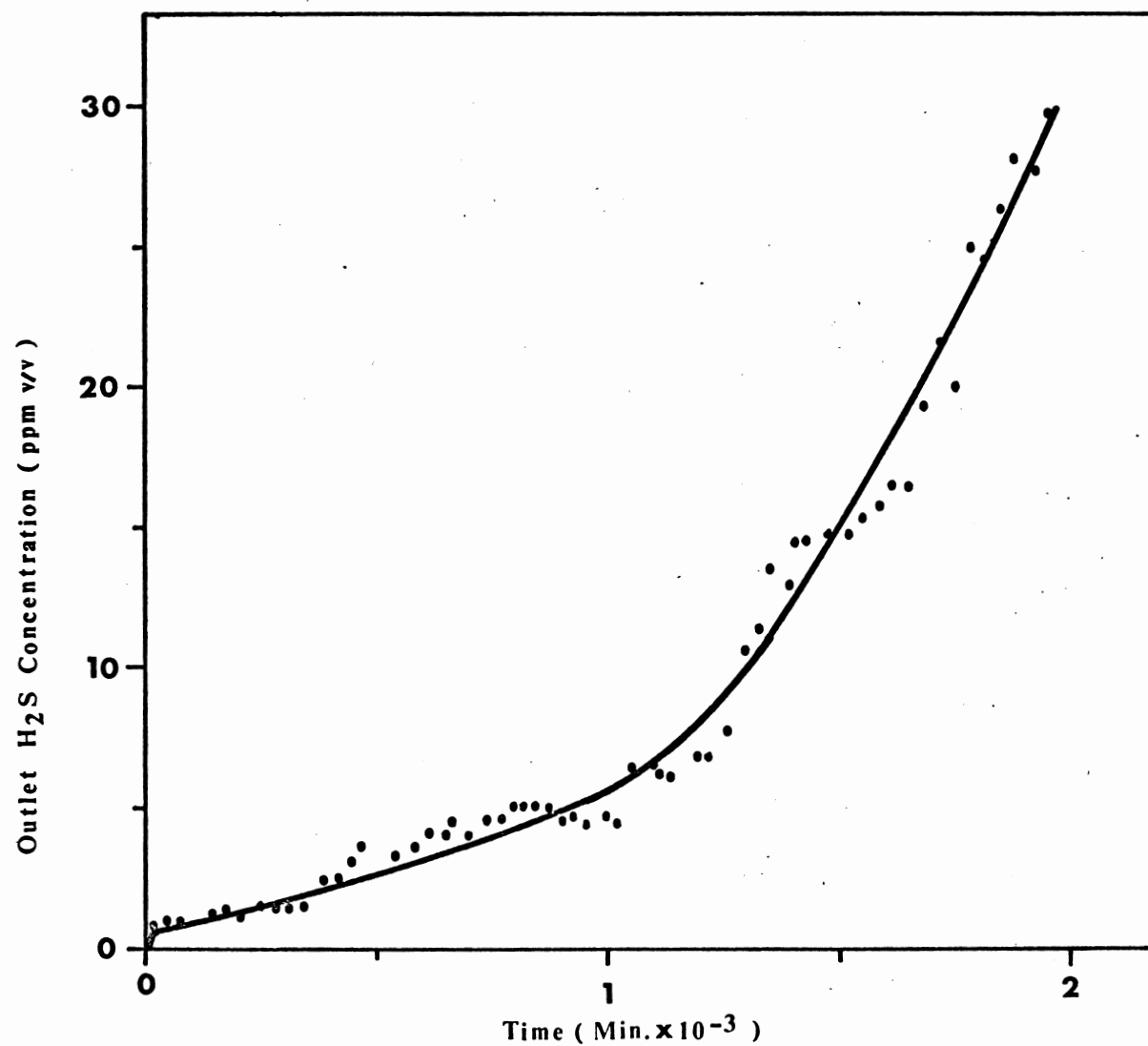


FIGURE 3.7 VARIATION OF THE OUTLET HYDROGEN SULPHIDE CONCENTRATION  
WITH TIME ( RUN 3.19 )

Runs numbered 3.20 to 3.22 demonstrate that the form of the manganese species may also be important. Each of these runs utilised an absorption solution containing a precipitate of "manganese oxide" of unknown composition. The precipitate for runs 3.20 and 3.21 was prepared by the neutralisation and air oxidation of manganous chloride solution, while the precipitate for run 3.22 was prepared by reaction of aqueous  $\text{KMnO}_4$  solution with excess sodium sulphide solution, followed by neutralisation and air oxidation. The manganese content of the solutions used in each of these runs was similar, approximating that found in 0.02%  $\text{KMnO}_4$  solution. Since it would be reasonable to assume that the chloride ion has no effect on the reaction, then the results emphasise the superiority of the oxide prepared for run 3.22.

The importance of manganese in this absorption process is further demonstrated by the results of runs 3.23 to 3.25. Here the aqueous solvent solution contained 0.02% potassium dichromate by weight, and was buffered to pH 9.2, 7.0 and 10.9 respectively. In no case did the results indicate the existence of a reaction mechanism capable of enhancing the absorptive capacity much beyond that obtainable with buffered water alone.

Overall, these results confirm the findings of POSSELT and REIDIES (72) who used a similar reactor and 1%  $\text{KMnO}_4$  solution to obtain "rapid and complete" oxidation of  $\text{H}_2\text{S}$ .

However, there is no evidence to suggest that a 1%  $\text{KMnO}_4$  solution is superior, per unit of permanganate usage, to solutions containing as little as 0.01% by weight.

Under the conditions of these tests, which were deliberately chosen to simulate practical situations, the reaction product itself appeared to be an efficient agent capable of promoting sulphide oxidation, and thus capable of continuing the  $\text{H}_2\text{S}$  elimination far beyond the point at which all permanganate ions had disappeared from solution.

#### Ethyl Mercaptan Absorption.

Runs numbered 3.28 to 3.36 (Tables B11 and B12) were carried out using ethyl mercaptan as the gaseous air stream contaminant. While run 3.33 and run 3,34 both employed only buffered water as the solvent, the remainder employed aqueous  $\text{KMnO}_4$  solutions buffered with either potassium tetraborate ( $\text{K}_2\text{B}_4\text{O}_7 \cdot 5\text{H}_2\text{O}$ ) or anhydrous potassium carbonate.

Again the results indicated that reaction products with significant oxidative powers were formed. Thus for run 3.35, where all evidence of permanganate ion had disappeared before  $18 \times 10^{-3}$  g of  $\text{C}_2\text{H}_5\text{SH}$  had been absorbed, elimination of the pollutant continued at a reasonable level throughout the entire run. The outlet concentration of  $\text{C}_2\text{H}_5\text{SH}$ , as a function of the cumulative weight of pollutant absorbed, is given in Figure 3.8 for both runs 3.35 and 3.36. In the latter case, where the absorption solution contained 0.2%  $\text{KMnO}_4$  by weight, all evidence of the permanganate ion had disappeared before a cumulative

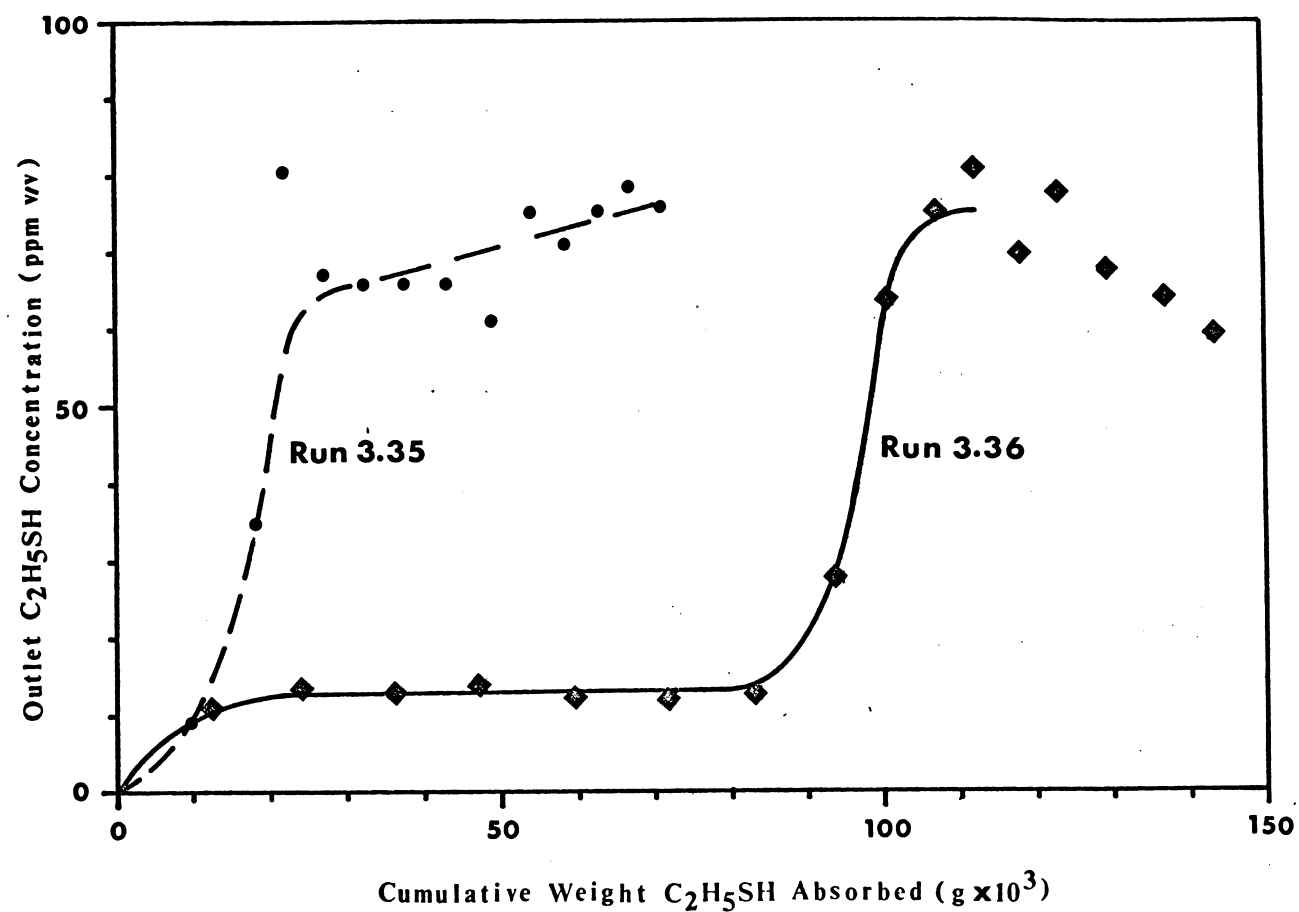


FIGURE 3.8 ETHYL MERCAPTAN ABSORPTION, OUTLET MERCAPTAN  
CONCENTRATION VERSUS CUMULATIVE WEIGHT  
ABSORBED FOR RUNS NO. 3.35 & 3.36

total of about 0.1 g of  $C_2H_5SH$  had been absorbed. By reference to the above figure it is obvious that the oxidative powers of the reaction products, while greatly inferior to that of the permanganate, were still significant.

#### Odour Measurements.

The easiest means of expressing the efficiency of odour removal is to assume that it is a direct function of the pollutant concentrations before and after the removal process. Under these conditions maximum efficiency would occur when the outlet pollutant concentration was less than the odour threshold.

As shown in Table B13, measurements over a number of runs failed to yield a consistent relationship between the odour levels and the respective pollutant concentrations. Nevertheless the results serve to emphasise the dramatic decrease in odour levels which can occur under the conditions of the tests.

CHAPTER 4.

THE REACTION OF HYDROGEN SULPHIDE  
AND ETHYL MERCAPTAN WITH POTASSIUM  
PERMANGANATE IN THE PRESENCE OF AIR.

#### 4.1 Introduction.

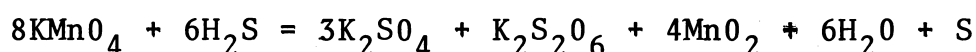
From the initial absorption trials, reported in Chapter 3, it was obvious that the equation describing the reaction of  $\text{H}_2\text{S}$  and  $\text{C}_2\text{H}_5\text{SH}$  with  $\text{KMnO}_4$  in the presence of air was considerably more complex than at first thought. Thus, the following tests were designed to clarify this situation, and to investigate the usefulness of the Stability Field Diagram for describing such systems.



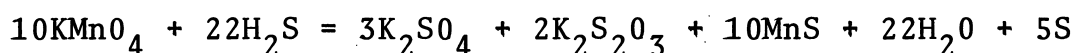
#### 4.2 The Reaction of $\text{H}_2\text{S}$ with $\text{KMnO}_4$ .

The reaction of  $\text{H}_2\text{S}$  with  $\text{KMnO}_4$  in neutral aqueous solution (turning alkaline) has been studied in detail by DUNNICLIFF and NIJHAWAN (88) (89) and MOHAMMAD and BEDI (90).

In general, they found that the reaction progressed in stages. The evidence presented in their papers indicates that the first stage may be represented by the equation,



With excess  $\text{H}_2\text{S}$  the hydrated  $\text{MnO}_2$  gave manganese sulphide, sulphur also being produced, whilst the dithionate yielded the sulphate and thiosulphate. The overall reaction might thus be represented by the equation,



In cold, neutral water, the reaction between dissolved  $\text{H}_2\text{S}$  and  $\text{KMnO}_4$  has been represented by the following equation(91),



##### 4.2.1 The Relevant Solid Phases of Manganese.

Manganese forms a number of reactive solid compounds in alkaline solution, which are of importance in the process described herein.

Manganese Hydroxide. ( $\text{Mn}(\text{OH})_2$ ), precipitates as a well defined gelatinous, white compound in alkaline solution, (87) (104) (105) (106). It rapidly darkens in the presence of oxygen, due to the formation of manganese oxide, generally believed to a hydrated manganese sesquioxide  $\text{Mn}_2\text{O}_3 \cdot x\text{H}_2\text{O}$ , which varies from

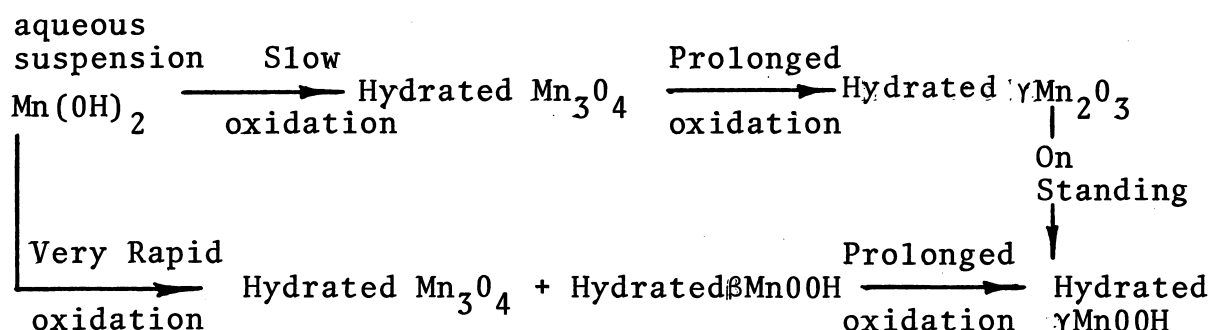
dark brown to black in colour (87) (105). BRICKER (107) who has made a detailed study of the manganese oxides, and the changes which occur during oxidation and reduction, has shown that the oxide resulting from the oxidation of the manganese hydroxide depends on the speed and severity of oxidation. Slow oxidation using either air free of  $\text{CO}_2$ , or oxygen gas, leads to the formation of  $\text{Mn}_3\text{O}_4 \cdot n\text{H}_2\text{O}$ , whilst rapid oxidation leads to the formation of a mixture of  $\text{Mn}_3\text{O}_4 \cdot n\text{H}_2\text{O}$  and  $\beta\text{MnOOH} \cdot z\text{H}_2\text{O}$ . Bricker's work supported the findings of OSWALD et al (109) who used air of accurately defined water vapour pressure to oxidise well crystallised  $\text{Mn}(\text{OH})_2$ .

Trimanganese Tetroxide ( $\text{Mn}_3\text{O}_4$ ) is a well defined cinnamon brown material which has been prepared in the laboratory by both thermal and aqueous techniques (107).

As mentioned above, it is a product of the slow oxidation of  $\text{Mn}(\text{OH})_2$ . After prolonged oxidation in an aqueous environment the tetroxide will darken in colour to yield  $\gamma\text{Mn}_2\text{O}_3 \cdot x\text{H}_2\text{O}$ .  $\gamma$  Manganese Sesquioxide ( $\gamma\text{Mn}_2\text{O}_3$ ) exhibits an X-ray diffraction pattern identical to that of the tetroxide with the exception of weakening or absence of some of the higher angle reflections. It is unstable at  $25^\circ\text{C}$  and one atmosphere total pressure, converting, after several months in suspension, to  $\gamma\text{MnOOH} \cdot y\text{H}_2\text{O}$  (107).

$\gamma$  Manganese Oxyhydroxide ( $\gamma\text{MnOOH}$ ) has been prepared in the laboratory by both thermal and aqueous techniques. It has a distinctive X-ray diffraction pattern, and is the final

product of air or oxygen oxidation of  $\text{Mn(OH)}_2$  (107)(109)(110). Thus the oxidation of an aqueous suspension of  $\text{Mn(OH)}_2$  by air or oxygen may be represented diagrammatically thus;



$\beta$  Manganese Oxyhydroxide ( $\beta \text{ MnOOH} \cdot z \text{ H}_2\text{O}$ ) is described in detail by BRICKER (107). It is one of the products obtained upon the rapid oxidation of  $\text{Mn(OH)}_2$ , and displays a distinctive x-ray diffraction pattern. It is unstable at  $25^\circ\text{C}$  and 1 atmosphere total pressure, yielding  $\gamma\text{MnOOH} \cdot \gamma \text{ H}_2\text{O}$ , after several months in suspension.

$\delta$ ,  $\beta$  and  $\gamma$  Manganese Dioxide. Both the  $\delta$  and the  $\gamma$  form of  $\text{MnO}_2$  can be prepared in the laboratory. However, the less reactive (104)  $\beta\text{MnO}_2$  (pyrolusite) is apparently the most stable form in the supergene environment, resisting synthesis at  $25^\circ\text{C}$  in the laboratory (107) (111).

A number of forms of  $\delta\text{MnO}_2$  have been prepared, varying in composition between  $\text{MnO}_{1.74}$  and  $\text{MnO}_{1.99}$ . These exhibit almost identical x-ray diffraction patterns, with the exception of line width and line intensity. Similarly a number of types of  $\gamma\text{MnO}_2$  have been prepared and examined.

Manganese Sulphide ( $\text{MnS}$ ) may be prepared in alkaline solution from Mn II salts (87) (104) or  $\text{KMnO}_4$ . Formation of sulphur may also occur during this step (112). It is not stable in air, gradually turning brown due to the formation of manganese oxides; both sulphate ion and elemental sulphur being formed.

There is some doubt as to whether the oxidation of  $\text{MnS}$  by a  $\text{CO}_2$  rich air stream will attain equilibrium in anything but an extended reaction period. HEM (108) who has examined the behaviour of suspended  $\text{MnS}$  in the presence of such an air stream, concluded that the oxidation of  $\text{MnS}$  is inhibited by the  $\text{MnCO}_3$  coating which forms around the particles.

#### 4.2.2 Discussion.

From the above data it appears to be well established that the major final product of the reduction of alkaline  $\text{KMnO}_4$  solution by  $\text{H}_2\text{S}$  is manganese sulphide. In the presence of oxygen the  $\text{MnS}$  is likely to react further, yielding various manganese oxides. The highest valency to be expected under the conditions of these experiments is the sesqui-oxide, the most likely form being  $\gamma\text{-MnOOH}$ .

#### 4.3 The Stability Field Diagram.

The stability field diagram, or Eh-pH diagram, is a plot of the redox potential against pH. It demonstrates the equilibrium relationships existing between the various soluble and insoluble compounds under consideration. Although application of this equilibrium diagram to the dynamic situation is theoretically impractical, it is useful insofar as it depicts

the limiting condition. Thus, it will diagrammatically depict the ultimate reaction path, whilst ignoring the relatively unstable intermediate products which are a feature of many reactions.

The diagrams are constructed using the following thermodynamic relationships (113) at 25°C and one atmosphere total pressure;

$$\Delta F^0 = -RT \ln K \quad - - - - 4.1$$

$$E_h = E^0 + \frac{RT}{nf} \ln \frac{a_{ox.}}{a_{red}} \quad - - - - 4.2$$

$$\text{where } E^0 = \frac{\Delta F^0}{nf} \quad - - - - 4.3$$

$$\text{and } R = 1.98717 \pm 0.00029 \text{ cal./deg.mol (114)}$$

$$T = 298.150^\circ K \text{ (113)}$$

$$f = 23,060.9 \pm 0.4 \text{ cal./abs. volt equiv. (114)}$$

Substituting in equ. 4.1.

$$\Delta F^0 = -1.3642 \log_{10} K \quad - - - - 4.4$$

and equ. 4.2.

$$E_h = E^0 + \frac{0.059157}{n} \log_{10} \frac{(a_{ox})}{(a_{red})} \quad - - - - 4.5$$

#### 4.3.1 The Reaction of H<sub>2</sub>S with Aqueous KMnO<sub>4</sub> in the Presence of Air - The Stability Field Diagram for the Experimental Conditions of This Study.

Stability field diagrams, depicting the probable systems existing during this experimental study were constructed (Figures 4.1 to 4.3) from various computed equilibria

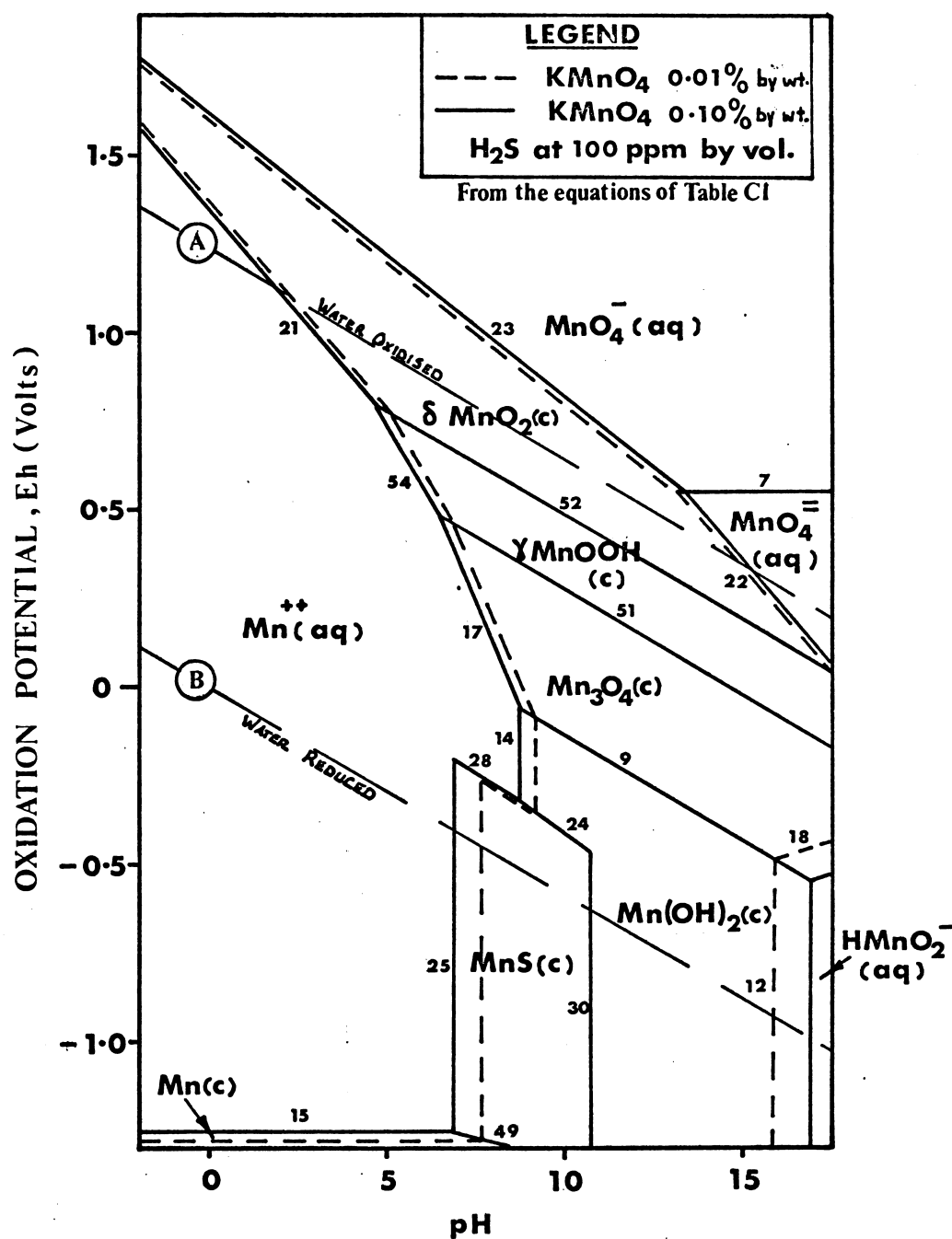
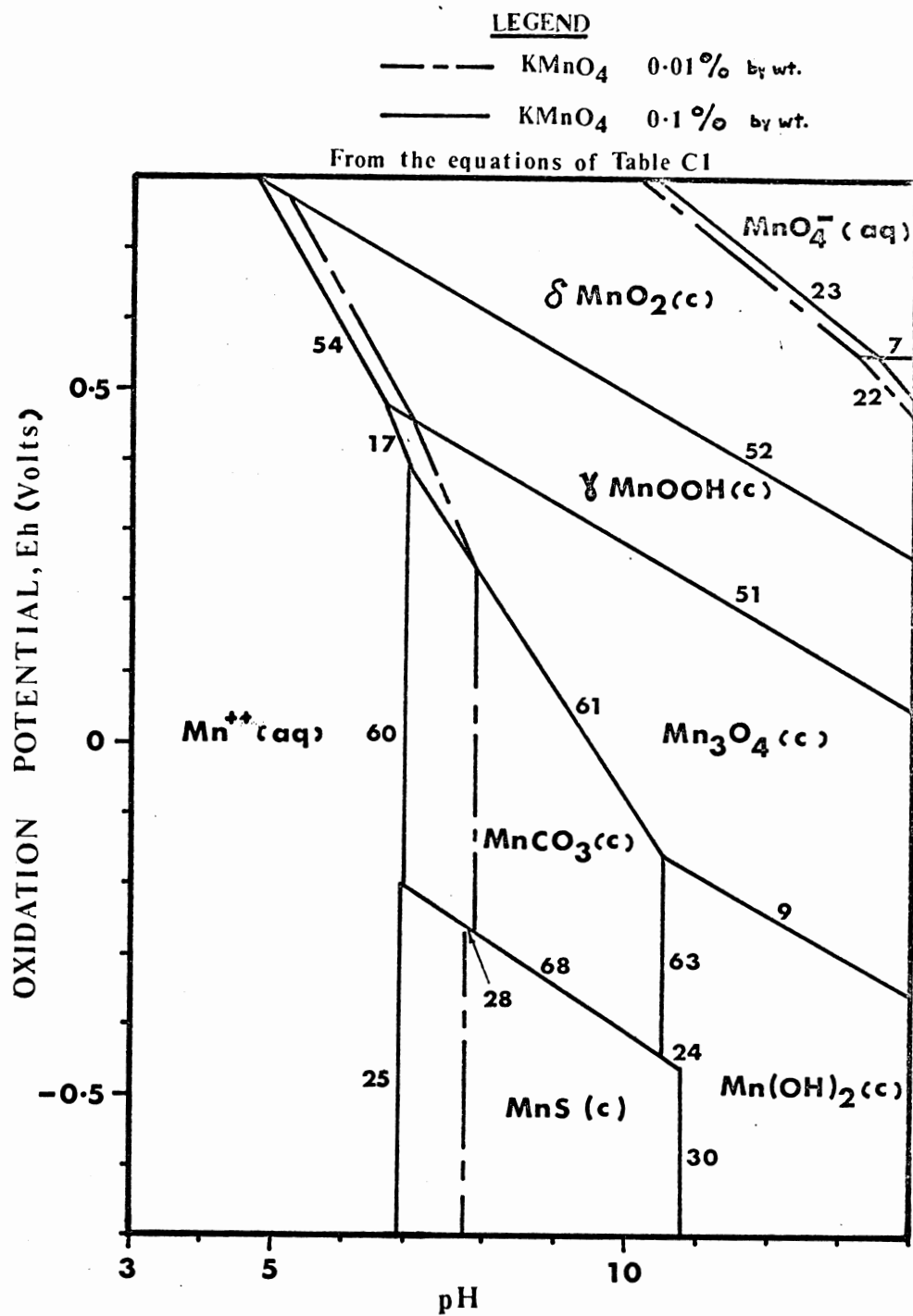


FIGURE 4.1

STABILITY FIELD DIAGRAM FOR MANGANESESPECIES AT 25°C(  $\text{KMnO}_4$  at 0.01% and 0.10% by wt. $\text{H}_2\text{S}$  at 100 ppm by vol. )



**FIGURE 4.2**

**STABILITY FIELD DIAGRAM FOR THE SYSTEM SHOWN  
 IN FIGURE 4.1 IN THE PRESENCE OF  $\text{CO}_2$**

**WHERE  $p\text{CO}_2 = 3 \times 10^{-6}$  ATM.**

**(Temp.  $25^\circ\text{C}$ )**

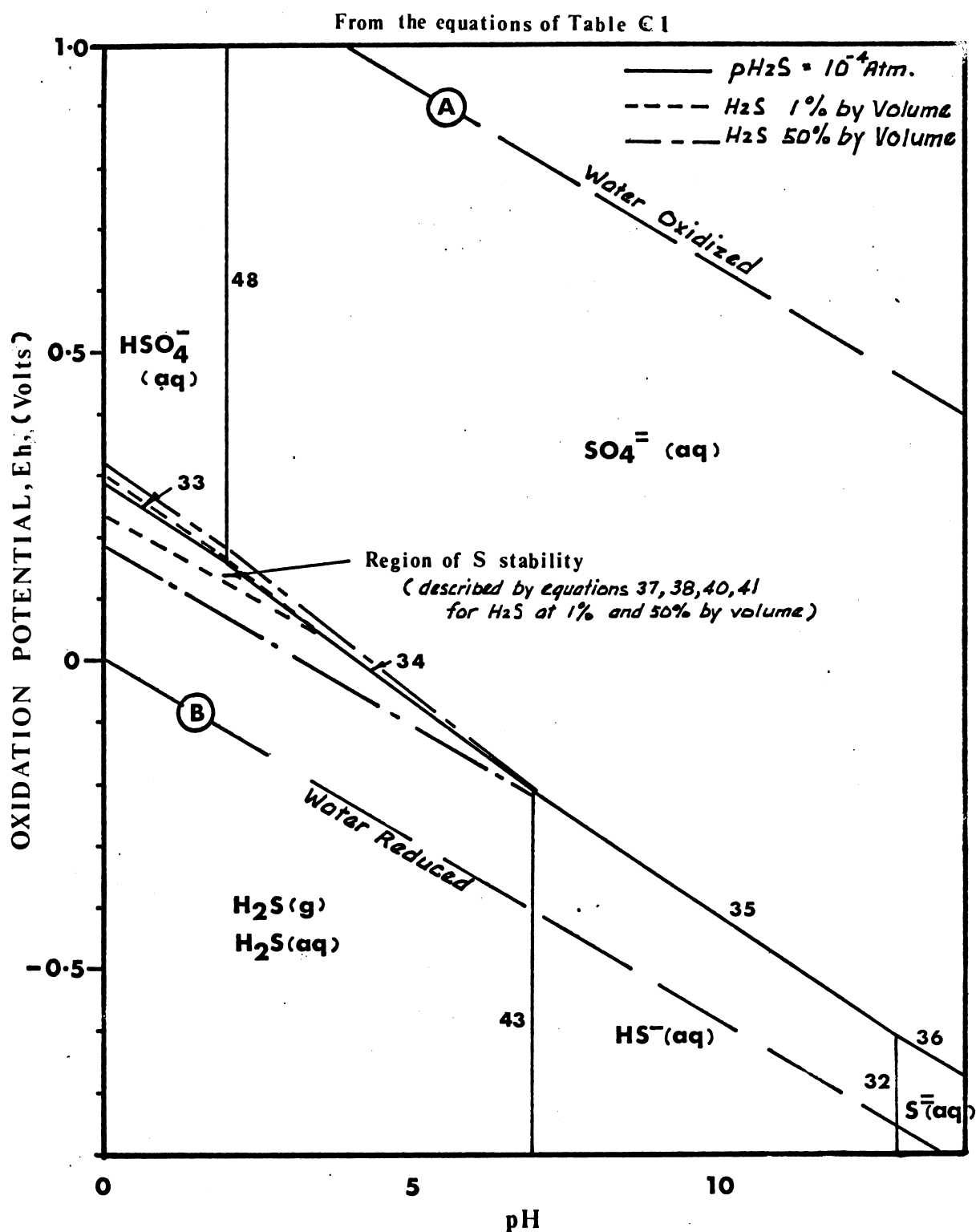


FIGURE 4.3

STABILITY FIELD DIAGRAM FOR THE  
SYSTEM S-H<sub>2</sub>O  
 (At 25°C)



data. Where more than one form of a species has been shown to exist, the form used in the preparation of the diagrams was chosen on the basis of evidence presented in the literature and reviewed in section 4.2.1.

The diagrams were based on the following conditions,

- a)  $\text{KMnO}_4$  concentrations of (i) 0.01%  
and(ii) 0.10%
- b) a  $\text{H}_2\text{S}$  partial pressure of  $100 \times 10^{-6}$  atm. and
- c)  $\text{CO}_2$  partial pressures of (i)  $5 \times 10^{-6}$  atm. and  
(ii)  $3 \times 10^{-4}$  atm.

The boundaries of the various species are numbered to correspond to the reaction mechanisms given in Table C.1. The equilibrium relationships were calculated using the free energy data listed in Table C.2.

By reference to the diagrams it becomes obvious that a  $\text{CO}_2$  partial pressure of  $5 \times 10^{-6}$  atm. has no effect on the equilibrium products. However, when the  $\text{CO}_2$  partial pressure is increased to  $3 \times 10^{-4}$  atm. (a value generally assumed to be equal to that found in the atmosphere)  $\text{MnCO}_3$  becomes an important equilibrium species. This is especially evident where the pH is in the optimum region for  $\text{KMnO}_4$  deodorisation (pH 8.5 to 10.0). Under these conditions mild oxidation of an aqueous suspension of MnS would yield hydrated  $\text{MnCO}_3$  at equilibrium, whilst stronger oxidation would yield one, or a mixture of hydrated  $\text{Mn}_3\text{O}_4$ ,  $\gamma$   $\text{MnOOH}$ , and  $\delta$   $\text{MnO}_2$ .

The stability field diagram for the S-H<sub>2</sub>O system at a H<sub>2</sub>S partial pressure of  $100 \times 10^{-6}$  atm. is shown in Figure 4.3. At this concentration no free sulphur exists at equilibrium. However, when the H<sub>2</sub>S concentration is increased it becomes possible to obtain large regions of sulphur stability. This is illustrated in the above diagram for H<sub>2</sub>S concentrations of 1% and 50% by volume.

#### 4.4 Examination of the Products from the H<sub>2</sub>S-KMnO<sub>4</sub> Reaction.

A sample of the product from the reaction between H<sub>2</sub>S and aqueous buffered KMnO<sub>4</sub> in the presence of air containing less than 7 p.p.m. v/v CO<sub>2</sub> was examined by x-ray diffraction.

##### 4.4.1 Preparation and Examination of the Product.

The sample for examination was prepared in the apparatus described in section 3.2. In this apparatus, a stream of relatively CO<sub>2</sub> free air containing about 100 ppm H<sub>2</sub>S was passed into a Drechsel bottle containing 300 ml. of 0.2% KMnO<sub>4</sub> buffered to a pH of 9.2 with potassium tetraborate. After a reaction time of six hours the container was removed and the aqueous product examined. It was noted that a yellow scum was present on the surface of the solution, and that the aqueous KMnO<sub>4</sub> solution itself had been decolourised. A brown, rapidly settling precipitate had also been formed.

The vessel temperature did not rise above the ambient temperature (26°C) at any time during the reaction.

The precipitate was then filtered, washed and

divided into two portions, one of which was dried at ambient temperature using alcohol, and the other of which was left undried.

Both portions of the product were then examined on a 50 kV Philips x-ray Diffractometer using a copper target and a nickel filter. It was noted that, although the wet sample shrank and cracked during the x-ray bombardment, both samples gave similar results. However, the clarity of the trace from the alcohol dried product was much superior.

#### 4.4.2 X-Ray Diffraction Evidence.

Table C3 lists the angles and intensity ratios for the above products. Comparison with the known x-ray diffraction patterns of the probable components produced no evidence to indicate the presence of either  $\text{MnS}$  or  $\text{MnCO}_3$  in concentrations sufficient to produce characteristic diffraction patterns. The absence of  $\text{MnCO}_3$  is to be expected in view of the low partial pressure of  $\text{CO}_2$  in the air stream. The absence of  $\text{MnS}$  may be explained by the transient nature of this compound in the presence of atmospheric oxygen.

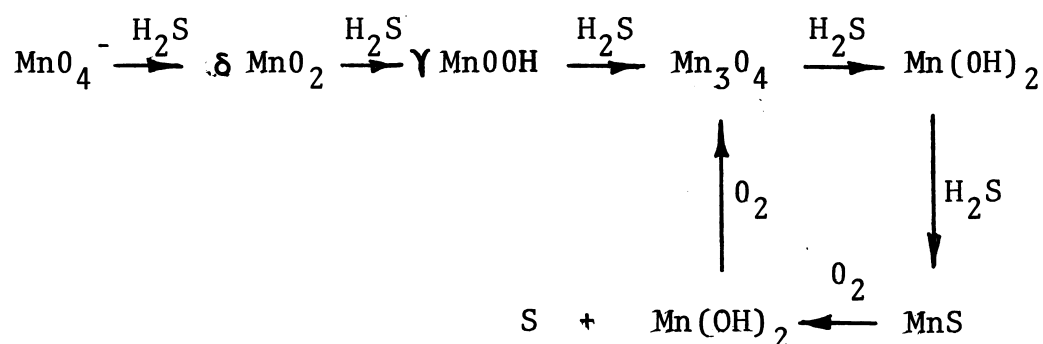
The x-ray diffraction patterns for  $\gamma \text{Mn}_2\text{O}_3$  (107) and  $\text{Mn}_3\text{O}_4$  (106) (107) (164) given in the literature, were found to be in excellent agreement with the experimental data. However the data was such that the x-ray patterns distinguishing the various reported forms of  $\text{Mn}_3\text{O}_4$  and  $\gamma \text{Mn}_2\text{O}_3$  could not be resolved clearly, so that it must be concluded that one or other, or both of these stoichiometric types were present.

The x-ray patterns provide no evidence indicating the presence of any other manganese species.

The evidence for the presence of orthorhombic sulphur is conclusive. However, the data is such that the possible presence of monoclinic sulphur is not to be excluded.

#### 4.4.3 The Probable Reaction Path.

From the above evidence it would appear probable that the reaction between aqueous alkaline  $\text{KMnO}_4$  and  $\text{H}_2\text{S}$ , in the presence of an almost  $\text{CO}_2$  free air stream, follows the path,



where each of the manganese species would, in fact, be hydrated. The  $\text{KMnO}_4$  probably reduces to the easily oxidised  $\text{MnS}$ , which, in the presence of the oxygen in the air stream, is oxidised to  $\text{Mn}_3\text{O}_4$ , liberating sulphur. The  $\text{Mn}_3\text{O}_4$  is then again reduced, and the cycle through  $\text{Mn(OH)}_2$ ,  $\text{MnS}$  and  $\text{Mn}_3\text{O}_4$  continued.

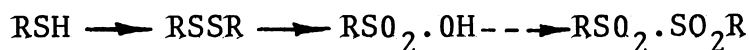
As in pointed out in Section 3.7, and illustrated in Figure 3.7, the absorption efficiency of the process gradually declines during extended runs, whereas the postulated reaction path described above indicates that the process

should maintain itself indefinitely without any such loss of efficiency. This might be due to some progressive blocking or poisoning of active sites on the precipitated solid surfaces, or to progressive changes in the actual nature of the precipitate. However, this question was not pursued.

#### 4.5 The Oxidation of Ethyl Mercaptan in Alkaline $\text{KMnO}_4$ Solution.

In alkaline solution the oxidation of mercaptans by air occurs readily and is assisted by such metals as arsenic, copper, antimony, zinc and cadmium, and by the presence of finely divided solids or by the dispersion of air in fine bubbles. However, the oxidation of pure mercaptans by air itself is an extremely slow process, and there appears to be some doubt as to whether it occurs at all in the absence of an appropriate catalyst (92).

In  $\text{KMnO}_4$  solution the mercaptan may be oxidised to the sulphonic acid, the potassium salt of the acid occurring in solution, (92) (93) (94) although, sometimes the disulphone may occur (92),



##### 4.5.1 Examination of Reaction Products.

Samples of the solid product from the reaction of  $\text{C}_2\text{H}_5\text{SH}$  with  $\text{KMnO}_4$  solution were prepared in the same manner as that described in Section 4.4.1 for  $\text{H}_2\text{S}$ .

Examination of these products using the Philips

Diffractionmeter, again in the same manner as that described above for  $\text{H}_2\text{S}$ , produced a pattern from which it was difficult to distinguish both the position and intensity of the various peaks. However, those peaks which could be distinguished indicated that the sample was identical to that produced by the reaction of  $\text{H}_2\text{S}$  with the permanganate, except that there was no proof of the existence of monoclinic sulphur.

Thus it would appear that the permanganate is undergoing a similar series of reduction steps as that proposed above for the reaction with  $\text{H}_2\text{S}$ .

CHAPTER 5.

MASS TRANSFER MEASUREMENTS.

### 5.1 Fundamentals of Gas Absorption.

When a gaseous component of a gas stream is being absorbed into a flowing liquid film, it is possible to calculate the rate of transfer from first principles if the concentration gradient on each side of the interface is known. However, a convenient means of expressing transfer rate ( $N_A$ ) in units of mass per unit time, is found in the equations:

$$N_A = k_G A (p_a - p_{ai}) \quad - - - - 5.1$$

$$\text{and } N_A = k_L A (C_a - C_{ai}) \quad - - - - 5.2$$

where  $p_a, p_{ai}$  = the partial pressure of component A  
in the bulk gas stream, and at the  
interface respectively,

$C_a, C_{ai}$  = concentration of component A in the  
bulk liquid stream and at the interface  
respectively,

$k_G, k_L$  = gas and liquid phase mass transfer co-  
efficients in units of mass time<sup>-1</sup>  
length<sup>-2</sup> pressure<sup>-1</sup> and mass time<sup>-1</sup>  
length<sup>-2</sup> conc.units<sup>-1</sup> respectively,

and component A = the absorbing component.

These equations are especially useful where the fluid or gas is in turbulent motion, and the concept of an orderly concentration gradient is hard to imagine.

Due to the difficulty in affixing values to the gas partial pressure and the liquid concentration at the interface,



the overall gas phase mass transfer coefficient,  $K_G$ , and the overall liquid phase mass transfer coefficient,  $K_L$ , are popular.

These are given by;

$$K_G = \frac{N_A}{A(p_a - p_a^*)} \quad - - - - 5.3$$

where  $p_a^*$  = the partial pressure of component A in the gas phase in equilibrium with  $C_a$ ,

and

$$K_L = \frac{N_A}{A(C_a - C_a^*)} \quad - - - - 5.4$$

where  $C_a^*$  = the concentration of component A in the liquid phase in equilibrium with  $p_a$ .

While it is possible to analyse mass transfer between phases without completely understanding the mechanism, a number of useful theories have been put forward. It has been suggested (161) that some of these theories, instead of being contradictory, represent extreme examples of the one general case. In the Two Film Theory, better known as the Whitman Theory (155) (156), it is assumed that there exists a thin film on either side of the interface in which all the resistance to transfer is situated. Mass transfer through these films is postulated to be by molecular diffusion alone.

This theory leads to the conclusion that;

$$k_L = \frac{D_L}{x_F} \quad - - - - 5.5$$

WHERE  $D_L$  = the diffusivity of the absorbing component in

the liquid,

and  $x_F$  = the thickness of the Whitman film.

HIGBIE (157) devised another theory called the Penetration Theory. He assumed that there was an exchange of surface elements with the bulk of the fluid, and that the periods of exposure of the elements to the gas phase were equal. As unsteady state conditions prevail;

$$D_L \frac{\partial^2 C}{\partial x^2} = \frac{\partial C}{\partial t} \quad - - - - 5.6$$

and the equation for  $k_L$  becomes:

$$k_L = 2 \sqrt{\frac{D_L}{\pi t_e}} \quad - - - - 5.7$$

where  $t_e$  = the time of exposure of the liquid to the gas.

The rate of absorption of component A is thus given by;

$$N_A = 2 (C_{ai} - C_a) \sqrt{\frac{D_L}{\pi t_e}} \quad - - - - 5.8$$

An extension to this theory is found in the work of DANCKWERTS (158) (159) who examined the case where the contact period of each of the elements of liquid with the gas phase was a matter of chance. From his analysis;

$$k_L = \sqrt{D_L S} \quad - - - - 5.9$$

where  $S$  = the rate of surface renewal.

While it could be expected that the Penetration Theory would not apply where the liquid film is in fully

developed laminar flow, LYNN et al (121) demonstrated its applicability to experimental liquid phase controlled gas absorption data obtained in wetted wall columns ranging in length between one and 22 cm. Other authors (138) (142) (149) have presented experimental data which supports the validity of the work of LYNN et al.

When the gas stream is in laminar flow, that is, when the gas Reynolds number,

$$Re = \frac{u \rho D}{\mu} \quad - - - - 5.10$$

is below about 2000, the interphase transfer is assumed to be by diffusion alone, and thus may be analysed from first principles.

## 5.2 Mass and Heat Transfer to Fluids and Gases in Laminar Flow.

Where a gas is in laminar flow within a tube of circular cross section, similarity between the laws of molecular diffusion and thermal conduction would be expected to prevail.

For a flowing fluid of constant physical properties, the continuity equation (131) for thermal conduction becomes, in cylindrical co-ordinates;

$$\begin{aligned} & \rho c \left[ v_r \frac{\partial T}{\partial r} + \frac{v_\theta}{r} \frac{\partial T}{\partial \theta} + v_z \frac{\partial T}{\partial z} \right] \\ = & k \left[ \frac{1}{r} \frac{\partial}{\partial r} \left( r \frac{\partial T}{\partial r} \right) + \frac{1}{r^2} \frac{\partial^2 T}{\partial \theta^2} + \frac{\partial^2 T}{\partial z^2} \right] \quad - - - - 5.11 \end{aligned}$$

Similarly, the continuity equation for mass transfer in moving gas streams is given by (131), again in cylindrical co-ordinates;

$$\begin{aligned}
 & \left( v_r \frac{\partial p_a}{\partial r} + \frac{v_\theta}{r} \frac{\partial p_a}{\partial \theta} + v_z \frac{\partial p_a}{\partial z} \right) \\
 = & D_v \left[ \frac{1}{r} \frac{\partial}{\partial r} \left( r \frac{\partial p_a}{\partial r} \right) + \frac{1}{r^2} \left( \frac{\partial^2 p_a}{\partial \theta^2} \right) + \frac{\partial^2 p_a}{\partial z^2} \right] \quad \text{--- 5.12}
 \end{aligned}$$

When the gas is moving in streamline flow through a straight tube of circular cross section, the rate of mass transfer between the tube wall and the gas can be calculated from this equation provided a velocity distribution is established. Two possible flow patterns should be considered,

- a) rodlike flow, where the gas is assumed to move through the pipe as a solid rod, and
- b) the parabolic velocity profile, where the velocity distribution is assumed to be fully developed and parabolic.

For rodlike flow, when both  $p_{a1}$ , the initial partial pressure of A in the gas stream, and  $p_{ai}$ , the partial pressure of component A at the wall or phase boundary, are assumed to be constant, equation 5.12 is solved by elimination of redundant terms and re-arrangement, to yield a relationship amenable to analysis using Bessel functions. The final solution becomes,

$$\left( \frac{p_{a2} - p_{a1}}{p_{ai} - p_{a1}} \right) = 1 - 4 \sum_{n=1}^{\infty} \frac{1}{g_n^2} e^{-\left[ \frac{g_n^2 \pi D_v \rho L}{W} \right]} \quad \text{--- 5.13}$$

where  $p_{a2}$  = partial pressure of component A in outlet stream  
from transfer length

and  $g_n$  =  $n^{\text{th}}$  root of Bessel function of first kind, zero order,  $J_0(x) = 0$ .

This method of attack is similar to that originally used by GRAETZ (150), and by DREW (153) to solve the comparable forced convection heat transfer equation.

If the gas flowing inside a tube of circular cross section is in laminar flow with a fully developed parabolic velocity distribution, then the equation of continuity (equation 5.12) can be solved for the general boundary conditions,

(a)  $p_{a1}$ ,  $p_{a2}$ ,  $D_v$  and  $\rho$  ; constant, and

(b)  $v_r$ : everywhere zero,

using a procedure similar to that given above for the case of rodlike flow. The resultant series equation becomes,

$$\left( \frac{p_{a2} - p_{a1}}{p_{a1} - p_{a2}} \right) = 1 - 8\phi \quad - - - - 5.14$$

where

$$\phi = 0.10238e^{-14.6272m} + 0.0122e^{-89.22m} + 0.00237e^{-212m} \quad - - - - 5.15$$

$$\text{and } m = \left( \frac{\pi}{4} \right) \left( \frac{D_v \rho L}{W} \right) \quad - - - - 5.16$$

A satisfactory approximation of equation 5.14, for

$$\left( \frac{W}{D_v \rho L} \right) > 400, \text{ is given by the LEVEQUE (152) equation,}$$

$$\left( \frac{T_2 - T_1}{T_w - T_1} \right) = 5.5 \left( \frac{WC}{KL} \right)^{2/3} \quad - - - - 5.17$$

LINTON and SHERWOOD (126) modified this equation to satisfy the criteria of rodlike flow at values of  $\left( \frac{W}{D_v \rho L} \right)$  in excess of about 200. From their graphed data,

$$\left( \frac{p_{a2}-p_{a1}}{p_{ai}-p_{a1}} \right) = 4 \left( \frac{W}{D_v \rho L} \right)^{-\frac{1}{2}} \quad - - - - 5.18$$

The significance of each of the above equations for mass transfer to a gas in laminar flow (equations 5.13, 5.14, 5.17 and 5.18) may be observed by reference to Figure 5.1, where these equations are shown as plots of

$$\log \left( \frac{p_{a2}-p_{a1}}{p_{ai}-p_{a1}} \right) \text{ versus } \log \left( \frac{W}{D_v \rho L} \right)$$

An alternative representation of these theoretical relationships is possible if the abscissa in Figure 5.1 is reduced to a function involving the Reynolds and Schmidt numbers. By re-arrangement of equation 5.16,

$$\left( \frac{4}{\pi} \right) \left( \frac{W}{D_v \rho L} \right) = (Re) (Sc) \left( \frac{D}{L} \right) \quad - - - - 5.19$$

This merely represents a shift of abscissa values by the multiplicand  $(4/\pi)$ .

Similar graphs to those shown in Figure 5.1 have been obtained for heat transfer (153) (127) by plotting  $\log \left( \frac{T_2-T_1}{T_w-T_1} \right)$  against  $\log \left( \frac{Wc}{kL} \right)$ .

### 5.2.1 Previous Experimental Results.

Experimental data for mass transfer to fluids in laminar flow is rather scanty, and is generally in conflict with the appropriate Graetz equation. Data has been collected by,

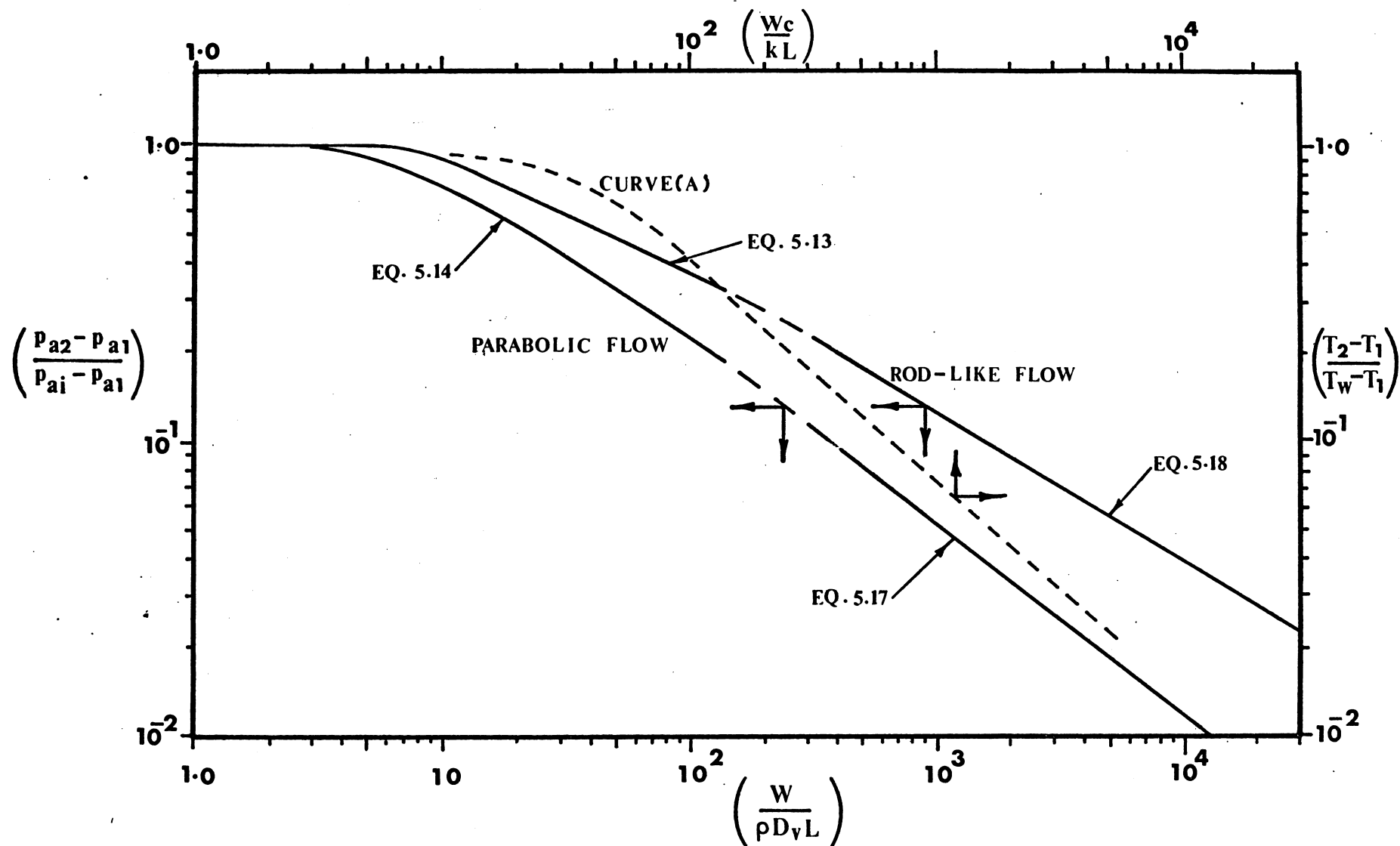


**FIGURE 5.1**      **THEORETICAL CURVES DESCRIBING MASS TRANSFER TO**  
**FLUIDS AND GASES IN STREAMLINE FLOW**

WITH THE EMPIRICAL HEAT TRANSFER CURVE OF DREW ET AL (127) (CURVE A) ALSO SHOWN  
 FOR COMPARISON

- (a) vaporization of liquids into air flowing in a wetted wall column,
- (b) absorption of sulphur dioxide and ammonia from air streams into water,
- (c) dissolution of cast tubes in flowing water, and
- (d) vaporization of solids into air streams.

GILLILAND and SHERWOOD (122) studied the vaporization of a number of different liquids from the wall of a relatively long wetted wall column into an isothermal laminar air stream for values of  $(W/D_v \rho L)$  less than about 100. Under these conditions theory would predict agreement of experimental data with the Graetz equation for a parabolic velocity gradient (equation 5.14). However, instead, they found that their data correlated extremely well with the theoretical line for rodlike flow (equation 5.13). When they also plotted the data of HASLAM et al (123), they found their results further substantiated. No explanation was offered for this obvious departure from theory.

However, BOELTER (124) critically analysed the situation within the wetted wall column used by GILLILAND and SHERWOOD (122), and came to the conclusion that free convection, generated by density variation across the column section, was modifying the parabolic velocity distribution sufficiently to yield a profile close to that for rodlike flow. A similar situation would be expected to exist in the column used by HASLAM et al (123), where changes in solute gas concentration



were rapid and large.

On the basis of this argument, Boelter then proceeded to modify the Graetz equation, taking into account gas density variations. Re-examination of the results of Gilliland and Sherwood using his solution, which consisted of a family of curves, gave reasonable agreement. The fact that there was still some variation of experimental results from his expanded theory was attributed, in part, to the fact that Gilliland and Sherwood used the absolute gas velocity for their original calculations, instead of the velocity relative to the liquid surface.

An examination of mass transfer to water in laminar flow was carried out by LINTON and SHERWOOD (126), but only for values of  $\frac{(W)}{D_v \rho L}$  between about  $6 \times 10^4$  and  $4 \times 10^6$ , where the LEVEQUE equation (equation 5.17) for parabolic velocity distribution applied. Their data was obtained by measurement of the rate of solution of cast tubes of benzoic acid, cinnamic acid and  $\beta$ -naphthol. Generally, experimental results were in good agreement with the line represented by Leveque equation.

Working in square ducts, PLEWES et al (125) succeeded in measuring the rate of vaporization of pure solids into air streams in laminar flow in the region covered by the Leveque equation. However, unlike the results of Linton and Sherwood, their data showed poor agreement with theory.

MUNAKATA et al (154), who measured vapourisation rates into air in laminar flow, reported exceptionally good agreement with the Graetz equation (eq. 5.14) for parabolic velocity distribution.

### 5.3 The Wetted Wall Column as an Experimental Unit.

A "wetted wall column" consists of a vertical tube down which a liquid flows in the form of a thin film under the force of gravity. This flow may be either down the inner or the outer (121) surface of the tube, the former being the most common. The gas and liquid streams are arranged such that intimate contact is achieved between the two phases.

The main advantage that the wetted wall column offers over most other means of examining fundamental mass transfer characteristics lies in its ability to expose an accurately known liquid surface area to the gas stream. Secondary benefits accrue from the ease with which liquor and gas rates can be measured and controlled, and the simplicity of the equations used to describe the flow characteristics of the gas and liquor streams.

However, when using wetted wall columns, experimental techniques and analysis must be carefully devised. Particular attention must be paid to the elimination of;

- a) disturbances in the film,
- b) end effects, and
- c) the "stagnant layer".

In addition, an accurate relationship describing film velocity and thickness must be used.

These items are discussed below.

#### 5.3.1 The Short Wetted Wall Column.

The short wetted wall column such as that illustrated in Figure 5.7 below, where the exposed film is no longer than about 10 cm, is designed to utilise, as the absorbing phase, the relatively short ripple-free length of film which is formed at the liquid inlet. Elimination of rippling in the absorbing laminar liquid film is important, since rippling can lead to an inaccurate estimate of the transfer surface area. It may also indicate some mixing in the fluid phase and disturbances in the layer of gas immediately adjacent to the wall.

With the many advantages possessed by this column (140) (142), it is not surprising that considerable data has been obtained using it as an experimental unit. A similar column to that shown in Figure 5.7 has been used for examination of the liquid side resistance in gas absorption (142), interfacial turbulence during absorption (141), the effect of solute concentration level on gas absorption (138) and gas absorption with chemical reaction (139) (140).

### 5.4 Film Flow.

#### 5.4.1 The Regimes of Film Flow.

Whilst both laminar and turbulent flow can be achieved in the falling liquid film, the presence of a relatively non-turbulent laminar sublayer which can exist over

a substantial thickness of the film up to quite high liquor flowrates, produces difficulty in identifying the transition from one flow regime to another. Nevertheless, it is generally accepted (128) that turbulence in films begins at a film Reynolds number ( $Re'$ ) of between 1000 and 2000, where

$$Re' = \frac{4\Gamma}{\mu} \quad - - - - 5.20$$

and  $\Gamma$  = the mass flowrate of liquor per unit perimeter.

However, TAILBY and PORTALSKI (129) in their examination of wave formation in liquid films, identified five regimes.

(a)	True laminar	$Re' < 25$
(b)	Pseudo laminar	$25 < Re' < 350$
(c)	Transitional	$350 < Re' < 1600$
(d)	Pseudo turbulent	$1600 < Re' < 2100$
(e)	Turbulent	$Re' > 2100$

The presence of waves on the surface of the flowing liquid film is no indication that the flow, as a whole, is turbulent. Thus, in fully developed flow, under suitable conditions, one may have (130) either,

- a) smooth laminar flow,
- b) wavy laminar flow, or
- c) wavy turbulent flow.

#### 5.4.2 Analysis of Film Flow.

When the wetted wall column is used to examine heat and mass transfer characteristics, film flows are generally maintained within the laminar region. For fully developed

two dimensional flow, which is both steady and uniform, the velocity distribution for film velocity  $v$  is given by the semiparabolic equation (131)

$$v = \frac{\rho g \sin \theta}{\mu} \left( \delta x - \frac{x^2}{2} \right) \quad - - - - 5.21$$

where  $\theta$  = the slope of the two dimensional system

$\delta$  = the film thickness

$x$  = the distance from the wall into the film.

This is equivalent to the well known equation developed by NUSSELT (136).

From this equation expressions may be obtained for the maximum film velocity  $v_{\max}$ , the average film velocity  $\bar{v}$ , and the film thickness  $\delta$

$$v_{\max} = \frac{\rho g \delta^2 \sin \theta}{2 \mu} \quad - - - - 5.22$$

$$\bar{v} = \frac{v_{\max}}{1.5} \quad - - - - 5.23$$

$$\delta = \left( \frac{3 \mu Q}{\rho g W' \sin \theta} \right)^{1/3} \quad - - - - 5.24$$

where  $W'$  = the width of the two dimensional system.

With  $\sin \theta = 0$ , the above equations are also applicable to the case of a film flowing down a vertical cylindrical surface, but only when the film thickness is small in comparison to the tube diameter. Where the effect of film thickness is appreciable, exact solutions are required. An exact solution for the velocity distribution within a film flowing down the inside surface of a vertical tube may be obtained from a shell momentum balance. Where the radius of

the tube is  $R$ , and the inside surface of the film occurs at a distance  $aR$  from the centre of the tube, solution of the above momentum balance yields an expression for the film velocity  $v$ , which, upon integration, yields the volume flow-rate;

$$Q = \frac{\pi \rho g R^4}{8 \mu} (1 - 4a^2 + a^4 (3 - 4 \ln a)) \quad - - - - 5.25$$

The film thickness can be found from this equation by trial and error.

#### 5.4.3 Wave Inception & Suppression in the Laminar Film.

The various correlations describing the critical film Reynolds number ( $Re_i$ ) at which waves first appear in the laminar film, have been reviewed by FULFORD (130). These appear to indicate that for the case of water flowing down a vertical wall, the value of  $Re_i$  would be in the vicinity of 6. However, wherever wavy laminar flow is present in a liquid film, there is an initial smooth entry region between the liquid inlet point and the point of wave inception. Where the adjoining gas flowrate is negligible, the length of this region is a function of the liquid flowrate alone, although the manner in which the liquid is introduced could have some effect (129).

The point of wave inception as a function of film Reynolds number, has been investigated by JACKSON (128) and TAILBY and PORTALSKI (129). A summary of their data is presented below in Table 5.1. While the former study used-

water films on the inner surface of a tube, the latter used flat plates.

STAINTHORP and ALLEN (135) have also published data collected in a tube which essentially verify the results of TAILBY and PORTALSKI (129) for film Reynolds numbers between about 100 and 200.

This rippling may be suppressed by addition of small quantities of surface active agents (137). In the past there appears to have been some doubt as to the effect of the wetting agent on the absorption rate (137), although it is now generally believed that these variations were a function of the minute traces of impurities which are always present in the agent (143)

TABLE 5.1.

The Point of Wave Inception as a Function of  
Film Reynolds Number for Water Films  
Falling in Laminar Flow in Wetted Wall Columns.

Distance from the liquid distributor to the point of wave inception (cm). (a)	Film Reynolds Number (b)	Reference (c)
0	15	JACKSON (128) from tabulated data.
10.2	530	"
20.3	1030	"

TABLE 5.1 (continued)

(a)	(b)	(c)
6	100	TAILBY and PORTALSKI (129) from graphed data
10	300	
14.5	530	
20.5	1030	

#### 5.4.4 A Critical Examination of Film Flow in The Short Wetted Wall Column.

When mass transfer characteristics are examined in any wetted wall column, imperfections in the film, or inaccuracies in the analysis of the film hydrodynamics, can seriously affect the overall accuracy of the results. However, when the column length is short, these factors assume even greater importance. Generally, there are three main sources of error associated with the flowing film,

- a) end effects,
- b) the "stagnant layer", and
- c) the use of incorrect relationships to describe the film surface velocity and the film exposure time.

These will each be considered in turn.

##### a) End Effects.

Wetted wall column end effects are due to the unmeasured areas of liquid-gas contact associated with the introduction and removal of the liquid from the column. The design of the short wetted wall column used in these experiments was specifically chosen such that the liquid was brought into and out of



the column without any gas-liquid contact other than on the wetted wall itself.

b) The "Stagnant Layer".

On the film surface in a wetted wall column a narrow horizontal band of ripples may be observed some distance upstream from the liquid exit slot. Visual observation of the film in this region (121) has lead to the conclusion that the surface is nearly stagnant.

This stagnant effect can be diminished or eliminated if disturbances in the outlet slot are deliberately produced at regular, widely spaced intervals (143).

c) The Accelerating Laminar Film in The Short Wetted Wall Column.

Generally, when analysing laminar film flow in short wetted wall columns, it is assumed that velocity functions and gas-liquid exposure times are calculable from the equations describing fully developed streamline flow. From inspection of a typical short wetted wall column (Figure 5.7), it is obvious that the liquid entering such a column must accelerate from some velocity close to, or equal to zero at the liquid inlet slot, to a final velocity, which depending on the length of the column, could equal the fully developed steady state velocity.

Both theoretical and experimental studies (144) (145) (146) (147) appear to indicate that this effect could be significant.

## 5.5 The Diffusion Coefficients.

The diffusion coefficients of  $\text{H}_2\text{S}$  in air,  $\text{C}_2\text{H}_5\text{SH}$  in air,

and  $\text{CO}_2$  in water were required for this study.

#### 5.5.1 The Diffusivity of Hydrogen Sulphide in Air and Ethyl Mercaptan in Air.

In the absence of experimental values for the diffusivity of  $\text{H}_2\text{S}$  in air and  $\text{C}_2\text{H}_5\text{SH}$  in air, the prediction methods of WILKE and LEE (117), SLATTERY and BIRD (119) and ANDRUSSOW (120) were examined.

For  $\text{H}_2\text{S}$  it was considered that the safest course would be to calculate  $D_v$  using Andrussov's method. This gave a value of  $D_v$  at  $20^\circ\text{C}$  and one atmosphere which was between those calculated using the other two methods, but which deviated no more than 5% from either.

For  $\text{C}_2\text{H}_5\text{SH}$ , the values of  $D_v$  calculated for a temperature of  $20^\circ\text{C}$  and a pressure of one atmosphere (absolute) differed by less than 1%. On this basis the relatively simple equation of Slattery and Bird was chosen for calculation.

#### 5.5.2 The Diffusivity of Carbon Dioxide in Water.

The values for the diffusivity of  $\text{CO}_2$  in water, tabulated by VIVIAN and PEACEMAN (142) were plotted against the inverse absolute temperature to give the regression line,

$$\log D_L = -4.72765 - 0.8388 \times 10^3 \left( \frac{1}{T} - 3.37729 \times 10^{-3} \right) \quad - - - - 5.26$$

#### 5.6 Experimental Apparatus.

The experimental apparatus was constructed to specifically examine the absorption of either hydrogen sulphide or ethyl mercaptan from a gas stream in laminar flow in relatively

short wetted wall columns. However, alterations to sections of the apparatus also allowed a check to be made on the performance of the columns in relation to previously reported columns. To achieve this latter point an examination was made also of the rate of desorption of carbon dioxide from water.

5.6.1 Experimental Apparatus for Examination of the Absorption of Hydrogen Sulphide and Ethyl Mercaptan into Alkaline Solutions.

Air containing a low concentration of either  $\text{H}_2\text{S}$  or  $\text{C}_2\text{H}_5\text{SH}$  was produced in the apparatus described in section 3.2. In this apparatus the air was freed of all impurities, and all but about 8 p.p.m. of the carbon dioxide, before being saturated with water.

The odorous material was then injected into the gas stream at a slow and steady rate using the mechanism previously described (section 3.2). As illustrated in Figures 5.2 and 5.3, a 10 l. mixing vessel was provided downstream of the injection point, the gas issuing from this vessel being divided into two streams, one passing to the wetted wall column section, and the other to the odour measuring system.

The main stream then passed through the wetted wall column, where some of the solute gas was dissolved, and thence into vessels containing alkaline potassium permanganate and glass wool to remove all traces of contaminants before introduction to a gas meter. This meter was of the "dry"

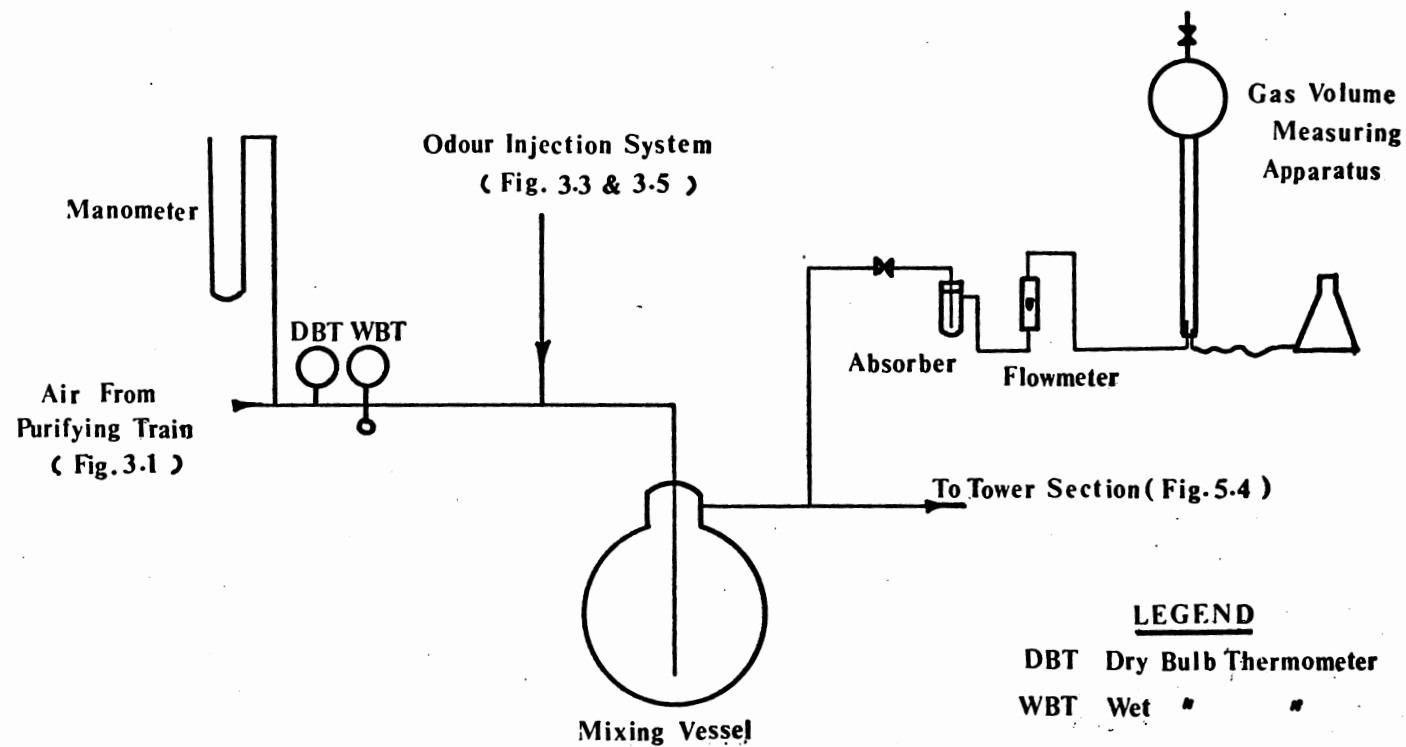
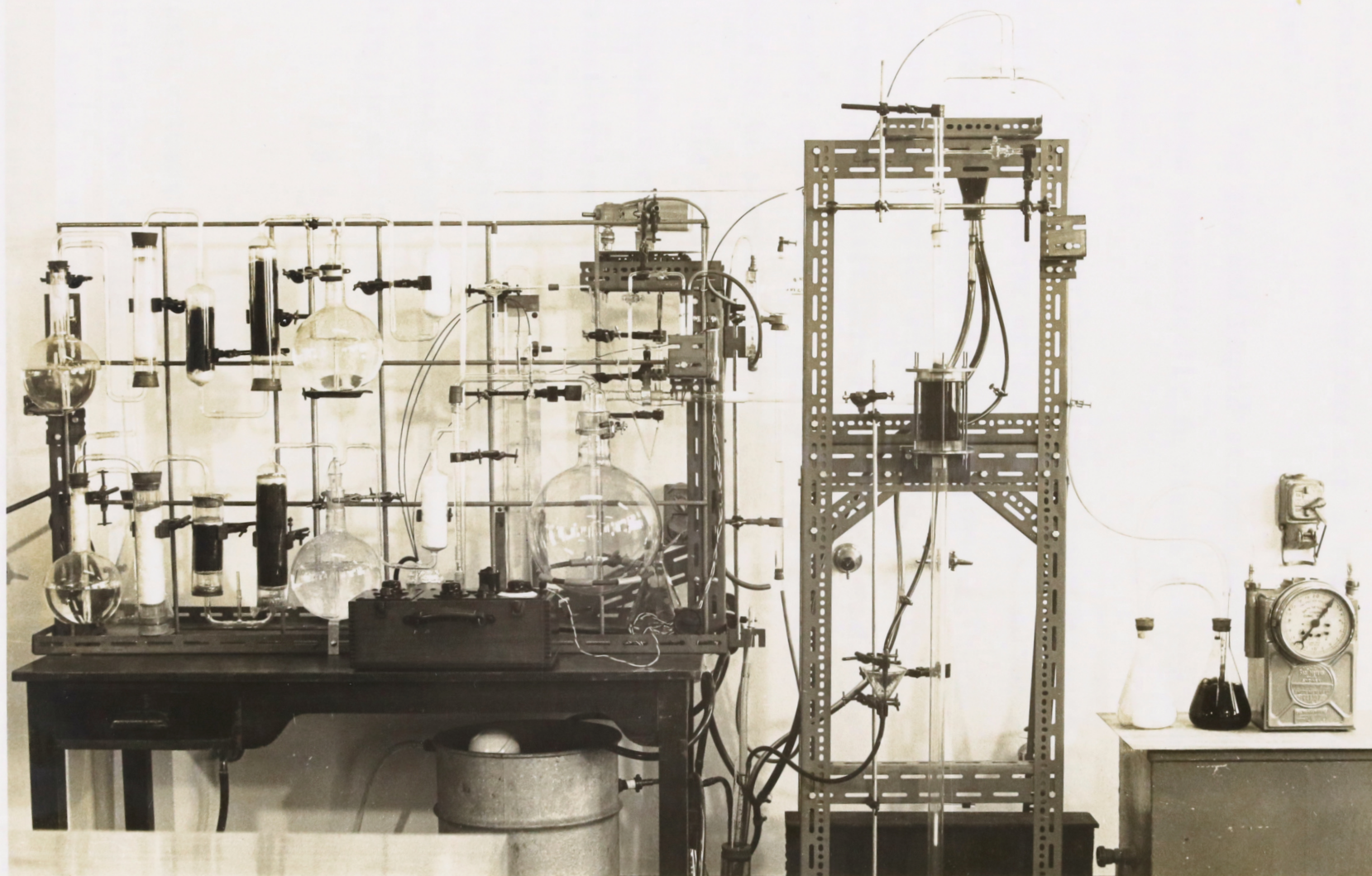


**FIGURE 5.2**  
**FLWSHEET, ODOUR INJECTION AND**  
**MEASURING SYSTEM**

FIGURE 5.3  
PHOTOGRAPH SHOWING THE  
APPARATUS USED FOR GAS  
ABSORPTION AND DESORPTION  
MEASUREMENTS



test type with a 6" diameter face and a least count of 0.02 cubic feet.

The gas and liquid streams around the column section are shown schematically in Figure 5.4 and photographically in Figure 5.5.

The ambient temperature, together with the wet and dry bulb temperatures of both inlet and outlet gas streams were measured using precalibrated copper-constantan thermocouples with an ice-water solution cold junction. Thermocouple output potentials were read using a Cambridge portable potentiometer calibrated to 0.01 mV. Temperature readings were found to be accurate to  $0.1^{\circ}\text{C}$ .

The atmospheric pressure was measured using a Fortin barometer calibrated to 0.01 inches of mercury, while the internal pressure within the system was measured using a water filled manometer. Measurements, using this manometer, showed that the pressure drop along the gas line, between the odour injection point and the column outlet sampling point was negligible for air flowrates up to 12 l./min.

#### 5.6.1.1 The Wetted Wall Column and Ancillary Equipment.

During these experiments, all glass wetted wall columns of three different lengths were used. The main details shown in Figure 5.6 were common to all, the only variation being in the length of the wetted wall section. The various lengths were 10.1 cm., 8.4 cm., and 7.5 cm. for columns

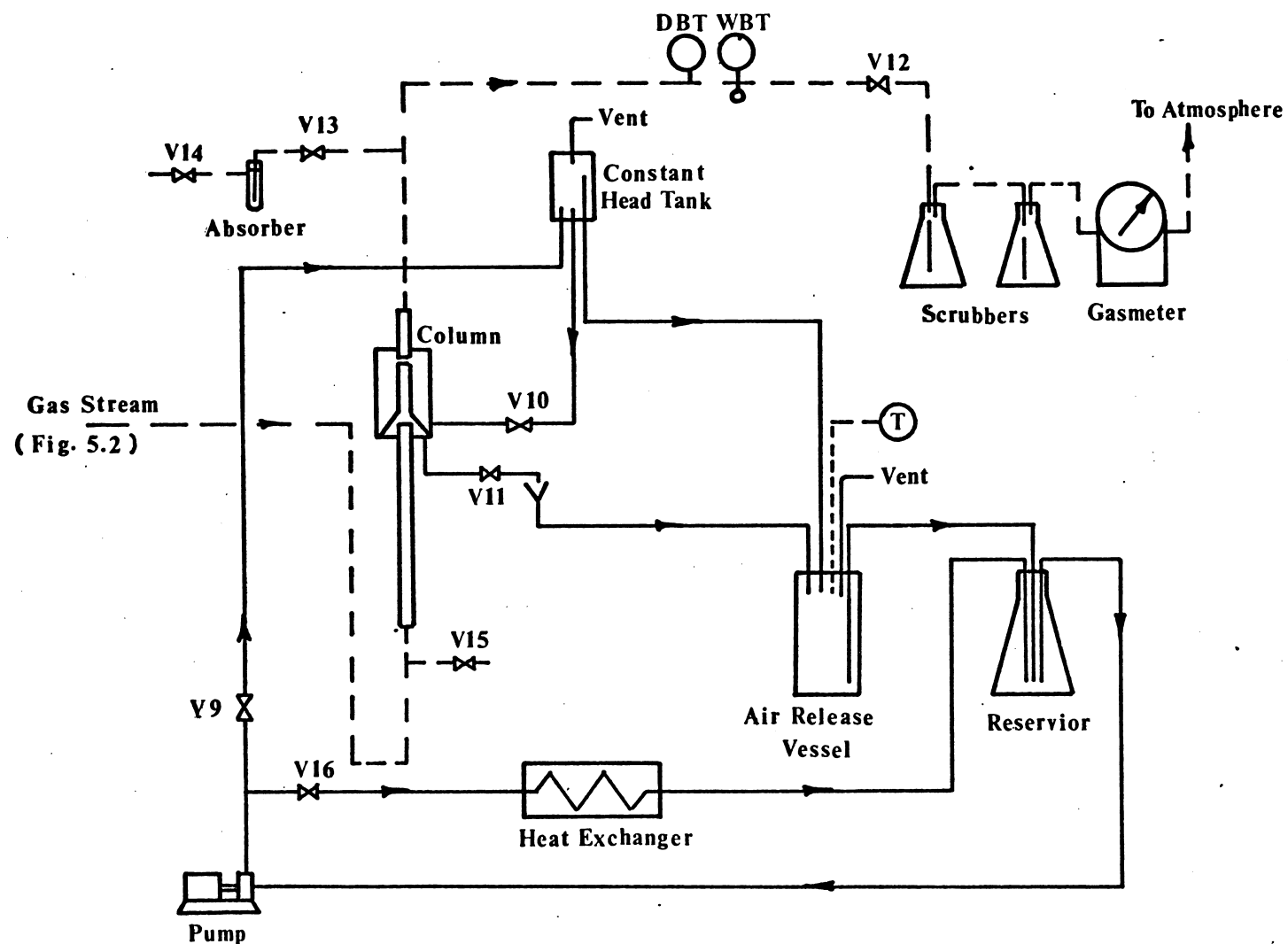
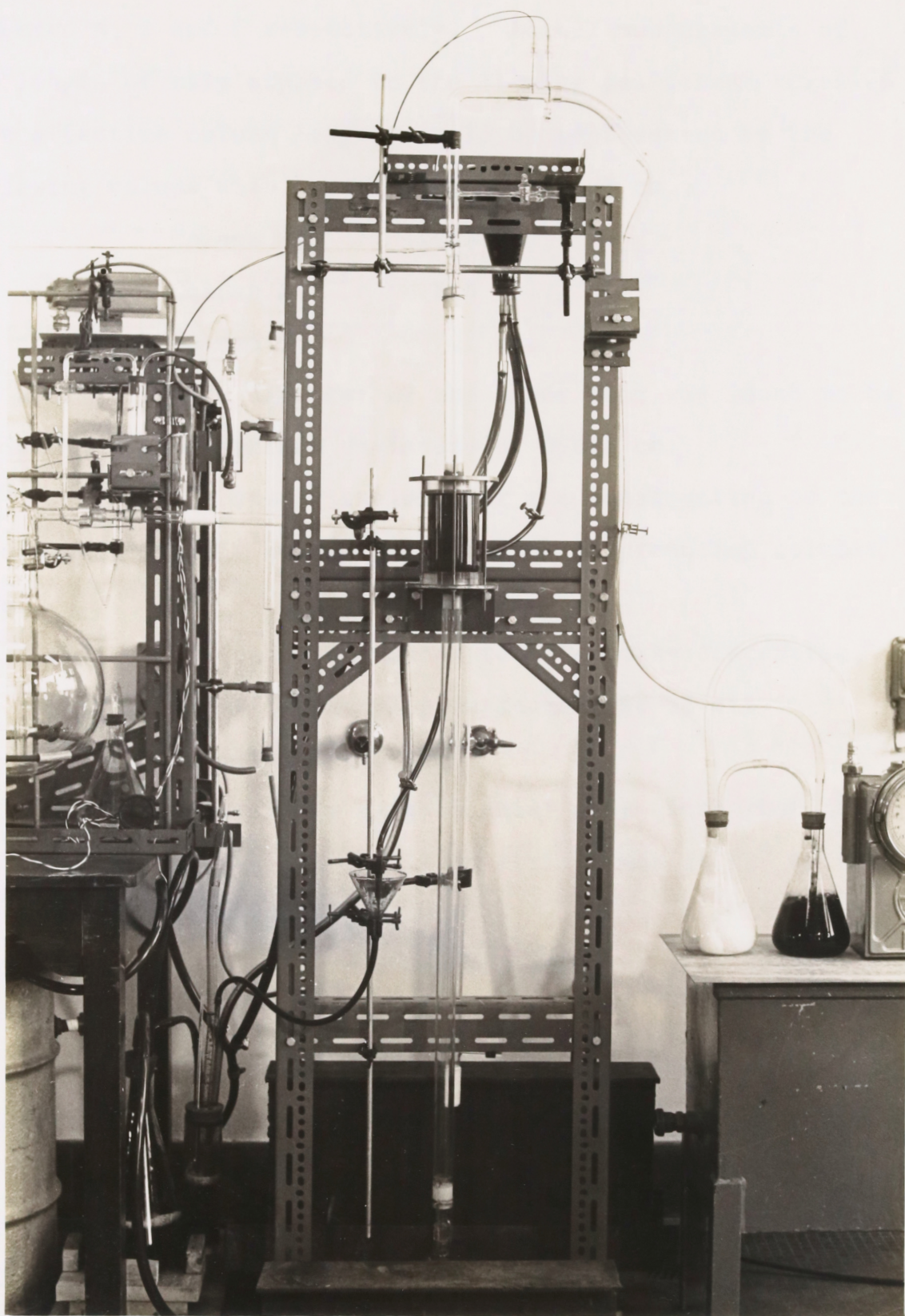


**FIGURE 5.4 FLOWSHEET, SHOWING THE GAS AND LIQUID STREAMS  
AROUND THE COLUMN**



FIGURE 5.5  
PHOTOGRAPH OF THE  
TOWER SECTION



numbered A, B and C respectively. Actual measurements of the length of film exposed to the flowing gas stream revealed that effective column lengths could be represented by the following values with an accuracy of  $\pm 0.05$  cm.;

Column A;            10.3 cm.,

Column B:            8.6 cm.,

Column C;            7.7 cm.

The average inside diameter of the inner tube was found to be 2.456 cm. with a maximum deviation of 0.005 cm.

The specifications for the construction of the column particularly noted the necessity of producing columns with,

- (a)        the inner and outer tubes exactly concentric,
- (b)        the film carrying surfaces free of all imperfections, and
- (c)        a carefully aligned inlet weir, such that the projection in all directions was at  $90^{\circ}$  to the vertical inner tube.

Basically, the column design was based on the unit described by VIVIAN and PEACEMAN (142).

Details of the column assembly are shown schematically in Figure 5.7 and photographically in Figure 5.5.

By reference to the former diagram, it may be observed that the column was designed to produce a thin liquid film on the inner wall of the central tube. To achieve this, the liquid entered the column assembly at the point indicated, and flowed vertically

upwards through a layer of stainless steel gauze in the annulus between the inner and outer tubes, finally entering the inner tube through the chamfered inlet slot. The film thus formed flowed down the column wall under the influence of gravity, eventually leaving the gas-liquid contact region via the conical outlet chamber, before passing completely out of the assembly through a  $5/16$ " O.D. glass tube located in the perspex end plate.

The gas flow was always countercurrent to the liquid film flow.

To minimise disturbances in the liquid film, the column assembly was bracketed to a rigid frame secured to the floor. Attachment of the glass column section was achieved by sandwiching it between two 2 cm. thick perspex end plates, with soft rubber gaskets at all mating surfaces, and securing it to the bracket with a brass support plate and  $1/4$ " diameter studs and nuts. This arrangement, which facilitated the rapid substitution of one glass column for another, is illustrated in Figure 5.7.

The inlet and outlet gas tubes to the column were constructed from 1" I.D. perspex tubing screwed  $1\frac{1}{4}$ " B.S.F. for a part of their length. During operation, the inlet tube was always kept as close as possible to the flowing liquid film, and the outlet tube as close as possible to the inner column consistent with formation of a steady film. To allow the unhindered rotation of these tubes, conical glass joints

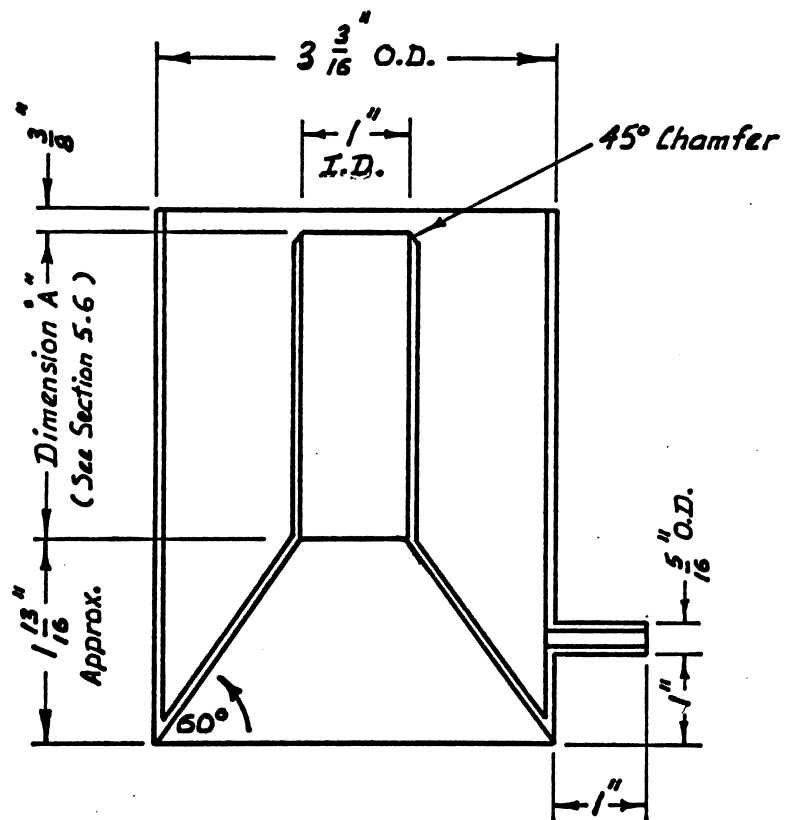


**FIGURE 5.6**

**DETAILS OF WETTED WALL COLUMN**

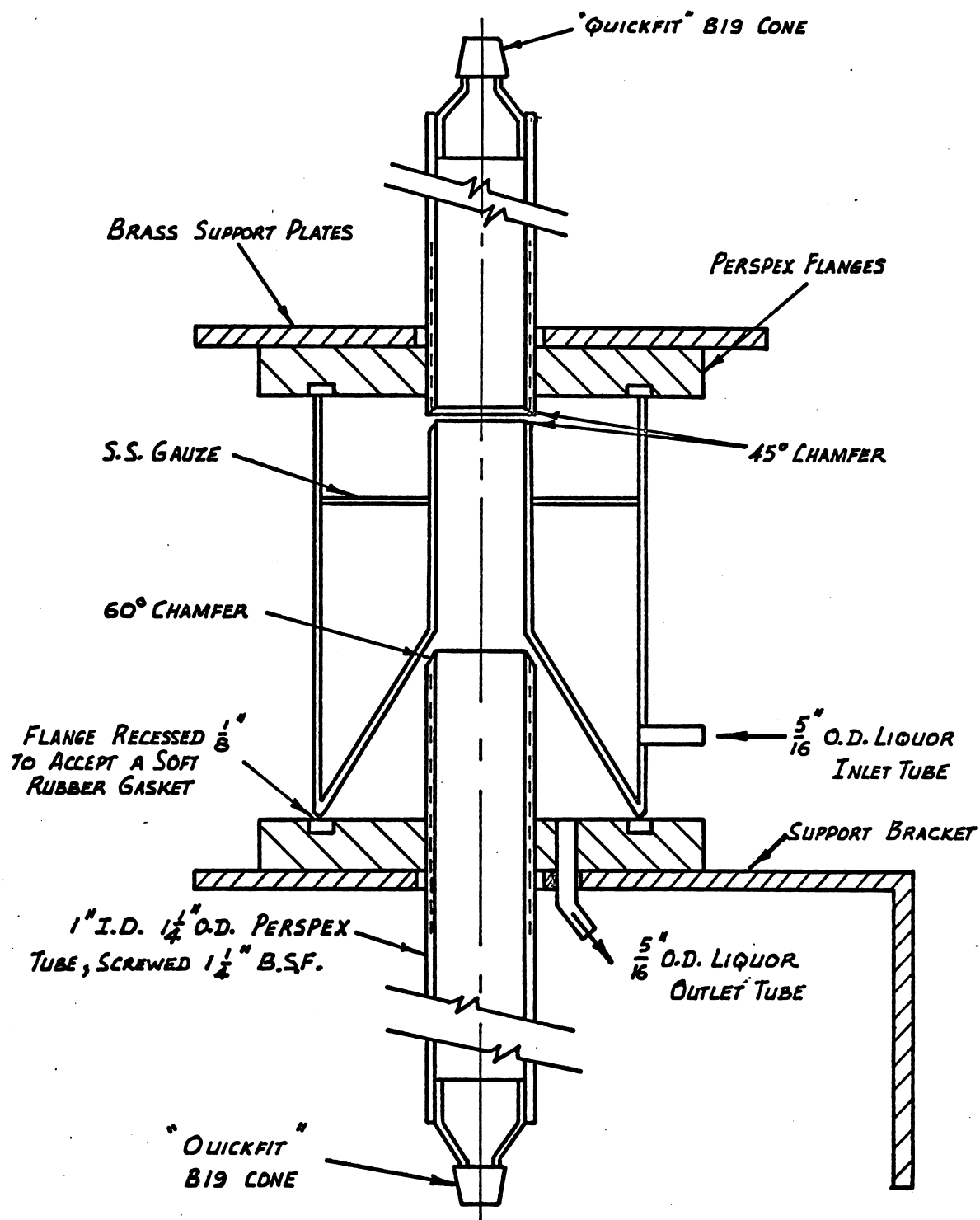


FIGURE 5.7

ASSEMBLY, WETTED WALL COLUMN AND ANCILLARY  
EQUIPMENT

were fixed into their free ends with an epoxy resin adhesive.

The straight 110 cm long perspex gas inlet tube immediately preceding the column was designed to ensure a fully developed gas velocity profile at the commencement of gas-liquid contact. Its length was well in excess of the entrance lengths predicted by the equations of KNUDSEN and KATZ (163), and so included a considerable safety margin.

Due to the distance of the column from the inlet gas sampling point, checks were made to determine whether there were any solute gas losses en route. However, no measurable losses were found.

Whenever a column was changed or cleaned, it was necessary to readjust its perpendicularity. To do this, the column was initially adjusted against a spirit level by shimming the column assembly support bracket. Finally, the vertical displacement of the inner column was measured using a Hilger and Watts theodolite, by assuming that light refraction through the outer column had no effect on the accuracy. From these measurements it was found that the greatest angular displacement of the inner column from the vertical did not exceed 4 minutes.

#### 5.6.1.2 Liquid Streams Around the Column.

The various liquid streams around the column are shown schematically in Figure 5.4. The system was designed to recirculate the liquid stream at a constant flowrate for extended periods without significant variation in temperature.

The liquid was drawn from a 5 litre reservoir by a Stuart centrifugal pump, and delivered to a constant head tank situated above the column. The liquid from this tank then ran into the wetted wall column via a pinch valve (V10) which was used to control film flowrates. Liquid leaving the column assembly ran, via another pinch valve (V11) into a funnel connected to a cylindrical vessel of about one litre capacity. This vessel was found a necessary adjunct to the system, and was designed to allow the release of air entrained in the liquid streams returning from both the column and the constant head tank. De-aerated solution then passed into the reservoir, in preparation for another cycle.

It was found that this system operated most efficiently with an overall liquid volume of 3.8 litres in the circuit.

Liquid temperatures were measured using a mercury in glass thermometer inserted in the air release vessel. The thermometer was checked against a standard thermometer and found to be accurate to its minimum calibration ( $0.1^{\circ}\text{C}$ ).

Due to the tendency of the centrifugal pump to produce a significant temperature increase in the fluid during runs of duration in excess of about 10 minutes, pinch valves V9 and V16 were used to bypass a fraction of the liquid through a heat exchanger consisting of ten 60 cm lengths of about one cm I.D. glass tubing in a large water bath. This enabled the liquid and ambient temperatures to be kept within about  $0.3^{\circ}\text{C}$ .



### 5.6.2 Experimental Apparatus for Examination of the Desorption of CO<sub>2</sub> from Water.

For these experiments, the columns and the column assembly described in section 5.6.1 were used without alteration. However, as shown in Figure 5.8, the gas and liquid streams around the column were extensively re-arranged.

The carbonated water for the column assembly was supplied from a constant head tank constructed from a 10 litre plastic container fitted with a sintered glass sparger (porosity 1) connected to a cylinder of CO<sub>2</sub>. The liquid level within this vessel was maintained at a constant height, corresponding to the inlet of an overflow pipe, using liquid gravity fed from a larger container possessing a capacity of five gallons. The latter vessel was fitted with a similar gas sparging arrangement.

Tee pieces were fitted to both the liquid inlet and outlet points on the column assembly, with the free leg of each tee connected, via a pinch valve, to a 25 ml pipette.

The air for the apparatus was drawn from the normal laboratory supply through a pressure reducing valve set to give a maximum outlet pressure of 5 p.s.i.g. It then passed through a two litre vessel packed with glass wool into a one foot diameter coil of ¼" O.D. stainless steel tubing situated within the five gallon liquid reservoir. After passage through this coil, the air, now at a temperature within about 0.2C° of the liquid temperature, was saturated with water

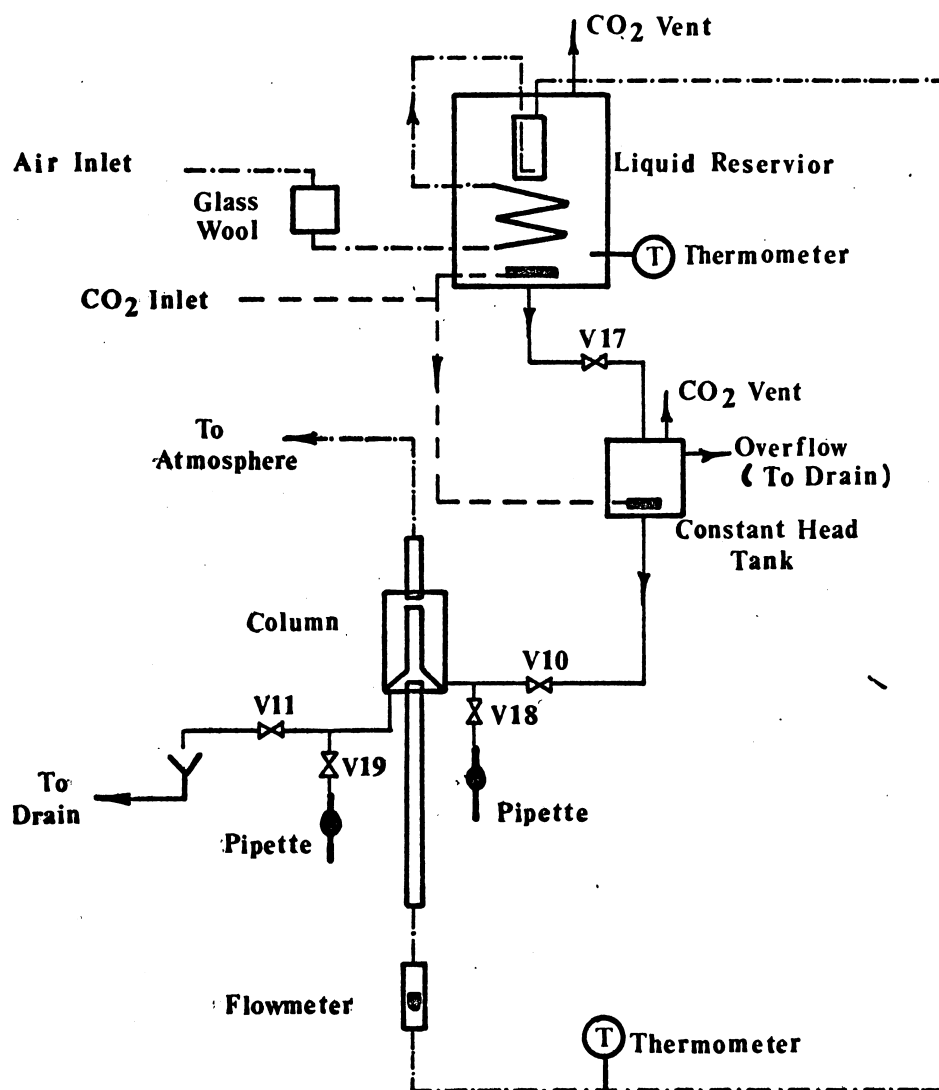


**FIGURE 5.8**

**LAYOUT OF GAS AND LIQUID STREAMS - CARBON**  
**DIOXIDE DESORPTION EXPERIMENTS**

by sparging it through a 500 ml gas sparging vessel held within the same container, and thus, at about the same temperature. The air then passed through a "Gapmeter" brand flowmeter, calibrated for a maximum flowrate of 10l/min., before finally passing through the column assembly counter-current to the falling liquid film. A check on the wet and dry bulb temperatures revealed that the air stream entering the column was completely saturated with water.

All temperatures were measured to  $\pm 0.05^\circ\text{C}$  using precalibrated mercury in glass thermometers.

#### 5.7 The Desorption of $\text{CO}_2$ from Water.

These experiments were designed to use experimentally determined physical absorption coefficients to compare the performance of the three short wetted wall columns described in Section 5.6.1.1 with those reported in the literature.

A number of investigators have reported experimental data for physical absorption coefficients obtained using short wetted wall columns of a design similar to that mentioned above (138) (140) (141) (142). Of these, perhaps the simplest method of attack is that described by VIVIAN and PEACEMAN (142), who examined the desorption of  $\text{CO}_2$  from water. Advantages of this system may be found in the simplicity of the required apparatus and the fact that comparatively accurate data for the diffusivity of  $\text{CO}_2$  in water is available.

##### 5.7.1 Theory.

From the equations of section 5.4, the maximum

velocity,

$$V_{\max} = \left( \frac{9 g \Gamma^2}{8 \mu \rho} \right)^{1/3} \quad - - - - 5.27$$

Where the penetration theory is valid, this value may be substituted into eq. 5.7, with

$$t_g = L/V_{\max} \quad - - - - 5.28$$

to give,

$$k_L = 2 \sqrt{\frac{D_L}{\pi L}} \left( \frac{9 g \Gamma^2}{8 \mu \rho} \right)^{1/6} \quad - - - - 5.29$$

which may be conveniently represented by a logarithmic plot of  $K_L \sqrt{\frac{L}{D_L}}$  versus  $\Gamma$ . Where the experimental data is collected at various temperatures, it may be corrected to a constant temperature of, say, 25°C, by altering the abscissa to  $\frac{\Gamma}{\sqrt{\epsilon}}$  where;

$$\epsilon = \left( \frac{\mu}{\mu_{25^\circ\text{C}}} \right) \left( \frac{\rho}{\rho_{25^\circ\text{C}}} \right) \quad - - - - 5.30$$

The above relationship for the liquid side mass transfer coefficient is strictly limited in its application by all the assumptions in the above analysis.

#### 5.7.2 Experimental Procedures Using CO<sub>2</sub>.

The wetted wall column was thoroughly cleaned before each run by immersion in a mixture of sulphuric acid and potassium dichromate. The perpendicularity of the re-assembled column was then adjusted using the method described in section 5.6.1.1.

With all the valves closed, and both the liquid

reservoir and the constant head tank full of distilled water, the  $\text{CO}_2$  was introduced through the sparging system. When the water was considered to be sufficiently saturated with  $\text{CO}_2$  to give a measurable desorption in the column, valves V17, V10 and V11 were adjusted to give a smooth film within the column and a constant but slow overflow of water from the constant head tank. Valves V18 and V19 were then opened such that a constant flow of liquid passed through the previously filled pipettes.

Valve V10 was then readjusted to give the required liquid flowrate, the flowrate being measured by weighing the liquid issuing from both V11 and V19 over a known time interval. The gas inlet and outlet tubes to the column, shown in detail in Figure 5.7, were then adjusted such that the inlet tube was as close as possible to the flowing liquid film, and the outlet tube as close as possible to the inner column consistent with formation of a steady film. Valve V11 was then readjusted to give a liquid level within the column outlet chamber which was as close as possible to the outlet slot. Under these conditions, which are necessary to reduce the outlet end effects, the liquid within the outlet chamber must be watched at all times so as to prevent overflow into the gas inlet tube.

The air flowrate was then adjusted to give a flowmeter reading of about 8 l /min. The liquid flowrate was also rechecked. After allowing about five minutes for the

conditions to attain equilibrium, valves V19 and V18 were closed, the pipettes removed, and then allowed to drain to the graduation mark.

The samples were then discharged into a flask containing 25 ml. of reagent solution under a nitrogen blanket. The reagent solution consisted of a standardised solution of sodium hydroxide with excess barium chloride. After precipitation of the barium carbonate by the  $\text{CO}_2$  in the water, the remaining hydroxyl ions were titrated against standard 0.1N hydrochloric acid using phenolphthalein as the indicator. A steady trickle of nitrogen was maintained within the analytical vessel during all these operations.

A total of 14 runs were performed, with five runs being carried out using Column A, five using Column B and four using Column C.

### 5.7.3 Calculations and Results.

The tabulated results are given in Tables D1 and D2 of Appendix D. A sample calculation is also given in Appendix E.

For the conditions existing in this experiment, the value for  $k_L$  may be calculated from the following equation, which is a modification of equation 5.2,

$$\begin{aligned} k_L &= \frac{N_A}{A} \frac{(C_1 - C_2)}{C_0 - C_1} \\ &= \frac{N_A}{A} \left(1 - \frac{C_2}{C_1}\right) \end{aligned} \quad \text{--- 5.31}$$

where  $C_1, C_2$  = inlet and outlet liquid concentrations.

$C_o$  = average concentration at start of absorption  
 period =  $C_1$   
 and  $C_i$  = 0 (assumed)

Since a value for the liquid film thickness,  $\delta$ , was required for calculation of the interfacial area,  $A$ , both the approximate equation (eq.5.24) and the exact equation (eq.5.25) for  $\delta$  were assessed. It was found that use of the approximate equation resulted in values which differed by less than  $\frac{1}{2}\%$  from the exact values.

#### 5.7.4 Discussion of Results.

The experimental results are plotted in Figure 5.9 on log-log paper with the group  $k_L \sqrt{\frac{L}{D_L}}$  as the ordinate, and the group  $\frac{\Gamma}{\sqrt{\epsilon}}$  as the abscissa. The units used for these co-ordinates are not homogeneous, being  $(\text{cm}/\text{sec})^{\frac{1}{2}}$  and  $(\text{g}/(\text{cm.})(\text{min.}))$  respectively. However, this system of units ensures compatibility with published data.

Linear regression of  $\log (k_L \sqrt{L/D_L})$  on  $\log (\frac{\Gamma}{\sqrt{\epsilon}})$  yielded the line

$$\log (k_L \sqrt{L/D_L}) = 0.28312 + 0.33386 \log (\frac{\Gamma}{\sqrt{\epsilon}}) \quad \text{--- 5.32}$$
 with a correlation coefficient of 0.8 and a standard deviation of 0.0369.

This equation reduces directly to the relationship,
 
$$k_L \sqrt{L/D_L} = 1.92 (\frac{\Gamma}{\sqrt{\epsilon}})^{0.33} \quad \text{--- 5.33}$$

where the units of  $\Gamma$  are  $(\text{g}/(\text{cm.})(\text{min.}))$

However in consistent units this equation becomes,

$$k_L \sqrt{L/D_L} = 7.41 (\frac{\Gamma}{\sqrt{\epsilon}})^{0.33} \quad \text{--- 5.34}$$

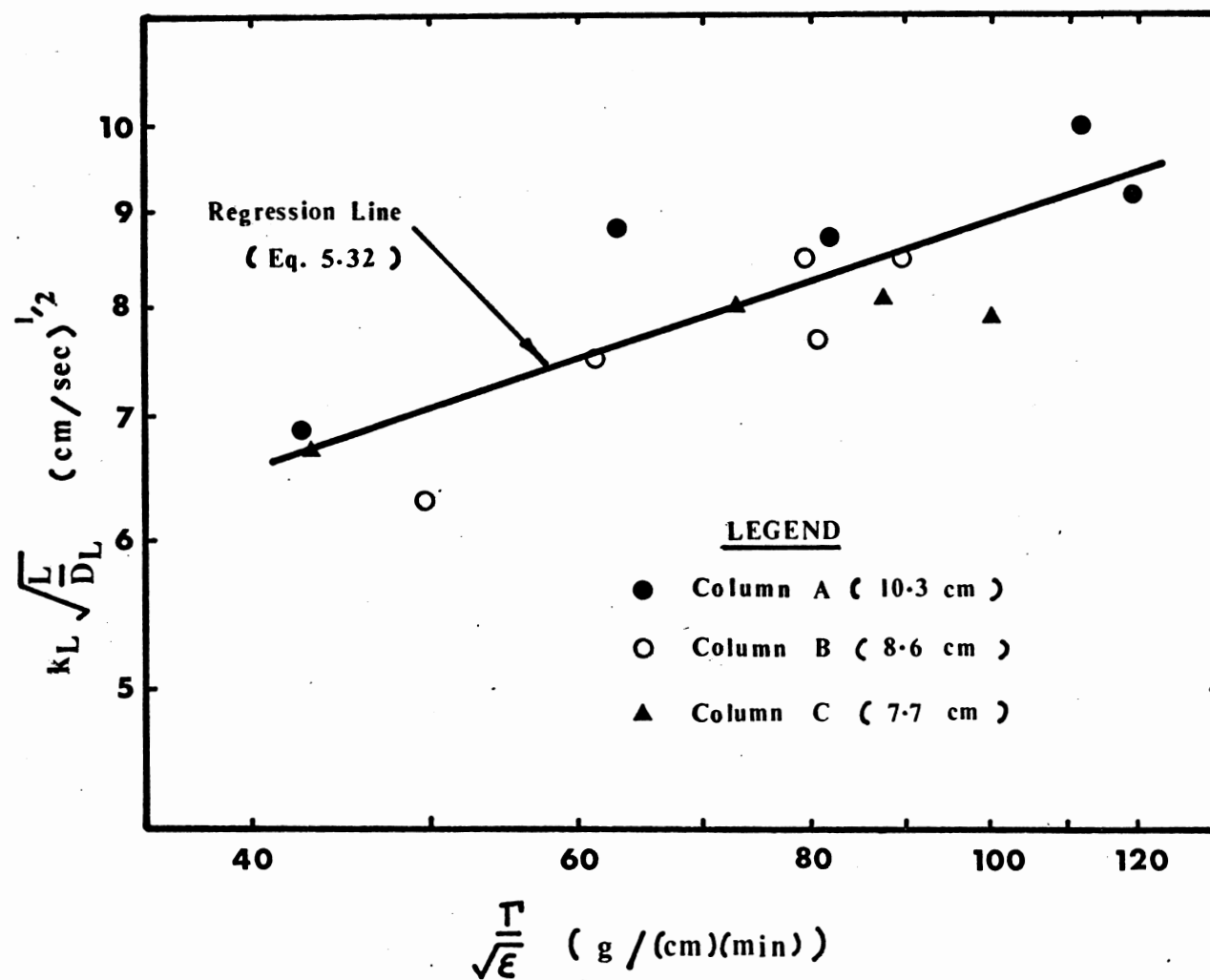


**FIGURE 5.9** EXPERIMENTAL RESULTS-DESORPTION OF CARBON DIOXIDE FROM WATER



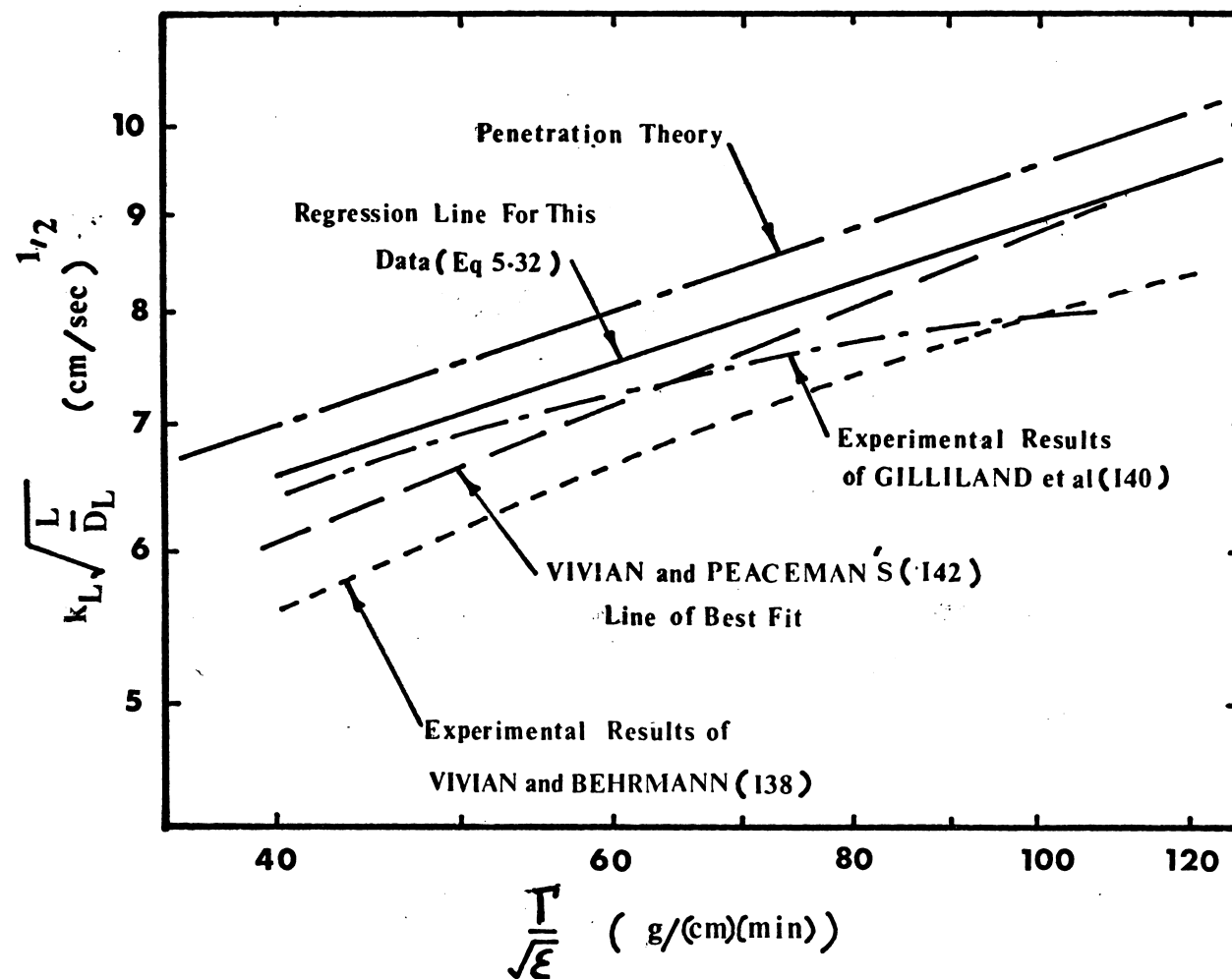


**FIGURE 5.10** COMPARISON OF EXPERIMENTAL AND THEORETICAL  
DATA- DESORPTION OF CARBON DIOXIDE FROM WATER

It may be noted that the deviation of experimental points from the regression line is no greater than that obtained by other investigators (138)(140)(141)(142) using similar apparatus.

The regression line for this data is also shown in Figure 5.10 together with a line representing the theoretical relationship from the Penetration Theory and a number of experimentally determined curves from the literature. The data produced in these experiments gives a line parallel to, but slightly below the theoretical. It is generally in slightly better agreement with the theoretical than the data of either VIVIAN and PEACEMAN (142) VIVIAN and BEHRMANN (138) or GILLILAND et al (140).

It is interesting to analyse the data from these experiments in an effort to determine the most probable cause of this small deviation from theory. The design of apparatus, together with its method of operation, would suggest that end effects, the stagnant layer and wave inception are not responsible. However, the assumption that fully developed laminar flow exists throughout the length of the film, implied by the method of calculation, is an obvious source of error. Assessment of the significance of this factor may be obtained using one of the methods mentioned in section 5.4.5, although these methods lack either ready applicability or experimental verification.

In a simple test designed to examine this effect,

a stream of methyl red dye was injected into the liquid and a high speed movie camera used to record its passage down the inner surface of the column. The liquid film velocities were then calculated from a knowledge of the movie film speed and the distance of dye movement.

This method of film velocity measurement is of dubious accuracy. It probably measures a velocity somewhere between the maximum and the average, where the dye stream is of sufficient concentration to give a photographic imprint. In addition it does not allow for the small density differences which would exist within the flow dye stream.

Nevertheless, the results, given in Table 5.2, emphasise the change in velocities occurring over the length of the falling film. In each of the two cases where a velocity measurement of the upper half of the falling film was obtained, this velocity was 75% of the overall measured velocity.

Thus, it would appear that the accelerating film effect was the predominant reason for the lack of agreement between the theoretical and experimental results.

TABLE 5.2  
Comparison of the Measured and  
Calculated Liquor Velocities  
For the 10.3 cm Long Column.

Run No.	Water Flowrate (ml /min)	Water Temp. ( $^{\circ}\text{C}$ )	Measured Velocity (cm/sec)		Calculated Velocity (cm/sec)	
			Overall	Upper Section	Average	Maximum
1	720	22	32	24	43	64
2	750	21	36	27	44	65
3	470	21	30	-	32	48
4	750	21	36	-	44	65
5	776	21	39	-	45	67

#### 5.8 Mass Transfer from a Gas in Laminar Flow.

In the study of mass transfer to fluids and gases in laminar flow, the partial differential equation for diffusion can be solved directly to yield a relationship describing the transfer rate (section 5.2). Most of the attempts to experimentally verify this theory have failed.

The experiments reported herein were designed to examine the absorption of  $\text{H}_2\text{S}$  and  $\text{C}_2\text{H}_5\text{SH}$  from an air stream in laminar flow, where the absorbing media comprised an alkaline solution flowing down a short wetted wall column. Particular attention was paid to the design of both the apparatus and the experimental procedure, in an attempt to overcome the errors associated with previous investigations.

#### 5.8.1 Experimental Apparatus.

The apparatus is described in detail in section 5.6.1.

#### 5.8.2 Experimental Procedure.

The wetted wall was cleaned and assembled as described in section 5.7.2.

A stream of air was then purified by passage through the scrubbing train described in section 3.2.1. This air, which was essentially  $\text{CO}_2$  free and saturated with respect to water, was then steadily and continuously injected with the required amount of  $\text{H}_2\text{S}$  or  $\text{C}_2\text{H}_5\text{SH}$ . Operation of the injection system has also been described in section 3.2.3.

The gas stream from this source then passed through the wetted wall column where some of the solute gas was dissolved, and thence into the gas scrubbing system, before finally being ejected into the atmosphere via the dry gas meter. Tests showed that there was no loss of solute gas during the passage of the air stream from the solute gas injection point to the column inlet point.

Measurement of the concentration of solute gas in the air stream, both before and after the column, was achieved using the Fluorometric method described in Chapter 2, and a reagent consisting of 25 mls. of 0.0120% TMF solution in 0.01N NaOH.

To commence circulation of liquid through the column and the associated liquor circuit, the reservoir was

first filled with 3.6 litres of the absorbing liquid, and the pump primed with a further 0.2 litres. The absorbing liquid phase in these tests consisted of either  $\text{KMnO}_4$  solution or water buffered to a pH greater than 9.0.

The pump was then started and valves V9 and V16 (Figure 5.4) adjusted such that liquid flowed through both the constant head tank and the heat exchanger. Liquid was then introduced into the column by carefully opening valve V10. In some cases it was necessary to gently tap the column assembly to obtain a uniform film over all wetted surfaces.

The gas inlet and outlet tubes to the column, shown in detail in Figure 5.7, were then adjusted such that the inlet tube was as close as possible to the flowing liquid film and the outlet tube as close as possible to the inner column consistent with formation of a steady film. Valve V11 was then adjusted to give a liquid level within the column outlet chamber which was as close as possible to the outlet slot. These conditions produced a liquid level which was liable to overflow into the gas inlet tube at the slightest provocation. Whenever this occurred, the gas inlet tube was removed and dried and the run repeated.

Valves V10 and V11 were then readjusted to give the required liquid flowrate while still maintaining the conditions established in the preceding operations. Measurement of the liquid flowrate was achieved by weighing the liquid issuing from valve V11 over a known time interval.

By operation of valve V16, the valve controlling the liquid flowrate through the heat exchanger, the temperature in the liquid circuit was maintained as close as possible to the gas temperature.

Whenever the liquid phase contained  $\text{KMnO}_4$ , the concentration of this reactant was determined before and after each run. The method of analysis has been described by VOGEL (95). Due to the inherent instability of this reagent, especially in the presence of light, there was a small, but measurable decrease in its concentration during recycling, even in the absence of reactants in the gaseous phase. For instance, in 30 minutes of recirculation with no gas flow, the normality of a  $1.016 \times 10^{-2}$  N. solution was found to decrease to  $1.014 \times 10^{-2}$  N.

At first, both the wet and dry bulb temperatures of both inlet and outlet gas streams were recorded during each run. However, it soon became apparent that, for each run, these temperatures were all within about  $0.1^\circ\text{C}$  and could be replaced by a single average value with no significant effect. Readings were also taken of the ambient temperature, the atmospheric pressure, and the internal pressure within the column. Gas flowrates were established

from the gas meter readings, the volume of gas used in each fluorometric analysis, and the overall time of the run.

### 5.8.3 Calculation of Results

The method of calculation is best illustrated by reference to the sample given in Appendix E.

It may be observed that the assumption of zero solute gas concentration at the gas/liquid interface has played an important part in these calculations. For the case of  $\text{H}_2\text{S}$  absorption, this assumption was supported by the existence of laminar flow in the gas stream together with an instantaneous chemical reaction in the liquid phase. Evidence for the latter statement may be found in the analysis of ASTARITA and GIOIA (165)(166), who critically examined the chemical absorption of  $\text{H}_2\text{S}$  in aqueous alkaline solutions.

For the case of  $\text{C}_2\text{H}_5\text{SH}$  absorption, where the chemical reactions occurring in solution would be expected to be more complex, the assumption of zero solute gas concentration at the interface was again made.

### 5.8.4 Discussion of Results

The results, both experimental and calculated



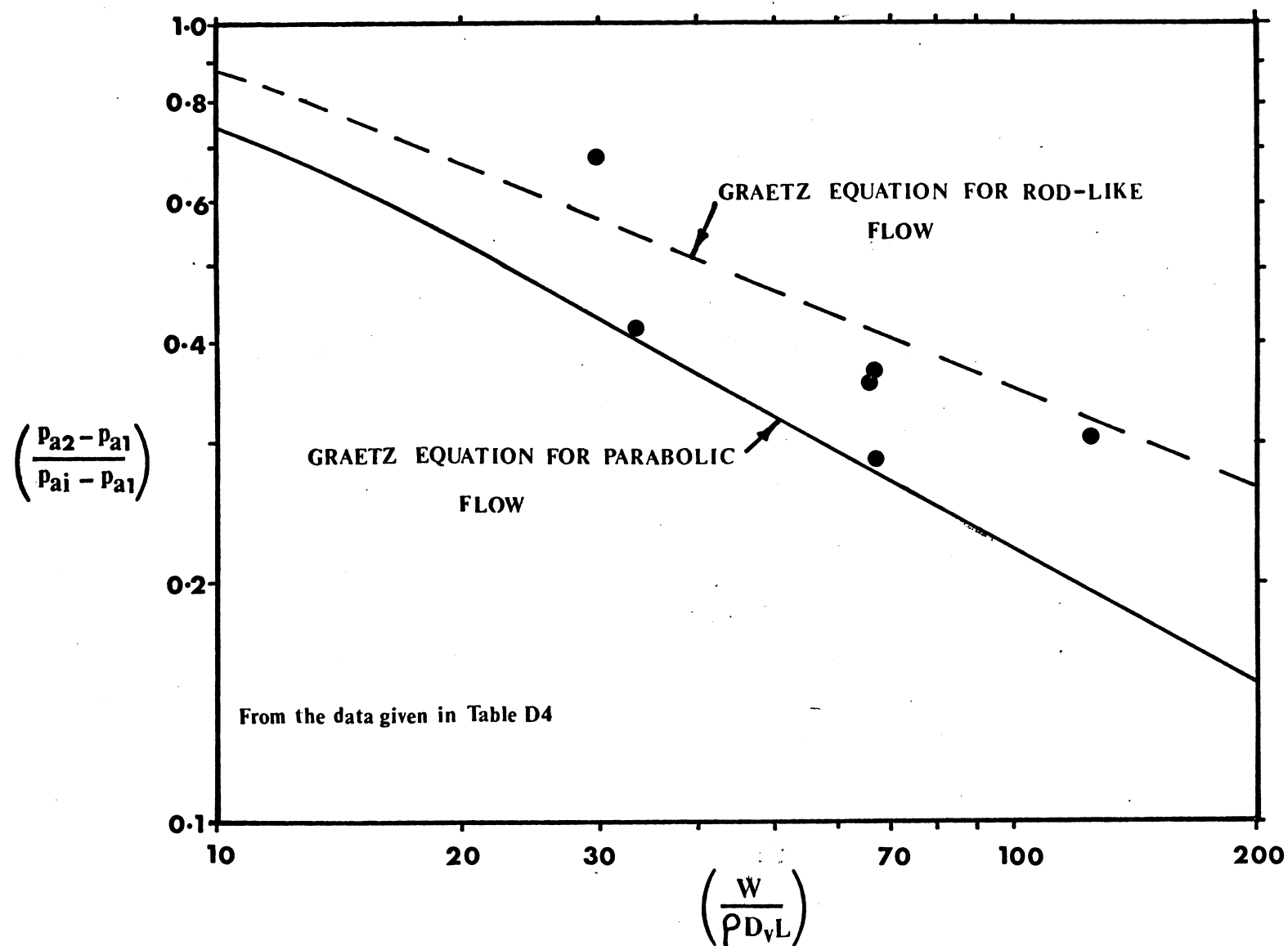


**FIGURE 5.11** COMPARISON OF EXPERIMENTAL RESULTS WITH THEORY - ABSORPTION OF ETHYL MERCAPTAN FROM AIR STREAMS IN LAMINAR FLOW

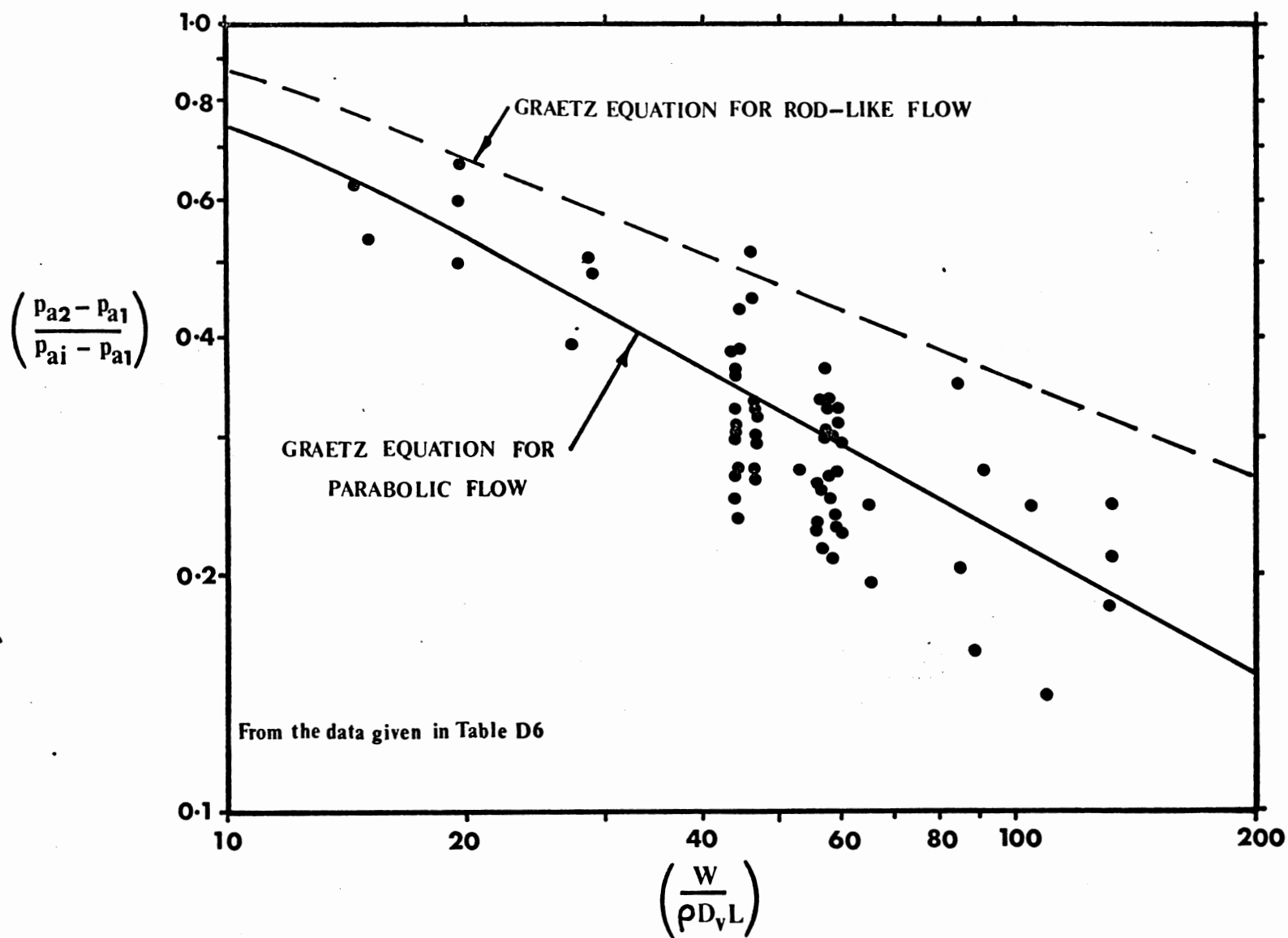


**FIGURE 5.12** COMPARISON OF EXPERIMENTAL DATA WITH THEORY—ABSORPTION OF HYDROGEN SULPHIDE FROM AIR STREAMS IN LAMINAR FLOW

are given in Tables D3 to D6 of Appendix D. The calculated results are also shown in Figures 5.11 and 5.12 as a log-log plot with the group  $\left(\frac{Pa_2 - Pa_1}{Pa_i - Pa_1}\right)$  as the ordinate, and the group  $\left(\frac{W}{D_v L \rho}\right)$  as the abscissa.

The absorption of  $C_2H_5SH$  from air was only examined in six of the 73 runs carried out in the wetted wall columns. The results of these six runs, plotted in Figure 5.11, do not appear to agree with either of the Graetz theoretical curves. However, the few results obtained, as well as the uncertainty in the value of  $D_v$  used in the associated calculations, make the results inconclusive.

The remaining 67 runs were designed to examine the absorption of  $H_2S$  under various conditions, and in columns of three different lengths. The results, which are plotted in Figure 5.12 show very good agreement with the curve representing the Graetz equation for parabolic flow. As explained in section 5.8, some of the investigators who have attempted to verify this equation experimentally have found poor agreement between their data and the appropriate theory.

The relatively good agreement of this data with theory is probably due to the precautions exercised during the experiments. For instance, gas density variations during absorption, which have been shown (124) to be a significant factor in the poor results of GILLILAND and SHERWOOD (122), were eliminated by;

- (a) carefully controlling all temperatures;

- (b) using very low concentrations of solute gas within the incoming air stream, and
- (c) using very short transfer sections.

To this end, the concentration of the solute gases  $\text{H}_2\text{S}$  and  $\text{C}_2\text{H}_5\text{SH}$ , in the air streams, ranged between  $0.6 \times 10^{-6}$  and  $1.7 \times 10^{-6}$  g mole/l, and  $1.8 \times 10^{-6}$  and  $5.3 \times 10^{-6}$  g mole/l respectively. In addition generally less than 50% of the solute gas was absorbed from the incoming air stream.

The length of the transfer section is also critical for another reason. When considering the absorption of a soluble gas from an air stream flowing in a column, where the absorbing media is flowing down the wall of the column, the normal parabolic profile for the gas stream is modified during passage through the column, by the movement of the liquid film.

The necessity to account for this alteration in the velocity profile would be expected to disappear when the wetted section is sufficiently short. While this phenomenon has not been theoretically considered as yet, the case of unsteady state "start up" flow has been solved (131). The latter analysis would suggest that the time required for an air stream to reach 90% of its final velocity profile, after commencement of flow, is of the order of 20 seconds.

While the overall agreement of the experimental data of this study with the theoretical curve is good,

individual points show considerable scatter. The scatter is no larger than that obtained by other investigators in this field (132) (126). This is more noticeable when the graphs of their results are expanded to a scale size similar to that of Figures 5.11 and 5.12.

CHAPTER 6.

RECOMMENDATIONS AND CONCLUSIONS.

## CONCLUSIONS

Hydrogen sulphide and ethyl mercaptan will readily absorb from air mixtures into alkaline buffered solutions of potassium permanganate, the absorption continuing well beyond the point at which all permanganate ion has disappeared from solution. Examination of this phenomenon has shown that, in the presence of air, the precipitated manganese species acts as a catalyst. On the basis of the experimental evidence it is believed that the oxygen from the air stream reacts with the final product of the permanganate reduction, manganese sulphide, to produce a reactive manganese oxide ( $\text{Mn}_3\text{O}_4$ ) which is capable of further reaction with the incoming sulphide.

The ability of hydrogen sulphide to progressively quench the fluorescence of alkaline solutions of fluorescein mercuric acetate and tetra-acetoxymercurifluorescein has been used as a basis for a rapid, yet accurate fluorometric method of analysis capable of determining low concentrations of the sulphide in air. Solutions of the latter reagent can also be used in a similar fluorometric method for the determination of low concentrations of ethyl mercaptan in air. Rigorous testing of the reagent solutions has shown that they are not affected by the air present in the gas samples, and are capable of continuous use for periods up to about two weeks provided proper storage precautions are taken.

Measurement of odour levels using the A.S.T.M. D1391 procedure produced values which correlated poorly with concentration measurements.

When the limitations of the short wetted wall column are realised, and allowed for, such columns are useful for examining mass transfer fundamentals.

The absorption of solute gases from air streams in laminar flow has been examined in three short wetted wall columns ranging in length between 7.7 cm and 10.3 cm, under conditions designed to eliminate the errors associated with similar investigations reported in the literature.

Under these conditions the experimental data was found to be in agreement with the Graetz equation for a parabolic velocity profile.

A check on the performance of the short wetted wall columns by examination of the desorption of carbon dioxide from water, revealed that they were behaving in a similar manner to those reported in the literature. As with all of the previous investigations, there was some variation of the experimental regression line from that predicted by the penetration theory. One of the main reasons for this was shown to be the assumption of fully developed flow within the accelerating film.



## RECOMMENDATIONS

As a result of the above study, and the associated literature survey, the following avenues for further research have become apparent.

(1) The economics of the use of solutions of potassium permanganate for deodorization should be studied for some practical situations.

(2) A more detailed examination of the reactions occurring in the spent permanganate solution between the hydrogen sulphide, the oxygen, and the various manganese species. This examination would include an experimental verification of the Eh-pH relationships within the solution during the reaction, and the development of a better method of preparation of crystalline reaction products for X-ray diffraction examination.

The study should be extended to cover the case where the air contains carbon dioxide.

APPENDICES.

TABLE A1.

The Effect of Time on the Stability  
of Reacted Reagent Test Solutions.

Description of Reagent Solution (a)	Wt.H <sub>2</sub> S Equiv. Added to Reagent Solution (µg) (b)	Pf115* (c)	Pf114* (d)
No.FMA25/6 0.00025% FMA in 0.01N NaOH	0	100.0	100.0
	0.30	99.0	99.0
	0.76	90.5	90.0
	1.06	80.3	80.0
	1.51	51.5	51.8
	1.81	39.5	39.5
	2.27	37.0	36.8
	2.57	35.8	35.5
No.FMA25/8 0.00025% FMA in 0.01N NaOH	0	100.0	100.0
	0.48	96.0	96.0
	0.80	87.2	87.5
	1.11	76.0	76.5
	1.59	46.2	46.5
	1.91	38.0	38.0
	2.39	37.2	37.0
	2.70	36.0	35.5
No.FMA75/4 0.00075% FMA in 0.01N NaOH	0	100.0	100.0
	1.60	98.5	98.5
	3.20	93.5	93.0
	4.00	87.0	87.5
	4.80	78.3	78.5
	5.44	69.0	69.0
	6.08	56.0	56.0
	6.40	49.5	49.8
	8.00	37.0	36.5

TABLE A1 (Cont.)

(a)	(b)	(c)	(d)
No.TMF120/7	0	100.0	100.0
0.0120% TMF in 0.01N NaOH	8.0	93.5	93.0
	16.0	81.5	81.2
	24.0	71.0	70.0
	32.0	59.3	59.5
	40.0	45.5	45.5
	48.0	36.3	36.0
	56.0	27.0	27.0
	64.0	20.3	20.0

Pf115 = Mean photofluorometer reading 15 minutes  
after addition of sulphide solution.

Pf145 = Mean photofluorometer reading 45 minutes  
after addition of sulphide solution.

TABLE A2.

Calibration Data; 0.00025% FMA in 0.01N NaOH

(For H<sub>2</sub>S Measurement)

Reagent Solution		Crystalline Reagent		Wt.H <sub>2</sub> S	Mean
No.	Age(days)	Time Since First Used (days)	Period Stored Over Silica Gel (days)	Equiv.Added to Reagent Solution. (µg)	Photo-fluorometer Reading.
(a)	(b)	(c)	(d)	(e)	(f)
FMA25/1	1	0	0	0	100.0
				0.74	95.3
				0.88	94.3
				1.10	90.2
				1.47	77.0
				1.62	67.0
				1.84	53.5
				2.21	45.3
				2.57	43.0
FMA25/1	14	0	0	0	100.0
				0.31	99.0
				0.77	94.7
				1.08	90.5
				1.54	72.2
				1.85	54.0
				2.31	44.0
FMA25/1	22	0	0	0	100.0
				0.32	98.5
				0.79	93.0
				1.11	86.5
				1.58	60.2
				1.89	48.0
				2.37	42.5
FMA25/1	36	0	0	0	100.0
				0.32	98.0
				0.81	90.3
				1.13	79.8
				1.61	51.5
				1.93	44.2
				2.42	43.0

TABLE A2 (Cont)

(a)	(b)	(c)	(d)	(e)	(f)
FMA25/2	1	18	0	0	100.0
				0.38	98.5
				0.76	94.7
				1.14	88.7
				1.51	73.5
				1.89	49.0
				2.27	42.8
FMA25/3	1	36	0	0	100.0
				0.40	98.3
				0.81	93.0
				1.21	83.3
				1.61	61.0
				2.01	39.3
				2.42	38.0
FMA25/4	1	55	0	0	100.0
				0.82	92.0
				1.14	86.3
				1.63	49.8
				1.96	39.3
				2.45	38.0
FMA25/5	1	60	0	0	100.0
				0.80	91.7
				1.20	77.7
				1.60	52.7
				2.00	36.7
				2.40	35.0
FMA/25/6	1	408	270	0	100.0
				0.30	99.0
				0.76	90.5
				1.06	80.3
				1.51	51.5
				1.81	39.5
				2.27	37.0
				2.57	35.8

TABLE A2 (Cont)

(a)	(b)	(c)	(d)	(e)	(f)
FMA25/7	1	535	397	0	100.0
				0.47	97.5
				0.78	90.2
				1.09	78.0
				1.25	68.0
				1.56	47.5
				1.87	38.5
				2.34	37.0
				2.65	36.2
FMA25/7	13	535	397	0	100.0
				0.30	99.0
				0.75	99.0
				1.05	80.2
				1.51	47.5
				1.81	38.8
				2.26	36.5
FMA25/7	21	535	397	0	100.0
				0.31	98.5
				0.77	86.0
				1.08	66.0
				1.55	44.2
				1.86	38.8
				2.32	36.0
FMA25/7	45	535	397	0	100.0
				0.31	96.2
				0.78	70.0
				1.09	47.5
				1.56	38.8
				1.88	37.3
				2.34	36.0
FMA25/8	1	605	467	0	100.0
				0.48	96.0
				0.80	87.2
				1.11	76.0
				1.59	46.2
				1.91	38.0
				2.39	37.2
				2.70	36.0

TABLE A3/1

Calibration Data; 0.00075% FMA in 0.01N NaOH

(For  $H_2S$  Measurement.)

Reagent No.	Solution Age(days)	Crystalline Time Since First Use (days)	Reagent Period Stored Over Sili- ca Gel(days)	Wt. $H_2S$ Equiv. <sup>2</sup> Added to Reagent Solution( $\mu$ g)	Mean Photofluor- ometer Reading.
(a)	(b)	(c)	(d)	(e)	(f)
FMA75/1	1	6	0	0	100.0
				1.51	98.5
				3.02	97.5
				4.53	89.0
				5.29	79.5
				6.04	66.8
				6.80	52.0
				7.56	40.0
				8.31	37.5
FMA75/2	1	39	0	0	100.0
				1.01	98.5
				2.03	98.0
				3.04	95.2
				4.05	88.7
				5.06	77.5
				5.47	72.0
				6.08	61.5
				7.09	43.5
				8.10	36.0
FMA75/3	1	237	99	0	100.0
				1.51	97.8
				2.26	96.0
				3.01	92.2
				3.76	88.5
				4.52	79.2
				5.27	66.5
				6.02	52.8
				6.77	39.0
				7.53	34.0



TABLE A3/2

Calibration Data; 0.00075% FMA in 0.01N NaOH

(For H<sub>2</sub>S Measurement)

Simultaneously Prepared Solutions

No.FMA75/4 to FMA75/7

Conditions: Crystalline reagent first used 406 days before preparation of these solutions, and stored over silica gel for 268 of these days.

Reagent Solution Age(days)	Wt.H <sub>2</sub> S Equiv.Added to Reagent Solution(μg)	Mean Photofluorometer Reading			
		FMA75/4	FMA75/5	FMA75/6	FMA75/7
(a)	(b)	(c)	(d)	(e)	(f)
2	0	100.0	100.0	100.0	100.0
	1.60	98.5	98.5	98.5	98.5
	3.20	93.5	92.5	93.0	93.0
	4.00	87.0	88.0	88.0	88.0
	4.80	78.3	78.5	79.0	79.5
	5.44	69.0	69.5	69.5	69.0
	6.08	56.0	57.0	57.5	57.5
	6.40	49.5	50.0	50.0	49.5
	8.00	37.0	36.3	36.0	36.0
9	0	100.0	100.0	100.0	100.0
	1.56	98.5	98.5	-	-
	3.12	94.5	94.5	-	-
	3.90	88.0	88.0	88.0	88.0
	4.68	80.0	79.5	-	-
	5.46	68.5	69.0	69.0	69.0
	6.24	52.5	52.5	-	-
	7.80	37.0	37.5	37.0	37.0
16	0	100.0	100.0	100.0	100.0
	3.22	92.0	92.0	92.0	92.0
	4.02	87.0	87.0	87.0	87.0
	4.82	77.5	78.5	77.0	77.0
	5.63	66.0	68.5	66.0	66.0
	6.43	48.5	50.5	48.3	48.3

TABLE A3/2 (Cont)

(a)	(b)	(c)	(d)	(e)	(f)
42	0	100.0	Insuff-	100.0	100.0
	3.09	91.0	iciently	92.5	92.5
	3.86	85.0		86.5	86.0
	4.62	77.5	Fluores-	78.5	77.0
	5.39	62.5	cent	61.0	61.5
	6.16	45.0		45.0	45.0
	7.70	35.5		35.5	35.5
51	0	100.0	Insuff-	100.0	100.0
	3.13	90.5	iciently	91.5	91.5
	3.91	83.5		84.0	83.5
	4.70	75.0	Fluores-	74.0	74.0
	5.48	55.0	cent	54.5	54.0
	6.26	39.5		40.0	39.5
	7.83	34.0		34.0	34.0

TABLE A3/3

Calibration Data; 0.00075% FMA in 0.01N NaOH(For H<sub>2</sub>S Measurement)Simultaneously Prepared SolutionsNo.FMA75/8 to FMA75/10

Conditions: Crystalline reagent first used 511 days before preparation of these solutions, and stored over silica gel for 373 of these days.

Reagent Solution Age(days)	Wt.H <sub>2</sub> S Equiv.Added to Reagent Solution(µg)	Mean Photofluorometer Reading		
		FMA75/8	FMA75/9	FMA75/10
1	0	100.0	100.0	100.0
	3.21	93.0	93.0	92.5
	4.01	87.5	88.0	86.5
	4.81	78.5	78.5	78.0
	5.61	65.5	64.5	64.0
	6.41	49.5	49.5	45.5
8	0	100.0	100.0	100.0
	3.98	87.0	87.0	87.5
	4.77	78.5	78.5	78.0
	6.34	51.5	51.5	49.0

TABLE A4

Calibration Data; 0.0120% TMF in 0.01N NaOH

(For H<sub>2</sub>S Measurement)

Reagent Solution No.	Solution Age(days)	Crystalline Reagent Time Since First Use (days)	Reagent Period Stored Over Silica Gel (days)	Wt.H <sub>2</sub> S Equiv.Added to Reagent Solution(μg)	Mean Photofluorometer Reading.
(a)	(b)	(c)	(d)	(e)	(f)
TMF120/1	1	0	0	0	100.0
				8.0	96.0
				16.0	88.2
				24.1	76.0
				32.1	65.2
				40.1	54.0
				48.1	43.5
				56.1	33.8
				64.2	25.5
				72.2	19.0
TMF120/1	5	0	0	0	100.0
				15.3	89.0
				30.6	67.0
				46.0	46.2
				61.3	28.0
TMF120/1	14	0	0	0	100.0
				16.4	86.5
				32.8	64.0
				49.2	42.0
				65.6	24.5
TMF120/1	18	0	0	0	100.0
				15.8	87.3
				31.5	65.0
				47.3	44.0
				63.1	26.0

TABLE A4 (Cont)

(a)	(b)	(c)	(d)	(e)	(f)
TMF120/1	27	0	0	0	100.0
				8.2	93.0
				16.3	84.0
				24.5	71.3
				32.6	60.3
				40.8	50.0
				49.0	40.0
				65.3	23.8
TMF120/2	1	38	0	0	100.0
				16.1	87.5
				24.2	76.3
				32.3	62.5
				40.3	54.3
				48.4	42.5
				56.5	33.7
				64.5	25.0
TMF120/2	12	38	0	0	100.0
				16.0	86.3
				32.1	63.0
				48.1	41.5
TMF120/2	21	38	0	0	100.0
				7.7	96.0
				15.4	81.7
				23.1	72.0
				30.8	62.2
				38.6	53.0
				46.3	43.8
				54.0	35.5
TMF120/3	1	38	0	0	100.0
				16.1	87.5
				24.2	75.7
				32.3	64.0
				40.3	53.0
				48.4	42.3
				56.5	32.5
				64.5	25.0

TABLE A4 (Cont)

(a)	(b)	(c)	(d)	(e)	(f)
TMF120/3	12	38	0	0	100.0
				16.0	86.0
				32.1	63.5
				48.1	42.0
TMF120/3	21	38	0	0	100.0
				7.7	95.5
				15.4	81.0
				23.1	70.5
				30.8	60.5
				38.6	53.0
				46.3	43.0
TMF120/3	21	38	0	54.0	35.0
TMF120/4	1	106	0	0	100.0
				7.9	95.5
				15.8	82.5
				23.6	71.5
				31.5	59.0
				39.4	48.8
				47.3	37.5
				63.0	20.0
TMF120/5	1	130	0	0	100.0
				16.2	80.2
				32.4	56.0
				48.6	35.5
TMF120/5	1	130	0	64.8	17.0
				0	100.0
				7.6	94.0
				15.1	81.0
				22.7	70.0
				30.2	59.0
				37.8	48.3
TMF120/6	1	132	0	45.3	38.8
				52.9	29.5
				60.4	21.5

TABLE A4 (Cont)

(a)	(b)	(c)	(d)	(e)	(f)
TMF120/7	1	489	350	0	100.0
				8.0	93.5
				16.0	81.5
				24.0	71.0
				32.0	59.3
				40.0	45.5
				48.0	36.3
				56.0	27.0
				64.0	20.3
TMF120/8	1	489	350	0	100.0
				8.0	94.0
				16.0	82.0
				24.0	70.5
				32.0	58.8
				40.0	48.0
				48.0	37.5
				56.0	27.5
				64.0	19.7
TMF120/9	1	649	510	0	100.0
				8.4	92.2
				16.9	79.2
				25.3	68.0
				33.7	56.3
				42.1	45.0
				50.6	34.8
				59.0	24.8
				67.4	17.2
TMF120/9	13	649	510	0	100.0
				8.6	92.5
				17.2	80.0
				25.8	67.8
				34.4	55.2
				43.0	44.3
				51.6	33.8
				60.2	23.7
				68.8	16.7
TMF120/9	25	649	510	0	100.0
				7.9	91.3
				15.7	78.0
				23.6	68.0
				31.5	55.5
				39.3	45.7
				47.2	36.5
				62.9	22.0

TABLE A5

Student's "t" Test, Applied to the  
Differences in the Data of Table A1.

	FMA25/6	FMA25/8	FMA75/4	TMF120/7
$(Y_{15} - Y_{45})$	1.0	-0.4	0	2.2
$(Y_{15} - Y_{45})^2$	0.56	0.72	0.88	1.56
Sd <sup>2</sup>	0.069	0.116	0.126	0.136
Sd	0.26	0.34	0.355	0.37
t'	1.46	-0.44	-	2.10

Tabulated t' value (Ref.100)  
 (6 degrees of freedom, 95%  
 Significance level) -  
 -2.45 to + 2.45.

Tabulated t' value (100)  
 (7 degrees of freedom, 95%  
 Significance level) -  
 -2.37 to + 2.37.



TABLE A6

Experimental ResultsFluorometric Measurements of the H<sub>2</sub>S Concentrationof Known Gaseous Mixtures.0.006% FMA in 0.01 N NaOHand0.0120% TMF in 0.01N NaOH

RUN NO.	H <sub>2</sub> S Purity ( $\mu\text{g/ml}$ ) $\times 10^{-3}$	Syringe Displace- ment (vs) (ml/inch)	Atmospheric Pressure (in.Hg.abs)	Internal Pressure (cm.H <sub>2</sub> Og)	Ambient Temp. °F.	Time of Test (mins)	Photofluorometer Reading	
							0.006%FMA	0.0120%TMF
1	1.00	1.70	30.00	5.0	80.0	0.80	43.5	37.0
2	1.00	"	30.04	"	80.0	0.80	42.0	36.0
3	0.85	"	30.15	"	81.0	0.93	45.2	40.2
4	0.85	"	30.15	"	81.0	0.77	59.0	50.5
5	0.83	"	29.81	16.5	85.1	0.70	64.0	55.0
6	0.83	"	29.81	"	85.1	0.75	59.3	53.5
7	0.82	"	29.95	16.0	81.1	0.77	59.8	52.1
8	0.82	"	29.95	"	81.1	0.70	65.2	57.0
9	0.75	"	29.86	"	81.1	0.83	60.0	52.0
10	0.75	"	29.86	"	81.1	0.87	57.2	49.8
11	1.02	2.73	29.87	5.0	79.0	0.53	60.2	54.0
12	1.02	"	29.87	"	79.0	0.52	61.0	53.0

Gear train input shaft speed, Runs F1 - F10 = 50 RPM

Runs F11- F12 = 36 RPM

TABLE A7

Calculated Results from the Data of Table A6Measurements of the H<sub>2</sub>S Concentrationof Known Gaseous Mixtures.

(Using 0.006% FMA in 0.01N NaOH)

RUN NO.	Known H <sub>2</sub> S Input ( $\mu$ g) (From H <sub>2</sub> S Injection Rate and Eq. 2.2) $X_1$	H <sub>2</sub> S Found ( $\mu$ g) From Photoflu- orometer Reading. $X_2$	( $X_2 - X_1$ )
1	52.5	52.5	0
2	52.5	53.5	1.0
3	51.1	51.5	0.4
4	42.3	41.8	-0.5
5	38.0	38.0	0
6	40.6	41.5	0.9
7	41.4	41.1	-0.3
8	37.3	37.0	-0.3
9	40.6	41.0	0.4
10	42.8	43.0	0.2
11	40.8	40.8	0
12	40.3	40.2	-0.1

Student's "t" test for Paired Data

$$S_d^2 = 0.215$$

$$t = 1.06$$

Tabulated value of  $t_n$ , from DIXON and MASSEY (100), for 95%  
level of significance = - 2.20, 2.20

Thus the differences between samples are not significant.

TABLE A8

Calculated Results from the Data of Table A6Measurements of the H<sub>2</sub>S Concentrationof Known Gaseous Mixtures.

(Using 0.0120% TMF in 0.01N NaOH and the  
Calibration Curve shown in Fig. 2.9 )

RUN NO.	Known H <sub>2</sub> S Input	H <sub>2</sub> S Found	(X <sub>2</sub> -X <sub>1</sub> )
	(µg)	(µg)	
	(From H <sub>2</sub> S Inject- ion Rate and Eq.2.2) X <sub>1</sub>	From Photoflu- orometer Reading. X <sub>2</sub>	
1	52.5	52.7	0.2
2	52.5	53.5	1.0
3	51.1	50.0	-1.1
4	42.3	42.0	-0.3
5	38.0	38.6	0.6
6	40.6	39.8	-0.8
7	41.4	41.1	-0.3
8	37.3	37.0	-0.3
9	40.6	41.0	0.4
10	42.8	42.6	-0.2
11	40.8	39.5	-1.3
12	40.3	40.2	-0.1

Student's "t" Test for Paired Data.

$$S_d^2 = 0.456$$

$$t = -0.94$$

Tabulated value of t<sub>α</sub>, from DIXON and MASSEY (100), for 95%  
level of significance = - 2.20, 2.20

Thus the differences between samples are not significant.

TABLE A9.CALIBRATION DATA, C<sub>2</sub>H<sub>5</sub>SH MEASUREMENT.(0.0120% TMF in NaOH (0.01N aq.))

Test No.	Wt. C <sub>2</sub> H <sub>5</sub> SH Added to Reagent Solution. (μg)	Average Photofluorometer Reading
I	0	100.0
	35.0	96.0
	69.9	87.2
	104.9	73.5
	139.8	61.2
	174.8	50.0
II	0	100.0
	63.7	87.0
	95.6	76.5
	127.4	68.0
	159.3	55.9
	191.2	43.4
	223.0	35.3
	254.9	28.0

TABLE A10  
VALUES OF THE 95% CONFIDENCE INTERVAL FOR  
THE CALIBRATION CURVE OF FIGURE 2.14.

(Equation 2.3)

C<sub>2</sub>H<sub>5</sub>SH Measurement

Interval into which the mean value ( $\bar{y}$ ) of a number of  $y$  values (for a particular value of  $X$ ) should fall - 95% confidence.

---

$Y = 40$	$40 - 1.38$	$< \bar{y}$	$< 40 + 1.38$
$Y = 60$	$60 - 0.83$	$< \bar{y}$	$< 60 + 0.83$
$Y = 80$	$80 - 0.96$	$< \bar{y}$	$< 80 + 0.96$
$Y = 100$	$100 - 1.61$	$< \bar{y}$	$< 100 + 1.61$

---

Interval into which a single  $y$  value, (corresponding to a single  $X$  value) should fall - 95% confidence.

$Y = 40$	$40 - 2.94$	$< y$	$< 40 + 2.94$
$Y = 60$	$60 - 2.74$	$< y$	$< 60 + 2.74$
$Y = 80$	$80 - 2.77$	$< y$	$< 80 + 2.77$
$Y = 100$	$100 - 3.06$	$< y$	$< 100 + 3.06$

TABLE A11

Results, Fluorometric Measurements of the  $C_2H_5SH$  Concentration  
of Known Gaseous Mixtures.

RUN NO.	$C_2H_5SH$ Input ( $\mu g$ ) (Wtm, Eq. 2.5) (Calculated from Injection Rate) $X_1$	Photofluorometer Reading	$C_2H_5SH$ Input ( $\mu g$ ) (Found from Photofluoro- meter Reading and Eq. 2.3) $X_2$	$(X_2 - X_1)$
E1	189.7	42.7	198.0	8.3
E2	210.8	38.0	212.1	1.3
E3	249.5	30.0	236.1	-13.4
E4	147.8	57.5	153.5	5.7
E5	152.6	56.8	155.6	3.0
E6	196.6	43.5	195.6	-1.0
E7	196.6	43.2	196.5	-0.1
E8	181.9	47.8	181.7	-0.2
E9	241.4	29.0	240.5	-0.9
E10	145.1	60.0	144.5	-0.6
E11	199.4	45.0	191.1	-8.3
E12	199.4	46.0	188.1	-11.3
E13	200.5	45.0	191.1	-9.4
E14	200.5	46.0	188.1	-12.4
E15	200.5	44.5	192.6	-7.9
E16	191.6	45.0	191.1	-0.5

$$\sum (X_2 - X_1) = -47.7 \quad (\overline{X_2 - X_1}) = -2.98 \quad \sum (X_2 - X_1)^2 = 795.21$$

$$Sd = 6.6 \quad t' = -1.81$$

Tabulated  $t'$  (100) at a 95% level of significance, 15 degrees of freedom =  $\pm 2.13$ .

Then, the differences between samples are not significant.

TABLE B1

Experimental ResultsH<sub>2</sub>S Absorption, Runs. No. 3.1 to 3.11

Run No.		3.1	3.2
<u>H<sub>2</sub>S Measurement</u>			
<u>Inlet Air.</u>			
Sample time (sec.)	(a)	42.5	45.1
Wt. H <sub>2</sub> S in reagent soln. (μg.)	(b)	38.0	41.5
<u>Outlet Air.</u>			
Sample time (sec.)	(c)	46.4	59.8
Wt. H <sub>2</sub> S in reagent soln. (μg.)	(d)	14.0	4.0
Time Occupied by Run (min.)	(e)	23.0	22.5
<u>Air Stream Data.</u>			
Average Temperature (°F.)	(f)	82.0	85.1
Vol. registered by gas meter (ft <sup>3</sup> )	(g)	1.42	1.35
External Pressure (in. Hg.)	(h)	29.97	29.81
Apparatus internal pressure (cm.H <sub>2</sub> Og)	(j)	16.0	16.5
<u>Absorber Solution Data.</u>			
Titration (initial) (ml)	(k)	19.60	39.68
" (final) (ml)	(l)	19.83	40.70
pH control by	(m)	-	KOH
pH initial value	(n)	6.80	8.50
pH final value	(p)	6.90	7.80

TABLE B 1 (Cont.)

Run No.	3.3	3.4	3.5	3.6	3.7			3.8
					.1	.2	.3	
(a)	44.5	43.5	47.5	43.6	49.0	47.2	45.5	47.4
(b)	41.1	37.0	41.0	30.5	39.5	38.5	40.0	35.8
(c)	55.5	47.6	40.2	44.8	43.0	43.5	45.5	44.9
(d)	6.08	5.80	2.00	2.52	3.65	3.67	3.75	2.00
(e)	21.7	24.0	24.0	23.0	24.0	24.0	25.0	25.0
(f)	81.1	76.2	81.1	80.3				77.1
(g)	1.37	1.56	2.48	1.54	75.8 4.34			2.23
(h)	29.95	29.73	29.86	29.80	30.02			29.96
(j)	16.0	16.0	16.0	16.5	16.0			16.5
(k)	39.20	39.20	39.20	39.35	39.70			39.18
(l)	39.97	39.70	40.88	40.28	42.18			40.28
(m)	KOH	KOH	MIXT *	Borax	(0.1%) Borax			Borax (0.1%)
(n)	8.50	8.50	8.50	9.10	8.50			9.15
(p)	7.85	7.80	9.00	9.05	7.50			9.15

\* MIXT. =  $\text{KHCO}_3$ /KOH mixture



TABLE B1. (Cont.)

Run No.	3.9	3.10		3.11	
		.1	.2	.1	.2
(a)	45.0	43.7	45.0	40.0	40.0
(b)	32.8	33.0	33.2	45.4	44.4
(c)	35.0	60.0	60.0	60.0	120.0
(d)	5.87	2.04	1.85	2.04	2.15
(e)	24.0	25.0	25.5	29.25	30.75
(f)	78.8	80.4		81.4	
(g)	1.58	2.91		3.47	
(h)	29.70	29.8		30.11	
(j)	16.5	16.0		16.0	
(k)	39.53	39.88		39.78	
(l)	40.08	40.78		43.80	
(m)	-	$K_2B_4O_7$ (0.1%)		$K_2B_4O_7$ (0.1%)	
(n)	6.70	9.25		9.25	
(p)	6.90	9.25		9.25	

TABLE B2

Experimental ResultsH<sub>2</sub>S Absorption, Run No. 3.12

Run No.	Time T <sub>m</sub> (min)	GMV (ft <sup>3</sup> )	Inlet		Tr (min)	Outlet	
			WTI (μg)	STI (sec)		WTO (μg)	STO (sec)
3.12.1	32.0	2.21	49.9	35.0	15	2.26	60.0
					26	2.42	60.0
3.12.2	33.0	2.13	49.9	35.0	5	3.11	45.0
					13	2.02	"
					20	2.35	"
					25	2.50	"
					31	2.35	"

Conditions.Air Stream Data.

Av. temperature (°F)	81.4
External pressure (in.Hg.)	29.96
Apparatus Internal pressure (cm.H <sub>2</sub> Og.)	16.0

Absorber Solution Data.

Av. titration, unreacted KMnO <sub>4</sub> (ml)	80.20
Av. " reacted " (ml)	(nil)
Solution pH adjusted with	K <sub>2</sub> B <sub>4</sub> O <sub>7</sub>
Initial solution pH	9.25
Final " pH	9.25

TABLE B3

Experimental ResultsH<sub>2</sub>S Absorption, Run No. 3.13

Run No.	Time T <sub>m</sub> (min)	GMV (ft <sup>3</sup> )	Inlet		Tr (min)	Outlet	
			WTI (μg)	STI (sec)		WTO (μg)	WTO (sec)
3.13.1	32.0	2.28	34.0	39.6	15	1.08	35.0
					26	1.08	35.0
3.13.2	31.5	2.17	33.5	40.0	15.	1.08	35.0
					23	1.13	30.0
					28	1.13	30.0
3.13.3	29.5	1.86	36.2	40.0	4	1.20	30.0
					8	1.08	30.0
					12	1.15	"
					17	1.02	"
					21	1.08	"
					24	1.13	"
					28	1.13	"
3.13.4	32.0	2.16	36.5	40.0	3	1.20	"
					9	1.20	"
					15	1.15	"
					20	1.20	"
					25	1.28	"
					31	1.25	"
3.13.5	31.0	2.06	35.4	40.0	7	1.46	"
					12	1.20	"
					23	1.28	"
3.13.6	33.0	2.42	36.2	40.0	11	1.46	"
					26	1.20	"

TABLE B3 (Cont).

3.13.7	25.0	1.75	37.0	40.0	15	1.43	30.0
					24	1.38	"

ConditionsAir Stream Data.

Av. Temperature ( $^{\circ}\text{F}$ )	81.8
External Pressure (in.Hg.)	29.97
Apparatus internal pressure (cm.H <sub>2</sub> Og.)	16.0

Absorber Solution Data.

Av. Titration, unreacted KMnO <sub>4</sub> (ml)	80.4
Av. " reacted " (ml)	(nil)
Solution pH adjusted with	K <sub>2</sub> B <sub>4</sub> O <sub>7</sub>
Initial solution pH	9.25
Final solution pH	9.25

TABLE B4  
Experimental Results  
H<sub>2</sub>S Absorption Tests Using Water,  
Buffered and Unbuffered, Run No.  
3.14 to 3.18.

Run No.	Time T <sub>m</sub> (min)	GMV (ft <sup>3</sup> )	Inlet		Tr (min)	Outlet	
			WTI (μg)	STI (sec)		WTO (μg)	STO (sec)
3.14	24.0	1.77	27.5	40.0	10. 20	5.75	45.0
						5.17	30.0
3.15	10.0	0.55	27.5	40.0	5.0	5.00	16.0
3.16	10.0	0.58	27.5	40.0	5	0.75	45.0
3.17	10.0	0.55	27.5	40.0	5.	0.71	75.0
3.18.1	30.0	1.61	39.8	20.0	10	3.17	30.0
			39.5	20.0	21	5.95	25.0
3.18.2	27.0	1.51	41.0	20.0	12	6.02	13.0
			40.2	20.0	25	6.50	10.0

Conditions

Run No.	3.14	3.15	3.16	3.17	3.18
Solution pH adjusted with	K <sub>2</sub> B <sub>4</sub> O <sub>7</sub>	-	K <sub>2</sub> B <sub>4</sub> O <sub>7</sub>	K <sub>2</sub> B <sub>4</sub> O <sub>7</sub>	K <sub>2</sub> B <sub>4</sub> O <sub>7</sub>
Initial solution pH	9.25	6.90	9.25	9.25	9.25
Final solution pH	9.25	6.80	9.25	9.25	9.25
Average air stream temp. (°F).	81.7		80.5		81.1
External pressure (in.Hg).	29.93		29.98		30.02
Apparatus internal pressure (cm.H <sub>2</sub> Og.)	16.0		16.0		16.0

TABLE B5

Experimental ResultsH<sub>2</sub>S Absorption, Run No. 3.19

Run No.	Time T <sub>m</sub> (min)	GMV (ft <sup>3</sup> )	Inlet		Outlet		Average P <sub>ext</sub> (in.Hg.)	Average Temp. (°F.)
			WTI (μg.)	STI (sec)	WTO (μg)	STO (sec)		
(a)	(b)	(c)	(d)	(e)	(f)	(g)	(h)	(j)
3.19.1	34.0	2.25	42.1	20.0	1.60	50.0	29.78	81.0
.2	33.0	2.18	45.2	"	1.88	50.0		
.3	33.0	2.16	45.2	"	1.63	40.0		
.4	32.0	2.08	45.8	"	1.90	40.0		
.5	33.0	2.14	42.1	"	1.85	35.0		
.6	32.0	2.12	42.0	"	1.83	33.0		
3.19.7	30.0	1.96	37.0	20.0	1.58	30.0	30.06	78.5
.8	20.0	1.30	38.5	"	2.00	32.0		
.9	28.0	1.78	38.5	"	1.88	30.0		
.10	31.5	2.00	37.2	"	1.83	30.0		
.11	27.0	1.74	37.2	"	1.84	30.0		
.12	33.0	2.12	38.5	"	1.85	30.0		
.13	33.0	2.12	38.5	"	5.90	55.0		
3.19.14	33.0	2.08	38.5	"	4.20	40.0	30.10	78.7
.15	33.0	2.06	38.5	"	3.80	30.0		
.16	33.0	2.09	37.8	"	4.55	30.0		
.17	33.5	2.14	44.3	"	3.65	30.0		
.18	33.0	2.10	43.8	"	3.80	30.0		
3.19.19	33.0	2.11	41.0	20.0	4.65	30.0		
.20	33.5	2.10	47.5	"	5.00	30.0		
.21	33.5	2.09	43.5	"	5.15	30.0		

TABLE B5 (Cont)

(a)	(b)	(c)	(d)	(e)	(f)	(g)	(h)	(j)
.22	33.5	2.12	46.2	20.0	5.70	30.0	29.89	77.9
.23	33.0	2.12	43.0	"	4.30	25.0		
.24	33.0	2.14	40.7	"	4.98	25.0		
.25	33.0	2.14	41.0	"	5.00	25.0		
3.19.26	33.0	2.11	42.5	20.0	5.22	25.0		
.27	33.0	2.10	39.5	"	5.40	"		
.28	33.0	2.11	40.7	"	5.34	"		
.29	33.0	2.11	43.0	"	4.86	"	29.87	77.9
.30	21.0	1.35	36.8	"	5.00	"		
.31	33.0	2.12	36.8	"	4.75	"		
.32	33.0	2.10	36.8	"	4.85	"		
.33	33.0	2.11	39.0	"	4.55	"		
3.19.34	34.25	2.23	42.0	19.0	5.47	20.0		
.35	33.0	2.17	42.0	"	5.75	"		
.36	35.5	2.30	42.5	"	5.26	"		
.37	34.0	2.21	37.8	16.0	5.13	"	29.84	77.7
.38	34.0	2.20	37.8	19.0	5.80	"		
.39	32.0	2.08	37.8	"	5.87	"		
.40	34.0	2.26	38.5	"	5.70	17.0		
3.19.41	33.0	2.06	41.9	17.0	27.0	60.0		
.42	34.5	2.19	37.8	"	29.2	"		
.43	33.0	2.11	44.2	"	5.81	10.0		
.44	33.0	2.10	39.5	"	33.5	60.0	30.08	77.8
.45	33.0	2.10	39.5	"	37.8	"		
.46	31.0	1.98	37.8	"	38.5	"		
.47	34.0	2.18	37.8	"	39.0	"		
3.19.48	33.0	2.09	37.8	20.0	37.8	60.0		
.49	32.0	2.03	37.8	"	40.2	"		
.50	33.0	2.13	38.5	"	42.0	"	30.21	76.3
.51	33.5	2.11	37.0	"	42.6	"		

TABLE B5 (Cont)

(a)	(b)	(c)	(d)	(e)	(f)	(g)	(h)	(j)
3.19.52	33.0	2.17	37.0	18.0	43.4	60.0		
.53	33.0	2.15	38.5	"	51.6	60.0		
.54	34.0	2.24	36.3	17.0	47.3	49.0		
3.19.55	33.0	2.16	37.8	20.0	44.0	50.0		
.56	33.0	2.18	37.8	"	50.0	45.0		
.57	33.0	2.18	38.0	"	44.0	40.0		
.58	33.5	2.22	38.5	"	47.3	40.0	29.80	77.0
.59	33.5	2.22	37.8	"	44.0	35.0		
.60	33.0	2.19	37.8	"	37.0	30.0		
.61	33.0	2.20	37.8	"	40.2	30.0		
3.19.62	33.25	2.06	37.8	20.0	31.3	60.0		
.63	33.0	2.13	37.0	"	39.8	50.0		

ConditionsApparatus internal pressure: 16.2 cm. H<sub>2</sub>Og

Initial soln. pH: 9.25

Final soln. pH: 8.10

Initial average KMnO<sub>4</sub> titration: 40.10 ml(against 5 ml. 0.05N As<sub>2</sub>O<sub>3</sub>)



TABLE B6

Experimental Results, Runs 3.20 to 3.27H<sub>2</sub>S AbsorptionInternal Apparatus Pressure: 16.0cm H<sub>2</sub>Og.

Run No. (a)	Time T <sub>m</sub> (min) (b)	GMV (ft <sup>3</sup> ) (c)	Inlet		Outlet		P <sub>ext</sub> (in.Hg) (h)	Temp. (°F) (j)	pH (k)
			WTI (μg) (d)	STI (sec) (e)	WTO (μg) (f)	STO (sec) (g)			
3.20.1	33.0	1.87	36.0	20.0	4.5	30.0	29.68	70.0	9.25
.2	33.25	1.91	35.2	"	5.7	30.0			
.3	33.0	1.84	39.0	"	18.8	60.0			
.4	34.0	1.89	35.2	"	18.8	"			
.5	33.0	1.86	37.5	"	19.1	"			
.6	33.0	1.83	36.0	"	23.2	"	29.68	70.1	
3.20.7	33.0	1.83	46.0	20.0	23.2	60.0	29.86	66.0	
.8	"	1.84	45.5	"	24.0	"			
.9	"	1.81	47.2	"	25.0	"			
.10	"	1.83	46.5	"	27.0	"	29.88	66.2	
3.20.11	33.0	1.85	48.0	15.0	24.0	60.0	29.72	66.0	
.12	"	1.83	46.5	20.0	25.6	"			
.13	"	1.85	48.8	15.0	29.8	"			
.14	"	1.84	46.5	20.0	31.5	"	29.72	66.2	9.25
3.21.1	33.0	1.85	49.0	20.0	5.80	45.0	29.96	65.2	9.25
.2	31.0	1.75	45.2	"	5.22	30.0			
.3	33.0	1.85	51.7	"	19.1	60.0			
.4	"	1.84	44.0	15.0	17.3	"			
.5	"	1.85	51.7	20.0	17.5	"			
.6	"	1.85	48.5	15.0	18.7	"	29.96	65.4	9.25

TABLE B6 (Cont)

(a)	(b)	(c)	(d)	(e)	(f)	(g)	(h)	(j)	(k)
3.22.1	34.0	1.92	42.0	15.0	0.95	45.0	29.59	63.2	9.25
.2	32.0	1.81	43.6	"	2.33	"			
.3	25.0	1.42	43.6	"	2.60	"	29.59	63.4	9.25
3.23.1	33.25	1.84	50.0	15.0	43.6	60.0	29.64	62.9	9.2
.2	33.0	<del>1.87</del>	<del>51.85</del>	<del>15.0</del>	52.8	45.0			
.3	"	1.86	51.2	"	53.0	35.0			
.4	"	1.85	51.5	"	51.5	30.0			
.5	30.0	1.71	51.5	"	48.0	25.0	29.62	63.1	9.1
3.24.1	34.0	1.93	44.0	20.0	52.5	30.0	29.77	62.4	7.0
.2	28.0	1.58	45.8	"	54.0	"	29.77	62.6	7.2
3.25.1	33.0	1.86	45.8	15.0	2.35	60.0	29.76	64.1	10.9
.2	33.0	1.84	46.6	"	3.10	"			
.3	33.0	1.86	43.5	"	3.30	"			
.4	33.25	1.90	44.1	"	3.94	"	29.78	64.3	
3.25.5	<del>33.0</del>	1.85	38.5	20.0	4.45	60.0	29.85	63.3	
.6	33.0	1.86	38.5	"	7.10	55.0			
.7	32.0	1.81	38.5	"	5.68	30.0			
.8	30.0	1.71	42.0	15.0	7.50	30.0	29.85	63.6	
3.25.9	33.0	1.89	42.0	15.0	5.75	20.0	29.51	64.0	
.10	33.0	1.87	42.5	"	27.5	60.0			
.11	33.0	1.86	44.0	"	31.7	"			
.12	33.0	1.86	42.5	"	38.5	"			
.13	33.0	1.82	42.5	"	43.4	"			
.14	33.0	1.86	44.0	"	39.0	45.0	29.51	64.4	10.9

TABLE B6 (Cont)

(a)	(b)	(c)	(d)	(e)	(f)	(g)	(h)	(j)	(k)
3.26.1	33.0	1.83	41.4	20.0	1.50	60.0	29.86	62.0	11.0
.2	"	1.86	42.6	"	1.25	40.0			
.3	"	1.86	43.2	"	1.59	"			
.4	"	1.86	41.7	"	1.63	"	29.86	62.4	11.0
3.27.1	33.0	1.80	39.0	20.0	0	60.0	30.14	60.8	11.0
.2	"	1.82	38.7	"	0	"			
.3	"	1.81	38.5	"	0.18	"	30.14	60.8	11.0

TABLE B7

Computed Results, H<sub>2</sub>S Removal by KMnO<sub>4</sub>

Runs 3.1 to 3.11

Run No.	Inlet Conc. H <sub>2</sub> S (ppm)	Outlet Conc. H <sub>2</sub> S (ppm)	Average Gas Flowrate (l/min)	Wt. H <sub>2</sub> S Absorbed (g x 10 <sup>3</sup> )	Wt. KMnO <sub>4</sub> Reduced (g x 10 <sup>2</sup> )	Ratio "R"
3.1	21.4	7.2	1.7	0.8	0.7	1.8
3.2	21.9	1.6	1.8	1.1	0.7	1.4
3.3	20.6	2.5	2.0	1.0	0.6	1.2
3.4	18.7	2.7	2.0	1.0	0.4	0.8
3.5	12.0	0.7	3.1	1.1	0.7	1.4
3.6	15.0	1.2	2.0	0.9	0.7	1.8
3.7.1	19.1	2.0	1.8	3.2	1.8	1.2
3.7.2	19.3	"				
3.7.3.	21.4	"				
3.8	12.1	0.7	2.7	1.0	0.8	1.7
3.9	15.7	3.7	2.0	0.8	0.4	1.1
3.10.1	18.3	0.9	1.8	2.1	1.4	1.5
3.10.2	18.2	0.8				
3.11.1	27.6	0.8	1.8	3.9	2.7	1.5
3.11.2	28.3	0.5				

Conc. KMnO<sub>4</sub>    Run 3.1:- 0.2%

Runs 3.2 to 3.11:- 0.1%

TABLE B8  
Computed Results, H<sub>2</sub>S Absorption  
Runs 3.12 to 3.18

Run No. (a)	Average Gas Flowrate (l/min) (b)	Inlet Conc. H <sub>2</sub> S (ppm) (c)	Outlet Conc. H <sub>2</sub> S (ppm) (d)
3.12.1	2.1	25.3	0.8 0.8
3.12.2	2.1	25.4	1.4 0.9 1.1 1.1 1.1
3.13.1	2.1	17.5	0.7 0.7
3.13.2	2.1	17.4	0.6 0.8 0.8
3.13.3	2.1	18.9	0.8 0.8 0.8 0.7 0.8 0.8 0.8
3.13.4	2.2	18.3	0.8 0.8 0.8 0.8 0.8 0.9 0.8
3.13.5	2.0	19.0	1.0 0.9 0.9

TABLE B8 (Cont).

(a)	(b)	(c)	(d)
3.13.6	2.2	18.0	1.0 0.8
3.13.7	2.1	19.0	1.0 0.9
3.14	2.3	13.2	2.4 3.3
3.15	1.7	13.2	8.4
3.16	1.7	13.2	0.4
3.17	1.7	13.2	0.3
3.18.1	1.6	27.0 26.8	2.9 6.5
3.18.2	1.7	27.0 26.5	12.3 17.2

TABLE B9  
Computed Results, H<sub>2</sub>S Absorption,  
Run No. 3.19.

Run No. (a)	Inlet Conc. H <sub>2</sub> S (ppm) (b)	Outlet Conc. H <sub>2</sub> S (ppm) (c)	Cumulative Time (min) (d)
3.19.1	47.3	0.7	24
.2	50.8	0.9	56
.3	51.6	0.9	89
.4	52.6	1.1	121
.5	48.6	1.2	153
.6	47.5	1.3	185
3.19.7	41.8	1.2	215
.8	43.0	1.4	234
.9	44.6	1.5	262
.10	43.3	1.4	293
.11	42.5	1.4	320
.12	44.3	1.4	352
.13	43.8	2.4	385
3.19.14	44.9	2.5	418
.15	45.6	3.0	451
.16	44.1	3.5	483
.17	51.3	2.8	516
.18	50.9	2.9	549
3.19.19	47.7	3.6	582
.20	56.4	4.0	615
.21	51.9	4.1	670
.22	54.4	4.5	681
.23	50.0	4.0	714
.24	46.8	4.6	745
.25	47.2	4.6	779
3.19.26	49.6	4.9	812
.27	46.3	5.1	845
.28	47.5	5.0	877
.29	50.2	4.5	910
.30	42.1	4.6	931
.31	42.7	4.4	963
.32	43.1	4.6	996
.33	45.5	4.3	1029

TABLE B9 (Cont).

(a)	(b)	(c)	(d)
3.19.34	50.9	6.3	1062
.35	50.3	6.6	1095
.36	51.8	6.1	1130
.37	54.5	5.9	1164
.38	46.1	6.7	1198
.39	45.8	6.8	1229
.40	45.7	7.6	1263
3.19.41	57.5	10.5	1296
.42	51.1	11.2	1330
.43	60.8	13.6	1363
.44	53.2	12.8	1395
.45	53.2	14.4	1428
.46	50.6	14.6	1459
.47	50.6	14.8	1493
3.19.48	43.1	14.4	1525
.49	43.0	15.2	1557
.50	43.1	15.7	1590
.51	42.4	16.3	1623
3.19.52	46.0	16.2	1656
.53	48.3	19.4	1688
.54	48.1	21.7	1722
3.19.55	42.5	19.8	1755
.56	42.3	24.9	1787
.57	42.6	24.7	1820
.58	43.0	26.4	1853
.59	42.4	28.2	1886
.60	42.4	27.7	1919
.61	42.2	29.9	1952
3.19.62	44	12.3	1985
.63	42	18.1	2017



TABLE B9 (Cont)

Summary - Run 3.19

Vol. absorption solution = 300 ml.

Initial  $\text{KMnO}_4$  content of absorption soln. = 0.02%

Buffer ( $\text{K}_2\text{B}_4\text{O}_7$ ) \* 0.4 g/l.

Total wt. of  $\text{H}_2\text{S}$  absorbed (computed from the individual  $\text{H}_2\text{S}$  measurements) = 0.20 g.

Total time  $\text{KMnO}_4$  solution on stream = 2017 min.

Average air flowrate = 1.9 l/min.

Average temperature = 78.1 °F.

Average conc. of  $\text{H}_2\text{S}$  in inlet stream  
= 47.4 ppm by vol.

Analysis of Product.

Equivalent wt. of  $\text{H}_2\text{S}$ . (total), in both solid and liquid products, determined by gravimetric means after oxidation of all sulphur values to  $\text{SO}_4^{=}$  ( see VOGEL (95) )  
= 0.18 g .

TABLE B10  
Computed Results, H<sub>2</sub>S Absorption

Runs 3.20 to 3.27.

Run No.	Inlet Conc. H <sub>2</sub> S (ppm)	Outlet Conc. H <sub>2</sub> S (ppm)	Cumulative Wt. H <sub>2</sub> S Absorbed (g x 10 <sup>3</sup> )	Average Inlet Conc. H <sub>2</sub> S (ppm)
(a)	(b)	(c)	(d)	(e)
3.20.1	46.9	3.9	3.2	47.4
.2	45.2	4.9	6.3	
.3	50.8	8.2	9.5	
.4	46.0	8.2	12.5	
.5	48.3	8.2	15.5	
.6	47.1	10.1	18.3	
3.20.7	59.4	10.0	22.0	59.9
.8	58.4	10.3	25.7	
.9	61.6	10.9	29.5	
.10	60.1	11.6	33.2	
3.20.11	82.4	10.3	38.7	71.6
.12	60.4	11.1	42.4	
.13	83.8	12.8	47.8	
.14	60.0	13.6	51.4	
<u>Summary</u> - Run 3.20				
Average conc. H <sub>2</sub> S in inlet stream = 57.9 ppm by vol.				
Average air flowrate = 1.6 l/min.				
Average air temperature= 67.8 °F.				
Total time KMnO <sub>4</sub> absorption solution on stream = 459 min.				
3.21.1	62.8	3.3	4.5	68.4
.2	57.9	4.5	8.4	
.3	65.8	8.1	12.8	
.4	75.2	7.4	18.0	
.5	65.8	7.4	22.5	
.6	82.5	8.0	28.3	

TABLE B10 (Cont)

(a)	(b)	(c)	(d)	(e)
3.22.1	72.1	0.5	5.6	73.5
.2	74.6	1.3	11.1	
.3	73.6	1.5	15.3	
3.23.1	86.7	18.9	5.2	87.4
.2	87.9	30.0	9.6	
.3	88.3	39.1	13.3	
.4	89.5	44.8	16.7	
.5	88.1	49.3	19.4	
3.24.1	55.8	44.4	0.9	56.3
.2	58.2	45.7	1.7	
3.25.1	77.8	1.0	5.9	76.4
.2	80.0	1.3	11.9	
.3	73.9	1.4	17.5	
.4	73.9	1.7	23.2	
3.25.5	49.0	1.9	26.8	53.7
.6	48.8	3.3	30.4	
.7	49.3	4.9	33.7	
.8	71.2	6.4	38.2	
3.25.9	72.3	7.4	43.1	73.9
.10	72.4	11.7	47.8	
.11	75.4	13.6	52.5	
.12	72.8	16.5	56.8	
.13	74.4	19.0	61.0	
.14	76.0	22.5	65.1	
3.26.1	53.2	1.1	4.0	54.0
.2	54.5	1.3	8.1	
.3	55.2	1.7	12.3	
.4	53.7	1.7	16.3	
3.27.1	51.0	0.005	3.8	50.4
.2	50.1	0.005	7.6	
.3	50.1	0.080	11.4	

TABLE B11

Experimental Results; Ethyl Mercaptan Absorption in Alkaline Solutions

Run No.	(a)	3.28	3.29	3.30	3.31				
					.1	.2	.3	.4	.5
Photofluorometer Reading (inlet)	(b)	29.0	60.0	48.5	42.0	45.0	44.5	42.0	42.0
" " (outlet)	(c)	83.0	92.5	87.5	89.5	88.5	89.0	88.5	85.0
Sample time (inlet)	(d)	40	30	30	30	30	30	30	30
" " (outlet)	(e)	90	60	60	60	60	60	60	60
Test Period (min)	(f)	26	30	30	30	30	31	30	24
Vol. Registered by Gas Meter (ft <sup>3</sup> )	(g)	1.05	1.14	1.15	1.18	1.17	1.20	1.16	0.95
Av. Temp. Air (°C)	(h)	21.4	21.4	22.8	23.6	23.6	23.7	23.8	23.9
Av. Atm. Pressure (in Hg)	(j)	30.15	30.25	30.00	29.92				
Soln. pH Adjusted with* (g/l)	(k)	KT(0.5)	KT(0.5)	KT(0.5)	KT(0.8)				
Soln. pH; start	(l)	9.25	9.25	9.25	9.25				
" " ; finish	(m)	9.25	9.25	9.25	9.25				
Av. Titration Unreacted KMnO <sub>4</sub> Soln. (ml)	(n)	39.17	39.68	39.25	39.67				
" " Reacted " " "	(o)	43.43	42.67	44.30	70.40				
Vol. 0.05N As <sub>2</sub> O <sub>3</sub> Soln. (ml)	(p)	25.0	25.0	25.0	25.0				

TABLE B11 (continued)

(a)	3.32							3.33		3.34		3.35			
	.1	.2	.3	.4	.5	.6	.7	.1	.2	.1	.2	.1	.2	.3	.4
(b)	42.0	42.0	42.0	42.0	42.0	42.0	42.0	48.0	49.5	45.0	44.5	47.0	47.0	47.0	47.0
(c)	56.0	54.5	52.0	51.5	51.5	55.5	56.3	44.5	56.0	57.0	55.0	98.0	81.5	61.5	68.4
(d)	30	30	30	30	30	30	30	30	30	30	30	30	30	30	30
(e)	60	40	35	35	35	30	30	35	30	30	30	60	45	35	35
(f)	30	30	30	30	30	30	30	32	30	30	27	30	30	30	30
(g)	1.18	1.19	1.24	1.21	1.22	1.15	1.17	1.26	1.18	1.19	1.09	1.15	1.19	1.19	1.20
(h)	23.3							23.3		23.0		22.2	22.3	22.4	22.4
(j)	28.85							30.23		30.19		29.93			
(k)	KT(0.5)							KT(0.5)		KC(0.5)					
(l)	9.25							9.25		11.0					
(m)	9.20							9.25		11.0					
(n)	80.10							-		-					
(o)	-							-		-					
(p)	10.0							-		-					

TABLE B11 (continued)

(a)	3.35									3.36					
	.5	.6	.7	.8	.9	.10	.11	.12	.13	.1	.2	.3	.4	.5	.6
(b)	47.0	47.0	47.0	47.0	48.0	48.0	48.5	48.5	48.0	46.0	45.0	46.0	46.0	45.0	45.0
(c)	69.0	69.5	69.5	72.0	65.0	67.5	65.0	63.5	64.0	97.0	94.2	95.0	93.5	95.5	96.0
(d)	30	30	30	30	30	30	30	30	30	30	30	30	30	30	30
(e)	35	35	35	35	35	35	35	35	35	60	60	60	60	60	60
(f)	32	32	33	32	32	32	32	32	30	35	35	35	35	35	35
(g)	1.31	1.28	1.33	1.31	1.28	1.27	1.27	1.26	1.20	1.38	1.39	1.38	1.41	1.38	1.38
(h)	22.5	22.5	22.7	22.8	22.8					25.6	25.4	25.2	25.0	25.3	25.4
(j)					29.69					29.58					
(k)	KC(0.5)														
(l)	11.0														
(m)	11.0														
(n)	80.50														
(o)	-														
(p)	10.0														

TABLE B11 (continued)

	3.36									
(a)	.7	.8	.9	.10	.11	.12	.13	.14	.15	.16
(b)	46.0	46.0	46.0	44.0	45.0	46.0	45.0	45.0	45.0	45.0
(c)	95.0	80.5	46.0	53.5	55.0	63.0	63.5	69.0	71.0	73.5
(d)	30	30	30	30	30	30	30	30	30	30
(e)	60	60	60	45	40	40	35	35	35	35
(f)	35	35	35	40	35	35	35	35	36	35
(g)	1.40	1.39	1.40	1.60	1.42	1.40	1.41	1.42	1.45	1.42
(h)	25.5	25.7	25.7	25.8	26.0	26.2	25.6	25.6	25.6	25.6
(j)							29.85			
(k)	KT(1.0)									
(l)	9.25									
(m)	9.25									
(n)	19.92									
(o)	-									
(p)	25.0									

Apparatus internal pressure = 16.0 cm H<sub>2</sub>O g

\* KT = potassium tetraborate, K<sub>2</sub>B<sub>4</sub>O<sub>7</sub>·5H<sub>2</sub>O

KC = potassium carbonate, K<sub>2</sub>CO<sub>3</sub> anhydrous

TABLE B12

Computed Results - Ethyl Mercaptan Absorption  
in Alkaline Solutions.

Run No.	Inlet Conc. C <sub>2</sub> H <sub>5</sub> SH (ppm)	Outlet Conc. C <sub>2</sub> H <sub>5</sub> SH (ppm)	Cumulative Wt. C <sub>2</sub> H <sub>5</sub> SH Absorbed (g x 10 <sup>3</sup> )	Initial Conc. KMnO <sub>4</sub> %	Ratio R
(a)	(b)	(c)	(d)	(e)	(f)
3.28	111.3	15.5	8.0	0.1	1.5
3.29	98.7	15.7	7.3	0.1	1.1
3.30	123.0	20.9	9.0	0.1	1.5
3.31.1	133.8	18.5	10.3	0.1	1.1
.2	128.8	19.7	20.0		
.3	131.0	19.3	30.1		
.4	136.2	19.8	40.4		
.5	131.3	22.6	48.3		
3.32.1	134.0	52.7	7.2	0.02	-
.2	134.4	81.6	11.9		
.3	129.4	94.0	15.2		
.4	134.9	98.9	18.5		
.5	131.5	96.4	21.7		
.6	130.2	103.4	24.0		
.7	137.5	107.5	26.6		
3.33.1	122.1	110.8	1.0		
.2	119.2	105.9	2.2		
3.34.1	127.4	103.0	2.2		
.2	125.7	104.8	3.9		
3.35.1	126.1	10.0	10.1	0.02	-
.2	123.0	35.3	18.0		
.3	123.7	80.7	21.9		
.4	122.7	67.9	26.8		
.5	120.2	65.6	32.2		
.6	123.0	66.3	37.6		
.7	122.3	65.9	43.3		
.8	120.3	60.6	49.1		
.9	122.2	74.9	53.6		
.10	123.1	71.0	58.5		
.11	122.1	75.4	63.0		
.12	123.1	78.7	67.1		
.13	121.9	76.4	71.2		



TABLE B12 (Cont)

(a)	(b)	(c)	(d)	(e)	(f)
3.26.1	128.6	11.1	12.0	0.2	-
.2	129.6	13.9	23.9		
.3	128.4	13.2	35.7		
.4	125.6	14.4	47.4		
.5	130.9	12.7	59.5		
.6	130.9	12.1	71.6		
.7	127.0	13.0	83.4		
.8	128.0	28.2	93.7		
.9	127.1	63.5	100.3		
.10	131.8	75.3	106.9		
.11	128.7	81.1	111.8		
.12	128.6	69.8	117.9		
.13	128.3	77.5	123.2		
.14	127.4	67.4	129.5		
.15	128.5	64.4	136.3		
.16	127.4	59.5	143.4		

Range of air flowrates = 1.1 to 1.2 l/min.

TABLE B13  
ODOUR MEASUREMENTS

Run No. (a)	Inlet Stream		Outlet Stream	
	Odour Conc. (odour units/ft <sup>3</sup> ) (b)	Pollutant Conc. (ppm) (v/v) (c)	Odour Conc. (odour units/ft <sup>3</sup> ) (d)	Pollutant Conc. (ppm) (v/v) (e)
3.1	510	21.4	50	7.2
3.2	500	21.9	10	1.6
3.3	500	20.6	20	2.5
3.4	500	18.7	16	2.7
3.5	300	12.0	5	0.7
3.6	300	15.0	5	1.2
3.7.1	400	19.1	20	2.0
3.8	300	12.1	10	0.7
3.9	400	15.7	35	3.7
3.10.1	410	18.3	5	0.9
3.11.1	600	27.6	5	0.8
3.12.1	610	25.3	5	0.8
3.13.1	400	17.5	5	0.7
3.19.1	1300	47.3	5	0.7
3.19.14	1150	44.9	25	2.5
3.19.63	1100	42.0	450	18.1
3.28	3500	111	35	15.5
3.30	4000	123	45	20.9
3.33.1	4200	122	2700	11.1
3.35.1	4000	126	30	10.0

TABLE C1.  
The Important Reactions Derived For  
The Stability Field Diagrams,  
Figures Numbered 4.1 to 4.3

NO.	REACTION
1.	$\text{Mn}^{++} + 2\text{H}_2\text{O} = \text{HMnO}_2^- + 3\text{H}^+$
2.	$\text{Mn}^{++} = \text{Mn}^{+++} + e$
3.	$\text{Mn}^{++} + 4\text{H}_2\text{O} = \text{MnO}_4^- + 8\text{H}^+ + 4e$
4.	$\text{HMnO}_2^- + 2\text{H}_2\text{O} = \text{MnO}_4^- + 5\text{H}^+ + 4e$
5.	$\text{Mn}^{++} + 4\text{H}_2\text{O} = \text{MnO}_4^- + 8\text{H}^+ + 5e$
6.	$\text{Mn}^{+++} + 4\text{H}_2\text{O} = \text{MnO}_4^- + 8\text{H}^+ + 4e$
7.	$\text{MnO}_4^- = \text{MnO}_4^{2-} + e$
8.	$\text{Mn}^{++} + \text{H}_2\text{O} = \text{MnOH}^+ + \text{H}^+$
9.	$3\text{Mn}(\text{OH})_2 = \text{Mn}_3\text{O}_4 + 2\text{H}^+ + 2\text{H}_2\text{O} + 2e$
10.	$2\text{Mn}_3\text{O}_4 + \text{H}_2\text{O} = 3\text{Mn}_2\text{O}_3 + 2\text{H}^+ + 2e$
11.	$\text{Mn}_2\text{O}_3 + \text{H}_2\text{O} = 2\text{MnO}_2 + 2\text{H}^+ + 2e$
12.	$\text{Mn}(\text{OH})_2 = \text{HMnO}_2^- + \text{H}^+$
13.	$\text{MnOH}^+ + \text{H}_2\text{O} = \text{Mn}(\text{OH})_2 + \text{H}^+$
14.	$\text{Mn}^{++} + 2\text{H}_2\text{O} = \text{Mn}(\text{OH})_2 + 2\text{H}^+$
15.	$\text{Mn} = \text{Mn}^{++} + 2e$
16.	$\text{Mn}^+ + 2\text{H}_2\text{O} = \text{HMnO}_2^- + 3\text{H}^+ + 2e$
17.	$3\text{Mn}^{++} + 4\text{H}_2\text{O} = \text{Mn}_3\text{O}_4 + 8\text{H}^+ + 2e$
18.	$3\text{HMnO}_2^- + \text{H}^+ = \text{Mn}_3\text{O}_4 + 2\text{H}_2\text{O} + 2e$
19.	$2\text{Mn}^{++} + 3\text{H}_2\text{O} = \text{Mn}_2\text{O}_3 + 6\text{H}^+ + 2e$

TABLE C1 (cont).

NO.	REACTION
20.	$2\text{HMnO}_2^- = \text{Mn}_2\text{O}_3 + \text{H}_2\text{O} + \text{H}_2\text{O} + 2\text{e}$
21.	$\text{Mn}^{++} + 2\text{H}_2\text{O} = \text{MnO}_2 + 4\text{H}^+ + 2\text{e}$
22.	$\text{MnO}_2 + 2\text{H}_2\text{O} = \text{MnO}_4^- + 4\text{H}^+ + 2\text{e}$
23.	$\text{MnO}_2 + 2\text{H}_2\text{O} = \text{MnO}_4^- + 4\text{H}^+ + 3\text{e}$
24.	$\text{MnS} + 6\text{H}_2\text{O} = \text{Mn}(\text{OH})_2 + \text{SO}_4^{=} + 10\text{H}^+ + 8\text{e}$
25.	$\text{Mn}^{++} + \text{HS}^- = \text{MnS} + \text{H}^+$
26.	$\text{Mn}^{++} + \text{H}_2\text{S} (\text{aq}) = \text{MnS} + 2\text{H}^+$
27.	$\text{MnS} + 2\text{H}_2\text{O} = \text{HMnO}_2^- + \text{HS}^- + 2\text{H}^+$
28.	$\text{MnS} + 4\text{H}_2\text{O} = \text{Mn}^{++} + \text{SO}_4^{=} + 8\text{H}^+ + 8\text{e}$
29.	$\text{MnS} + 6\text{H}_2\text{O} = \text{HMnO}_2^- + \text{SO}_4^{=} + 11\text{H}^+ + 8\text{e}$
30.	$\text{MnS} + 2\text{H}_2\text{O} = \text{Mn}(\text{OH})_2 + \text{HS}^- + \text{H}^+$
31.	$\text{H}_2\text{S}(\text{aq}) = \text{HS}^- + \text{H}^+$
32.	$\text{HS}^- = \text{S}^{=} + \text{H}^+$
33.	$\text{H}_2\text{S}(\text{aq}) + 4\text{H}_2\text{O} = \text{HSO}_4^- + 9\text{H}^+ + 8\text{e}$
34.	$\text{H}_2\text{S}(\text{aq}) + 4\text{H}_2\text{O} = \text{SO}_4^{=} + 10\text{H}^+ + 8\text{e}$
35.	$\text{HS}^- + 4\text{H}_2\text{O} = \text{SO}_4^{=} + 9\text{H}^+ + 8\text{e}$
36.	$\text{S}^{=} + 4\text{H}_2\text{O} = \text{SO}_4^{=} + 8\text{H}^+ + 8\text{e}$
37.	$\text{H}_2\text{S}(\text{aq}) = \text{S}(\text{c}) + 2\text{H}^+ + 2\text{e}$
38.	$\text{HS}^- = \text{S}(\text{c}) + \text{H}^+ + 2\text{e}$
39.	$\text{S}^{=} = \text{S}(\text{c}) + 2\text{e}$
40.	$\text{S}(\text{c}) + 4\text{H}_2\text{O} = \text{HSO}_4^- + 7\text{H}^+ + 6\text{e}$
41.	$\text{S}(\text{c}) + 4\text{H}_2\text{O} = \text{SO}_4^{=} + 8\text{H}^+ + 6\text{e}$
42.	$\text{H}_2\text{S} (\text{g}) = \text{H}_2\text{S} (\text{aq})$

TABLE C1 (cont)

NO.	REACTION
43.	$\text{H}_2\text{S (g)} = \text{HS}^- + \text{H}^+$
44.	$\text{H}_2\text{S(g)} = \text{S}^= + 2\text{H}^+$
45.	$\text{H}_2\text{S(g)} + 4\text{H}_2\text{O} = \text{SO}_4^= + 10\text{H}^+ + 8\text{e}$
46.	$\text{H}_2\text{S(g)} + 4\text{H}_2\text{O} = \text{HSO}_4^- + 9\text{H}^+ + 8\text{e}$
47.	$\text{H}_2\text{S (g)} = \text{S(c)} + 2\text{H}^+ + 2\text{e}$
48.	$\text{HSO}_4^- = \text{SO}_4^= + \text{H}^+$
49.	$\text{Mn} + \text{HS}^- = \text{MnS} + \text{H}^+ + 2\text{e}$
50.	$\text{HMnO}_2^- = \text{MnOOH} + \text{e}$
51.	$\text{Mn}_3\text{O}_4 + 2\text{H}_2\text{O} = 3\text{MnOOH} + \text{H}^+ + \text{e}$
52.	$\text{MnOOH} = \text{MnO}_2 + \text{H}^+ + \text{e}$
53.	$\text{Mn(OH)}_2 = \text{MnOOH} + \text{H}^+ + \text{e}$
54.	$\text{Mn}^{++} + 2\text{H}_2\text{O} = \text{MnOOH} + 3\text{H}^+ + \text{e}$
55.	$\text{Mn}_3\text{O}_4 + 2\text{H}_2\text{O} = 3\text{MnO}_2 + 4\text{H}^+ + 4\text{e}$
56.	$\text{Mn} + \text{H}_2\text{S (aq)} = \text{MnS} + 2\text{H}^+ + 2\text{e}$
57.	$\text{CO}_2 \text{ (g)} + \text{H}_2\text{O} = \text{H}_2\text{CO}_3\text{(aq)}$
58.	$\text{H}_2\text{CO}_3\text{(aq)} = \text{H}^+ + \text{HCO}_3^-$
59.	$\text{HCO}_3^- = \text{H}^+ + \text{CO}_3^=$
60.	$\text{Mn}^{++} + \text{HCO}_3^- = \text{MnCO}_3 + \text{H}^+$
61.	$3\text{MnCO}_3 + 4\text{H}_2\text{O} = \text{Mn}_3\text{O}_4 + 3\text{HCO}_3^- + 5\text{H}^+ + 2\text{e}$
62.	$3\text{MnCO}_3 + 4\text{H}_2\text{O} = \text{Mn}_3\text{O}_4 + 3\text{CO}_3^= + 8\text{H}^+ + 2\text{e}$
63.	$\text{MnCO}_3 + 2\text{H}_2\text{O} = \text{Mn(OH)}_2 + \text{CO}_3^= + 2\text{H}^+$
64.	$\text{MnCO}_3 + 2\text{H}_2\text{O} = \text{Mn(OH)}_2 + \text{HCO}_3^- + \text{H}^+$
65.	$\text{MnCO}_3 + 2\text{H}_2\text{O} = \text{MnOOH} + \text{HCO}_3^- + 2\text{H}^+ + \text{e}$

TABLE C2  
Standard Free Energy Data.

SPECIES	$\Delta F^0$ (kcal./mole)	SOURCE
(a)	(b)	(c)
$\text{Mn}^{++} \text{ (aq)}$	- 54.5	(115)
$\text{HMnO}_2^- \text{ (aq)}$	-120.9	(116)
$\text{H}_2\text{O} \text{ (l)}$	- 56.687	(114)
$\text{Mn}^{+++} \text{ (aq)}$	- 19.6	(116)
$\text{MnO}_4^- \text{ (aq)}$	-119.7	(115)
$\text{MnO}_4^- \text{ (aq)}$	-106.9	(115)
$\text{Mn(OH)}_2 \text{ (c)}$	-147.0	(115)
$\text{MnOH}^+ \text{ (aq)}$	- 96.8	(115)
$\text{Mn}_3\text{O}_4 \text{ (c)}$	-306.7	(115)
$\text{Mn}_3\text{O}_4 \text{ (c)}$ (aqu.suspension)	-306.5	(107)
$\text{Mn}_2\text{O}_3 \text{ (c)}$	-210.6	(115)
$\beta \text{ MnO}_2 \text{ (c)}$	-111.18	(115)
$\delta \text{ MnO}_2 \text{ (c)}$	-108.4	(107)
$\gamma \text{ MnO}_2 \text{ (c)}$	-109.2	(107)
$\text{MnS} \text{ (c)}$	-52.2	(115)
$\text{SO}_4^{=}\text{ (aq)}$	-177.97	(114)
$\text{HS}^- \text{ (aq)}$	2.88	(114)
$\text{H}_2\text{S} \text{ (aq)}$	-6.66	(114)
$\text{H}_2\text{S} \text{ (g)}$	-8.02	(114)
$\text{S}^{=}\text{ (aq)}$	20.5	(114)

TABLE C2 (cont)

(a)	(b)	(c)
$\text{HSO}_4^-$ (aq)	-180.69	(114)
$\text{Mn}(\text{OH})_3^-$ (aq)	-177.9	(115)
$\gamma$ $\text{MnOOH}$ (c)	-133.3	(107)
$\text{MnHCO}_3^+$ (aq)	-196.	(115)
$\text{MnCO}_3$ (c)	-195.2	(115)
$\text{CO}_2$ (g)	-94.254	(114)
$\text{CO}_2$ (aq)	-92.26	(114)
$\text{CO}_3^{=}$ (aq)	-126.17	(114)
$\text{HCO}_3^-$ (aq)	-140.26	(114)
$\text{H}_2\text{CO}_3$ (aq)	-148.94	(114)
$\text{SO}_4^{=}$ (aq)	-177.97	(114)
$\text{K}_2\text{CO}_3$ (c)	-255.5	(114)

TABLE C3

X-Ray Diffraction Results - H<sub>2</sub>S Absorption

Sample (1) Wet Sample		Sample (2) Dried with ethanol	
Angle (dA <sup>0</sup> )	Intensity Ratio ( $I/I_0$ )	Angle (dA <sup>0</sup> )	Intensity Ratio ( $I/I_0$ )
(a)	(b)	(a)	(b)
4.93	0.40	4.93	0.15
4.35	0.20	4.48	0.15
4.04	0.15	4.08	0.20
3.90	0.20	3.95	0.15
3.83	0.50	3.85	1.00
3.74	0.30	3.77	0.15
3.63	0.30	3.56	0.20
3.58	0.15	3.45	0.50
3.45	0.25	3.35	0.25
3.33	0.20	3.23	0.35
3.27	0.25	3.14	0.15
3.21	0.25	3.12	0.30
3.16	0.30	3.08	0.25
3.11	0.15	3.02	0.15
3.08	0.50	2.96	0.15
3.02	0.15	2.94	0.15
2.87	0.25	2.88	0.20
2.75	0.75	2.85	0.20
2.61	0.10	2.75	0.35
2.57	0.10	2.61	0.20
2.48	1.00	2.56	0.20
2.40	0.10	2.48	0.60
2.37	0.30	2.42	0.20
2.29	0.10	2.37	0.15
2.15	0.15	2.29	0.25
2.11	0.10	2.22	0.20
2.04	0.35	2.14	0.15
1.90	0.10	2.12	0.20
1.80	0.30	2.03	0.15
1.78	0.10	1.80	0.20
1.76	0.10	1.78	0.20
1.73	0.10	1.70	0.20
1.70	0.15	1.68	0.15
1.64	0.15		



TABLE C3. (Cont)

Sample (1)		Sample (2)	
(a)	(b)	(a)	(b)
1.58	0.25		
1.54	0.55		
1.44	0.20		
1.39	0.15		
1.35	0.15		

TABLE D1.  
EXPERIMENTAL RESULTS  
CARBON DIOXIDE DESORPTION FROM WATER.

RUN NO.	L Column Length (cm).	Liquor Temp. °C.	Titrations (ml.0.1N.HCl.)			W Liquor Flowrate (g./min.)
			Blank	Inlet Liquor	Outlet Liquor	
CL1	10.3	21.0	19.60	7.40	8.90	353
CL2	"	"	"	7.40	8.12	984
CL3	"	"	"	9.00	9.72	931
CL4	"	"	"	7.90	8.85	678
CL5	"	19.0	"	6.35	7.70	536
CL6	8.6	20.1	19.40	8.35	9.15	665
CL7	"	"	"	8.20	9.17	417
CL8	"	"	"	6.46	7.29	751
CL9	"	19.5	19.45	2.76	4.14	518
CL10	"	21.8	24.65	7.50	8.64	669
CL11	7.7	21.5	"	8.03	9.05	724
CL12	"	"	"	8.73	9.57	822
CL13	"	21.4	"	8.45	10.13	355
CL14	"	21.0	"	7.73	8.95	602

TABLE D2  
CALCULATED RESULTS  
CARBON DIOXIDE DESORPTION FROM WATER

RUN NO.	COL- UMN NO.	$D_L \times 10^5$ Diffusivity ( $\text{cm}^2/\text{sec}$ )	Liquor $\text{CO}_2$ (g./l)		Re	$\frac{\Gamma}{\sqrt{\epsilon}}$ (g./cm.min)	$k_L \sqrt{\frac{L}{D_L}}$ (cm/sec) $^{\frac{1}{2}}$
			$C_1$ Inlet	$C_2$ Outlet			
CL1	A	1.80	1.074	0.942	302	42.4	6.9
CL2	"	"	1.074	1.010	843	118.3	9.2
CL3	"	"	0.933	0.870	797	112.0	10.1
CL4	"	"	1.030	0.946	581	82.5	8.7
CL5	"	1.72	1.166	1.047	437	62.9	8.8
CL6	B	1.76	0.973	0.902	558	79.1	8.5
CL7	"	"	0.986	0.900	350	49.6	6.3
CL8	"	"	1.139	1.066	630	89.3	8.5
CL9	"	1.74	1.469	1.348	428	61.1	7.5
CL10	"	1.83	1.510	1.409	576	80.6	7.7
CL11	C	1.82	1.463	1.373	628	87.6	8.1
CL12	"	"	1.401	1.327	713	99.4	7.9
CL13	"	1.81	1.426	1.278	308	42.9	6.7
CL14	"	1.80	1.489	1.382	516	72.8	8.0

TABLE D3  
EXPERIMENTAL RESULTS, WETTED WALL COLUMNS - ABSORPTION OF C<sub>2</sub>H<sub>5</sub>SH

RUN NO.	Temperature (°C)			Pressure		Gas Thru Meter (ft <sup>3</sup> )	Over-all Time of Run (min)	Measurement of C <sub>2</sub> H <sub>5</sub> SH Conc. In Gas Stream.				Liquor	
	Amb-ient	Gas	Liquor	Atmos. (in.Hg. abs).	Int (cm. H <sub>2</sub> Og)			INLET		OUTLET		Norm-ality KMnO <sub>4</sub> Soln <sub>2</sub> x 10 <sup>2</sup>	Flow-rate g/min.
								Vol.Gas Thru Soln(ml)	Wt.of C <sub>2</sub> H <sub>5</sub> SH in Re-gent Soln. (µg).	Vol. Gas Thru Soln. (ml)	Wt.of C <sub>2</sub> H <sub>5</sub> SH in Re-gent Soln. (µg)		
P1	27.3	27.3	27.0	29.90	8.2	2.06	40.0	535	176.1	534	56.0	1.1	800
P2	25.0	25.0	25.6	30.11	8.5	9.85	170.0	546	111.9	587	71.0	1.2	"
P3	26.1	26.0	25.9	29.65	11.0	8.97	42.0	575	122.0	{545 528	{83.0 89.0}	"	762
P4	24.5	24.4	24.4	29.76	9.1	8.00	70.0	{541 596	{59.0 68.0	{582 603	{41.0 42.5}	1.5	770
P5	23.1	23.1	23.3	29.86	9.1	5.84	52.0	{544 545	{123.5 "	{535 553	{78.5 80.0}	"	765
P6	23.1	23.1	23.3	"	"	2.27	20.0	522	125.0	539	92.0	"	"

NOTES:

(a) Absorption Liquor; KMnO<sub>4</sub> + 0.5 g/l K<sub>2</sub>B<sub>4</sub>O<sub>7</sub>

(b) Column No.A used throughout these runs.

TABLE D4  
COMPUTED RESULTS, WETTED WALL COLUMN  
ABSORPTION OF ETHYL MERCAPTAN

RUN NO.	C <sub>2</sub> H <sub>5</sub> SH Absorption rate. (kg.mole/hr; x10 <sup>8</sup> ).	Kg (kg.mole/hr m <sup>2</sup> .atm)	Reynolds No.		$\left[ \frac{Pa_2 - Pa_1}{Pa_i - Pa_1} \right]$	$\left[ \frac{W}{\rho D_v L} \right]$
			Liquor	Gas		
P1	32.2	0.69	786	84	0.68	30
P2	12.8	0.35	762	95	0.42	34
P3	30.4	0.70	731	351	0.31	123
P4	13.0	0.62	714	189	0.37	67
P5	25.2	0.59	693	186	0.36	66
P6	21.7	0.46	693	188	0.29	67

TABLE D5/1  
EXPERIMENTAL CONDITIONS, WETTED WALL COLUMN  
ABSORPTION OF H<sub>2</sub>S

Run No.	Column No.	Temperature (°C)			Pressure	
		Ambient	Gas	Liquor	Atmos. (in.Hg.abs) (f)	Internal (cm.H <sub>2</sub> Og.) (g)
(a)	(b)	(c)	(d)	(e)	(f)	(g)
P7	A	25.4	25.3	25.1	30.12	9.1
P8	"	25.4	25.3	25.2	"	10.1
P9	"	25.4	25.3	25.2	"	10.1
P10	"	25.5	25.4	25.2	29.76	9.8
P11	"	"	"	"	29.74	5.5
P12	"	25.6	25.5	25.6	"	"
P13	"	"	"	25.7	29.65	9.8
P14	"	24.9	24.8	24.7	29.95	"
P15	"	"	"	"	"	"
P16	"	24.4	24.2	24.1	29.97	"
P17	"	"	"	"	"	"
P18	"	25.7	25.5	25.8	30.02	"
P19	"	25.9	25.8	25.9	30.00	"
P20	"	26.0	"	"	"	"
P21	"	"	"	"	"	"
P22	"	27.4	27.3	27.1	29.95	"
P23	"	27.5	"	27.2	29.91	"
P24	"	24.2	24.0	24.2	29.87	6.8
P25	"	25.6	25.6	25.5	29.91	9.8
P26	"	25.7	25.6	24.7	30.05	9.7
P27	"	25.7	25.6	25.0	"	"
P28	"	"	"	"	"	"
P29	"	26.5	26.3	26.0	29.82	"
P30	"	"	"	26.1	29.80	"
P31	"	25.8	25.5	25.4	"	"
P32	"	25.9	"	25.5	29.82	"
P33	C	25.6	"	25.3	29.83	"
P34	"	"	25.6	"	"	"
P35	"	26.1	25.9	25.6	"	"
P36	"	"	26.0	"	29.84	"
P37	"	23.9	23.7	23.2	29.89	"
P38	"	23.8	"	23.3	"	"
P39	"	"	"	"	"	"
P40	"	"	"	"	"	"
P41	"	27.0	26.8	26.2	29.86	"
P42	"	"	"	"	29.85	"
P43	"	"	"	"	"	"

TABLE D5/1 (Cont)

(a)	(b)	(c)	(d)	(e)	(f)	(g)
P44	C	22.2	22.1	21.7	30.15	9.7
P45	"	"	"	22.0	"	12.6
P46	"	21.1	21.0	20.0	30.37	12.6
P47	"	"	"	"	"	9.6
P48	B	20.8	20.7	20.9	30.33	"
P49	"	"	"	"	"	6.8
P50	A	19.4	19.2	19.7	29.55	"
P51	"	"	19.4	"	"	"
P52	"	"	"	"	"	8.7
P53	B	19.2	19.2	19.2	30.19	"
P54	B	"	"	19.2	30.08	"
P55	B	19.4	19.2	19.7	30.04	"
P56	"	"	"	"	30.02	"
P57	C	18.6	18.6	18.6	29.95	"
P58	"	18.9	18.8	19.2	29.94	8.7
P59	"	"	"	"	"	5.2
P60	"	19.4	19.2	19.4	29.74	8.7
P61	"	"	"	"	"	"
P62	"	"	"	"	"	"
P63	"	19.2	19.2	19.2	30.13	"
P64	"	19.4	19.4	19.4	"	"
P65	"	"	"	"	30.08	"
P66	"	"	"	19.4	"	"
P67	"	18.3	18.2	18.6	29.94	5.3
P68	"	"	18.3	"	"	"
P69	"	18.9	18.9	19.7	30.23	12.0
P70	"	"	"	20.0	"	"
P71	"	19.0	19.0	20.0	29.80	12.2
P72	"	"	"	19.2	"	12.2
P73	"	"	"	"	"	9.8

TABLE D5/2

## EXPERIMENTAL RESULTS, WETTED WALL COLUMN

ABSORPTION OF H<sub>2</sub>S

Run No.	Gas Thru Meter (ft <sup>3</sup> )	Overall Time of Run (min.)	INLET H <sub>2</sub> S CONC.		OUTLET H <sub>2</sub> S CONC.		LIQUOR	
			Vol. Gas Sample Taken (ml)	Corresponding Wt. H <sub>2</sub> S (μg)	Vol. Gas Sample Taken (ml)	Corresponding Wt. H <sub>2</sub> S (μg)	Normality KMnO <sub>4</sub> Soln. x 10 <sup>2</sup>	Flowrate (g./min.)
(a)	(b)	(c)	(d)	(e)	(f)	(g)	(h)	(j)
P7	3.54	31.0	1108	27.0	1114	15.3	1.4	743
P8	5.27	31.0	1134	31.3	1128	23.5	"	"
P9	4.90	29.0	1105	29.3	1132	24.2	"	512
P10	5.68	37.0	1118	36.5	1128	24.8	"	744
P11	1.73	34.3	1134	35.8	1140	12.1	"	604
P12	1.33	27.0	1122	36.3	1114	18.1	"	480
P13	4.90	32.0	1116	36.7	1131	27.2	"	748
P14	5.45	36.0	1130	37.3	1126	25.0	1.5	916
P15	4.28	28.0	1128	37.3	1202	29.0	"	798
P16	5.49	36.0	1123	37.8	1156	27.2	1.4	756
P17	4.73	31.0	1152	39.1	1178	27.5	"	918
P18	5.19	34.0	1128	35.0	1133	26.8	1.5	462
P19	5.20	34.0	1159	36.3	1160	27.9	"	570
P20	3.37	22.0	1158	36.3	1156	27.9	1.4	696
P21	3.63	24.0	1160	36.2	1156	28.5	"	816
P22	5.31	35.0	1156	37.0	1144	28.2	"	512
P23	4.27	28.0	1156	37.0	1149	27.5	"	748
P24	2.77	37.0	1127	40.0	1150	21.2	"	600
P25	4.28	15.0	1159	41.0	1152	35.0	"	725
P26	5.14	34.0	1129	31.7	1126	21.3	"	712
P27	4.17	28.0	1100	41.6	1148	30.4	"	"
P28	3.31	22.0	604	25.0	1138	32.8	"	"



TABLE D5/2 (Cont)

(a)	(b)	(c)	(d)	(e)	(f)	(g)	(h)	(j)
P29	4.81	32.0	1150	31.1	1148	21.6	6.7	768
P30	5.44	36.0	1125	34.0	1142	21.9	5.5	"
P31	3.14	21.0	1127	34.0	1140	23.0	4.5	"
P32	3.31	22.0	1127	34.0	1139	23.0	2.8	"
P33	4.92	32.0	1119	34.2	1114	23.5	1.5	800
P34	4.48	29.0	1145	37.0	1142	26.8	"	696
P35	3.38	22.0	1144	37.0	1145	27.1	"	580
P36	3.22	21.0	1143	37.0	1155	28.5	1.4	460
P37	4.10	27.0	1122	46.0	1131	32.5	"	806
P38	3.97	26.0	1123	46.0	1149	32.5	"	680
P39	3.03	20.0	1123	46.0	1158	33.2	"	600
P40	4.58	30.0	1114	45.0	1154	35.0	"	484
P41	4.66	30.0	1140	46.4	1120	29.0	"	772
P42	3.85	25.0	1136	55.0	1139	37.4	"	"
P43	3.10	20.0	604	34.8	1135	40.3	"	"
P44	4.74	31.0	1130	38.5	1152	24.2	"	760
P45	6.37	22.0	1124	40.6	1107	31.9	"	745
P46	6.12	21.4	1127	48.8	1154	32.5	"	660
P47	4.80	32.0	1156	38.0	1160	24.2	"	"
P48	4.63	31.0	1160	34.8	1158	25.3	1.5	"
P49	5.25	18.1	1138	37.0	1134	27.8	"	"
P50	2.19	32.0	1124	39.5	1122	23.9	nil	548
P51	2.23	31.0	1122	38.0	1126	19.0	nil	692
P52	2.78	18.0	1145	42.2	1126	29.2	nil	776
P53	5.78	37.0	1146	42.2	1150	31.4	nil	595
P54	4.85	31.0	1155	38.6	1145	30.0	"	"
P55	5.35	34.1	1156	38.0	1150	29.2	"	700
P56	4.54	29.0	1147	37.4	1154	27.8	"	780
P57	4.03	26.0	1147	38.0	1153	27.8	"	584

TABLE D5/2 (Cont)

(a)	(b)	(c)	(d)	(e)	(f)	(g)	(h)	(j)
P58	4.85	31.2	1151	37.4	1151	26.4	nil	700
P59	1.31	21.0	1153	37.4	1151	15.3	"	795
P60	5.04	32.2	1151	21.8	1155	14.8	"	690
P61	5.35	34.1	1151	41.7	1150	23.0	"	790
P62	3.09	20.0	1151	41.7	1150	20.2	"	872
P63	5.97	38.2	1150	23.5	1150	17.3	"	815
P64	4.84	31.0	1149	29.6	1151	20.8	"	947
P65	5.18	33.0	1142	40.0	1149	27.5	"	815
P66	4.99	32.0	1150	40.8	1149	27.3	"	920
P67	1.56	32.0	1137	43.0	1125	19.7	"	735
P68	1.64	35.3	1151	43.0	1151	16.2	"	"
P69	5.98	20.3	1122	38.5	1124	32.4	1.4	665
P70	14.05	32.2	1120	34.5	1131	28.5	"	675
P71	7.35	17.0	1152	39.2	1116	29.9	"	660
P72	6.97	16.0	1151	38.5	1147	28.9	"	704
P73	6.27	21.0	1149	35.5	1151	25.2	"	805

NOTES:  $\text{KMnO}_4$  Runs P7 - P 28, P33 - P49, P69- P73 buffered with  
 $0.5\text{g/l K}_2\text{B}_4\text{O}_7 \cdot 5\text{H}_2\text{O}$

$\text{KMnO}_4$  Runs P29 - P32 buffered with  $2.5\text{g/l K}_2\text{B}_4\text{O}_7 \cdot 5\text{H}_2\text{O}$

Water Runs P50 - P68 buffered with  $0.5\text{g/l K}_2\text{B}_4\text{O}_7 \cdot 5\text{H}_2\text{O}$

TABLE D6  
COMPUTED RESULTS, WETTED WALL COLUMN  
ABSORPTION OF HYDROGEN SULPHIDE

RUN NO.	H <sub>2</sub> S Ab- sorption Rate (kg. mole/hr x 10 <sup>8</sup> )	Kg (kg.mole/ hr.m <sup>2</sup> .atm)	Reynolds'No.		(Pa <sub>2</sub> -Pa <sub>1</sub> )	( W )
			Liquor	Gas	(Pai-Pa1)	(ρD <sub>v</sub> L)
(a)	(b)	(c)	(d)	(e)	(f)	(g)
P7	6.2	0.78	703	191	0.44	44
P8	5.8	0.57	"	282	0.25	66
P9	4.4	0.43	484	280	0.19	65
P10	8.3	0.72	704	254	0.33	59
P11	5.5	0.67	571	86	0.66	20
P12	4.1	0.41	460	85	0.50	20
P13	6.8	0.57	721	254	0.27	59
P14	8.3	0.72	846	251	0.33	58
P15	6.9	0.58	737	254	0.27	59
P16	7.8	0.65	698	253	0.30	59
P17	8.2	0.68	847	254	0.31	60
P18	5.7	0.49	428	253	0.24	59
P19	5.6	0.47	532	254	0.23	59
P20	5.5	0.47	650	256	0.23	60
P21	5.1	0.43	767	252	0.21	59
P22	5.5	0.45	481	243	0.23	56
P23	6.3	0.52	712	254	0.25	58
P24	6.6	0.60	498	126	0.48	29
P25	7.3	0.51	687	475	0.14	109
P26	7.0	0.71	665	251	0.33	58
P27	8.6	0.63	669	248	0.30	58
P28	9.6	0.65	669	250	0.30	58
P29	6.3	0.65	722	250	0.30	57
P30	8.4	0.81	727	250	0.37	57
P31	7.7	0.72	727	250	0.33	57
P32	7.7	0.72	727	252	0.33	58
P33	7.4	0.51	757	253	0.31	44
P34	6.9	0.44	658	257	0.27	45
P35	6.8	0.43	549	257	0.27	44
P36	6.0	0.37	436	257	0.24	44
P37	9.4	0.48	720	253	0.30	44
P38	9.8	0.51	612	255	0.31	44
P39	9.5	0.49	542	255	0.30	44
P40	7.8	0.39	437	254	0.25	44
P41	11.6	0.62	744	258	0.36	44
P42	12.2	0.53	744	257	0.32	44

TABLE D6 (Cont)

(a)	(b)	(c)	(d)	(e)	(f)	(g)
P43	17.4	0.66	744	258	0.38	44
P44	10.1	0.66	664	254	0.38	45
P45	10.7	0.59	653	479	0.20	85
P46	22.0	1.10	552	474	0.35	84
P47	9.1	0.61	552	249	0.37	44
P48	6.2	0.51	566	255	0.27	54
P49	11.7	0.87	566	494	0.25	104
P50	4.9	0.42	455	119	0.39	28
P51	6.3	0.62	574	125	0.50	29
P52	8.6	0.67	644	267	0.30	62
P53	7.5	0.50	488	266	0.26	57
P54	5.7	0.41	488	267	0.22	57
P55	6.0	0.44	581	268	0.23	56
P56	6.8	0.52	648	268	0.26	56
P57	7.1	0.45	472	266	0.27	47
P58	7.6	0.49	574	266	0.30	47
P59	6.5	0.54	652	111	0.60	20
P60	4.9	0.55	569	267	0.32	47
P61	12.9	0.84	651	268	0.45	47
P62	14.8	1.02	719	266	0.52	46
P63	4.3	0.43	668	266	0.26	47
P64	6.1	0.50	781	267	0.30	47
P65	8.8	0.54	672	268	0.32	47
P66	9.3	0.57	758	267	0.33	47
P67	5.2	0.35	594	86	0.54	15
P68	5.6	0.42	594	82	0.62	14
P69	8.2	0.46	552	501	0.16	89
P70	12.3	0.80	564	737	0.18	131
P71	15.8	1.46	590	734	0.21	131
P72	18.1	1.09	625	740	0.25	132
P73	12.7	0.85	581	508	0.27	91

## APPENDIX E

### Sample Calculations

#### E(1) Sample Calculations - Chapter 3

Calculations for this chapter are best demonstrated by the computer program given below, where the various terms are as follows,

VOL = GMV (see page xx)  
 WTI, WTO, STI, STO, Tm = defined in Nomenclature (page xx)  
 TEMP = average temperature ( $^{\circ}\text{C}$ )  
 PEXT = average external pressure (ins Hg)  
 PINT = average internal pressure (cm  $\text{H}_2\text{O}$  g)  
 TIME = Tm  
 TSS =  $\text{KMnO}_4$  stock solution titration with 0.05N  $\text{As}_2\text{O}_3$   
 TRS =  $\text{KMnO}_4$  reacted solution titration with 0.05N  $\text{As}_2\text{O}_3$   
 CI, CO = conc. of  $\text{H}_2\text{S}$  in inlet and outlet streams respectively (ppm)  
 WT = Wt of  $\text{H}_2\text{S}$  absorbed in  $\text{KMnO}_4$   
 WTHZS = total wt. of  $\text{H}_2\text{S}$  absorbed in  $\text{KMnO}_4$   
 TOT - total time  $\text{KMnO}_4$  in contact with gas stream (min)  
 AVFL = average flowrate  
 AVT = average temperature ( $^{\circ}\text{F}$ )  
 AVP = average total pressure (in Hg)  
 AVC = average conc. of  $\text{H}_2\text{S}$  in inlet gas stream (ppm)  
 R = reaction stoichiometry  
 WTK = Wt.  $\text{KMnO}_4$  reacted

### PROGRAM A

```

RUN 3.19
DIMENSION WTH(63),TKOS(63),F(63),T(63),P(63),C(63)
K=0
J=0
1 READ 50, TEMP, PEXT,PINT
2 VGM=(22414.0*29.921*(459.67+TEMP))/(PEXT*491.67)
3 READ 51,STI,STO,WTI,WTO,VOL,TIME
4 IF (STO) 19,19,5
5 FAV=(VOL*28316.1*60.0)/((60.0*TIME)-(STI+STO))
6 CI=(WTI*VGM*60.0)/(STI*34.08*FAV)
7 CO=(WTO*VGM*60.0)/(STO*FAV*34.08)
8 WT=((60.0*TIME)-(STI))*((WTI/STI)-(WTO/STO))/(1000000.0)
9 K=K+1
10 WTH(K)=WT
11 TOS=((60.0*TIME)-STI)/(60.0)
12 TKOS(K)=TOS
13 F(K)=TEMP*TOS
15 P(K)=(PEXT+((PINT)/(2.54*13.596)))*(TOS)
16 C(K)=CI*TOS

```

```

17 PRINT 52,CI,CO,WT
18 GO TO 3
19 J=J+1
20 IF (11-J) 21,21,1
21 WTH2S=0.0
22 DO 23 K=1,63
23 WTH2S=WTH2S+WTH(K)
24 TOT=0.0
25 DO 26 K=1,63
26 TOT=TOT+TKOS(K)
27 AVFL=0.0
28 DO 29 K=1,63
29 AVFL=AVFL+F(K)
30 AVFL=(AVFL)/(TOT)
31 AVT=0.0
32 DO 33 K=1,63
33 AVT=AVT+T(K)
34 AVT=(AVT)/(TOT)
35 AVP=0.0
36 DO 37 K=1,63
37 AVP=AVP+P(K)
38 AVP=(AVP)/(TOT)
39 AVC=0.0
40 DO 41 K=1,63
41 AVC=AVC+C(K)
42 AVC=(AVC)/(TOT)
43 PRINT 53,WTH2S,TOT,AVFL,AVT
44 PRINT 54,AVP,AVC
END

```

#### PROGRAM B

```

REACTION STOICHIOMETRY CHECK
DIMENSION WTH(2)
1 READ 50,TEMP,PEXT,TSS,TRS,J
2 VGM=(22414.0*29.921*(459.67+TEMP))/(PEXT*491.67)
  WTK=(0.375*31.606)*((1.0/TSS)-(1.0/TRS))
  CK=(0.05*2.5*31.606)/(TSS)
  K=0
3 READ 51,STI,STO,WTI,WTO,VOL,TIME
5 FAV=(VOL*28316.1*60.0)/((60.0*TIME)-(STI+STO))
6 CI=(WTI*VGM*60.0)/(STI*34.08*FAV)
7 CO=(WTO*VGM*60.0)/(STO*FAV*34.08)
8 WT=((60.0*TIME)-(STI))*((WTI/STI)-(WTO/STO))/((1000000.0)
PRINT 52,CI,CO,J
IF (10-J) 11,11,14
11 K=K+1
  WTH(K)=WT
  IF(K-2) 3,12,12
12 WT=0.0
  DO 13 K=1,2
13 WT=WT+WTH(K)
14 R=(34.08*WTK)/(158.04*WT)
PRINT 53,R,WT,WTK,CK,J

```

## E2 Sample Calculations - Chapter (5) - Desorption of CO<sub>2</sub> from Water

### Run CL1

From the experimental data given in Table D1

Concentration of CO<sub>2</sub> - Inlet gas stream

$$C_1 = (19.60 - 7.40) \times \frac{0.1}{25} \times \frac{44.011}{2}$$

where the molecular weight of CO<sub>2</sub> (95) = 44.011

$$\therefore C_1 = 1.074 \text{ g/l}$$

Similarly, in the outlet gas stream

$$\begin{aligned} C_2 &= (19.60 - 8.90) \times \frac{0.1}{25} \times \frac{44.011}{2} \\ &= 0.942 \text{ g/l} \end{aligned}$$

### Correction Factor

At 21°C, equation 5.30 becomes

$$\epsilon = \frac{\mu_{21}\rho_{21}}{\mu_{25}\rho_{25}}$$

For water (101)

$$\mu_{25} = 0.8937 \text{ cp}, \mu_{21} = 0.981 \text{ cp}$$

$$\rho_{25} = 0.997 \text{ g/cc}, \rho_{21} = 0.998 \text{ g/cc}$$

$$\therefore \epsilon = 1.0988$$

### Mass Flowrate of Liquor per Unit Perimeter

$$\Gamma = \frac{W}{\pi D}$$

where  $W = 353 \text{ g/min}, D = 2.526 \text{ cm}$

$$\therefore \Gamma = 44.5 \text{ g/cm min}$$

$$\therefore \frac{\Gamma}{\sqrt{\epsilon}} = 42.4 \text{ g/cm min}$$

### Liquor Reynolds' Number

$$Re = \frac{4 \times 44.5}{0.981 \times 0.01}$$

$$= 302$$

Film Thickness

Using approximate relationship : from equation 5.24

$$\delta = \left[ \frac{3\mu\Gamma}{\rho^2 g} \right]^{1/3} \quad \text{where } g = 979.6 \text{ cm/sec}^2 \quad (101)$$

$$= \left[ \frac{3 \times 0.981 \times 44.5 \times 0.01}{60 \times (0.998)^2 \times 979.6} \right]^{1/3}$$

$$= 0.0282 \text{ cm}$$

∴ Inside diameter of film

$$D = (2.526 - 2\delta)$$

$$= 2.47 \text{ cm}$$

Calculation  $k_L$  From equation 5.31

$$k_L = \frac{353}{60 \times \pi \times 2.47 \times 10.3} \left( 1 - \frac{0.942}{1.074} \right)$$

$$= 9.056 \times 10^{-3} \text{ cm/sec}$$

From equation 5.26,  $D_L = 1.8 \times 10^{-5} \text{ cm}^2/\text{sec}$

$$\text{Then } k_L \sqrt{\frac{L}{D_L}} = 6.9 \text{ (cm/sec)}^{1/2}$$

$$\text{for } L = 10.3 \text{ cm}$$

E3 Sample Calculations - Chapter (5) - Absorption of  $\text{H}_2\text{S}$  and  $\text{C}_2\text{H}_5\text{SH}$  by Alkaline  $\text{KMnO}_4$

Run P1

From the experimental data given in Table D3

(1) Concentration of  $\text{C}_2\text{H}_5\text{SH}$  in Gas Stream  
Inlet

From equation 2.3, when  $Y = 50.0$

$$X = 176.05 \mu\text{g}$$



And since the volume of gas tested = 535 ml (Table D3)

$$\begin{aligned}\therefore \text{Conc. } C_2H_5SH &= \frac{176.05}{535} \times 10^3 \\ &= 329.2 \text{ } \mu\text{g/l}\end{aligned}$$

### Outlet

Similarly when  $Y = 90.0$   
and the gas volume = 534 ml  
Conc  $C_2H_5SH$  in outlet gas stream = 104.9  $\mu\text{g/l}$

### (2) Partial Pressure of $C_2H_5SH$ in Gas Stream

$$\text{Generally, for this case, } p_a = \frac{nRT}{V}$$

### Inlet

$$\begin{aligned}\text{Mol.wt. } C_2H_5SH &= 62.13 \\ T_1 &= 300.5^\circ\text{K (Table D3)} \\ R &= 82.057 \text{ cc atm/deg mole} \quad (101)\end{aligned}$$

$$\begin{aligned}\therefore p_{a1} &= \frac{329.2 \times 10^{-6} \times 82.057 \times 300.5}{62.13 \times 10^3} \\ &= 1.306 \times 10^{-4} \text{ atm}\end{aligned}$$

### Outlet

$$\begin{aligned}\text{Similarly where } T_2 &= 300.5^\circ\text{K} \\ p_{a2} &= 0.416 \times 10^{-4} \text{ atm}\end{aligned}$$

### (3) Log Mean Partial Pressure Difference

By assuming that the partial pressure of  $C_2H_5SH$  in the exit liquor is zero

$$\begin{aligned}p_{LM} &= \frac{(p_{a1} - 0) - (p_{a2} - 0)}{2.30259 \log \frac{(p_{a1} - 0)}{(p_{a2} - 0)}} \\ &= 0.779 \times 10^{-4}\end{aligned}$$

(4) Gas Flowrate

$$\text{Gas flowrate, } F = \frac{(28.316G) + S_1 + S_2}{T_m}$$

where G = vol. gas through meter (ft<sup>3</sup>)

S<sub>1</sub>, S<sub>2</sub> = sample volumes (ℓ)

T<sub>m</sub> = time of run (min)

$$\begin{aligned} \therefore F &= \frac{(28.316 \times 2.06) + 0.535 + 0.534}{40} \\ &= 1.49 \text{ ℓ/min} \end{aligned}$$

(5) Absorption Rate

$$\begin{aligned} \text{Absorption rate} &= F \times 60 \times (n_{a1} - n_{a2}) \times 10^{-3} \\ &= \frac{1.49 \times 60 \times 10^{-6} (329.2 - 104.9) \times 10^{-3}}{62.13} \\ &= 3.216 \times 10^{-7} \text{ kg mole/hr} \end{aligned}$$

(6) Film Thickness

The film thickness may be calculated from the exact equation (e.g. 5.25). The liquid properties are assumed to equal those for pure water.

$$\begin{aligned} Q &= \frac{800}{(60p)} \text{ cc/sec} \\ \rho &= 0.996 \text{ g/cc} \quad (101) \\ g &= 979.64 \text{ cm/sec}^2 \quad (162) \\ \mu &= 0.855 \times 0.01 \text{ poise} \quad (101) \\ R &= \left( \frac{2.526}{2} \right) \text{ cm} \\ a &= 1 - z/R \end{aligned}$$

By trial and error  $z = 0.035 \text{ cm}$ .

For calculation of this function, equation 5.24 may also be used.

(7) Liquor Film Reynold's Number

$$\text{Re} = \frac{4 \times 800}{\pi \times 2.526 \times 0.01 \times 60 \times 0.855}$$

$$= 786$$

(8) Mass Transfer Coefficient

$$\text{KG} = \frac{\frac{[\text{absorption rate}]}{[\text{pLm}] \times [\text{film surface area}]}}{3.216 \times 10^{-7}}$$

$$= \frac{0.779 \times 10^{-4} \times \pi [(2.526 - (2 \times 0.035))] \times 7.7 \times 10^{-4}}{3.216 \times 10^{-7}}$$

where the length of the liquid film = 7.7 cm

$$= 0.69 \text{ kg mole/hr m}^2 \text{ atm}$$

(9) Gas Reynold's Number

Total pressure within the apparatus

$$= \left[ \frac{29.90}{29.92} \right] + \left[ \frac{8.2}{13.6 \times 76} \right]$$

$$= 1.007 \text{ atm}$$

$$\rho_{\text{air}} @ 0^\circ\text{C}, 1 \text{ atm} = 1.2928 \times 10^{-3} \text{ g/cc} \quad (101)$$

$$\rho_{\text{air}} @ 27.3^\circ\text{C}, 1.007 \text{ atm} = \frac{1.2928 \times 10^{-3} \times 1.007 \times 273.2}{300.5}$$

$$= 1.1836 \times 10^{-3} \text{ g/cc}$$

$$\mu_{\text{air}} = 60 \times 0.018 \text{ g/cm min} \quad (101)$$

The gas Reynold's Number is given by,

$$\text{Re} = \frac{u \rho D}{\mu} = \frac{4 F \rho}{\pi D \mu} \times 10^3$$

When the gas properties are assumed to equal those for pure air,

$$\therefore Re = \frac{4 \times 1.49 \times 10^3 \times 1.1836 \times 10^{-3} \times 10^3}{\pi \times (2.526 - 2 \times 0.035) \times 60 \times 0.018}$$

$$= 84.4$$

(10) Ratio of Partial Pressures

The group  $\frac{pa_2 - pa_1}{pa_i - pa_1}$ , may be readily calculated if the partial pressure of the  $C_2H_5SH$  at the interface,  $pa_i = 0$ .

$$\therefore \frac{pa_2 - pa_1}{pa_i - pa_1} = \frac{(0.416 - 1.306) \times 10^{-4}}{(0 - 1.306) \times 10^{-4}}$$

$$= 0.68$$

(11) The Group  $\left(\frac{W}{\rho D_V L}\right)$

From section 5.5.2 and reference (119), the value of  $D_V$  at  $20^\circ C$  and 1 atm abs. =  $0.104 \text{ cm}^2/\text{sec}$ .

Using the method of Slattery and Bird (119) to correct this value to  $27.3^\circ C$  and 1.007 atm.

$$D_V = \frac{0.104}{P} \left(\frac{T}{293.2}\right)^{1.823}$$

$$= \frac{0.104}{1.007} \left(\frac{300.5}{293.2}\right)^{1.823}$$

$$= 0.108 \text{ cm}^2/\text{sec}$$

Now,

$$\begin{aligned}\frac{W}{\rho D_V L} &= \frac{F}{D_V L} \\ &= \frac{1.49 \times 10^3}{60 \times 0.108 \times 7.7} \\ &= 29.8\end{aligned}$$

APPENDIX E.REFERENCES.

1. JACOBS, M.B., "The Chemical Analysis of Air Pollutants", Interscience Publishers, Inc., New York. (1960).
2. JACOBS, M.B., BRAVERMAN, M.M., and HOCHHEISER, S., Anal. Chem., 29, 1349-51, (1957).
3. SMITH, A.F., JENKINS, D.G., and CUNNINGWORTH, D.E., J. Appl. Chem., 11, 317-28, (1961).
4. SANDS, A.E., GRAFIUS, M.A., WAINWRIGHT, H.W., and WILSON, M.W., "The Determination of Low Concentrations of H<sub>2</sub>S in Gas by the Methylene Blue Method" U.S. Bureau of Mines, Report of Investigations No.4547 (1949).
5. LAHMANN, E., and PRESCHER, K.E., Staub. 25, 527-8 (1965).
6. POMEROY, R., Water Work and Sewerage, 83, 279-281 (1936).
7. POMEROY, R., Sewerage Works J, 8, 572-591 (1936). Also summarised in Water Works and Sewerage 83, 279-281 (1936).
8. CHANIN, G., ELWOOD, J.R., and CHOW, E.H., Sewerage and Indust. Wastes, 26, 1217-1230 (1954).
9. ADAMS, D.F., KOPPE, R.K., and TUTTLE, W.N., J. of the Air Poll. Cont. Assoc. 15, 31-33 (1965).
10. BAYER, E., "Gas Chromatography", Elsevier Publishing Co., Amsterdam. (1961).
11. DEMAIO, L., and CORN, M., Anal. Chem., 38, 131-133 (1966).
12. STERN, A.C., "Air Pollution", P.42, 2nd Ed., Vol.II, Academic Press Inc., N.Y., (1968).
13. WRONSKI, M., Z. Anal. Chem., 180, 185-188 (1961).
14. WRONSKI, M., Z. Anal. Chem., 175, 432-436 (1960).
15. WHITE, E.C., J. Am. Chem. Soc., 42, 2355-2366 (1920).
16. KARUSH, F., KLINMAN, N.R., and MARKS, R., Anal. Biochem., 9, 100-114 (1964).

17. ANDREW, T.R., and NICHOLS, P.N.R., The Analyst, 90, 367-370 (1965).
18. SUMMER, W., "Methods of Air Deodorization", Elsevier Publishing Co., Amsterdam (1963).
19. MCCORD, C.P., and WITHERIDGE, W.N., "Odors, Physiology and Control", McGraw-Hill Book Co. Inc., N.Y. (1949).
20. WRIGHT, R.H., "The Science of Smell", George Allen and Unwin LTD., London (1964).
21. RAMSAY, D.A., and HASLER, A.D., Science, 133, 56-57 (1961).
22. GORMAN, W., "Flavour, Taste and the Psychology of Smell", Charles C. Thomas. Publisher, Springfield, Illinois (1964).
23. AMERINE, M.A., PANGBORN, R.M., and ROESSLER, E.B., "Principles of Sensory Evaluation of Food", Academic Press Inc., N.Y., (1965).
24. SHAH, R.K., SHAIKH, A.A., and RABARI, L.F., Nature, 218, 593-594 (1968).
25. BAKER, R.A., pp. 87-107 of A.S.T.M. Spec. Tech. Publication No. 440, "Correlation of Subjective-Objective Methods in the Study of Odours and Taste" (1968).
26. TANYOLAC, N.N., Conf. Surface Effects Detection-Washington D.C., 1964, pp. 89-100, (pub.1965).
27. MONCRIEFF, R.W., "The Chemical Senses", Leonard Hill Ltd., London, (1951).
28. AMOORE, J.E., and VENSTROM, D., J. of Food Science, 31, 118-128 (1966).
29. AMOORE, J.E., JOHNSTON, J.W., and RUBIN, RM., Sci. American, 210, 42-49 (1964).
30. STERN, A.C., "Air Pollution", 2nd Ed., Vol. III, Academic Press Inc., N.Y., (1968).
31. VON BERGEN, J., Chem. Engrg., 64, 239-250 (1957).
32. STERN, A.C., "Air Pollution", 2nd Ed., Vol. I., Academic Press Inc., N.Y. (1968).

33. HENDERSON, Y., and HAGGARD, H.W., "Noxious Gases" 2nd Revised Ed., p. 245, Reinhold Pub. Corp. N.Y. (1943).
34. American Conference of Governmental Industrial Hygienists - Threshold Limit Values for 1968.
35. WITTES, J., and TURK, A., in A.S.T.M. Spec. Tech. Publication No. 440 (1968).
36. PRINCE, R.G.H., and INCE, J.H., J. Appl. Chem., 8, 314-321, (1958).
37. BENFORADO, D.M., ROTELLA, W.J., and HORTON, D.L., J. Air Poll. Cont. Assoc., 19, 101-105, (1969).
38. WILBY, F.V., J. Air Poll. Cont. Assoc., 19, 96-100, (1969).
39. MILLS, J.L., WALSH, R.T., LUEDTKE, K.D., and SMITH, L.K., J. Air Poll. Cont. Assoc., 13, 10- (1963).
40. LEONARDOS, G., KENDALL, D., and BARNARD, N., J. Air Poll. Cont. Assoc., 19, 91-95 (1969).
41. SAX, N.I., "Dangerous Properties of Industrial Materials", 3rd Ed., Reinhold Book Corp. N.Y. (1968).
42. SULLIVAN, D.C., ADAMS, D.F., and YOUNG, F.A., Atmos. Environment, 2, 121-133 (1968).
43. KATZ, S.H., and TALBERT, E.J., U.S. Bureau of Mines Tech. Paper No. 480, (1930).
44. American Society for Testing and Materials (ASTM) Designation D1391-57, "Measurement of Odour in Atmospheres (Dilution Method)", (1957).
45. DRAYNIEKS, A., in "Flavour Chemistry" in Advances in Chem. Series No. 56, American Chem. Soc., Washington (1966).
46. JONES, F.N., Science, 118, p. 333 (1953).
47. WASHBURN, E.W., (Ed.), "The International Critical Tables", Vol. 1, McGraw-Hill Book Co. Inc., N.Y. (1926).
48. DALLAVALLE, J.M., and DUDLEY, H.C., U.S. Public Health Reports, 54, 35-43 (1939).



49. OUGH, C.S., and STONE, H., J. Food Science, 26, 452-456 (1961).
50. SCHNEIDER, R.A., COSTILOE, J.D., VEGA, A., and WOLF, S., J. Appl. Physiol. 18, 414-417 (1963).
51. CEDERLÖF, R., EDFORS, M., FRIBERG, L., and LINDVALL, T., J. Air. Poll. Cont. Assoc., 16, 92-94, (1966).
52. RYAZONOV, V.A., Arch. Environmental Health, 5, 480-491, (1962).
53. ALLISON, V.C., and KATZ, S.H., J. of Indust. and Engrg. Chem., 11, 336-338 (1919).
54. FISCHER, E., and PENZOLDT, F., Sitzungsab. phys. med. Soc. Erlangen, 18, 7-10, (1886).
55. LAFFORT, P., Arch. Sci. Physiologiques, 17, 75-105, (1963).
56. YANT, W.P., Am. J. Public Health, 20, 598-608 (1930).
57. WEAVER, E.R., "Control of Odours", U.S. Bureau of Standards, Circular No.491 (1950).
58. TURK, A., Indust. Wastes, 3, 9-14, (1958).
59. LORENTZ, F., Chem. Engrg. Progress, 46, 377-379 (1950).
60. BROOMAN, D.L., and EDGERLEY, E., J. Air Poll. Cont. Assoc., 16, 25-29 (1966).
61. MANTELL, C.L., "Adsorption", 2nd Ed., McGraw-Hill Book Co., Inc., N.Y., (1951).
62. CARLSON, D.A., and LEISER, C.P., J. Water Poll. Cont. Fed., 38, 829-840 (1966).
63. ANDERSON, H.W.J., Aust. Patent 24,477, (1936) Chem. Abs. No.31-1539 2.
64. GRIFFITH, R.H., pp. 48-58 of "Special Study of Sulphur Removal and Recovery from Fuels", Papers for the Inaugural Conference of the Institute of Fuel, October, 1954.
65. CADLE, R.D., and LEDFORD, M., Air Water Pollution, 10, 25-30 (1966).

66. KOHL, A.L., and RIESENFELD, F.C., "Gas Purification", Mc-Graw Hill Book Co. Inc., N.Y. (1960).
67. JENSEN, G.A., ADAMS, D.F., and STERN, H., J. Air Poll. Cont. Assoc., 16, 248-253, (1966).
68. WELCH, W.A., J. Am. Water Works Assoc., 55, 735-741 (1963).
69. SPICHER, R.G., and SKRINDE, R.T., J. Am. Water Works Assoc., 55, 1174-1194 (1963).
70. ADAMS, R.B., J. Am. Water Works Assoc., 52, 219-228 (1960).
71. EMANUEL, A.G., Air Engrg., 7, 19-21, (1965).
72. POSSELT, H.S., and REIDIES, A.H., Indust. and Engrg. Chem. Product Research and Development, 4, 48-50, (1965).
73. BAILEY, D.A., and HUMPHREYS, F.E., J. of the Soc. of Leather Trades' Chemists, 51, No.5, pp. 154-172, (1967).
74. KUEHNER, R.L., and HOPKINS, N.E., U.S. Patent 2,876,507 (1959); Chem. Abs. 53-12542.
75. KUEHNER, R.L., U.S. Patent 2,683,074 (1954) Chem. Abs. 48-14062.
76. BORG WARNER CORP., U.S. Patent 3,049,399 B. Patent, 895,683 (1962), Chem. Abs. 57-5762.
77. Am. Cyanamid Co., Neth. Appl. 6,501, 093 (1965) Chem. Abs. 64-7267.
78. SWINARSKI, A., and ROZWADOWSKI, M., Chemia Stosowana, Ser. A., 9, (3), 287-294 (1965).
79. ROZWADOWSKI, M., and SWINARSKI, A., Chemia Stosowana, Ser. A., 10, (1), 11-18 (1966).
80. CONVISER, S.A., Oil Gas J., 63, (49), 130-135 (1965).
81. KHARKOVSKAYA, E.N., ZELVENSII, Y.D., and BRONINA, R.N., Khim. Prom., 42, 268-272 (1966).
82. MARSH, J.D.F., and RICH, J., Brit. Pat. 802,284 (1958) Chem. Abs. 54-13609.
83. THOMAS, M.D., IVIE, J.O., ABERSOLD, J.N., and HENDRICKS, R.H., Indust. and Engrg. Chem. Anal. Ed., 15, 287-290 (1943).

84. IVANOV, D., and KOSTADINOV, N, Godishnik Khim-Teknol. Inst. 11, 53-64 (1965).
85. ROMOVACEK, J., and BEWES, M., Paliva, 45, 19-22 (1965).
86. LYNN, C., and ELSEY, H.M., Trans. Am. Inst. Elect. Engrs., 68, Part I, 106-112 (1949).
87. COTTON, F.A., and WILKINSON, G., "Advanced Inorganic Chemistry", p.840 Interscience Publishers (John Wiley and Sons), London (1966).
88. DUNNICLIFF, H.B., and NIJHAWAN, S.D., J. Chem. Soc., pp.1-7 (1926).
89. JACOBSON, C.A., "Encyclopedia of Chemical Reactions" Vol.5, Reinhold Pub. Corp, N.Y. (1953).
90. MOHAMMAD, S., and SURENDAR NATH BEDI, J. Indian Chem. Soc., 21, 55-60 (1944).
91. WILLEY, B.F., JENNINGS, H., and MUROSKI, F., J. Am. Water Works Assoc., 56, 475-479 (1964).
92. REID, E.E., "Organic Chemistry of Bivalent Sulphur", Vol. I, Chemical Pub. Co. Inc., N.Y. (1958).
93. GILMAN, H., "Organic Chemistry, An Advanced Treatise", Vol.I, 2nd Ed., John Wiley and Sons Inc. N.Y. (1958).
94. FINAR, I.L., "Organic Chemistry", Longmans, Green and Co., London (1951).
95. VOGEL, A.I., "A Text-Book of Quantitative Inorganic Analysis", 3rd Ed., Longmans, Green and Co. Ltd., London, (1961).
96. WEAST, R.C., (Ed) "Handbook of Chemistry and Physics", 50th Edition, The Chemical Rubber Co., Ohio (1969).
97. TREADWELL, F.P., and HALL, W.T., "Analytical Chemistry" Vol. II, 9th Ed., John Wiley and Sons, Inc., N.Y. (1948).
98. WALTHER, J.E., and AMBERG, H.R., Chem. Engrg. Prog., 66, No.3, 73-80 (1970).
99. EZEKIEL, M., and FOX, K.A., "Methods of Correlation and Regression Analysis", 3rd Ed., John Wiley and Sons, Inc., N.Y. (1959).

100. DIXON, W.J., and MASSEY, F.J. "Introduction to Statistical Analysis", 2nd Ed., McGraw-Hill Book Co. Inc., N.Y. (1957).
101. PERRY, J.H., Editor, "Chemical Engineers' Handbook", 4th Ed., McGraw-Hill Book Co., Inc., N.Y. (1963).
102. FRITZ, J.S., and HAMMOND, G.S., "Quantitative Organic Analysis" John Wiley and Sons Inc., N.Y. (1957).
103. MELVILLE, Sir H., and GOWENLOCK, B.G., "Experimental Methods in Gas Reactions", Macmillan and Co. Ltd., London, (1964).
104. REMY, H., "Treatise on Inorganic Chemistry", Vol.II, Elsevier Publishing Co., Amsterdam (1956).
105. BARNETT, E., and WILSON, C.L., "Inorganic Chemistry", 2nd Ed., Longmans, London, (1960).
106. MOORE, T.E., ELLIS, M., and SELWOOD, P.W., J. Am. Chem. Soc., 72, 856-866 (1950).
107. BRICKER, O., The Am. Mineralogist, 50, 1296-1354, (1965).
108. HEM, J.D., "Chemical Equilibria and Rates of Manganese Oxidation", Geological Survey Water-Supply Paper 1667-A, U.S. Dept. Interior (1963).
109. OSWALD, H.R., FEITKNECHT, W., and BRUNNER, P., Symposium on Electron Microscopy, 141-160 (1963).
110. FEITKNECHT, W., BRUNNER, P., and OSWALD, H.R., Z. Anorganische und Allgemeine Chem., 316, 154-160 (1962).
111. POURBAIX, M.J.N. Atlas of Electrochemical Equilibria in Aqueous Solutions Pergamon (1966).
112. MELLOR, J.W., "A Comprehensive Treatise in Inorganic and Theoretical Chemistry", Vol. XII, Longman, Green & Co. Ltd., London (1932).
113. GARRELS, R.M., and CHRIST, C.L., "Solutions, Minerals, and Equilibria", Harper and Row Student Edition, Tokyo (1965).
114. U.S. Dept. Commerce, N.B.S. Tech. Note No.270-3, "Selected Values of Chemical Thermodynamic Properties" (Elements 1 through 34) (1968).

115. U.S. Dept. of Commerce, N.B.S. Tech. Note No.270-4, "Selected Values of Chemical Thermodynamic Properties", (Elements 35 through 53) (1969).
116. LATIMER, W.M., "Oxidation Potentials", 2nd Edition, Prentice Hall, N.Z. (1952).
117. WILKE, C.R., and LEE, C.Y., I. and E.C., 47, 1253-1257 (1955).
118. HIRSCHFELDER, J.O., BIRD, R.B., and SPOTZ, E.L., Trans. Am. Soc. Mech. Engrs., 71, 921-926 (1949).
119. SLATTERY, J.C., and BIRD, R.D., A.I. Ch.E. Journal 4, 137-142 (1958).
120. ANDRUSSOW, L., "Diffusivity, Viscosity and Conductivity of Gases", pp. 279-82 of Progress in International Research on Thermodynamic and Transport Properties, Papers presented at the 2nd Symposium on Thermophysical Properties; The American Soc. of Mech. Engrs., Academic Press, N.Y. (1962).
121. LYNN, S., STRAATEMEIER, J.R., and KRAMERS, H., Chem. Engrg. Sci., 4, (2), 58-62 and 49-58, (1958).
122. GILLILAND, E.R., and SHERWOOD, T.K., I.E.C., 26, (1), 516-523 (1934).
123. HASLAM, R.T., HERSHEY, R.L., and KEEN, R.H., I.E.C., 16, (12), 1224-1230 (1924).
124. BOELTER, L.M.K., Trans. A.I. Ch. E., 39, 557-564 (1943).
125. PLEWES, A.C., BUTLER, R.M., and MARSHALL, H.E., Chem. Engrg. Prog., 50 (2), 77-80, (1954).
126. LINTON, W.H., and SHERWOOD, T.K., Chem. Engrg. Prog., 46, (5), 258-264 (1950).
127. DREW, T.B., HOGAN, J.J., and McADAMS, W.H., I.E.C., 23, 936-945 (1931).
128. JACKSON, M.L., A.I. Ch. E. Journal, 1, 231-240 (1955).
129. TAILBY, S.R., and PORTALSKI, S., Chem. Engrg. Sci., 17, 283-290 (1962).
130. FULFORD, G.D., "The Flow of Liquids in Thin Films," in Advances in Chem. Engrg., 5, 151-236, Academic Press, N.Y., (1964).

131. BIRD, R.B., STEWART, W.E., and LIGHTFOOT, E.N., "Transport Phenomena", John Wiley and Sons Inc., N.Y. (1960).
132. PORTALSKI, S., Chem. Engrg. Sci., 19, 575-582 (1964).
133. WEST, D., and COLE, R., Chem. Engrg. Sci., 22, 1388-1389 (1967).
134. WILKES, J.O., and NEDDERMAN, R.M., Chem. Eng. Sci., 17, 177-187 (1962).
135. STAINTHORP, F.P., and ALLEN, J.M., Trans. Instn. Chem. Engrs., 43, T85-T91 (1965).
136. NUSSELT, W., Z. Ver. Deutsch Ing. 60, 541, 569, (1916).
137. NORMAN, W.S., "Absorption, Distillation and Cooling Towers", Longmans, Green & Co., London (1961).
138. VIVIAN, J.E., and BEHRMANN, W.C., A.I. Ch.E. Journal, 11, 656-661 (1965).
139. EMMERT, R.E., and PIGFORD, R.L., A.I.Ch.E. Journal, 8, 171-175 (1962).
140. GILLILAND, E.R., BADDOUR, R.F., and BRIAN, P.L.T., A.I. Ch. E. Journal, 4, 223-230 (1958).
141. BRIAN, P.L.T., VIVIAN, J.E., and MATIATOS, D.C., A.I. Ch. E. Journal, 13, 28-36 (1967).
142. VIVIAN, J.E., and PEACEMAN, D.W., A.I. Ch. E. Journal, 2, 437-443 (1956).
143. SCRIVEN, L.E., and PIGFORD, R.L., A.I. Ch.E. Journal, 4, 439-444 (1958).
144. CERRO, R.L., and WHITAKER, S., Chem. Engrg. Sci., 26, 785-798 (1971).
145. BRULEY, D.F., A.I. Ch.E. Journal, 11, 945-950 (1965).
146. SCRIVEN, L.E., and PIGFORD, R.L., A.I. Ch.E. Journal 4, 382- (1958).
147. LYNN, S., A.I. Ch. E. Journal, 6, 703-705 (1960).
148. ROBERTS, D., and DANCKWERTS, P.V., Chem. Engrg. Sci., 17, 961-969 (1962).

149. EMMERT, R.E., and PIGFORD, R.L., Chem. Engrg. Prog., 50, 87-93 (1954).
150. GRAETZ, L., Ann. Physik., 18, 79-86 (1883), and 25, 337-357 (1995).
151. NUSSELT, H., Z. Ver. Deut. Ing., 54, 1154-1160 (1910).
152. LEVEQUE, J., Ann. Mines, (12), 13, 201, 305 and 381 (1928).
153. DREW, T. B., Trans. A.I. Ch. E., 26, 26-79 (1931).
154. MUNAKATA, T., SHIOTA, S., and SHINOHARA, H., Kagaku Kogaku (Abridged Eng. Ed.) 2, 224-228 (1964).
155. LEWIS, W.K., and WHITMAN, W.G., I.E. Co, 16, 1215-1220 (1924).
156. WHITMAN, W.G., Chem. Met. Engrg., 29, 146-148 (1923).
157. HIGBIE, R., Trans. Am. Inst. Chem. Engrs., 31, 365-389 (1935).
158. DANCKWERTS, P.V., I.E.C., 43, 1460-1467 (1951).
159. DANCKWERTS, P.V., and KENNEDY, A.M., Trans. Am. Inst. Chem. Engrs., 32, 49-55 (1954).
160. MORRIS, G.A., and JACKSON, J., "Absorption Towers", Butterworth, London (1953).
161. TOOR, H.L., and MARCHELLO, J.M., A.I. Ch. E. Journal, 4, 97-101 (1958).
162. BARRACLOUGH, Sir Henry, "Abridged Mathematical Tables", Parts I and II, Angus and Robertson, Sydney (1961).
163. KNUDSEN, J.G., and KATZ (D.L.) "Fluid Dynamics and Heat Transfer" McGraw-Hill Book Co. Inc., N.Y. (1958).
164. BERRY, L.G., and THOMPSON, R.M., The Geological Society of America, Memoir 85, 195-196. (1962).
165. ASTARITA, G., and GIOIA, F., Chem Engrg. Sci., 19, 963-971, (1964).
166. GIOIA, F., and ASTARITA, G., Ind. and Engrg. Chem. Fundamentals, 6, 370-375, (1967)

APPENDIX GPUBLISHED PAPERS

- (1) HARDWICK, B.A., THISTLETHWAYTE, D.K.B., and FOWLER, R.T.,  
Atmospheric Environment, 4, 379-385, 1970 and 5, 281-282  
1971.
- (2) THISTLETHWAYTE, D.K.B., HARDWICK, B., and GOLEB, E.E.,  
Paper presented at the Congres International Le Genie  
Chimique Au Service De L'Homme, 2nd to 9th September 1972.



## A FLUOROMETRIC METHOD FOR DETERMINING LOW CONCENTRATIONS OF HYDROGEN SULPHIDE IN AIR

B. A. HARDWICK, D. K. B. THISTLETHWAYTE and R. T. FOWLER

School of Chemical Engineering, University of New South Wales

(First received 5 February 1970 and in final form 3 April 1970)

**Abstract**—A fluorometric technique for the determination of low concentrations of hydrogen sulphide in air streams is described and possible limitations examined. The method is particularly suitable where accurate measurements of these low hydrogen sulphide concentrations are required in small air sample volumes.

The reagent is a simple solution of fluorescein mercuric acetate (FMA—biochemical laboratory reagent grade), in dilute aqueous sodium hydroxide. Hydrogen sulphide reacts rapidly with the alkaline FMA solution, causing a quenching of fluorescence which is related in a definite way to the amount of hydrogen sulphide contained in the air stream.

Reagent stability, overall precision, and reproducibility of the method were found to be very satisfactory.

### 1. INTRODUCTION

IN THE chemical and related industries, hydrogen sulphide is a gas which can be both a valuable reactant and an annoying byproduct. It is extremely toxic, 600 ppm proving fatal within 30 min (HENDERSON and HAGGARD, 1943). Having the odour of rotten eggs, with reported odour threshold values varying between 0.007 ppm (CEDERLOF *et al.*, 1966) and 0.13 ppm (YANT, 1930), hydrogen sulphide is easily the most malodorous of the commoner industrial gases.

#### 1.1 Review of published methods

The measurement of hydrogen sulphide concentrations in air has received considerable attention and a number of analytical methods have been developed. JACOBS (1960) has reviewed the majority of these, whilst SMITH *et al.* (1961) have critically commented on their shortcomings.

Recently, WRONSKI (1961) described a procedure for the fluorometric titration of sulphides and mercaptans with tetra-acetoxymercurifluorescein (TMF)  $C_{20}H_8O_5$  (Hg OOC.CH<sub>3</sub>)<sub>4</sub>, a compound which he prepared following the method of WHITE (1920). The same compound was used by ANDREW and NICHOLS (1965), for an automatic instrumental method which they claimed could be used for on the spot measurements of hydrogen sulphide concentrations with satisfactory precision at concentrations even less than 5 parts of H<sub>2</sub>S in 10<sup>10</sup> parts of air, by volume. The technique depended on the reduction (quenching) of the fluorescence of the TMF reagent solution according to the amount of H<sub>2</sub>S absorbed.

This TMF compound is not available commercially and its preparation and purification is somewhat tedious. KARUSH *et al.* (1964) used a similar compound fluorescein mercuric acetate, (FMA)  $C_{20}H_{10}O_5$  (Hg OOC.CH<sub>3</sub>)<sub>2</sub> (which is marketed commercially) as a very sensitive test reagent for disulphide groups in proteins and peptides. The potential of this latter compound as a reagent for the determination of H<sub>2</sub>S in air does not appear to have been evaluated to date.

### 1.2 Preliminary experiments

It was required that an analytical procedure be selected and developed to satisfy the specific test requirements of an experimental study of hydrogen sulphide removal from air streams (HARDWICK, 1970). In particular it was necessary that the procedure be simple and reliable for accurate measurements of  $\text{H}_2\text{S}$  concentrations between about 0.05 ppm and 60 ppm by volume. In addition it had to be sensitive enough to measure  $\text{H}_2\text{S}$  concentrations of only 0.05 ppm using not more than 4–5 l. of air (about 0.3  $\mu\text{g}$  total  $\text{H}_2\text{S}$ ). The flowrate of the sample air was restricted to  $1\frac{1}{2} \text{ l min}^{-1}$  maximum.

Suitability of the FMA reagent system for the particular purpose envisaged also demanded (a) that the absorption apparatus be simple and readily connected to the main experimental set-up for  $\text{H}_2\text{S}$  removal studies, (b) that the reagent be stable enough for continued use throughout, say, at least 2 weeks together and (c) that measurements be accurate and reproducible with a precision generally around 1 per cent.

(a) It was found that a solution of FMA in dilute NaOH (0.01N aq.) would achieve 100 per cent measurable absorption of  $\text{H}_2\text{S}$  from air streams when a simple test tube bubbler was used. The body of this bubbler consisted of a glass test tube, 25 mm i.d. and about 150 mm long, and was charged with 25 ml of reagent solution. The inlet tube was constructed from 3.5 mm i.d. glass tubing drawn down to about 1.5 mm i.d. at the orifice, this orifice being located about 1.5 cm above the rounded bottom (centre) of the test tube. The outlet was also constructed from 3.5 mm i.d. glass tubing. Both inlet and outlet tubes were fitted through an appropriate red rubber laboratory grade stopper.

When two such bubbler tubes were used in series, it was found that for all gas flowrates used up to the maximum of  $1\frac{1}{2} \text{ l min}^{-1}$ , even when the fluorescence of the FMA solution in the first tube had been substantially reduced, that of the following tube showed no measurable difference from the fluorescence of the solution at the start of the test.

An advantage of the FMA reagent-bubbler system, in the hands of a trained worker, was that the progressive degree of quenching of the reagent could be observed by inspection reliably enough so that the amount of test sample passed through the bubbler, even though the  $\text{H}_2\text{S}$  concentration were unknown, could be regulated to an appropriate level.

(b) The stability of the FMA reagent proved to be satisfactory, there being no significant change over a period of up to about 16 days. Further tests of this and the longer term stability are described below.

(c) The overall reliability of the method was checked by testing air streams containing known proportions of  $\text{H}_2\text{S}$ . Preliminary runs showed that the method could be adapted to give results accurate to  $\pm 1$  per cent (see TABLE 1), even at low  $\text{H}_2\text{S}$  concentrations. Further detailed experiments were undertaken as described in the following, in which details of the procedure are given.

These experimental investigations not only showed that a technique based on FMA reagent satisfied these special requirements, but suggested that the technique could be adapted for measuring sulphide gas concentrations in air streams generally.

## 2. METHODS AND PROCEDURES

### 2.1 Fluorescence measurement

Measurement of the solution fluorescence was made directly using a model 12C photofluorometer (Coleman Instruments Inc. U.S.A.) in conjunction with primary filter number 12-224 (Corning Glass No. 5113) and secondary filter number 14-220 (Corning Glass No. 2424). Transmission characteristics for these filters are set out in the *Handbook of Chemistry and Physics* (WEAST, 1969).

### 2.2 Preparation of the test solution and calibration curves

The test solution was prepared by dissolving the required amount of FMA in sodium hydroxide (0.01 N aq.). This yellow-green solution was stored in a dark brown bottle in a dark cupboard, but was discarded and prepared afresh after 14 days. No special mixing technique appeared to be necessary, but as a precaution the fresh solution was always allowed to stand at least 24 hr after preparation, before use. Test solutions contained from 0.00025 to 0.006 per cent FMA.

The crystalline chemical itself was stored in a dark bottle, in a cool place, using silica gel as a desiccant.

Calibration curves similar to those shown in FIG. 1 were constructed from measurements of the fluorescence of 25 ml aliquots of the reagent solution, containing micro-pipetted quantities of sodium sulphide solution, prepared and standardized in accordance with the procedure described by SMITH *et al.* (1961). Care had to be taken with this preparation to avoid oxidation and polymerisation of the sodium sulphide in solution.

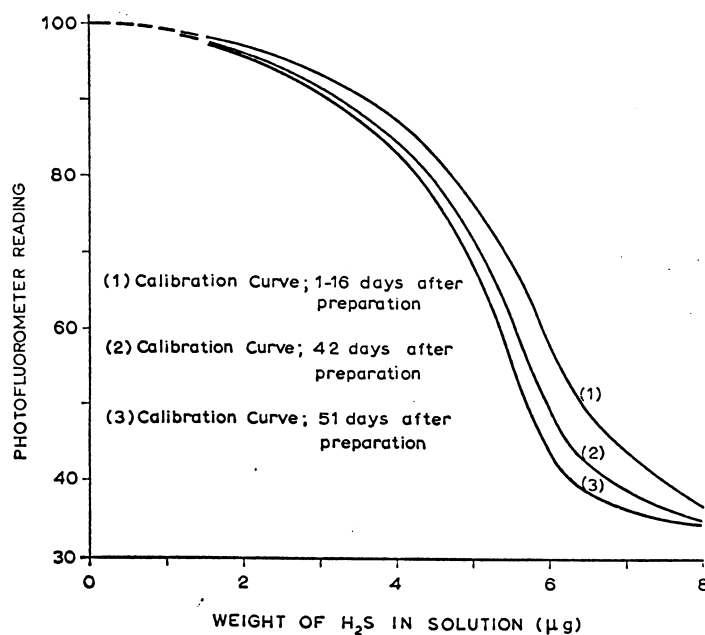


FIG. 1. Calibration curves 0.00075% FMA in 0.01 N NaOH.

### 2.3 H<sub>2</sub>S Concentration measurement procedure

Precise measurement of the H<sub>2</sub>S content of air streams was achieved by passing a known volume through a 25 ml portion of FMA solution contained within the absorber. The relative fluorescence of the solution was then determined using the photofluorometer.

The volume of the air stream and the concentration of the FMA solution were adjusted so that the corresponding photofluorometer test reading fell on the more linear portion of the calibration curve. This restricted the weight of H<sub>2</sub>S which was passed into solution to levels similar to those indicated in TABLE 1.

TABLE 1. TYPICAL FMA SOLUTION CONCENTRATIONS AND THEIR USEFUL RANGES

FMA solution strength (%)	Ranges of applicability	
	Precision $\pm 15\%$ or better	Precision $\pm 1\%$ or better
	$\mu\text{g H}_2\text{S}$	
0.00025	0.3-2.0	1.0-2.0
0.00075	2.0-7.0	3.5-7.0
0.006	15-60	20-60

### 3. SENSITIVITY AND ACCURACY: PRACTICAL CHECKS

Absolute overall checks of accuracy were made by preparing air-H<sub>2</sub>S mixtures containing known concentrations of H<sub>2</sub>S and carrying out measurements of these concentrations using the experimental method detailed above.

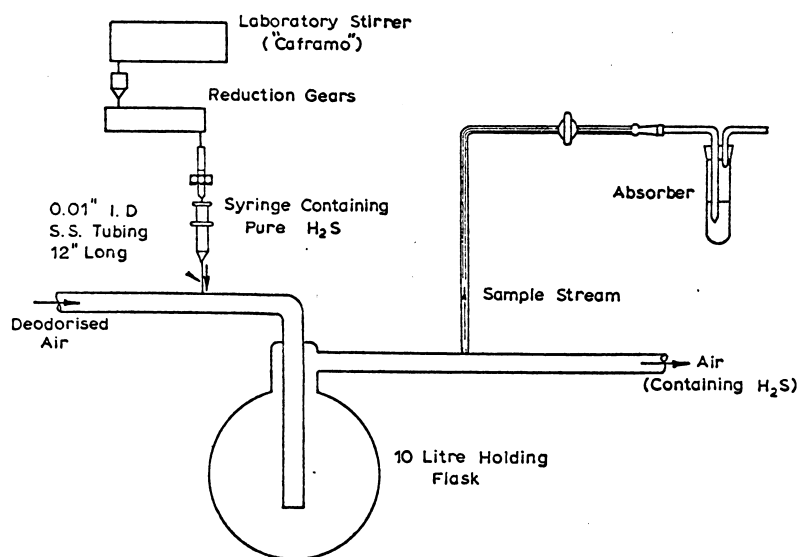


FIG. 2. Diagram of apparatus (for the production and measurement of air streams containing known concentrations of hydrogen sulphide).

H<sub>2</sub>S of known purity was dosed into a continuous stream of purified air at a constant predetermined rate from a mechanically operated, all glass hypodermic syringe as shown in FIG. 2. The mechanical system consisted of a laboratory stirrer connected by reduction gears to a threaded push rod which drove the syringe plunger at rates down to 0.04 in. min<sup>-1</sup>. This allowed precise calculation of the weight of H<sub>2</sub>S introduced into the gas stream in a known time period. These calculated values were compared with the observed values derived from the photofluorometer readings and the appropriate calibration curve for the FMA solution used.

The results of twelve such comparisons are given in TABLE 2.

TABLE 2. COMPARISON OF VALUES OF H<sub>2</sub>S INPUT INTO ABSORBER  
(0.006% FMA in 0.01 N NaOH)

H <sub>2</sub> S input (μg) (from H <sub>2</sub> S injection rate) X1	H <sub>2</sub> S found (μg) (from photofluorometer reading and calibration curve) X2	Difference (X2-X1) μg
52.5	52.5	0
52.5	53.5	1.0
51.1	51.5	0.4
42.3	41.8	-0.5
38.0	38.0	0
40.6	41.5	0.9
41.4	41.1	-0.3
37.3	37.0	-0.3
40.6	41.0	0.4
42.8	43.0	0.2
40.8	40.8	0
40.3	40.2	-0.1

Statistical examination of these data, using Student's *t* statistic at the 5 per cent significance level, showed that the differences between pairs of observations were not significant.

#### 4. REAGENT STABILITY

##### 4.1 Effect of light

A sample of 0.00075 per cent FMA in 0.01 N NaOH was left exposed to daylight in a clear glass stoppered container on the laboratory bench, whilst three control samples were stored as specified above in a dark cupboard.

After seven days no detectable variation could be found in the calibration curves, each reading falling on the curve (FIG. 1, curve 1). However, thereafter, the fluorescence of the sample exposed to the light was quenched progressively, so that 42 days after preparation the solution fluorescence was no longer measurable on the photofluorometer. On the other hand, after the same period, the control samples, stored in the dark, still showed considerable fluorescence (FIG. 1, curve 2), even though appreciably less than the original curve.

#### 4.2 *Effect of storage temperature*

A 15° change in the storage temperature was found to have no detectable effect on the calibration curve for 0.00075 per cent FMA solution in 0.01 N NaOH over the test period of 16 days.

#### 4.3 *Degradation of FMA test solution on standing*

Even when solutions of FMA are stored at ambient temperature, in a dark bottle and in the dark, the solutions degrade slowly.

The course of degradation of 0.00075 per cent FMA solution in 0.01 N NaOH is shown on FIG. 1 (curves 1, 2 and 3). These measurements, taken on a number of samples, 2, 7, 16, 42 and 56 days after preparation, demonstrate that the calibration curves show no significant change until after about 16 days storage.

#### 4.4 *Reacted reagent solution standing time*

Tests were carried out to determine whether the reacted solution standing time was critical.

A number of aliquots of solutions of 0.00075 per cent FMA in 0.01 N NaOH were reacted with sulphide ion and allowed to stand in a dark, cool place. Samples were withdrawn from these aliquots at times varying between 10 and 45 min after sulphide ion addition and the fluorescence measured.

No significant change in fluorescence was detectable in any instance.

#### 4.5 *Calibration curve reproducibility*

Groups of samples of 0.00075 per cent FMA in 0.01 N NaOH prepared 120 days apart were calibrated and calibration curves compared. No significant variation in curves was discovered, all plots following curve 1 (FIG. 1) almost exactly.

### 5. DISCUSSION OF RESULTS AND CONCLUSION

The method of hydrogen sulphide measurement described above appears to offer some advantages over others in common use today. It is a simple method, requiring a minimum of apparatus and instrumentation. It is capable of accurately measuring relatively low concentrations of the sulphide in only small volumes of air. In fact, concentrations as low as 0.05 ppm v/v H<sub>2</sub>S in 4.5 l. of air can be measured with 0.00025 per cent FMA solution (in 0.01 N NaOH) using the technique described in this paper.

The reagent solution appears to be unaffected by substantial variations in temperature and was found to be resistant to air degradation. However, the volume of air used did not exceed 4.5 l. It may be that acidic constituents, such as CO<sub>2</sub> and SO<sub>2</sub>, could affect measurements, particularly if the volume of air tested contained sufficient of such constituents to significantly change the reagent pH. For the reagent specified (using 0.01 N solutions of NaOH) the limits would be more than 500 ppm by volume of CO<sub>2</sub> plus SO<sub>2</sub> for 4.5 l. samples.

Where the H<sub>2</sub>S air stream contains other sulphidic gases (such as mercaptans and disulphides), which also tend to cause fluorescence quenching, this analytical method cannot be used directly.

The reproducibility of calibration curves was found to be excellent, it being found

unnecessary to carry out daily recalibrations. However, due to degradation of the fluorescence of the reagent solution on standing, it was found essential that prepared solutions be stored in the dark and then discarded after 14 days.

The fluorescence of FMA solutions was found to be not completely quenched, even by excess sulphide ion, and in this respect any calibration curve must be restricted, accordingly.

#### REFERENCES

- ANDREW T. R. and NICHOLS P. N. R. (1965) The determination of hydrogen sulphide in the atmosphere, *Analyst* **90**, 367-370.
- CEDERLOF R., EDFORS M., FRIBERG L. and LINDYALL T. (1966) On the determination of odour thresholds in air pollution control, *J. Air Pollut. Control Ass.* **16**, 92-94.
- HARDWICK B. A. (1970) Ph.D. Thesis in preparation. University of N.S.W.
- HENDERSON Y. and HAGGARD H. W. (1943) *Noxious Gases*, 2nd Revised Edition, p. 245. Reinhold Pub. Corp., N.Y.
- JACOBS M. B. (1960) *The Chemical Analysis of Air Pollutants*, pp. 182-188. Interscience Publishers, London.
- KARUSH F., KLINMAN N. R. and MARKS R. (1964) An assay method for disulphide groups by fluorescence quenching, *Analyt. Biochem.* **9**, 100-114.
- SMITH A. F., JENKINS D. G. and CUNNINGWORTH D. E. (1961) Measurement of trace quantities of hydrogen sulphide in industrial atmospheres, *J. appl. Chem.* **11**, 317-329.
- WEAST R. C. (1969) *Handbook of Chemistry and Physics*, 50th Edition, p. E238. The Chemical Rubber Co., Ohio.
- WHITE E. C. (1920) Mercury derivatives of phthaleins, *J. Am. chem. Soc.* **42**, 2355-2366.
- WRONSKI M. (1961), Fluorimetrische titration von Sulfiden und Mercaptanen mit Tetraquecksilberacetatfluorescein, *Z. anal. Chem.* **180**, 185-188.
- YANT W. P. (1930) Hydrogen sulphide in industry; occurrence, effects and treatment, *Am. J. Publ. Hlth* **20**, 598-608.

## DISCUSSION

### A FLUOROMETRIC METHOD FOR DETERMINING LOW CONCENTRATIONS OF HYDROGEN SULPHIDE IN AIR\*

(1) On page 6 it is mentioned that "acidic constituents such as  $\text{CO}_2$  and  $\text{SO}_2$  could affect measurements" and a limit of 500 ppm by volume of  $\text{CO}_2$  plus  $\text{SO}_2$  is given; probably on stoichiometric considerations for the neutralization of the NaOH content. From the above it is not clear whether this effect is dependent on the resultant pH of the FMA solution and if so, to what extent? Or else, whether the effect would come into play only after the NaOH is fully neutralized?

(2) In TABLE 1 one finds the range of applicability of the procedure from 0.3  $\mu\text{g}$  to 60  $\mu\text{g}$ . However, the experimental verification provided in TABLE 2 deals with only the near maximum concentrations of  $\text{H}_2\text{S}$  in the above range (37.3-52.5  $\mu\text{g}$ ). At these concentrations, particularly in purified air (page 5) almost all known methods of estimating  $\text{H}_2\text{S}$  at low concentrations will yield similar result.

To my mind it would have been better if the experimental verification could be presented at concentrations covering the entire range of applicability proposed in TABLE 1.

(3) One would agree with the authors that this is really a straight forward and simple procedure for the estimation of  $\text{H}_2\text{S}$  concentrations above 0.05 ppm in small volumes of air, provided the air stream is purified (page 5, 1st line). However, these days the environmental air in most of the places is very much polluted and the  $\text{H}_2\text{S}$  concentrations usually encountered in the atmosphere are around 0.01 ppm or even less, which will correspond to only about 0.08  $\mu\text{g}$  in a 5 l. parcel of air. This, to our mind, puts a serious limitation on the applicability of the present procedure to environmental sampling unless it is shown that serious interferences will not be encountered while sampling larger volumes of air necessary to bring the  $\text{H}_2\text{S}$  concentration in the absorber to a level at which it can be measured satisfactorily by the proposed method.

P. K. ZUTSHI

*Bhabha Atomic Research Centre  
(Air Monitoring Section)  
Bombay 85  
India*

\*B. A. Hardwick, D. K. B. Thistlethwayte and R. T. Fowler, *Atmospheric Environment* 4, 379 (1970)

## AUTHORS' REPLY

THE AUTHORS are in sympathy with the comment by P. K. ZUTSHI.

In respect of items 2 and 3, it is pointed out that the authors have not investigated the method as it might be applied directly to environmental air pollution studies. The paper was written because the authors believe the method does have useful applications, particularly in that field where extreme dilutions of sulphidic gases are of interest. As stated in the paper, the authors satisfied themselves fully as to the accuracy of the technique at very low concentrations of  $\text{H}_2\text{S}$ . They measured such concentrations in effluent air streams from their experimental purification systems. The calibrations were made against standardized solutions of sodium sulphide as outlined in the paper. TABLE 1, however, presents data collected during experimental deodorization runs. The air stream analysed for  $\text{H}_2\text{S}$  content had been dosed with precisely known amounts of  $\text{H}_2\text{S}$ , so that this data provided additional verification to the calibration curves but only in the 37-53  $\mu\text{g}$  range.

Items 1 and 3 refer more specifically to possible interference by other substances which also may occur in polluted air environments. In this connection it is emphasized that quenching of the FMA fluorescence is especially characteristic for sulphidic gases. The alkalinity of the FMA test solution is important in the main because  $\text{H}_2\text{S}$  (mercaptans also) is trapped with high efficiency at higher pH levels but not so efficiently near neutrality nor under "acid" conditions. The authors believe that if, for example, neutralization of the solution alkalinity by acidic gases such as  $\text{CO}_2$  and  $\text{SO}_2$  were to cause appreciable errors in determining  $\text{H}_2\text{S}$  contents, simple modifications of the technique would surely be found so as to obviate the inaccuracies.

The authors' work was not concerned with these questions, but they believe that what is presented here provides a goodly length start from which suggested applications for air pollution test runs might begin; and hope this justifies the publication as it stands.

B. A. HARDWICK, D. K. B. THISTLETHWAYTE and R. T. FOWLER

*School of Chemical Engineering  
University of New South Wales  
New South Wales  
Australia*



## DISCUSSION

THIS paper is well written and the problem clearly defined, but no appreciable interference studies from air pollutants are reported. The procedure has indeed a potential for measuring  $\text{H}_2\text{S}$  in air and merits further evaluation by other investigators under field conditions. I shall submit the procedure to the various sulfur subcommittee members for critical review and obtain their recommendations for collaborative testing.

However, I would like to raise several questions for the authors to discuss. These questions arise mostly from the work of AXELROD *et al.*, *Anal. Chem.* **41**, 1856 (1969); "Thus, the FMA must be added to the sample following the bubbling procedure. These data are not in agreement with the findings of ANDREW and NICHOLS", *Analyst* **90**, 367 (1965). This statement by Axelrod apparently contradicts the authors of the article under discussion as well. Do the authors have any explanation or is it because of the different concentration ranges of  $\text{H}_2\text{S}$  reported in the two papers?

AXELROD *et al.*, state "... air containing  $\text{NO}_2$  and  $\text{SO}_2$  containing  $2 \times 10^{-7} \text{ m s}^{-2}$  in 0.1 N NaOH. At concentrations greater than 10 ppb these gases tend to react with  $\text{S}^{2-}$ , changing it to a form that resists analysis". Does this apply only to the Axelrod procedure, since FMA is not incorporated into the absorbing solution? I suspect that this is the case, since sulfito ions and sulfido ions cannot coexist in solution. In any event,  $\text{SO}_2$  and  $\text{NO}_2$  should be checked as potential sources of interference in the procedures. Have the authors done any interference studies for these compounds?

Large amounts of organic materials contain fluorescent materials that are collected in an alkaline solution. In any event,  $\text{SO}_2$  and  $\text{NO}_2$  should be checked as potential sources of interference in the procedure. Have the authors done any interference studies for these compounds?

Large amounts of organic materials contain fluorescent materials that are collected in an alkaline solution (1 N). Would this produce a negative interference in the procedure as written? Do the authors have any data to indicate this occurs?

The authors indicate an alkalinity of 0.01 NaOH, while AXELROD *et al.*, prefer 0.1 N and 1 N NaOH. In view of the potential interference from acidic gases, would not the solution with higher alkalinity be preferred or is there some other reason for 0.01 NaOH?

FRANK P. SCARINGELLI

*Methods Development Section, ACB  
Division of Chemistry and Physics*

## AUTHORS' REPLY

HERE the authors point out again that they developed, applied and tested the reported procedure as ancillary—but of course essential—to their main project. They made no attempt to evaluate interference by potential atmospheric pollutants such as  $\text{SO}_2$  and  $\text{NO}_2$ . Accordingly, while refraining from any argument in that connection they wish to say only that they personally would have been optimistic if they had needed to apply the procedure for air-pollution analyses.

KARUSH *et al.* (1964) suggested 0.01 N for the NaOH concentration. This proved satisfactory, and the aspect of whether or not stronger solutions might or might not be equally satisfactory was not pursued. The use of the FMA by addition before passing the test air stream through the absorber-bubbler was adopted *de novo* as the simpler procedure, from an overall point of view. AXELROD *et al.*'s paper (1969) referred to was not available to the authors when the paper was prepared, but this work would rather have confirmed their use of the FMA solution during bubbling, than have suggested the reagent be added afterwards.

B. A. HARDWICK, D. K. B. THISTLETHWAYTE and R. T. FOWLER

*School of Chemical Engineering  
University of New South Wales  
New South Wales  
Australia*

## ODOUR NUISANCES FROM WASTE DISPOSAL WORKS AND TECHNIQUES

### FOR DEODORIZATION

by Thistlethwayte, D.K.B., Hardwick, B. and Goleb, E.E.  
Schools of Civil and Chemical Engineering, University of  
New South Wales, Australia. 2033.

Copy of a paper accepted for presentation at the  
CONGRES INTERNATIONAL LE GENIE CHIMIQUE AU SERVICE DE  
L'HOMME; 2nd. to 9th. SEPTEMBER 1972.

Air pollution problems stem from many sources, including industries as different in character as abattoirs, wool scours, fat-rendering plants, textile factories, paper mills, oilrefineries, various chemical factories, and waste disposal works. In the case of paper mills for example gaseous effluvia are spread widely through the atmosphere of the neighbouring localities, which usually are rural in character and would be expected otherwise to be free of such nuisance problems. The pollutants include terpenes along with various sulphur compounds such as methyl mercaptan, dimethyl sulphide and disulphide and other thiols, sulphones, etc. (1)

Such public or private odour nuisance problems arise either from particular odours such as these, or from combination of odours, as illustrated by Table 1.

The concentration levels of these gaseous pollutants vary greatly from place to place, and according to circumstances. Sulphide concentrations in highly septic sewages seldom reach levels as high as 10mg/l, whereas tannery wastes may carry up to 3000 mg/l or more of sulphide sulphur. However, such tannery wastes usually are highly alkaline and  $H_2S$  partial pressures are only correspondingly high when the pH is lowered by admixtures of acidic wastes. The gases flowing out of sewer ventstacks commonly contain  $H_2S$  at concentrations not above 10 p.p.m.

by volume, usually rather less. Methyl mercaptan and dimethyl sulphide together usually do not exceed about 0.1 p.p.m. Effluvia from fish-preserving plants might contain tens of p.p.m. of mono- and trimethylamines at the ventilation plant outlet.

TABLE 1

Odours and Air Pollution

Origin	Nature of Odours	Remarks
Tanneries	Sulphide, ammoniacal (organic amines, $\text{NH}_3$ , etc.)	$\text{H}_2\text{S}$ may be most dangerous but organic most penetrating.
Abattoirs	Sulphidics and amines	By-products mfr. may add aldehydes, organic acids: fermentation may increase proportions of $\text{H}_2\text{S}$ /
Paper pulping	Sulphidics prominent, with terpenes, etc.	Relatively high concentration evolved from "digesters"
Sulphur dyeing	$\text{H}_2\text{S}$ and amines mainly	
Chemical Manufacture	Variable not infrequently due mainly to a particular gas, e.g. $\text{H}_2\text{S}$ , $\text{NH}_3$ , $\text{HCl}$ , $\text{Cl}_2$ .	Especially synthetic chemical factories
Sewerage and sewage treatment	Sulphidics, amines, aldehydes, organic acids	Result of septic sewage fermentations.

The concentration levels which are likely to be associated with odour complaints would be about as follows (2)

TABLE 2

Practical Odour Nuisance Thresholds

<u>Gas</u>	<u>Threshold Dilution Value ppm</u>
H <sub>2</sub> S	0.02
CH <sub>3</sub> SH	0.04
CH <sub>3</sub> S CH <sub>3</sub>	0.004

AIR POLLUTION (ODOUR) CONTROL for such nuisance sources as these may depend upon one or more of the following techniques:-

(1) Simple dilution using mechanical, sometimes even natural draft, ventilation systems to ensure adequate proportions of diluting air so that "ground-level" concentrations are lower than those of Table 2, or the corresponding concentrations of other pollutants. One technique takes clean air into the ventilation duct at the base of the outlet ventsack.

(2) Incineration or Catalytic combustion.

(3) Deodorization, the literature reporting various means including mainly the following:

- (a) Chemical treatment using chlorine or hypochlorite applied mostly in solution. Disadvantages are related to the corrosive character of such solutions. High concentrations of CO<sub>2</sub> gas produce other problems.
- (b) Treatment by absorption in lime solutions.
- (c) Treatment by gaseous ozone (3). Despite optimistic reports, studies of gaseous ozone treatments are not encouraging (4) as indicated by the following

reaction rates.

TABLE 3

Ozone -  $\text{H}_2\text{S}$  Reaction Rates

<u>ppm <math>\text{H}_2\text{S}</math> in Air</u>	<u>ppm Ozone in Air</u>	<u>Oxidation of <math>\text{H}_2\text{S}</math> ppm per minute</u>
about 300	about 400	about 2
" 6000	" 700	" 10
" 1000	" 700	" 40

In addition, other workers have shown that the ozone  $\text{H}_2\text{S}$  reaction produces  $\text{SO}_3$  and  $\text{H}_2\text{SO}_4$ , not sulphur as has been claimed most commonly, suggesting that corrosion would also be a problem with ozone. Toxicity also could be a problem.

- (d) Treatment by Sulphur dioxide, which is likely to be both corrosive to plant and to nearby structures.
- (e) Treatment by other oxidants.
- (f) Biological treatment.

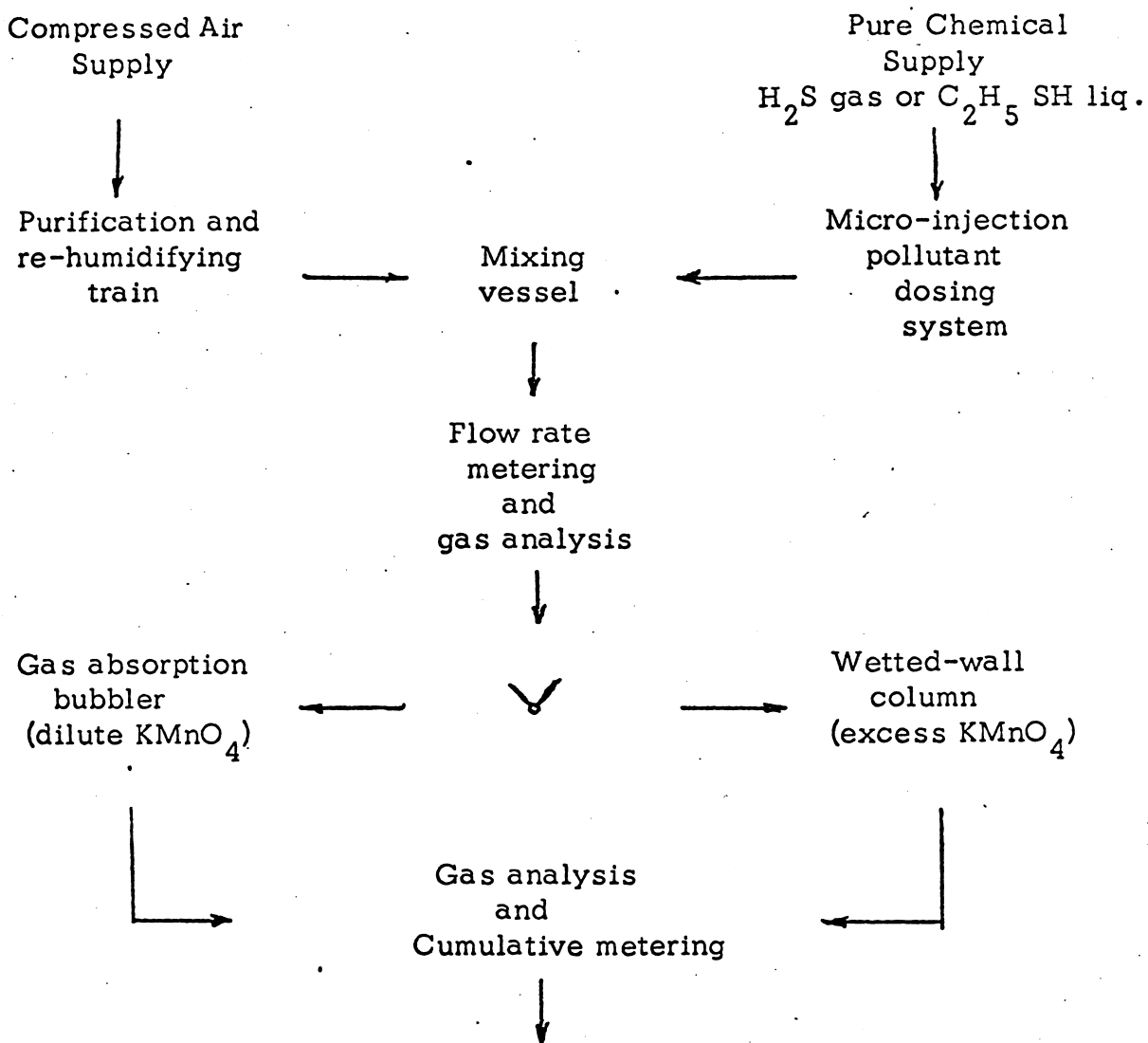
EXPERIMENTAL

The experimental investigations reported in this paper are part of studies of both a chemical and a biological system of oxidation. In the case of the chemical system, air streams were first polluted by precisely measured proportions of either  $\text{H}_2\text{S}$  alone or of ethane thiol alone; whereas proportions of  $\text{H}_2\text{S}$ , ethane thiol, di-ethylamine and butyraldehyde, alone or mixed, were used for the biological system which was based on the so-called trickling filter. These two sets of experiments are discussed separately in

the following.

DEODORIZATION OF AIR IN A CATALYTIC CHEMICAL PROCESS

A literature review led to the idea that potassium permanganate solutions would be suitable for oxidation of sulphidics, and apparatus was assembled to achieve the following sequence.



After due consideration, a fluorometric technique (5) was chosen as the standard method for measuring either the  $\text{H}_2\text{S}$  or the Et SH. Measurements showed that dosing accuracies were very satisfactory, variations from the mean dose rate being only about 10% at most.

The preliminary runs made using  $\text{KMnO}_4$  solution (0.02% buffered with  $\text{K}_2\text{B}_4\text{O}_7 \cdot 5\text{H}_2\text{O}$ , 0.4g/l, pH 9) yielded data such as that of Tables 4 and 5, from which it is to be seen that, after reduction of the permanganate and manganate ions, oxidation of the sulphidic pollutants continued practically at the same rate (which however showed a steady falling off over a period of several days) presumably due to the oxygen of the air stream, (see also Fig.1).

TABLE 4

Removal of  $\text{H}_2\text{S}$  from Air Streams

Room temperature - total pressure/atmosphere

Progressive time of run minutes	$\text{H}_2\text{S}$ Content of Effluent Air ppm v/v	Cumulative Total Input of $\text{H}_2\text{S}$ $\mu\text{g}$	Cumulative Total $\text{H}_2\text{S}$ Output $\mu\text{g}$	% Removal
34	0.7	4,200	33	99.2
461	3.0	56,000	1,730	96.9
941	4.6	119,000	6,530	94.5
1,438	14.4	184,000	19,180	89.5
1,962	29.9	247,000	49,580	79.5

Mean concentration of  $\text{H}_2\text{S}$  in inlet air 47.4 ppm v/v.

Rate of throughput of polluted air 1.88 l/min. About 200

minutes running, equal to 25,800  $\mu\text{g}$  of  $\text{H}_2\text{S}$ , is the stoichiometric equivalent of 300 cc of  $\text{KMnO}_4$  (0.02% aq, pH 9.2) for  $\text{Mn}^{7+} \rightarrow \text{Mn}^{3+}$ .

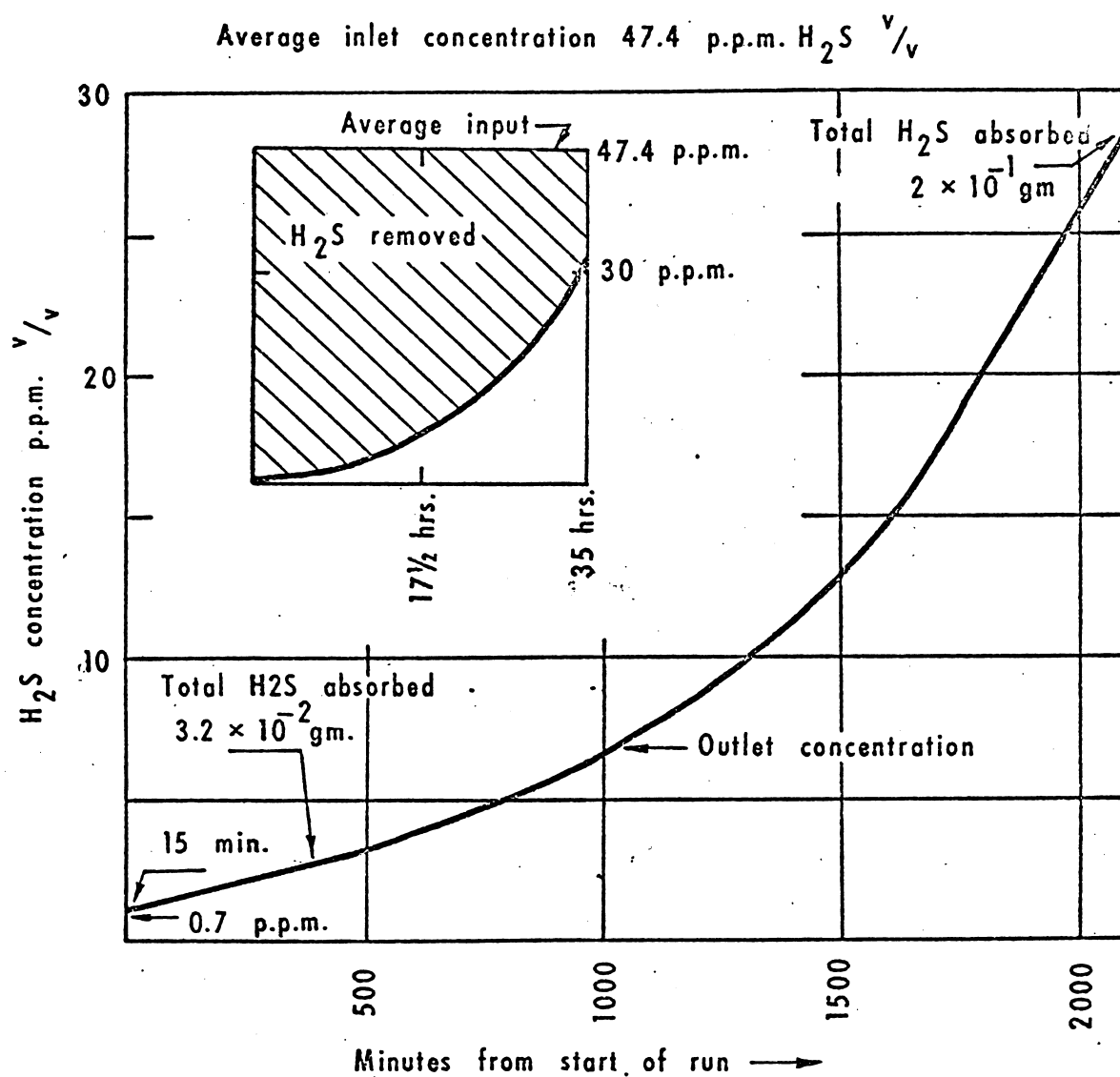


Fig. 1: Removal of  $\text{H}_2\text{S}$  from contaminated air  
 1.88 litres per minute passed through  
 300 mls. aq. solution containing initially  
 0.02%  $\text{KMnO}_4$ ; pH 9.2  
 (equivalent oxidising capacity  $3.2 \times 10^{-2}$  gm.  $\text{H}_2\text{S}$ )



TABLE 5

Removal of  $C_2H_5SH$  from Air Streams

Room temperature - total pressure/atmosphere

Progressive running time minutes	$C_2H_5SH$ in effluent air ppm v/v	Cumulative total $C_2H_5SH$ Input $\mu g$	Cumulative total $C_2H_5SH$ Output $\mu g$	% Removal
34	11.1	13,400	1,100	91.8
172	12.7	68,000	6,400	90.6
310	63.5	122,000	22,400	81.7
523	64.4	206,000	58,000	71.9

Mean concentration of  $C_2H_5SH$  in inlet air 129 ppm v/v.

Rate of throughput of polluted air 1.18 litre/min.

119 minutes running, equal to 47,000  $\mu g$   $C_2H_5SH$ , gives the stoichiometric equivalent of 300 cc of  $KMnO_4$  (0.02 % aq, pH 9.2),  $Mn^{7+} \rightarrow Mn^{3+}$ .

Fig. 2 illustrates diagrammatically the possible character of the catalytic reaction which effect the continuing oxidation of the Sulphidic gases in the polluted atmosphere when  $KMnO_4$  is no longer present. The slowing down of the rate of catalytic oxidation is attributed to a progressive "poisoning" of the system perhaps by precipitated sulphur.

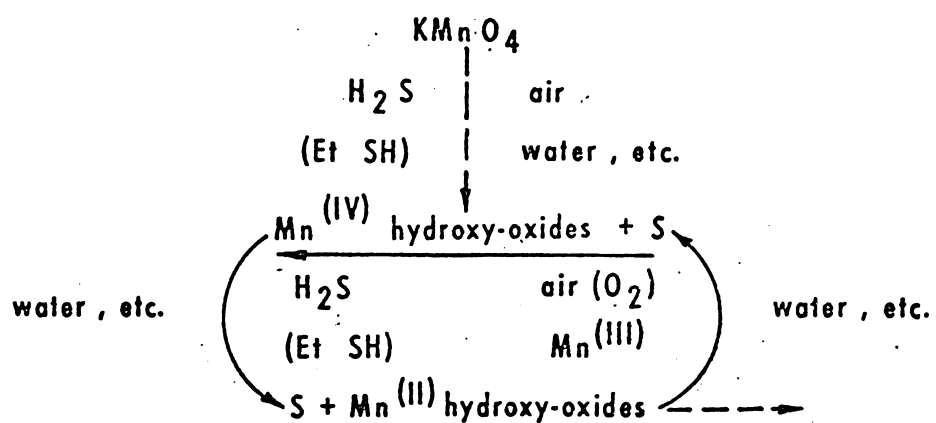


FIG. 2: Possible Catalytic Oxidation Systems

Absorption-reaction rate studies were made using short wetted-wall columns, substituted for the Drechsel bottle absorber. Three columns were used in turn, respectively 7.7, 8.6 and 10.3 cm long, 2.456 cm diameter, passing air streams at rates between about 1 and 12 litres/min. equal to upflow rates through the columns of 3-40 cm sec.<sup>-1</sup>. The arrangement of each column was as shown in Fig. 3 with weir-overflow feed and provision for very precise adjustments of clearances to ensure that the patterns of air-flow past the liquid film down-flow were substantially if not entirely free of entry and exit irregularities.

Experimental runs were made with each of the columns measuring the rate of desorption of CO<sub>2</sub> from water. The results generally were in accordance with those reported for example by Vivian, Behrmann and Peaceman<sup>(6)</sup>.

Data from the experiments with H<sub>2</sub>S and C<sub>2</sub>H<sub>5</sub>SH generally fit the theoretical concepts of Graetz<sup>(7)</sup> and Nusselt<sup>(8)</sup> assuming a parabolic velocity distribution of the gas stream. The overall values of the mass transfer coefficient K<sub>G</sub> expressed in units of kilogram-moles hr<sup>-1</sup> m<sup>-2</sup> atm<sup>-1</sup> range between the following values

range of (K <sub>G</sub> ) H <sub>2</sub> S	0.4 to 1.5
(K <sub>G</sub> ) C <sub>2</sub> H <sub>5</sub> SH	0.4 to 0.7

TABLE 7

Absorption rate data for  $\text{H}_2\text{S}$  and  $\text{C}_2\text{H}_5\text{SH}$ Wetted-wall columns with excess  $\text{KMnO}_4$ , 0.02% pH 9.2

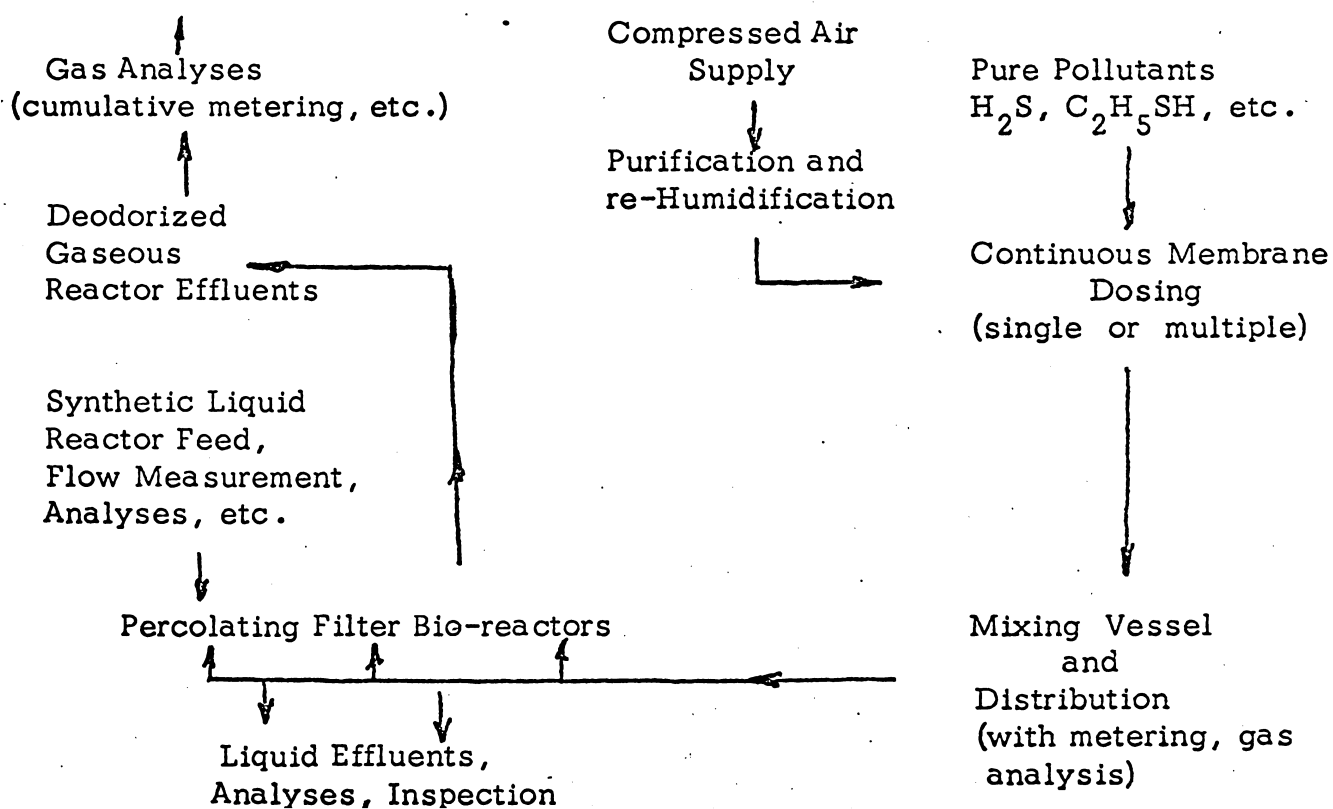
Length of Column used	Rate of Upflow of polluted air	$\text{H}_2\text{S}$ Concentrations	
		At entry ppm	At exit ppm
7.7 cm	$3.3 \text{ l. min}^{-1}$	17.5	9.9
10.3 cm	$12.4 \text{ l. min}^{-1}$	21.7	17.7
Ethanethiol			
7.7 cm	$6.1 \text{ l. min}^{-1}$	8.4	6.3

Column diameters 2.46 cm

Room temperatures, total pressure 1 atmosphere.

DEODORIZATION OF AIR IN A BIOLOGICAL FILTER SYSTEM

The experimental data in this connection were obtained by setting up apparatus according to the following flow-sheet.



Pollutant dosing for these experiments was controlled using permeation through tubular membranes, of selected diameters, length and wall thicknesses, made as required of polythene, polytetra fluoroethylenes and silicone rubbers, using assemblies such as those shown in Fig. 4 to feed precisely known amounts of  $\text{H}_2\text{S}$ ,  $\text{C}_2\text{H}_5\text{SH}$ ,  $(\text{C}_2\text{H}_5)_2\text{NH}$  and  $\text{C}_4\text{H}_9\text{CHO}$  either separately or as mixtures simulating the general character of sewer air.

The columns, representing so-called "percolating" or "trickling" filters, used for these preliminary experiments comprised pyrex glass cylinders of about  $2\frac{1}{4}$ " diameter, packed about 2 ft. deep either with river gravels, passing 1" and retained on  $\frac{3}{4}$ " wet mesh screens; or with glass balls of  $\frac{7}{8}$ " diameter roughened by rumbling with iron balls of  $\frac{1}{4}$ " size. They were not sterilized but cleaned with water of temperature  $85^\circ - 90^\circ \text{C}$ . Some of the columns were "seeded" with one or two stones taken from normal sewage treatment works, others were not seeded.

The liquid feed to the columns comprised "synthetic" sewage compositions prepared from yeast and beef extracts with glycosate, glucose, lactate and glycerol, and mineral salts containing Na, K, Mg,  $\text{NH}_4$ ,  $\text{PO}_4$ ,  $\text{CO}_3$ , and trace elements such as Fe, Cu, Zn, Mn, with a little EDTA.

Deodorization experiments in these experimental filters yielded results which are illustrated by the following Table No.8, (a) using  $\text{H}_2\text{S}$  only and (b) using  $\text{C}_2\text{H}_5\text{SH}$  only.

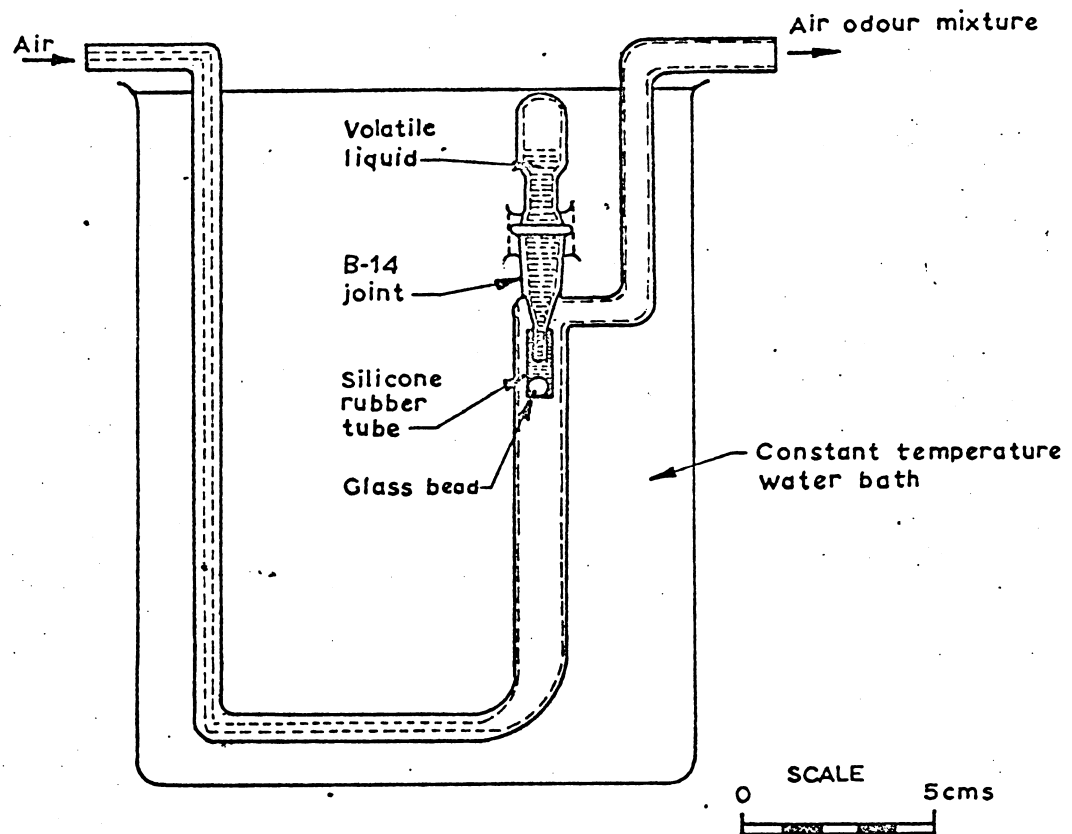


FIG.6: DOSING APPARATUS FOR PREPARING AIR ODOUR MIXTURES

TABLE 8 (a)

## Deodorization in Laboratory Scale Biological "Filters"

Mass Flow Rates		BOD <sub>5</sub> of Synthetic Sewage Feed mg/l		Gaseous Pollutants added $\mu\text{g min}^{-1}$	Filter No.3 Polluted Air Gaseous Concentrations ppm v/v		Percent Removal of Gaseous Pollutants
Synthetic Sewage ml/hr.	Polluted Air Stream $\text{cm sec}^{-1}$	Inlet	Outlet		Inlet	Outlet	
400 $\pm$ 50	1.55	100	50	H <sub>2</sub> S	5.0	Nil	100
	2.58	to	to	(only)	3.0	0.07	97 $\frac{1}{2}$
	3.61	110	60	21 $\pm$ 1	2.15	0.11	95
400 $\pm$ 50	1.03	110		45 $\pm$ 2	16.5	0.065	99.6
	2.06	to	about	H <sub>2</sub> S	8.25	0.210	97.1
	3.09	130	50 to	(only)	5.5	0.495	91
	5.16		60		3.2	0.510	83

TABLE 8 (b)

do.	0.52				1.6	0.065	96
	1.03				0.8	0.145	82
	1.55	Range	Range	C <sub>2</sub> H <sub>5</sub> SH (only)	0.57	0.17	70
	2.06	90	50		0.4	0.15	62
	2.58	to	to		0.32	0.14	57
	3.09	96	56	4.05	0.25	0.12	52
	3.61	pH 7.4	pH 7.3	± 0.12	0.23	0.122	47
	4.13				0.20	0.116	42
	4.64		23.5° C		0.18	0.108	40
	5.16				0.16	0.102	36

The filters were run at room temperatures, total pressures 1 atmosphere.



Diethylamine and butyraldehyde being far more soluble than the sulphidics were completely taken up by the biofilm. However in experiments with newly charged, practically sterile, columns using a liquid feed of clean tap water only, the proportion retained presumably by simple solution in the water was always very close to 100%. Analyses of effluent gas and effluent water taken together balanced exactly with the amount of amine used to pollute the input air, but when a biological filter was used, no diethylamine could be found in the effluent, presumably being metabolized by bacteria or other fungi.

Something similar was found with  $H_2S$ . Use of practically sterile columns likewise showed uptake of  $H_2S$  by the water, with roughly a balancing of the quantities of sulphide inputs and outputs but much lower proportions of  $H_2S$  being dissolved. As with the diethylamine, no  $H_2S$  could be detected in the normal effluents from ripened "filters", unless the filters were heavily overloaded with organic matter. In such cases  $H_2S$  is produced in the column.

Absorption-reaction rates for such columns are often calculated using expressions of similar type to those referred to earlier in connection with wetted wall columns, but proper allowances for film flow, effective areas, residence time and so on, are much less straightforward. Simple concepts developed by simple consideration of the material balance and physical dimensions of the system give the following relationships for a column element  $\Delta H$  at height  $H_x$  above the column base.

$$-\Delta Q = K_G \times S \times \Delta H \times C_{H_x} \times \Delta t \quad (3)$$

$$\text{and } C = \frac{\Delta Q}{V_G \times A \times \Delta t} \quad (4)$$

where  $-\Delta Q$  is the amount of gaseous pollutant absorbed on the element  $\Delta h$ ;

$K_G$  is the absorption rate coefficient per unit area and unit concentration difference;

$S$  is the effective surface area of the packing,  $\text{cm}^2$  per  $\text{cm}^3$ ;

$V_G$  is the nominal mass flow rate of the polluted air;

$A$  is the nominal cross-section of the column,  $\text{cm}^2$ ;

$\Delta C$  is the change in gaseous pollutant concentration at height  $Hx$ ;

and hence

$$\frac{K_G \times S \times C_{Hx} \times \Delta t \times \Delta H}{\Delta C = -V_G \times A \times \Delta t}$$

$$\int_{C_0}^{C_H} \frac{1}{C_{Hx}} \times dC = \int_{H_0}^H \frac{K_G}{V_G} \times \frac{S}{A} \times dh$$

$$2.303 (\log C_H - \log C_0) = K_G \times \frac{S}{V_G \times A} \times H$$

Calculated values for  $(K_G)_{H_2S}$ , ppm, in units of ml  $H_2S$  per sq. cm per second per ppm input concentration averaged about  $2 \times 10^{-4}$ , and for  $(K_G)_{C_2H_5SH}$ , ppm, about  $5 \times 10^{-5}$

Such coefficients could be applied to practical designs of polluted gas deodorizing plants. The catalytic chemical

process using  $\text{KMnO}_4$  solutions might for example consist of a simple tunnel system; with say 3 droplet spray units alternating with 3 zones filled with checker brickwork, the polluted air moving counter current to sprayed reactant mixtures. The mixture at the downstream end would comprise an appropriate fresh  $\text{KMnO}_4$  solution feed with some recirculation. The next spray (closer upstream in the moving air) might also include some  $\text{KMnO}_4$ , but rather less in proportion, but the first spray contacting the polluted air would consist only of recirculated hydroxy-oxides of manganese suspensions.

The biological systems might best consist of normal low rate trickling filter structures using say 30 mm to 50 mm size gravel packing but with special arrangements for polluted air distribution under the media. The liquid fed from above might be restricted to flow rates say  $10 \times 10^6$  litres per hectare daily of weak settled wastes,  $\text{BOD}_{5\text{-day}}$  contents say 50 to 100 mg/l or less. Rectangular filters may be specially suitable.

---

#### ACKNOWLEDGEMENTS:

The experimental work referred to herein was carried out in the Public Health Engineering Laboratories of the School of Civil Engineering with financial support for the catalytic chemical method studies through the School of Chemical Engineering. The biological method studies were carried out under the sponsorship and financial support of the Metropolitan Water Sewerage and Drainage Board of Sydney. The authors make these acknowledgements gratefully.

REFERENCES:

- (1) Reid, H.A., "The Odour Problem at Maryvale", Proc. Australian Pulp and Paper Ind. Technical Assoc'n. 3(1949), 18th June.
- (2) Derived from practical experience especially with sewer odour nuisances.  
  
Stern, A.C., (Editor) "Air Pollution" (1962) Academic N.Y. gives extensive data, but see also  
  
Leonardos, G., Kendall, D. and Barnard, N., J. Air Poll. Control Assoc. 19(1969) 91.
- (3) Gregor, I.K., and Martin, R.L., Australian J. Chem. 14, (1961) 462.
- (4) Hales, J.M., Wilkes, J.O., and York, J.L., Atmospheric Environ. 3(1969) (vi) 657.
- (5) Hardwick, B.A., Thistlethwayte, D.K.B., and Fowler, R.T., Atmospheric Environ. 4(1970) 379, and discussion Idem, 5(1971) 281-2.
- (6) Vivian, J.E. and Peaceman, D.W., also Vivian, J.E. and Behrmann, Amer. Inst. Chem. Eng. J. 2 (1956) 437 and 11 (1965) 656.
- (7) Graetz, L., Ann. der Physik 48 (1883) 79.
- (8) Nurselt, H., Ver. deutsch. Ing. 54 (1910) 1154.